UNIVERSITY OF OKLAHOMA

GRADUATE COLLEGE

TRILOBITES FROM A CAMBRIAN EXTINCTION INTERVAL AT THE BASE OF THE STEPTOEAN STAGE, RILEY FORMATION, CENTRAL TEXAS

A THESIS

SUBMITTED TO THE GRADUATE FACULTY

in partial fulfillment of the requirements for the

Degree of

MASTER OF SCIENCE

By

MADISON LAYNE ARMSTRONG
Norman, Oklahoma
2018

TRILOBITES FROM A CAMBRIAN EXTINCTION INTERVAL AT THE BASE OF THE STEPTOEAN STAGE, RILEY FORMATION, CENTRAL TEXAS

A THESIS APPROVED FOR THE
CONOCOPHILLIPS SCHOOL OF GEOLOGY AND GEOPHYSICS

BY

_____
Dr. Stephen Westrop, Chair

_____
Dr. Richard Cifelli

_____
Dr. Richard Lupia

Acknowledgements

First, I must express my gratitude to Dr. Steve Westrop for giving me this project and for providing insight, guidance, and patience while I figured out what I was doing; as well as for instilling in me an appreciation for the greatest arthropod to ever roam the seafloor. A big thanks to Roger Burkhalter for his assistance in the collections and lab, and for his insight on fossils over the years. Thank you to my committee, Dr. Rick Lupia and Dr. Rich Cifelli for your time and for providing feedback. A special thanks to Dr. Mike Engel for his important role in the geochemistry aspect by providing his time and lab; as well as to Sarah Engel-Barnett for her assistance in preparing carbonate samples. Thanks to Dr. Doug Elmore, for his guidance and advice on thin sections and all things diagenesis. I must thank my friends and family who have provided support and encouragement over the course of my education; especially Justin for his love, support, and patience while I spent our engagement in graduate school. And lastly, a shout-out to my cat, Minerva, for keeping me company during late night study and writing sessions.

Table of Contents

Acknowledgements iv
List of Tables viii
List of Figures ix
Abstract x
Chapter I: Introduction 1
Geologic Setting 3
Localities 4
Chapter II: Biostratigraphy and Geochemistry 19
Introduction 19
Biostratigraphy 19
Carbon Isotope Stratigraphy 21
Geochemical Analysis Procedure 23
Carbon Isotope Results 25
SPICE in Central Texas 25
Diagenesis 27
Petrographic Description 29
Discussion 30
Chapter III: Systematics of Genus *Blountia* and Relatives 50
Introduction 50
Localities and Stratigraphic Setting 50
Phylogenetic Analysis 55
Taxon Selection and Coding Sources 56
Character Coding 56
Results 56
Systematic Paleontology 57
Family Kingstoniidae Kobayashi, 1933 58
Genus *Blountia* Walcott, 1916 58
Blountia mimula Walcott, 1916 59
Blountia angela sp. nov. 63
Blountia bristolensis Resser, 1938 66

Blountia cora Lochman, 1944 68
Blountia janei Lochman, 1944 70
Blountia montanensis Duncan, 1944 72
Blountia cf. *montanensis* (Duncan, 1944) 74
Blountia gaspensis Rasetti, 1946 75
Blountia nasuta Rasetti, 1946 76
Blountia nevadensis sp. nov. 78
Blountia morgancreekensis sp. nov. 82
Blountia newfoundlandensis sp. nov. 87
Genus *Maryvillia* Walcott, 1916 89
Maryvillia arion Walcott, 1916 90
Maryvillia triangularis (Lochman, 1944) 93
Genus *Blountina* Lochman, 1944 95
Blountina eleanora Lochman, 1944 96
Chapter IV: Genus *Aphelaspis* 108
Introduction 108
Stratigraphic Setting 108
Systematic Paleontology 109
Family Pterocephaliidae Kobayashi, 1935 109
Genus *Aphelaspis* Resser, 1935 110
Aphelaspis cf. *walcotti* (Resser, 1938a) 111
Aphelaspis constricta Palmer, 1954 116
Aphelaspis longifrons Palmer, 1954 118
Aphelaspis spinosa Palmer, 1954 120
Chapter V: Other Genera in the Riley Formation 124
Systematic Paleontology 124
Family Cheilocephalidae Shaw, 1956 124
Genus *Cheilocephalus* Berkey, 1898 124
Cheilocephalus brevilobus Walcott, 1916 124
Cheilocephalus cf. *granulosus* (Palmer, 1965) 128
Family Elviniidae Kobayashi, 1935 129
Genus *Dunderbergia* Walcott, 1924 129

Dunderbergia cf. *variagranula* (Palmer, 1954).....129
Family Lonchocephalidae Hupé, 1955.....130
Genus *Glaphyraspis* Resser, 1937.....130
Glaphyraspis parva (Walcott, 1899).....130
Glaphyraspis dianae sp. nov. 133
Glaphyraspis richardi sp. nov. 136
Family Crepicephalidae Kobayashi, 1935.....137
Genus *Coosella* Lochman, 1936 137
Coosella cf. *perplexa* (Palmer, 1954).....137
Genus *Coosina* Rasetti, 1956 138
Coosina cf. *ariston* (Walcott, 1916).....138
Family Llanoaspididae Lochman, in Lochman and Duncan, 1944.....139
Genus *Llanoaspis* Lochman, 1938 139
Llanoaspis cf. *peculiaris* (Resser, 1938a) 139
Family Pterocephaliidae Kobayashi, 1935 140
Genus *Blandicephalus* Palmer, 1954.....140
Blandicephalus texanus Palmer, 1954 140
Genus *Labiostria* Palmer, 1954.....141
Labiostria convexiimarginata Palmer, 1954 141
Labiostria sigmoidalis Palmer, 1954 142
Labiostria platifrons Palmer, 1954 143
Gen. nov. aff. *Dunderbergia*.....143
APPENDIX A: Abundances and Distributions 146
APPENDIX B: Phylogenetic Analysis Character List.....153
APPENDIX C: Plates.....154

List of Tables

Table 1: Carbon and Oxygen Isotope Values in the Riley Formation. 37

Table 2: Phylogenetic Analysis Matrix for Blountia and Related Taxa.....102

Table 3: Individuals of Species by Section 146

Table 4: Genera Abundance by Biozone.....147

Table 5: Species Abundance by Biozone 148

Table 6: Species and Sclerite Distribution by Section 149

List of Figures

Figure 1: Stratigraphy of the Riley Formation.....7

Figure 2: Upper Cambrian Timescale. 9

Figure 3: Map of Localities. 11

Figure 4: Locality Section Correlation.....13

Figure 5: Depositional Envrionment of Lion Mountain.....15

Figure 6: Images of Study Area 17

Figure 7: Carbon Isotope and Biostratigraphy.....40

Figure 8: The SPICE in Central Texas and the Great Basin.....42

Figure 9: The SPICE in Central Texas and Newfoundland.....44

Figure 10: Thin Section Images of the Cap Mountain Limestone.....46

Figure 11: Thin Section Images of the Lion Mountain Sandstone 48

Figure 12: Strict Consensus Cladogram of *Blountia* and Related Taxa.....104

Figure 13: Character Optimization of *Blountia* and Related Taxa 106

Abstract

The Riley Formation of central Texas provides the only record of Steptoean trilobites in the southern mid-continent region. The objective of this thesis is to document the faunal assemblages associated with the globally documented extinction event at the base of the Steptoean (Saltzman et al., 2000) and its aftermath. A positive carbon isotope excursion (SPICE; e.g., Saltzman et al., 2000) that has been recognized on several continents but not previously in the southern mid-continent of Laurentia, is also documented. Peak SPICE $\delta^{13}C$ values have been recorded up to +5‰; the Riley Formation records the climbing limb of the SPICE and a peak $\delta^{13}C$ value of +3‰. The SPICE is also associated with marine transgression and deposition of siliclastic sediments, which is characteristic of the Cap Mountain and Lion Mountain members of the Riley Formation.

Palmer (1954) recognized two faunal assemblage in the Riley Formation, the *Aphelaspis* Zone and the overlying post-*Aphelaspis* Zone. Here the zones are revised into species-based assemblages: the *Coosella perplexa* Zone, *Aphelaspis spinosa* Zone, *Aphelaspis longifrons* Zone, and *Blandicephalus texanus* Zone. The most recent study of the trilobites in the Riley Formation is over 60 years old (Palmer, 1954) so here select taxa is revised from the Cap Mountain Limestone and the Lion Mountain Sandstone. The genus *Blountia* is of particular interest because it is one of the few genera to survive the extinction at the base of the Steptoean. Pre- and post-extinction species from across Laurentia are revised and a preliminary phylogenetic analysis investigates the relationship between the species, and the relationship with two

relatives, *Maryvillia* and *Blountina*, which some authors (e.g., Pratt, 1992; Rasetti, 1956) consider to be synonymous with *Blountia*. *Aphelaspis*, *Blandicephalus*, *Cheilocephalus*, *Coosella*, *Coosina*, *Dunderbergia*, *Glaphyraspis*, *Llanoaspis*, *Labiostria*, and a new genus related to *Dunderbergia* are also looked at. New species include *Blountia morgancreekensis*, *Blountia nevadensis*, *Blountia angela*, *Blountia newfoundlandensis*, *Glaphyraspis dianae*, and *Glaphyraspis richardi*.

Chapter I: Introduction

The Riley Formation of the Moore Hollow Group in central Texas is a succession of carbonates and glauconitic sands deposited during the middle to late Cambrian when the area was covered by shallow seas. The Riley Formation consists of the Hickory Sandstone Member, the Cap Mountain Limestone Member, and the Lion Mountain Sandstone Member (Fig. 1), of which the latter two are the focus of this thesis. These rocks are the only record of Steptoean-aged trilobites (Ludvigsen and Westrop, 1985) in the southern mid-continent region and are of interest because of a globally documented extinction at its base (Saltzman et al., 2000).

Chapter II examines the biostratigraphy of the trilobite fauna in the study area and relates it to a new carbon isotope stratigraphy from the same succession. The two biozones proposed by Palmer (1954), the *Aphelaspis* and post-*Aphelaspis* Zones, are revised into a more detailed scheme based on the occurrence of species in the upper Cap Mountain Limestone and Lion Mountain Sandstone. Cambrian carbon isotope stratigraphy has not been documented previously from the southern mid-continent region, and the succession in the study region records a positive carbon isotope excursion beginning at the base of the Steptoean. It can be correlated with the globally identified SPICE excursion (Saltzman et al. 2000) during sea level regression (Saltzman et al., 2004). Most areas that document the SPICE show a $\delta^{13}C$ increase of +1–5‰, and in the Riley Formation in central Texas, $\delta^{13}C$ peaks at around +3‰. Thin section analysis suggests that much of the diagenesis occurred early as the limestone is

dominated by early marine cements, indicating the isotopes should reflect the seawater chemistry at the time. Combining isotope analysis with the biostratigraphy provides an improved basis for correlating the Texas succession to other regions.

Chapter III focuses on the genus *Blountia*, which is a genus that survived the extinction at the base of the Steptoean Stage and persisted through part of the *Aphelaspis* Zone. To use the words of Jablonski (2002, p. 8139), the genus became a "dead clade walking"; a short-lived survivor that failed to recover. Exemplar species of *Blountia* and its close relatives *Maryvillia* and *Blountina* are revised using new photographs of previously illustrated taxa (e.g., Lochman and Duncan, 1944), and their relationships are explored through a phylogenetic analysis of pre- and post-extinction species.

Chapter IV focuses on the genus *Aphelaspis* and its species occurring in the classic *Aphelaspis* zone (herein divided into the *Coosella perplexa*, *Aphelaspis spinosa*, and *Aphelaspis longifrons* Zones in central Texas; see Chapter II) of the Riley Formation. *Aphelaspis* is a wide-spread genus that is documented across North America (e.g., Palmer, 1965; Rasetti, 1965; Pratt, 1992). Palmer (1954) recognizes four species in the Riley Formation. However, these species were based on only a handful of specimens. Here, expanded samples illustrated with high resolution digital images allow a greatly improved evaluation to be made.

Chapter V covers additional genera and taxa that occur in the study areas, some of which require further evaluation in future projects. They include *Glaphyraspis*, *Cheilocephalus*, *Coosella*, *Coosina*, *Llanoaspis*, *Blandicephalus*, *Dunderbergia*, *Labiostria*, *Cheilocephalus*, and a new genus related to *Dunderbergia*.

Geologic Setting

The Riley Formation is exposed across several counties in central Texas. The study areas for this thesis lie in the eastern region of the outcrop belt in Burnet County. In this region, the Cap Mountain Limestone is a bioclastic grainstone composed of dominantly sparry calcite cements and variable amounts of mature quartz sand, glauconite, brachiopod, echinoderm, and trilobite sclerites. King and Chafetz (1983) described the lower, siliciclastic-rich and upper, carbonate-rich strata of the Cap Mountain as being tidal flat, tidal channel, and shallow subtidal deposits during a transgressive-regressive couplet. The siliciclastic facies, which occur in the northern and western regions, are interpreted as channel fills from tidal channels draining into tidal flat deposits. The carbonate strata are gradational with the siliciclastic deposits and were assigned to three facies by King and Chafetz (1983): sponge banks, adjacent to oolite shoals, and shallow shelf deposits with trilobite, brachiopod, and echinoderm debris that formed above wave base. The latter of these facies is expressed in the study areas in Burnet County.

The overlying Lion Mountain Sandstone member was deposited during a time of regression and underlies a craton-wide unconformity (the Sauk II–Sauk III boundary; Palmer, 1998). The succession in Burnet County is mostly a sandstone dominated by glauconite and mature quartz sand with cross-bedding (Fig. 6A), some shale layers (Fig. 6D), and carbonate lenses filled with sparry calcite and trilobite sclerites (Fig. 6E). The sandy deposits are interpreted to be migratory tidal inlet channels of a barrier island complex that passed landward into a lagoon recorded by unfossiliferous, unbioturbated

shale (Chafetz, 1978) (Fig. 5). The lack of bioturbation and presence of evaporite clasts in the shale suggests the lagoon was hypersaline (Chafetz, 1980). The carbonate lenses may have originated in troughs of the cross-beds where trilobite sclerites accumulated; early diagenetic, marine calcite cements began to nucleate off the allochems, growing outward to lithify the lenses (Chafetz, 1988).

Localities

This study is based on data from two areas, Morgan Creek and Hoover Point, located in Burnet County, Texas (Fig. 3) which provided lithologic logs, trilobite samples, and samples for geochemical analysis. There were five localities from the Morgan Creek area exposed at road cuts and along Morgan Creek: Morgan Creek North extended sections 1 and 2 (MCNe1 and MCNe2, respectively), Morgan Creek North (MCN), Morgan Creek South (MCS), and Lake Buchanan (LB). Correlation of the Morgan Creek localities yields around 26 meters of section, which includes about 11 meters of the upper Cap Mountain Member and nearly the entire Lion Mountain Member. The Hoover Point (HP) locality is located about 23 kilometers (14.2 miles) south of Morgan Creek and exposes the uppermost Cap Mountain Limestone and about 8 meters of Lion Mountain Sandstone along a highway overlook. A composite section of all six localities (Fig. 3) is shown in Figure 4.

References

Chafetz, H.S., 1978, A trough cross-stratified glaucarenite: a Cambrian tidal inlet accumulation: Sedimentology, v. 25, p. 545–559, doi: 10.1111/j.1365-3091.1978.tb02079.x.

Jablonski, D., 2002, Survival without recovery after mass extinctions: Proceedings of the National Academy of Sciences, v. 99, p. 8139–8144, doi: 10.1073/pnas.102163299.

King Jr., D.T., and Chafetz, H.S., 1983, Tidal-flat to Shallow-shelf Deposits in the Cap Mountain Limestone Member of the Riley Formation, Upper Cambrian of Central Texas: SEPM Journal of Sedimentary Research, v. 53, p. 261–273, doi: 10.1306/212f81a2-2b24-11d7-8648000102c1865d.

Lochman, C., and Duncan, D., 1944, Early Upper Cambrian Faunas of Central Montana: Geological Society of America Special Papers, v. 54, p. 1–172, doi: 10.1130/spe54-p1.

Ludvigsen, R., and Westrop, S.R., 1985, Three new Upper Cambrian stages for North America: Geology, v. 13, p. 139–143, doi: 10.1130/0091-7613(1985)13<139:TNUCSF>2.0.CO;2.

Ogg, J.G., Ogg, G., and Gradstein, F.M., 2016, A Concise Geologic Time Scale: 2016: Amsterdam, Elsevier, p. 42.

Palmer, A.R., 1954, The faunas of the Riley Formation in central Texas: Journal of Paleontology, v. 28, p. 709–786.

Palmer, A.R., 1998, A proposed nomenclature for stages and series for the Cambrian of Laurentia: Canadian Journal of Earth Sciences, v. 35, p. 323–328, doi: 10.1139/e97-098.

Saltzman, M.R., Ripperdan, R.L., Brasier, M.D., Lohmann, K.C., Robison, R.A., Chang, W.T., Peng, S., Ergaliev, E.K., and Runnegar, B., 2000, A global carbon isotope excursion (SPICE) during the Late Cambrian: relation to trilobite extinctions, organic-matter burial and sea level: Palaeogeography, Palaeoclimatology, Palaeoecology, v. 162, p. 211–223, doi: 10.1016/S0031-0182(00)00128-0.

Saltzman, M.R., Cowan, C.A., Runkel, A.C., Runnegar, B., Stewart, M.C., and Palmer, A.R., 2004, The Late Cambrian SPICE ($\delta^{13}C$) event and the Sauk II–Sauk III regression: new evidence from Laurentian basins in Utah, Iowa, and Newfoundland: Journal of Sedimentary Research, v. 74, p 366–377, doi: 10.1306/120203740366.

Figure 1: Stratigraphic column of members of the Riley Formation in the Moore Hollow Group, including the overlying member of the Wilberns Formation. Modified from Palmer, 1954, Fig. 3. Not drawn to scale.

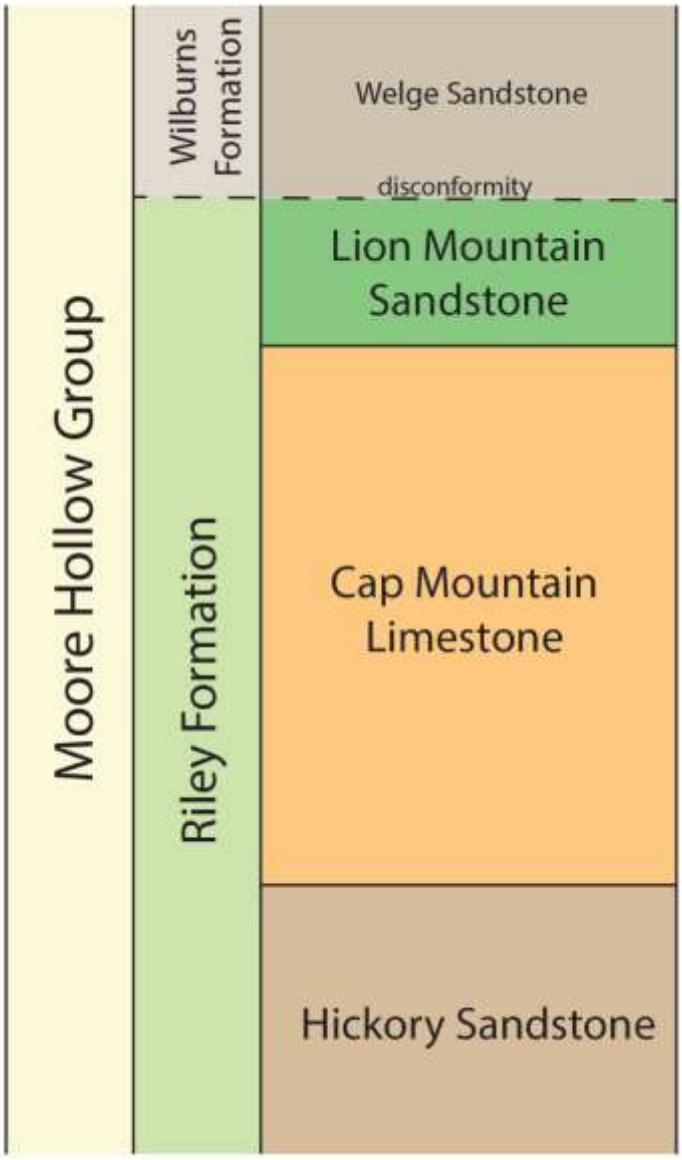
Moore Hollow Group
Wilburns Formation
Welge Sandstone
disconformity
Riley Formation
Lion Mountain Sandstone
Cap Mountain Limestone
Hickory Sandstone

Figure 2: Upper Cambrian timescale of stages, indicating the time of deposition of the Riley Formation in the study areas at the end of the Marjuman and through the Steptoean. Modified from Ogg et al., 2016, fig. 5.1.

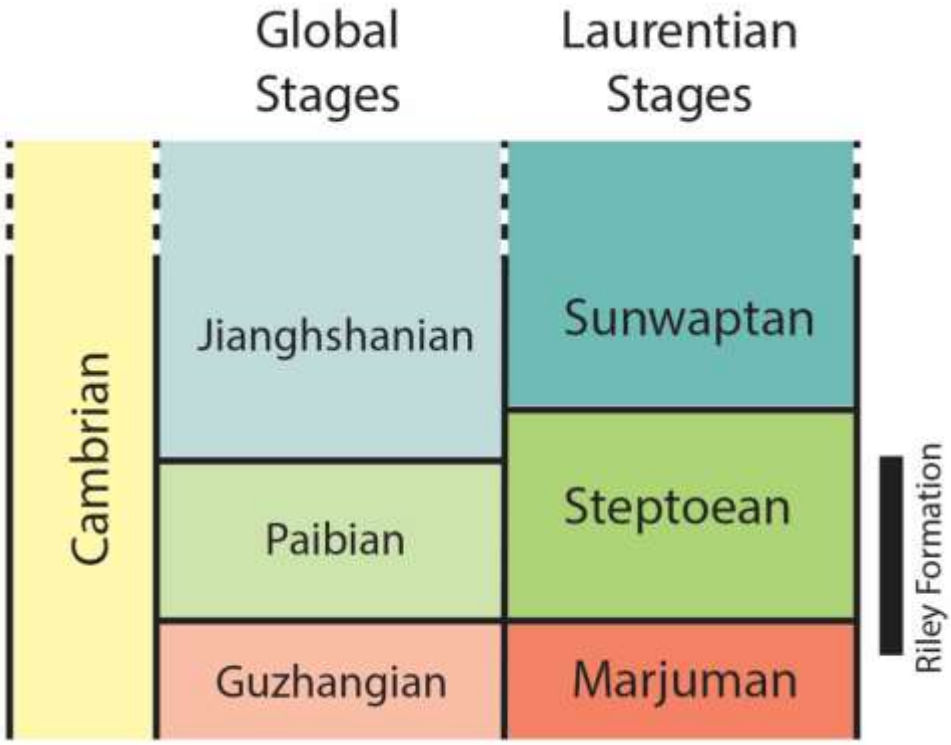
Global Stages
Laurentian Stages
Cambrian
Jianghshanian
Paibian
Guzhangian
Sunwaptan
Steptoean
Marjuman
Riley Formation

Figure 3: Map of the localities for this project in Burnet County, Texas. Morgan Creek area includes five localities: MCN, MCNe1, MCNe2, MCS, and LB. The Hoover Point (HP) is located about 23 kilometers (14.2 miles) south of Morgan Creek.

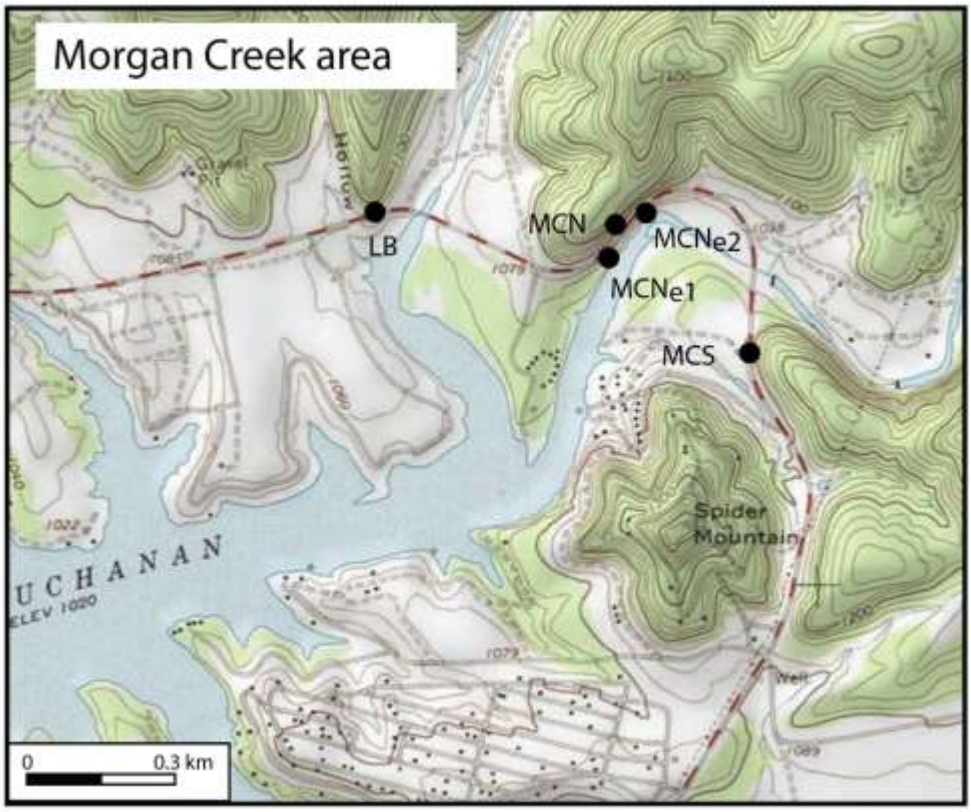
Morgan Creek area
LB
MCN
MCNe2
MCNe1
MCS
Spider Mountain
0
0.3 km

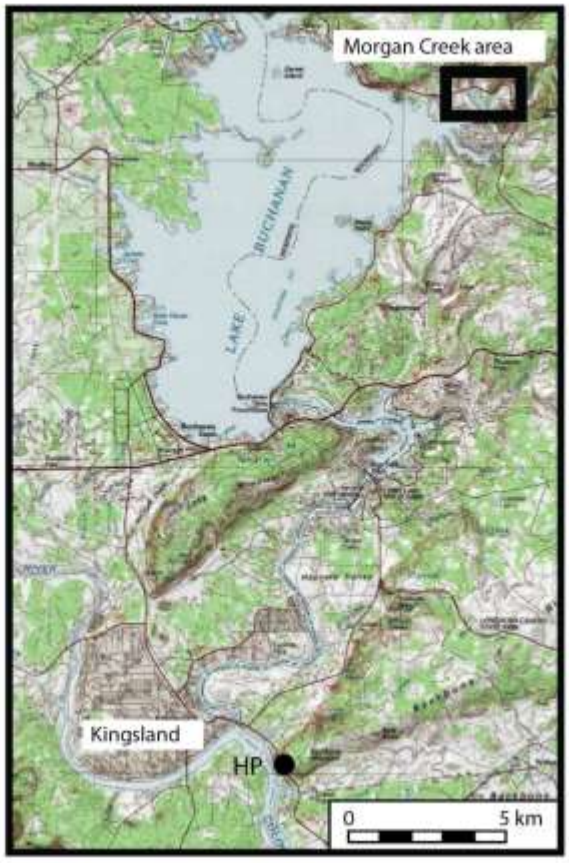
Morgan Creek area
Kingsland
HP
0
5 km

Figure 4: Section correlation of the five localities, their approximate distances apart, and a composite section. Sections are measured in meters. Cap Mountain Limestone member (tan) and Lion Mountain Sandstone member (green) of the Riley Formation are differentiated; shale layers represented in black. The presence of *Coosella* cf. *perplexa* indicates the base of the Steptoean from the underlying Marjuman Stage. Carbon isotope ($\delta^{13}C$) values are noted next to section numbers. Composition section includes approximate meterage, section number, and carbon isotope value.

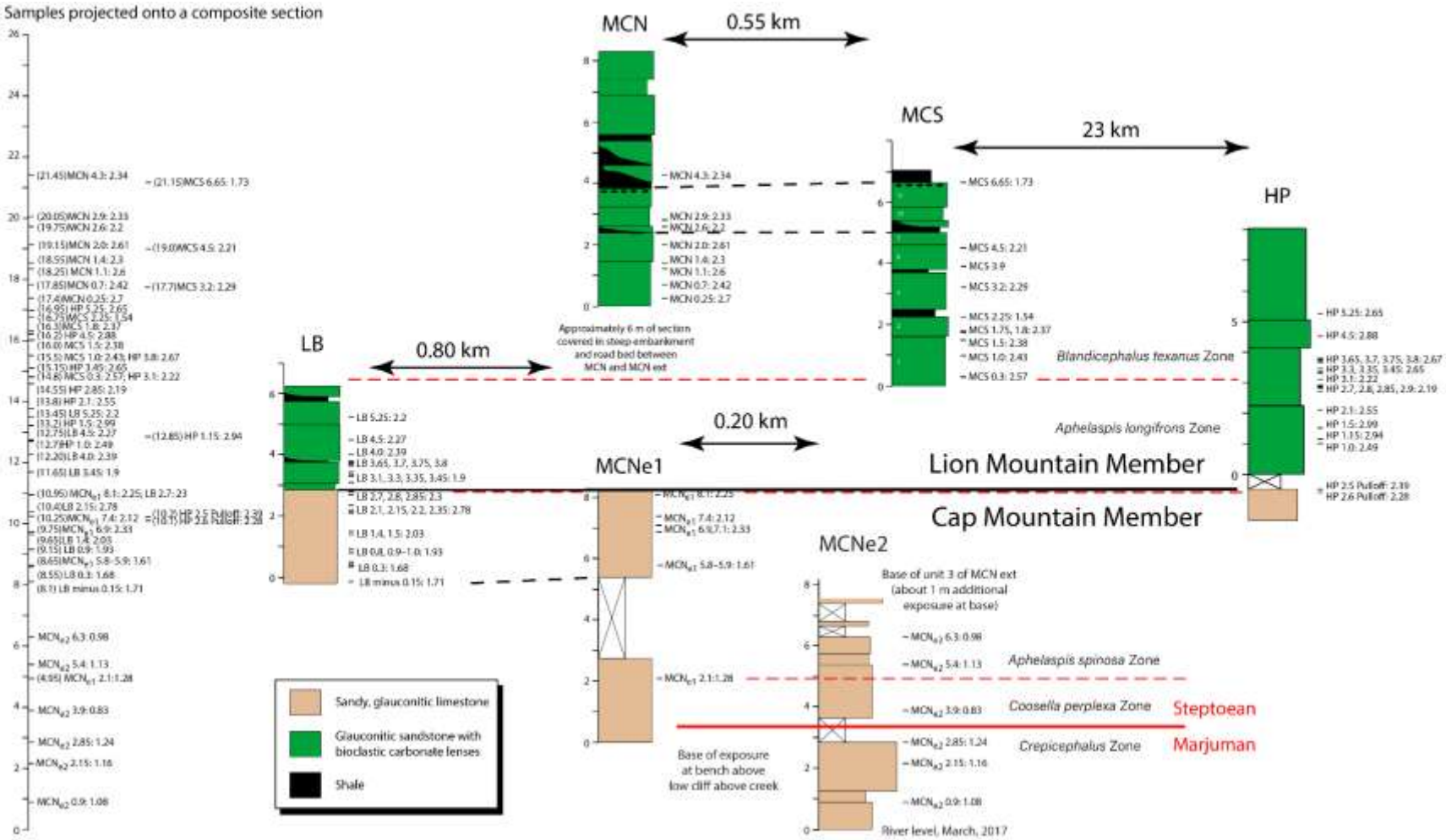
Samples projected onto a composite section
MCN
0.55 km
MCS
23 km
HP
LB
0.80 km
0.20 km
MCNe1
MCNe2
Blandicephalus texanus Zone
Aphelaspis longifrons Zone
Lion Mountain Member
Cap Mountain Member
Aphelaspis spinosa Zone
Coosella perplexa Zone
Steptoean
Crepicephalus Zone
Marjuman
Approximately 6 m of section covered in steep embankment and road bed between MCN and MCN ext
Base of unit 3 of MCN ext (about 1 m additional exposure at base)
Base of exposure at bench above low cliff above creek
River level, March, 2017
Sandy, glauconitic limestone
Glauconitic sandstone with bioclastic carbonate lenses
Shale

Figure 5: Illustration of the tidal inlet, migrating tidal channels, and flood deltas in the lagoon deposits of the Lion Mountain Sandstone. Figure modified from Chafetz, 1978, Fig. 8.

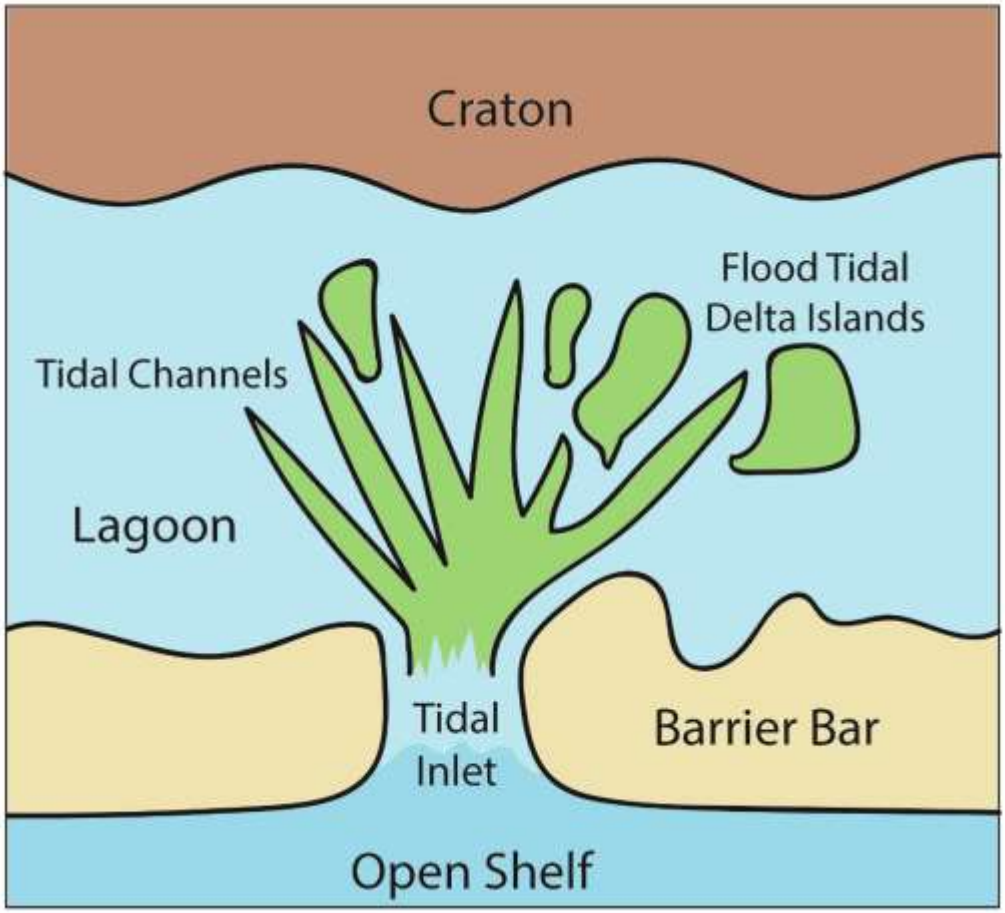
Craton
Flood Tidal
Delta Islands
Tidal Channels
Lagoon
Tidal
Inlet
Barrier Bar
Open Shelf

Figure 6: Images of lithologic features and outcrops of the Cap Mountain and Lion Mountain members of the Riley Formation, Burnet County, Texas. Field notebook for scale is 6.5 inches long. Images from March 2017.

A. Cross-beds (indicated by white lines) in glauconite-rich sandstone with white carbonate lenses following along cross-beds, Lion Mountain Sandstone, MCN locality.

B. Road outcrop of Lion Mountain Sandstone at MCN locality.

C. Tidal channel deposits of glauconitic sand (G) cutting through shale beds (S), Lion Mountain Sandstone, MCN locality; rock hammer for scale.

D. Glauconitic sandstone (G) with carbonate lenses (C) disrupted by thin shale layer (S), Lion Mountain Sandstone, MCN locality.

E. White carbonate lenses along cross-beds in glauconitic sand, Lion Mountain Sandstone, MCS locality.

F. Carbonate lenses weathered/dissolved out, leaving voids in the glauconitic sandstone host rock, LB section.

G. Carbonate lenses (C) in glauconitic sandstone (G), Lion Mountain Sandstone at HP section.

H. Cap Mountain Limestone exposed through vegetation overgrowth at MCN extended section.

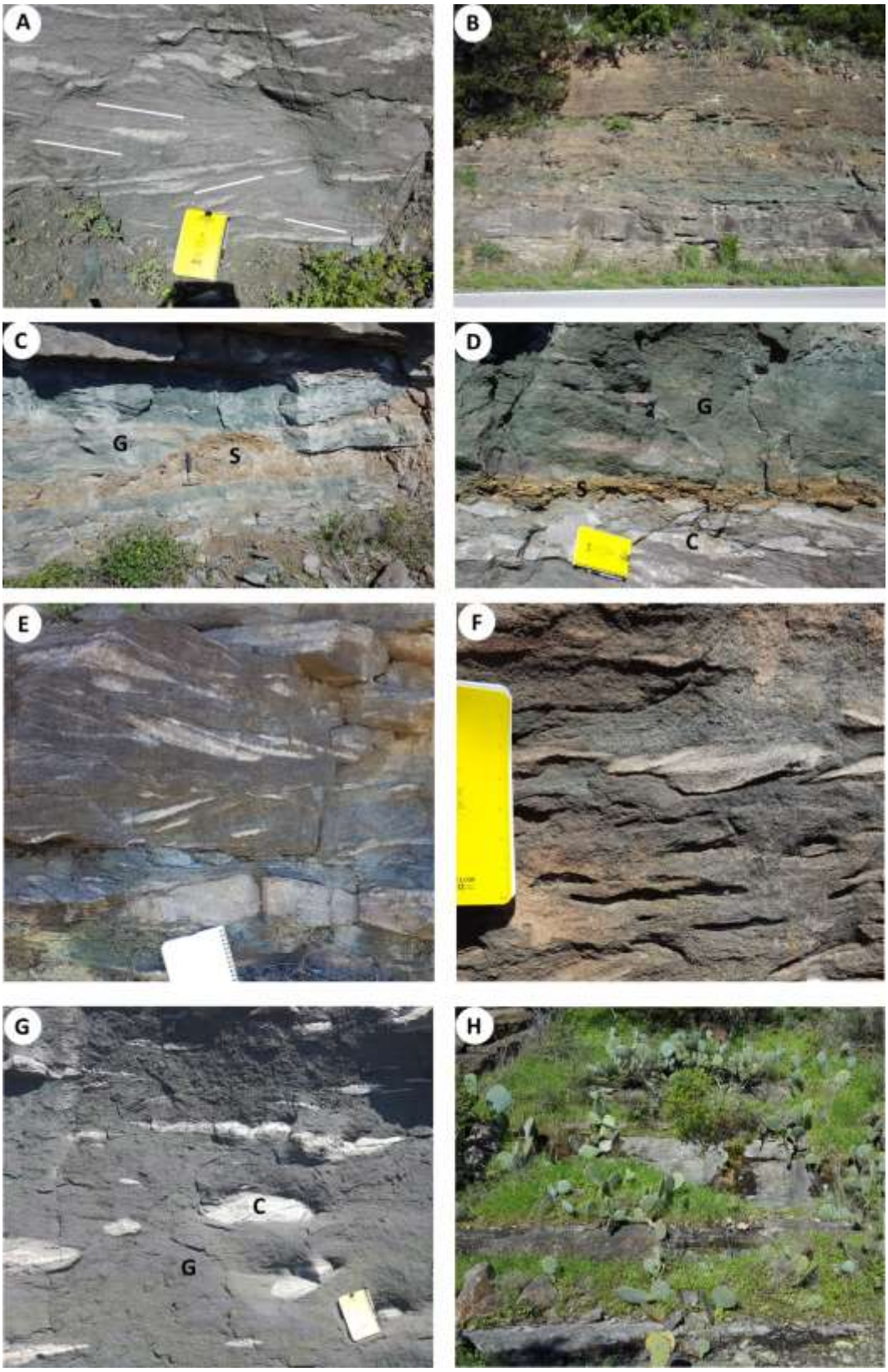
A
B
C
G
S
D
G
S
C
E
F
G
C
G
H

Chapter II: Biostratigraphy and Geochemistry

Introduction

This chapter focuses on the biostratigraphy and revision of biozones previously recognized by Palmer (1954) as the *Aphelaspis* and post-*Aphelaspis* Zones in the Riley Formation of central Texas. The biostratigraphy is correlated to the carbon isotope signatures from early marine cements and documents a positive $\delta^{13}C$ excursion peaking at +3‰, which is recognized as the Steptoean Positive Carbon Isotope Excursion (SPICE) (e.g., Saltzman et al., 1998; Saltzman et al., 2000, Saltzman et al., 2004). The SPICE has been documented globally, including in Newfoundland and the Great Basin of North America, China, Australia, Siberia, and Kazakhstan, but has not previously been documented in central Texas.

Biostratigraphy

In Texas, Palmer (1954) recognized two faunal assemblages: the *Aphelaspis* Zone, which is identified throughout North America, and the overlying post-*Aphelaspis* Zone. In this paper, the *Aphelaspis* Zone interval is recast as a set of species-based zones (Fig. 7) that offer higher resolution correlation in central Texas. The post-*Aphelaspis* Zone is renamed the *Blandicephalus texanus* Zone, after a characteristic species. See Appendix A for taxon distribution by sections and biozones.

Coosella perplexa Zone

The *Coosella perplexa* Zone marks the lower boundary of the Steptoean Stage of Laurentian North America (Ludvigsen and Westrop, 1985) and approximates the base of the global Paibian Stage (Peng et al., 2004); it is defined by the lowest occurrence of the nominate species. A single small sample (MCNe2 3.9) includes *C.* cf. *perplexa* (Palmer, 1954), *Llanoaspis* cf. *peculiaris*, and *Coosina* cf. *ariston*.

Faunas correlative with the *C. perplexa* Zone have been recorded from the Nolichucky Formation of Tennessee (Rasetti, 1965). The zone has also been recognized in Nevada and Utah (Palmer, 1979, 1984, 1998). It marks the onset of the extinction event at the base of the Steptoean Stage (Westrop and Cuggy, 1999).

Aphelaspis spinosa Zone

In addition to *Aphelaspis spinosa* Palmer, 1954, *A.* cf. *walcotti* Resser, 1938, *Blountia mogancreekensis* sp. nov., *Cheilocephalus* cf. *granulosa* Palmer, 1965 and *Glaphyraspis parva* (Walcott, 1889) make their first appearances at the base of the zone. Only the latter species occurs outside of central Texas, and has been recorded from Wyoming (Shaw, 1956), Montana (Lochman and Hu, 1962) Tennessee (Rasetti, 1965), Nevada and Utah (Palmer, 1965) and the Mackenzie Mountains of northern Canada (Pratt, 1992). Where *G. parva* has been placed into a detailed biostratigraphic zonation, it enters the succession in association with *C. perplexa* (e.g., Rasetti, 1965; Palmer, 1979). The absence of the species from the *C. perplexa* Zone at Morgan Creek may reflect the very small sample size. Other species which occur later in the *A. spinosa* Zone include Glaphyraspis *dianae* and *G. richardi*.

Aphelaspis longifrons Zone

Aphelaspis longifrons Palmer, 1954 is a distinctive and abundant species that enters the succession near the top of the Cap Mountain Member; *A. constricta* Palmer, 1954 also occurs in the lower part of the zone, whereas *Labiostria platifrons* Palmer, 1954 occurs in a largely barren upper interval. Although neither of these species occurs outside of central Texas, the base of the zone is readily identifiable and provides a significant datum for correlation within the region.

Blandicephalus texanus Zone

Time permitted only a cursory examination of the trilobites of the Lion Mountain Member, which Palmer (1954) assigned to his post-*Aphelaspis* Fauna. New collections from Morgan Creek and Hoover Point confirm that this fauna is distinct from those of the underlying *Aphelaspis*-rich zones, and it is redefined as species-based zone marked by the first occurrence of *B. texanus*. Other species occurring in the zone include *Labiostria sigmoidalis* Palmer, 1954, *L. conveximarginata* Palmer, 1954, *L. platifrons* Palmer, 1954, *Dunderbergia* cf. *variagranula, Cheilocephalus brevilobus* Walcott, 1916 and an undescribed species related to *Dunderbergia*.

Most of the species are confined to Texas. The presence of *Dunderbergia* supports a correlation with the *Dunderbergia* Zone of Nevada and Utah (Palmer, 1965). *Cheilocephalus brevilobus* is rare and has been reported as low as the *C. perplexa* Zone.

Carbon Isotope Stratigraphy

When marine limestones are deposited, the carbon isotope ($\delta^{13}C$) composition of the surrounding water is recorded in the rock. In the case of major biotic events, like

mass extinctions, carbon isotopes may reflect this ecological change and can be used as a way to correlate time-equivalent successions at a high resolution. During the Phanerozoic, $\delta^{13}C$ values are typically 1–2‰ above the PDB (Pee Dee Belemnite) baseline of $\delta^{13}C$=0‰; short-lived increases of $\delta^{13}C$ have been correlated with times of marine invertebrate extinctions (Saltzman et al., 2000). Carbon isotope excursions occur at least once during most periods of the Paleozoic and have been interpreted to be due to isotopically light organic carbon burial as a result of increased productivity, high sedimentation rates, or burial in anoxic conditions (Saltzman et al., 2004).

The Steptoean Positive Carbon Isotope Excursion (SPICE) was coined by Saltzman et al. (1998) after carbon isotopes of middle to late Cambrian strata in the Great Basin showed a positive shift (+4‰). It is one of the earliest recorded globally distributed positive isotope excursions, having been documented in North America, China, Australia, Siberia, and Kazakhstan (Saltzman et al., 1998; Glumac and Walker, 1996; Saltzman et al., 2000; Saltzman et al., 2004; Kouchinsky et al., 2008; Gill et al., 2011). The SPICE was first recognized by Brasier (1993) in the Great Basin in the Pterocephaliid biomere (Palmer, 1984), equivalent to the Steptoean Stage (Ludvigsen and Westrop, 1985). The onset begins at the base of the *Aphelaspis* Zone and peaks in strata equivalent to the *Dunderbergia* Zone with values ranging from +1–5‰. The SPICE lasted about 3.6 million years; the increase lasting about 2.8 million years and the decrease about 0.8 million (Saltzman et al., 2004). The rising limb of the SPICE coincides with a time of sea level regression and the aftermath of the extinction at the base of the Steptoean when diversity was low. The $\delta^{13}C$ peak coincides with the Sauk II–Sauk III boundary (Palmer, 1981), a sea level lowstand (Saltzman et al., 2004).

Unlike other carbon excursions, species diversity is high during the peak of the SPICE, and faunal turnover and replacement of trilobite faunas occurs with the onset of a positive shifts in $\delta^{13}C$ (Saltzman et al., 2000). The SPICE has also been shown to occur along with a sulfate ($\delta^{34}S$) excursion of approximately +20‰ (Gill et al., 2011), supporting the notion that the SPICE was a result of ocean anoxia, upwelling, and benthic extinction. It is not documented everywhere though; carbon isotopes do not record the SPICE in Wyoming (Saltzman et al., 1998) and Vermont (Glumac and Spivak-Birndorf, 2002), likely the result of a sedimentary hiatus.

In this chapter, a carbon isotope excursion is documented from carbonate samples from the Cap Mountain Limestone and the overlying Lion Mountain Sandstone members of the Riley Formation in Burnet County, Texas. The strata were deposited during the upper Marjuman and the Steptoean stages of the late Cambrian and record the faunal turnover from the *Coosella perplexa* Zone into the *Blandicephalus texanus* Zone. The overall trend shows a modest drop of $\delta^{13}C$ by about 0.5 per mil across the base of the Steptoean followed by a recording the rising limb of the SPICE through the *Aphelaspis spinosa* Zone with peak values of $\delta^{13}C$ into the post-*Aphelaspis* Zone, reaching a peak value of +2.7–2.99 in the *A. longifrons* and *B. texanus* Zones.

Geochemical Analysis Procedure

Representative samples with freshly exposed surfaces were selected from each section analyzed in order to have decreased diagenetic (e.g., meteoric) influences. For each sample, an electric drill was used to powder carbonate from exposed calcite spar, avoiding other lithologic components (e.g., glauconite) as much as possible.

Approximately 200–300 µg of the powder was placed into a 12 mL borosilicate exetainer vial (Labco 938 W) and sealed with a butyl rubber septa cap. The samples were then placed in a thermostated sample tray heated to 50°C and flushed with ultra-high purity He (99.999%) using a ThermoGas Bench II equipped with a PAL automatic sampler flushing needle for 360 seconds to remove the air. Then, using a syringe, 0.4 mL of 100% phosphoric acid was manually injected into the vials and left to react for two hours at 50°C. Afterwards, using the PAL measurement needle, the vials were sampled and the headspace CO_2 was analyzed for $\delta^{13}C$ and $\delta^{18}O$ using a Thermo Delta V Plus isotope ratio mass spectrometer.

The carbon and oxygen isotopic compositions are expressed as (Coplen, 2011):

$$\delta^{13}C_{VPDB} = [R(^{13}C/^{12}C)_P / R(^{13}C/^{12}C)_{VPDB}] - 1$$

$$\text{and, } \delta^{18}O_{VPDB} = [R(^{18}O/^{16}O)_P / R(^{18}O/^{16}O)_{VPDB}] - 1$$

where $R(^{13}C/^{12}C)_P = N(^{13}C)_P / N(^{12}C)_P$ which is the ratio of the number of ^{13}C and ^{12}C atoms in sample P and equivalent parameters apply for Vienna Pee Dee Belemnite (VPDB), and where $R(^{18}O/^{16}O)_P = N(^{18}O)_P / N(^{16}O)_P$ which is the ratio of the number of ^{18}O and ^{16}O atoms in sample P and equivalent parameters apply for VPDB (Vienna Pee Dee Belemnite).

The $\delta^{13}C$ values are reported relative to VPDB on a scale normalized so that the $\delta^{13}C$ of N-bromosuccinimide (NBS) 18 is -5.01 per mL (Kim et al., 2015), and the $\delta^{18}O_{VPDB}$ values are reported on a scale normalized such that the $\delta^{18}O$ of Standard Light Antarctic Precipitation (SLAP) is -55.5 per mL relative to the Vienna Standard Mean Ocean Water (VSMOW). On this $\delta^{18}O_{VPDB}$ scale, the values of NBS 18 and NBS 19 are

-23.01 per mL and -2.2 per mL, respectively (Brand et al., 2014). The oxygen isotope acid fractionation factor for calcite used for 50°C is 1.00934 (Kim et al., 2015).

Carbon Isotope Results

The isotope analysis results from fifty carbonate samples from the Cap Mountain Limestone and Lion Mountain Sandstone are recorded in Table 1 and Figure 7. Samples from the six localities are distributed through approximately 21.60 meters, against which the isotope values are plotted. The $\delta^{13}C$ values follow an increasing trend from 1.08‰ at the first section analyzed at 0.90 meters (section MCNe2 0.9) to a sharp increase to 2.78‰ at 10.40 meters (section LB 2.15). Carbon isotope ratios fluctuate and continue to stay high, peaking at 2.99‰ at 13.20 meters (section HP 1.5), with two outliers that are more negative (1.54‰ at 16.75 m from MCS 2.25, and 1.73‰ at 21.15 m from MCN 6.65). Oxygen isotopes fluctuate between approximately -6 to -8‰ from the basal unit until meter 13.8 (section HP 2.1) where fluctuations increase up to about -4.5‰

SPICE in Central Texas

The carbon isotopes documented in Texas follows the trend expected during the SPICE. The rise of the SPICE begins at a global extinction interval at the base of the *Glyptagnostus reticulatus* Zone (Saltzman et al., 2000). In Texas, the rising limb of the $\delta^{13}C$ (Fig. 7) begins in the *Coosella perplexa* Zone and increases during a time of diversification of *Aphelaspis* species, along with the entry of holdover genera from the Marjuman (*Blountia*; *Glaphyraspis*). The $\delta^{13}C$ values reach maximum values near the

base of the *A. longifrons* Zone, which is near the base of the Lion Mountain Sandstone during sea level regression and remain elevated through the sampled extent of the *Blandicephalus texanus* Zone.

Comparison of the carbon isotope data in Texas shows a similar trend to the data in the Great Basin (fig. 8) and in Newfoundland (fig. 9), with a rising limb beginning towards the base of the Steptoean and reaching maximum $\delta^{13}C$ in the *Dunderbergia* Zone and Texas-equivalent *Blandicephalus texanus* Zone. The Great Basin records higher $\delta^{13}C$ values, peaking around +4–5‰ (fig. 8). In Texas, the sections analyzed recorded a maximum $\delta^{13}C$ value of 2.99‰ which is comparable to the values recorded in Newfoundland that peaked at +2.20‰ (fig. 9); Saltzman et al. (2004) suggested the lower $\delta^{13}C$ values in Newfoundland could be the result of local conditions influencing the carbon signature. The late Cambrian rocks in Newfoundland were deposited in shallow waters, much like the deposits of the Riley Formation, and similar local influences may have caused a lower carbon isotope signature in central Texas. In both the Great Basin and Newfoundland, carbon isotope data continues through the *Elvinia* Zone where the $\delta^{13}C$ signature begins to decrease to pre-SPICE levels. Isotope data during this interval is unobtainable in Texas due to the disconformity between the Riley Formation and overlying Wilberns Formation,

Perfetta et al. (1999) documented a slight negative excursion just before the SPICE in South Dakota and interpreted it to the result of a shift of a thermocline onto the shelf or ocean turnover. The data in Texas may also reflect this excursion at 10.25 meters where the $\delta^{13}C$ decreases before the first large positive pulse; however, there is

no direct sedimentary evidence for cooling or anoxia in shallow water carbonates of the Cap Mountain Member to support this.

The faunal turnover and carbon isotopes trend associated with the SPICE has been interpreted as the result of cold, dysoxic waters upwelling onto shelves (Perfetta et al., 1999; Gill et al., 2011), but as noted above independent sedimentary evidence for this (e.g., black shale) is lacking. Kump et al. (1999) suggested the positive carbon isotope excursion at the end of the Ordovician was due to increased carbonate weathering as glaciation decreased rates of clastic weathering and lowering sea levels exposed more carbonate. Due to the lack of ice sheets during the late Cambrian, this mechanism would not applicable to the SPICE. Saltzman et al. (2004) favored a mechanism that increased carbonate and terrestrial weathering during falling sea levels, which would have increased sedimentary influx and carbon burial in the ocean, caused the increased $\delta^{13}C$ signature in the seawater. The high percentage of mature quartz sand in the Riley Formation introduced from terrestrial sources and channels (King and Chafetz, 1983), is consistent with this explanation. The SPICE may not be the result of a sole mechanism, but rather an orchestration of several contributing factors. The modest negative excursion before the onset of the $\delta^{13}C$ peak documented in Texas could be the result of upwelling of cold, anoxic deep waters (Perfetta et al., 1999), but there is no change in facies to support this.

Diagenesis

Modern limestones are isotopically heterogenous and it has been suggested that early, low temperature diagenesis may cause averaging of the original isotope

components (Saltzman et al., 1998). Isotopes can be influenced over time from later diagenesis; for example, meteoric waters and terrestrial soils can introduce more negative $\delta^{13}C$ values, so analysis of carbonates deposited in open ocean with little meteoric influence is more ideal (Saltzman and Thomas, 2011). The Cap Mountain Limestone formed on a shallow shelf with influx of clastic sediments and the Lion Mountain Sandstone was deposited during marine regression with increased quartz sand influx from the craton interior. Understanding the diagenetic history of these units help support the accuracy of the isotope values recorded in the carbonate.

Thin sections were made from ten of the horizons analyzed for isotopes, five from the Cap Mountain Limestone (MCNe2 0.90, MCNe1 5.80–5.90, MCNe1 6.90, LB -0.15, LB 2.15) and five from the Lion Mountain Sandstone (MCS 1.80, MCS 6.65, MCN 0.25, MCN 2.00, MCN 4.50). Most of the samples chosen lie along the general trend $\delta^{13}C$ values, although some outliers in $\delta^{13}C$ were included to check for any diagenetic differences. Thin sections polished to 30 μm were viewed with a petrographic microscope in plain, polarized, and reflective light. Alizarin Red dye was used on one section to distinguish dolomite from calcite. Overall, the diagenetic composition of the sections was dominantly calcite spar cement with minimal alteration and variable amounts of quartz grains, glauconite grains with iron oxide replacement, and fossil debris. Sections with outlying $\delta^{13}C$ values did not have any clear differences in composition or diagenesis. The spar cements formed early and appear to have undergone minimal diagenesis, suggesting that the original isotope signature would be retained (McBride, 1988).

Petrographic Description

The Cap Mountain Limestone is a bioclastic grainstone and has sparry calcite cement that is isopachous forming around allochems, particularly trilobite sclerites (Fig. 10, images 3–4). Grains vary from approximately 5–40% of the composition, consisting of subrounded, moderately-sorted quartz, glauconite, and sparse microcline grains (compare Fig. 10, images 1 and 3). Glauconite is present mostly amongst quartz grains and is sometimes melded together (Fig. 10, image 1). Many glauconite grains have opaque iron oxide rims or are partially to completely replaced by iron oxide. The two opaque minerals identified under reflective light are hematite with its reddish hue and a fully opaque mineral, likely goethite or its hydrous form, limonite (Barnes and Bell, 1977; McBride, 1988). Iron oxide has also replaced small amounts of the calcite matrix. Small quartz overgrowths are present but not common, some having formed after iron oxide coated the quartz grain. The edges of many quartz grains are being consumed by the matrix. Lower samples (MCNe2 0.9) preserve dolomite rhombohedrons (Fig. 10, images 5–6), often present alongside iron oxide mineral. Well-rounded micrite intraclasts are present, but not common. Trilobite sclerites are the most abundant fossil allochems, and are mostly unaltered, displaying the characteristic sweeping extinction; some sclerites have been replaced by cement and retain a ghost outline with the isopachous calcite rim still present. Linguliform brachiopods (Fig. 10, image 1–2) are also common and most preserve the original phosphatic composition, but some are partly replaced by calcite. Echinoderm fragments are not as common and most are replaced by the matrix, and sponge spicules are rare. There are a few occurrences of

iron oxide-filled microstyolites and calcite veins cutting through the rock, as well as some quartz and glauconite grains having fractures filled in with calcite.

The Lion Mountain Sandstone is a bioclastic grainstone with similar components and diagenetic alterations as the underlying Cap Mountain Sandstone, but in different abundances and degrees. It can be separated into a greensand facies, the host rock, and a carbonate facies, from the carbonate lenses. Sparry calcite cement, fossil fragments including trilobites, linguliform brachiopods, and echinoderm debris (Fig. 11, images 1–2) are present in both facies; fossils tend to be more broken in the greensand compared to the carbonate facies. Well-rounded, moderately-sorted, coarser quartz and glauconite grains are very abundant in the greensand facies (60–90%) (Fig. 11, images 3–4). The amount of these grains in the carbonate facies is comparable to that in the Cap Mountain Limestone (10–40%) (Fig. 11, image 5–6). More of the iron oxide minerals have a red hue in the Lion Mountain Sandstone, suggesting more hematite than limonite or goethite. The occurrence of the iron oxide minerals is in association with glauconite, so is typically more abundant, and forms rim around and replaces more allochems than in the Cap Mountain Limestone Fig. 11, image 1–2). Microstyolites are present throughout, often filled with iron oxide.

Discussion

Stylolites in outcrop and microstylolites in thin sections are the result of compaction and pressure solution and are often filled with iron oxide. In hand sample, small dendritic precipitation of dark mineral are present, likely iron oxide or manganese oxide, a result of mineral-rich fluids passing through. Iron oxide and glauconite are

often co-occurring because glauconite forms iron oxide by releasing potassium and releasing and/or oxidizing iron (McRae, 1972). Iron oxide also coats non-glauconitic grains and replaces cement, and so the introduction of iron oxide appears to have occurred later in the diagenetic history relative to the genesis of glauconite and cement formation.

Glauconite formation is poorly understood, but a widely accepted model proposed by Odin and Matter (1981) suggests glauconite precipitation occurs in micropores (5–10 μm) while simultaneously dissolving the host mineral, then later undergoes further diagenesis and maturation (Chafetz, 2000). Potassium and iron are important ions for glauconite to form, and the decomposition of organic material can provide an ideal environment for its formation (McRae, 1972). Host material providing means for glauconite formation in the Riley Formation would have included quartz, feldspar (if originally abundant), calcite, and degradation of skeletal grains (e.g., echinoderms).

Modern glauconite has been reported in marine depths greater than 50 meters and with increasing abundance with depth. It has also been suggested to form during slow sedimentation rates (Chafetz and Reid, 2000). Marine transgression events in the rock record are usually associated with glauconite since rising sea levels are accompanied by low sedimentation rates and organic matter from terrestrial soils can provide ideal conditions (McRae, 1972). The presence of abundant glauconite in the Riley Formation appears to be anomalous. In the Cambrian, since life had yet to establish on land, marine life in the photic zone may have been a sufficient source of organics, but the Lion Mountain Sandstone, which is the glauconite-rich unit, deviates

from these hypotheses because it deposited during a marine regression with a high influx of quartz sand and in a high energy environment, supported by cross-beds. A lack of nearby deep-water deposits in central Texas supports that the glauconite in the shallow water deposits of the Riley Formation is autochthonous and did not formed in a deeper marine setting, in addition to the glauconite grains lacking abrasion that would be expected to occur during transport (Chafetz and Reid, 2000).

The glauconite in both units occurs as ovate and deformed grains that are often melded together due to presumed compaction. The undeformed glauconite as well as unfragmented fossil pieces are surrounded by isopachous and blocky spar calcite, suggesting that some of the cement formed prior to compaction, adding support to grains. McBride (1988) suggested that the cement in the carbonate lenses of the Lion Mountain Sandstone deposited early, forming at or close to the seafloor, in contact with the seawater, based on the cement forming off unbroken fossils and extending towards the glauconitic host rock. The host rock has more broken shell fragments, indicating that there was compaction from burial before cementation occurred. The ubiquitous isopachous cement that rims allochems throughout both members offers support for the hypothesis of early marine diagenesis. McBride also reported carbon and oxygen isotope values from the different components (lenses, rinds, host rock, trilobite sclerites) of the Lion Mountain Sandstone that showed consistent values, suggesting the components formed from waters with uniform composition. McBride suggested that maximum burial of the units occurred by the end of the Ordovician, compacting the glauconite grains during this time. The diagenesis of the rocks in the Cap Mountain

Limestone and Lion Mountain Sandstone appear to be early and likely record the original isotope composition.

References

Brand, W.A., Coplen, T.B., Vogl, J., Rosner, M. and Prohaska, T., 2014, Assessment of international reference materials for isotope-ratio analysis (IUPAC technical report): Pure and applied Chem, v. 86, p. 425–467, doi: 10.1515/pac-2013-1023.

Chafetz, H.S., and Reid, A., 2000, Syndepositional Shallow-Water Precipitation of Glauconitic Minerals: Sedimentary Geology, v. 136, p. 29–42, doi: 10.1016/S0037-0738(00)00082-8.

Coplen, T.B., 2011, Guidelines and recommended terms for expression of stable-isotope-ratio and gas-ratio measurement results. Rapid Communications in Mass Spectrometry, v. 25, p. 2538-2560, doi: 10.1002/rcm.5129.

Kim S.T., Coplen T.B., and Horita, J., 2015, Normalization of stable isotope data for carbonate minerals: Implementation of IUPAC guidelines: Geochim.et Cosmochimic Acta, v. 158, p. 276–289, doi: 10.1016/j.gca.2015.02.011.

Gill, B.C., Lyons, T.W., Young, S.A., Kump, L.R., Knoll, A.H., and Saltzman, M.R., 2011, Geochemical evidence for widespread euxinia in the Later Cambrian ocean: Nature, v. 469, p. 80–83, doi: 10.1038/nature09700.

Glumac, B., and Spivak-Birndorf, M.L., 2002, Stable isotopes of carbon as an invaluable stratigraphic tool: An example from the Cambrian of the northern Appalachians, USA: Geology, v. 30, p. 563–566, doi: 10.1130/0091-7613(2002)030<0563:siocaa>2.0.co;2.

Kump, L.R., Arthur, M.A., Patzkowsky, M.E., Gibbs, M.T., Pinkus, D.S., and Sheehan, P.M., 1999, A weathering hypothesis for glaciation at high atmospheric pCO2 during the Late Ordovician: Palaeogeography, Palaeoclimatology, Palaeoecology, v. 152, p. 173–187, doi: 10.1016/S0009-2541(99)00086-8.

Ludvigsen, R., and Westrop, S.R., 1985, Three new Upper Cambrian stages for North America: Geology, v. 13, p. 139–143, doi: 10.1130/0091-7613(1985)13<139:tnucsf>2.0.CO;2.

McBride, E.F., 1988, Contrasting diagenetic histories of concretions and host rock, Lion Mountain Sandstone (Cambrian), Texas: Geological Society of America Bulletin, v. 100, p. 1803–1810, doi: 10.1130/0016-7606(1988)100<1803:cdhoca>2.3.CO;2.

McRae, S.G., 1972, Glauconite: Earth-Science Reviews, v. 8, p. 397–440, doi: 10.1016/0012-8252(72)90063-3.

Odin, G.S. and Matter, A., 1981, De glauconiarum origine: Sedimentology, v. 28, p. 611–641, doi: 10.1111/j.1365-3091.1981.tb01925.x.

Öpik, A.A., 1966, The early Upper Cambrian crisis and its correlation: Journal and Proceedings of the Royal Society of New South Wales, v. 100, p. 9–14

Palmer, A.R., 1965, Trilobites of the late Cambrian Pterocephaliid biomere in the Great Basin, United States: U.S. Geological Survey Professional Papers, no. 493.

Perfetta, P.J., Shelton, K.L., and Stitt, J.H., 1999, Carbon isotope evidence for deep-water invasion at the Marjumiid-Pterocephaliid biomere boundary, Black Hills, USA: A common origin for biotic crises on Late Cambrian shelves: Geology, v. 27, p. 403–406, doi: 10.1130/0091-7613(1999)027<0403:ciefdw>2.3.CO;2.

Saltzman, M.R., Runnegar, B., and Lohmann, K.C., 1998, Carbon isotope stratigraphy of Upper Cambrian (Steptoean Stage) sequences of the eastern Great Basin: Record of a global oceanographic event: Geological Society of America Bulletin, v. 110, p. 285–297, doi: 10.1130/0016-7606(1998)110<0285:CISOUC>2.3.CO;2.

Saltzman, M.R., Ripperdan, R.L., Brasier, M.D., Lohmann, K.C., Robison, R.A., Chang, W.T., Peng, S., Ergaliev, E.K., and Runnegar, B., 2000, A global carbon isotope excursion (SPICE) during the Late Cambrian: relation to trilobite extinctions, organic-matter burial and sea level: Palaeogeography, Palaeoclimatology, Palaeoecology, v. 162, p. 211–223, doi: 10.1016/S0031-0182(00)00128-0.

Saltzman, M.R., Cowan, C.A., Runkel, A.C., Runnegar, B., Stewart, M.C., and Palmer, A.R., 2004, The Late Cambrian SPICE ($\delta^{13}C$) event and the Sauk II–Sauk III regression: new evidence from Laurentian basins in Utah, Iowa, and Newfoundland: Journal of Sedimentary Research, v. 74, p 366–377, doi: 10.1306/120203740366.

Saltzman, M., and Thomas, E., 2012, Carbon Isotope Stratigraphy: The Geologic Time Scale, p. 207–232, doi: 10.1016/b978-0-444-59425-9.00011-1.

Scholle, P.A., and Ulmer-Scholle, D.S., 2003, A Color Guide to the Petrography of Carbonate Rocks: Grains, Textures, Porosity, Diagenesis: Tulsa, Oklahoma, AAPG Memoir 77, 459 p. doi: 10.1306/M77973.

Walcott, C.D., 1916, The Cambrian Fauna of Eastern Asia: Washington D.C., The Smithsonian Institution, The Smithsonian Miscellaneous Collections, v. 3.

Table 1: Carbon ($\delta^{13}C$) and oxygen ($\delta^{18}O$) isotope values in each section analyzed from the Riley Formation, Burnet County, Texas. Projected composite section in meters.

m	section	$\delta^{13}C_{VPDB\text{-}LSVEC}$	$\delta^{18}O_{VPDB}$
21.60	MCN 4.50	2.34	-6.24
21.15	MCS 6.65	1.73	-6.78
20.05	MCN 2.90	2.33	-7.72
19.75	MCN 2.60	2.2	-6.1
19.15	MCN 2.00	2.61	-6.2
19.00	MCS 4.50	2.21	-6.8
18.55	MCN 1.40	2.3	-5.32
18.25	MCN 1.10	2.6	-6.03
17.9	MCS 3.40	2.45	-6.13
17.85	MCN 0.70	2.42	-5.59
17.70	MCS 3.20	2.29	-7.75
17.40	MCN 0.25	2.7	-6.62
16.95	HP 5.25	2.65	-6.28
16.75	MCS 2.25	1.54	-6.73
16.30	MCS 1.80	2.37	-7.57
16.20	HP 4.50	2.88	-5.91
16.00	MCS 1.50	2.38	-6.65
15.50	MCS 1.00	2.43	-7.64
15.50	HP 3.80	2.67	-5.85
15.15	HP 3.45	2.65	-5.4
14.80	MCS 0.30	2.57	-6.7
14.80	HP 3.10	2.22	-4.41
14.55	HP 2.85	2.19	-5.08
13.80	HP 2.10	2.55	-4.81
13.45	LB 5.25	2.2	-6.62
13.20	HP 1.50	2.99	-7
12.85	HP 1.15	2.94	-6.2
12.70	LB 4.45	2.27	-6.67
12.70	HP 1.00	2.49	-6.92
12.20	LB 4.00	2.39	-6.66
11.60	LB 3.40	1.9	-7.51
10.95	MCNe1 8.10	2.25	-7.29
10.95	LB 2.70	2.3	-7.51
10.40	LB 2.15	2.78	-6.21
10.25	MCNe1 7.40	2.12	-7.96
10.20	HP 2.50 Pulloff	2.39	-7.01
10.10	HP 2.60 Pulloff	2.28	-6.28
9.75	MCNe1 6.90	2.33	-7.4
9.65	LB 1.40	2.03	-7.42
9.15	LB 0.90–1.00	1.93	-7.74
8.65	MCNe1 5.80–5.90	1.61	-7.56
8.55	LB 0.30	1.68	-7.52

m	section	$\delta^{13}C_{VPDB\text{-}LSVEC}$	$\delta^{18}O_{VPDB}$
8.10	LB -0.15	1.71	-7.63
6.30	MCNe2 6.30	0.98	-7.62
5.40	MCNe2 5.40	1.13	-6.34
4.95	MCNe1 2.10	1.28	-7.26
3.90	MCNe2 3.90	0.83	-6.52
2.85	MCNe2 2.85	1.24	-7.31
2.15	MCNe2.15	1.16	-7.35
0.90	MCNe2 0.90	1.08	-7.02

Figure 7: Stratigraphic carbon isotope ($\delta^{13}C$) data for the Cap Mountain and Lion Mountain members of the Riley Formation, Burnet County, Texas. Isotope data are differentiated by localities (closed circles are MCNe2; hexagrams are MCNe1, plus signs are LB; stars are HP; triangles are MCS; and open circles are MCN). The biostratigraphic ranges of the species documented at the localities is to scale with the isotope graph and the species-based biozones are indicated.

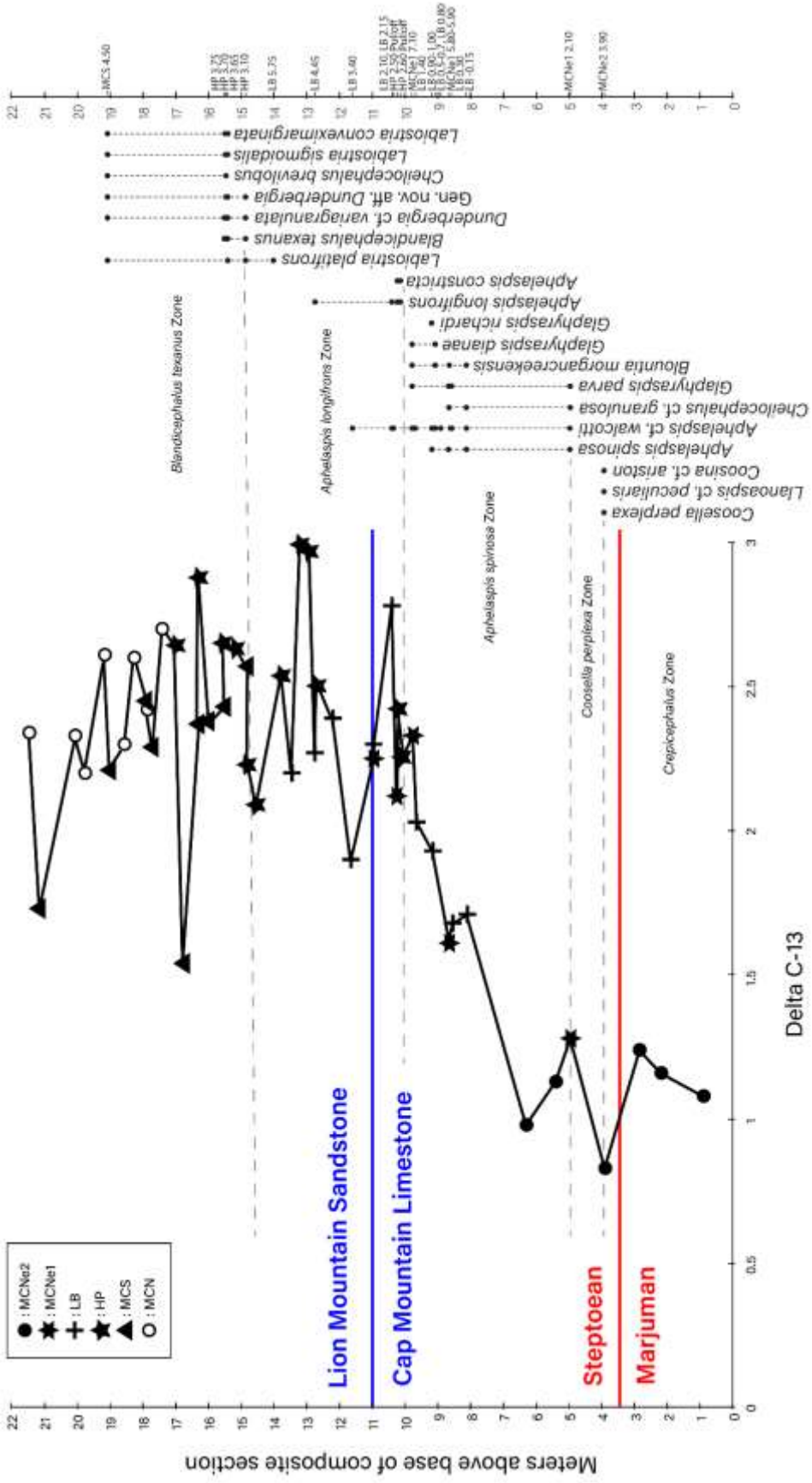
Meters above base of composite section
Delta C-13
Lion Mountain Sandstone
Cap Mountain Limestone
Steptoean
Marjuman
Blandicephalus texanus Zone
Aphelaspis longifrons Zone
Aphelaspis spinosa Zone
Cossella perplexa Zone
Crepicephalus Zone
Labiostria platirons
Blandicephalus texanus
Dunderbergia cf. variagranulata
Gen. nov. aff. Dunderbergia
Cheilocephalus brevilobus
Labiostria sigmoidalis
Labiostria convexima rginata
Glaphyraspis richardi
Glaphyraspis dianae
Blountia morgancreekensis
Glaphyraspis parva
Cheilocephalus cf. granulosa
Aphelaspis cf. walcotti
Aphelaspis spinosa
Cossina cf. ariston
Llanoaspis cf. peculiaris
Cossella perplexa
: MCNa2
: MCNe1
: LB
: HP
: MCS
: MCN

Figure 8: Carbon isotope ratios ($\delta^{13}C$) recording the SPICE in the Riley Formation of central Texas compared to the carbon isotopes in Nevada and Utah (modified from Saltzman et al., 1998, fig. 3). The *Aphelaspis* Zone in the Great Basin and equivalent *Aphelaspis spinosa* and *Aphelaspis longifrons* Zones in Texas are outline in red, and the *Dunderbergia* Zone in the Great Basin and equivalent *Blandicephalus texanus* Zone in Texas are outlined in blue. Scale in Texas is in meters.

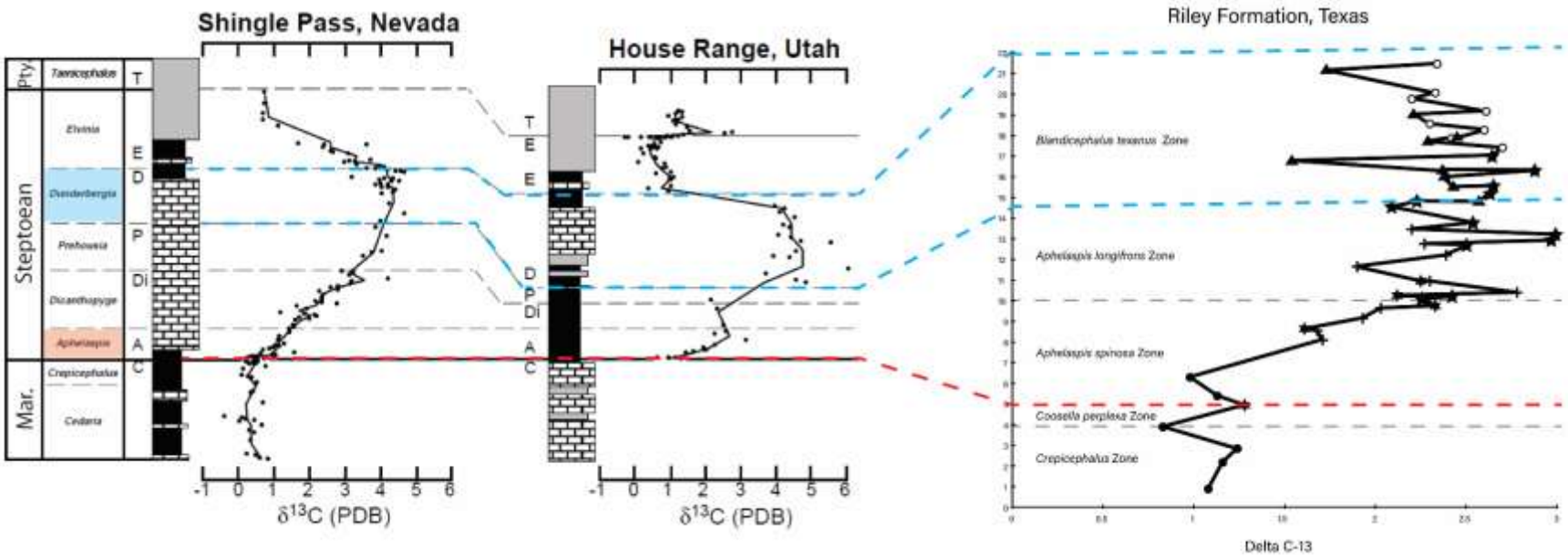
Shingle Pass, Nevada
House Range, Utah
Riley Formation, Texas
Pty
Mar.
Steptoean
Taenicephalus
Elvinia
Dunderbergia
Prehousia
Dicanthopyge
Aphelaspis
Crepicephalus
Cedaria
T
E
D
P
Di
A
C
-1 0 1 2 3 4 5 6
δ13C (PDB)
Blandicephalus texanus Zone
Aphelaspis longifrons Zone
Aphelaspis spinosa Zone
Coosella perplexa Zone
Crepicephalus Zone
Delta C-13

Figure 9: Carbon isotope ratios ($\delta^{13}C$) recording the SPICE in the Riley Formation compared to data in Newfoundland (modified from Saltzman et al., 2004, fig. 6). The *Aphelaspis* Zone in Newfoundland and equivalent *Aphelaspis spinosa* and *Aphelaspis longifrons* Zones in Texas are outline in red, and the *Dunderbergia* Zone in Newfoundland and equivalent *Blandicephalus texanus* Zone in Texas are outlined in blue. Scale in Texas is in meters.

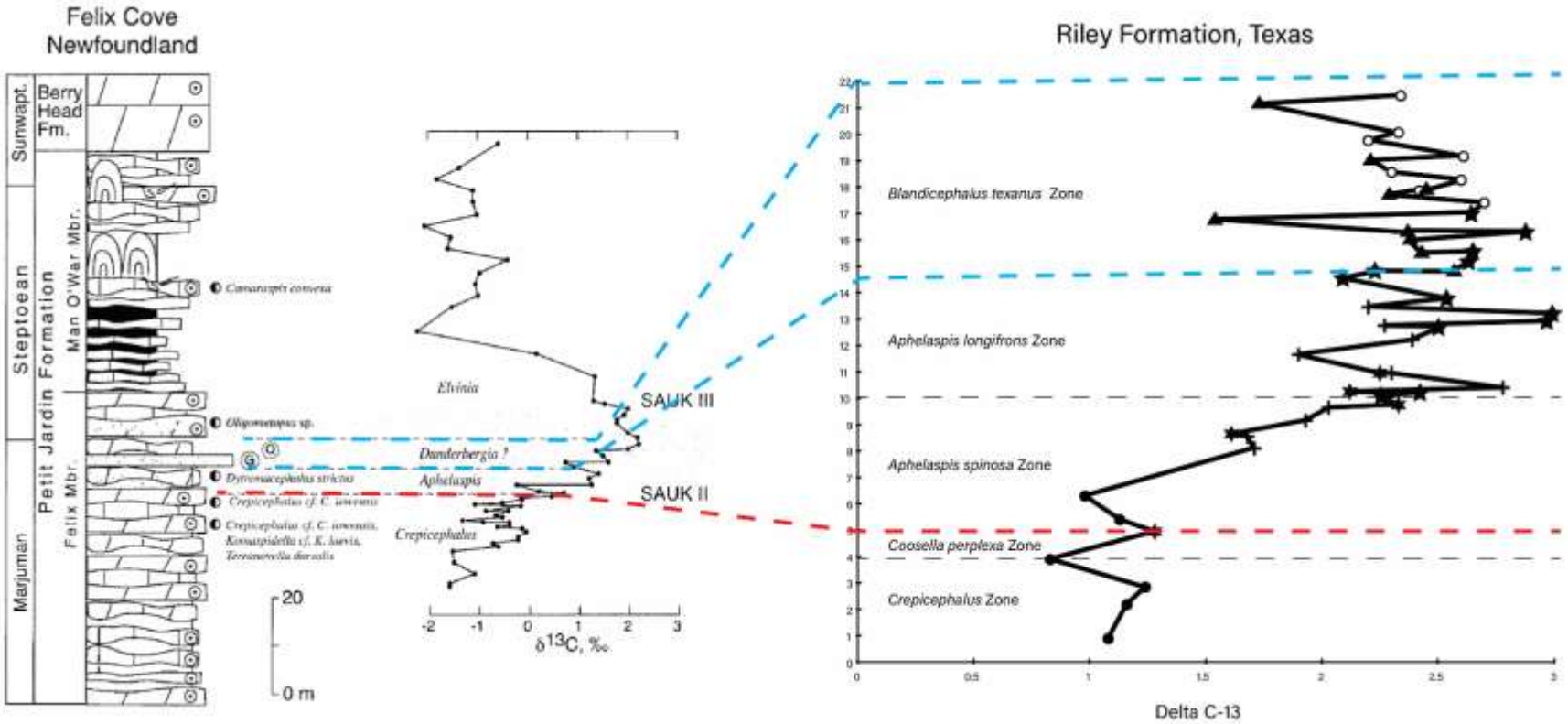
Felix Cove
Newfoundland
Sunwapt.
Steptoean
Marjuman
Berry Head Fm.
Petit Jardin Formation
Man O'War Mbr.
Felix Mbr.
Camaraspis convexa
Oligometopus sp.
Dunderbergia ?
Dytremacephalus stricta
Aphelaspis
Crepicephalus cf. C. iowensis
Crepicephalus cf. C. iowensis, Komaspidella cf. K. laevis, Terranovella dorsalis
Crepicephalus
Elvinia
20
0 m
SAUK III
SAUK II
-2 -1 0 1 2 3
δ13C, ‰
Riley Formation, Texas
Blandicephalus texanus Zone
Aphelaspis longifrons Zone
Aphelaspis spinosa Zone
Coosella perplexa Zone
Crepicephalus Zone
0 0.5 1 1.5 2 2.5 3
Delta C-13

Figure 10: Thin section images of limestone from the Cap Mountain member of the Riley Formation, Burnet County, Texas.

1: Plain polarized light. Quartz grains (Q). Some glauconite (G) is alternating to iron oxide (IO). Phosphatic brachiopod fragments (B). Calcite spar cement (C). Trilobite (T) sclerite fragments. (LB -0.15)

2: Cross polarized light. Same as image 1.

3: Plain polarized light. Trilobite sclerite fragments (T) throughout. Isopachous calcite cement dominating. (MCNe1 6.90)

4: Cross polarized light. Same as image 3; arrowing pointing out isopachous cement radiating off trilobite sclerite (T).

5: Cross polarized light. Calcite spar (C) dominating. Dolomite (D) rhombohedrons present. Some glauconite (G). (MCNe2 0.90)

6: Cross polarized light. Same as image 5.

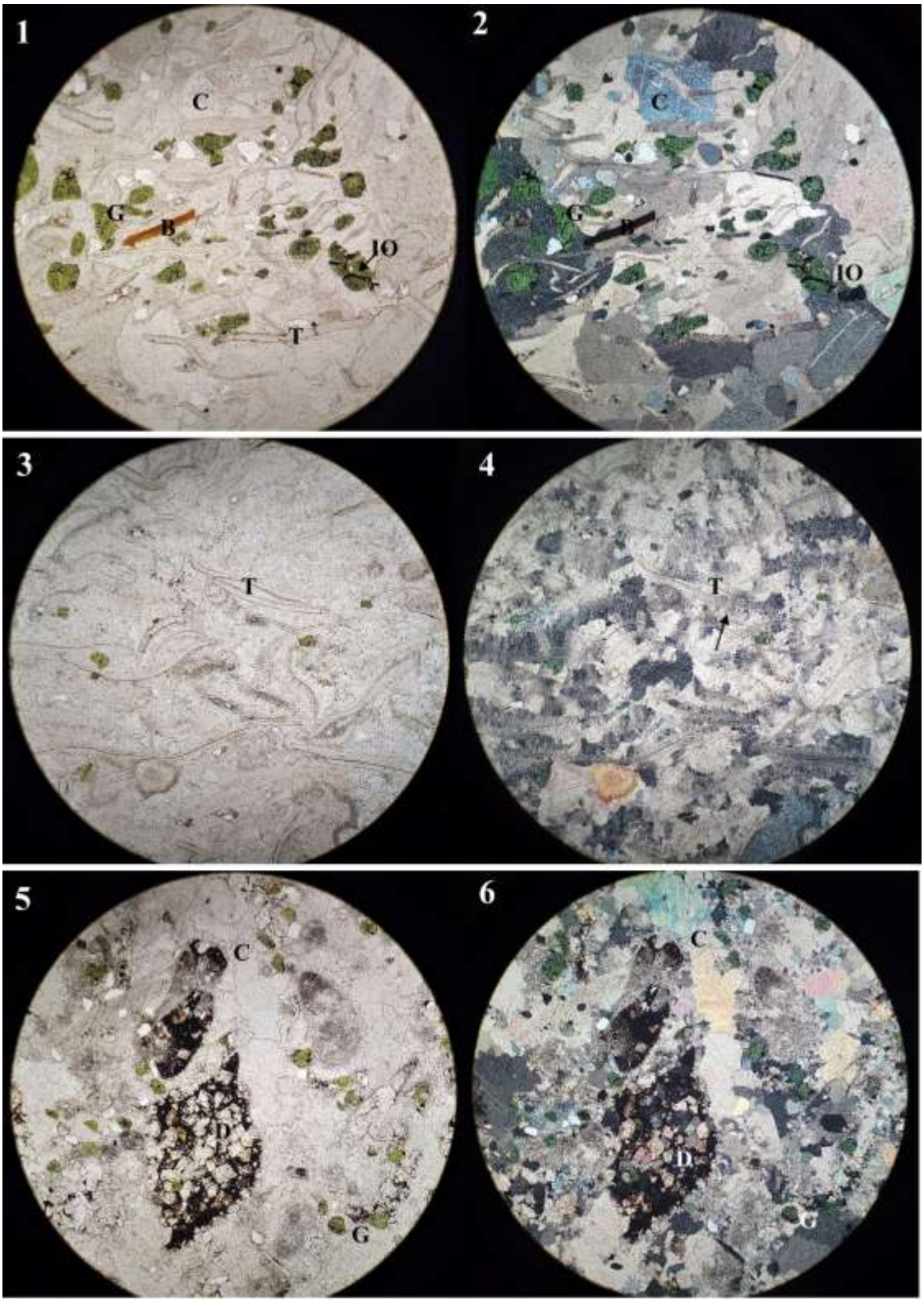
1
C
G
B
IO
T
2
C
G
IO
3
T
4
T
5
C
D
G
6
C
D
G

Figure 11: Thin section images of the Lion Mountain Sandstone member of the Riley Formation in Burnet County, Texas.

1: Plain polarized light. Glauconite (G) and quartz grains (Q). Echinoderm (E) debris replaced by iron-oxide (IR). Phosphatic brachiopod (B) fragments. Calcite spar cement. (MCS 1.80)

2: Cross polarized light. Same as image 1.

3: Plain polarized light. Glauconite (G) grains melded together, some with alteration to iron oxide (IO). Quartz grains (Q). (MCN 2.00)

4: Cross polarized light. Same as image 3.

5: Plain polarized light. Trilobite (T) sclerites with isopachous calcite cement radiating off. (MCN 4.50)

6: Cross polarized light. Same as image 5.

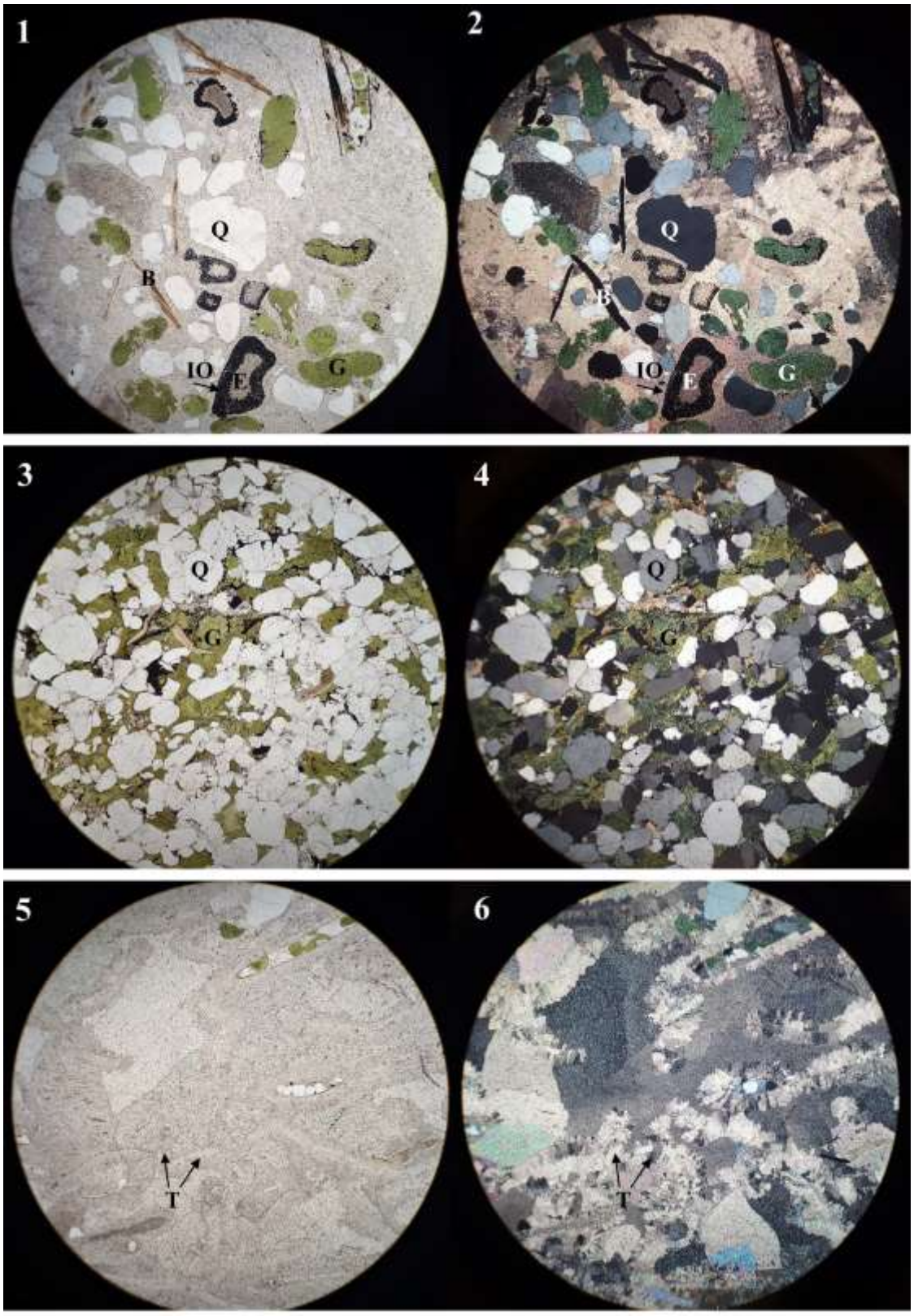
1
Q
B
IO
E
G
2
Q
B
IO
E
G
3
Q
G
4
Q
G
5
T
6
T

Chapter III: Systematics of Genus *Blountia* and Relatives

Introduction

The late Cambrian kingstoniid trilobite *Blountia* Walcott, 1916 is of interest because it is among the few Laurentian shelf genera that survive, albeit briefly, the extinction at the end of Marjuman Stage (Guzhangian Stage of global nomenclature). The most recent revisions of the surviving Steptoean members, now more than 50 years old (Palmer, 1965; Rasetti, 1965), recognized no more than two species, *B. mimula* Walcott, 1916 and *B. bristolensis* Resser, 1938. However, new material from Texas and Newfoundland indicates more diversity is present among these survivors, and the genus may record a geographically structured species group perhaps similar to those reported from other Cambrian extinction intervals (Westrop and Adrain, 2007). This chapter revises selected species of *Blountia* and related genera from the uppermost Marjuman (*Crepicephalus* Zone) and lower Steptoean (*Aphelaspis* Zone) and describes new ones from Texas and Newfoundland. A preliminary phylogenetic analysis is used to explore the relationships between species of *Blountia* and the related genera, *Maryvillia* Walcott, 1916 and *Blountina* Lochman, in Lochman and Duncan, 1944.

Localities and Stratigraphic Setting

Texas.—Palmer (1954, pl. 79 fig. 4) illustrated a single cranidium (pl. 24, fig. E–G) from an archival collection made by E.O. Urlich and colleagues from the Cap Mountain Member of the Riley Formation, two miles southeast of the mouth of Fall Creek, 27.3

km northwest of Burnet, Burnet County, central Texas (Palmer, 1954, p. 782). Resser (1942) assigned this specimen to *Maryvillia hybrida* (see Palmer, 1954, p. 722 for discussion) but Palmer identified it as *Blountia bristolensis*. However numerous sclerites from a new collection shows that it belongs to a new species, *Blountia morgancreekensis* sp. nov. This new collection is from Palmer's (1954, p. 781) Morgan Creek section on the north bank of the south fork of Morgan Creek, Burnet County, Texas. We measured and logged the section, which is now overgrown in places, in segments beginning at the water line in Morgan Creek, and ending at the limit of accessible exposures in the road cut of Ranch Road 2341 above the creek. The new collection (MCNe1 7.4) is from the Cap Mountain Member, 5.3 m above the lowest occurrence of *Aphelaspis spinosa*, and no more than about 6.5 m above the base of the Steptoean Stage. The lower boundary of the Cap Mountain is not exposed at Morgan Creek, and the upper boundary interval with the overlying Lion Mountain Member is covered. Correlation with a second section in a road cut about 0.8 km to the west that does expose the upper boundary indicates that collection MCNe1 7.4 is located less than a meter (about 0.7 m) below the base of the Lion Mountain Member. *Blountia morgancreekensis* is also present but less abundant in three other collections, MCNe1 2.1, LB -0.15, and LB 0.8.

Tennessee and Virginia.— Walcott (1916) reported new several species from Tennessee, including the type species, *B. mimula*, as occurring in the Maryville Limestone. Resser (1938, pp. 12, 14), noted that this formation name was commonly used in error in early studies, and subsequent work by Rasetti (1965) showed that Walcott's species are in fact from the Nolichucky Formation or the overlying

Maynardville Limestone. The holotype and paratypes of *B. mimula* are from USNM localities 120 and 107c (Walcott, 1916, p. 444), respectively. According to Rasetti (1965, p. 16), locality 120 is at Shields Ridge, Jefferson County, and Walcott's collection is a mixture of material from the *Crepicephalus* and *Aphelaspis* zones. Sclerites illustrated and identified as *B. mimula* by Rasetti (1965; pl. 2) are from the *Aphelaspis* Zone at his Hurricane Hollow section in Union County, but they almost certainly represent a distinct species (= *B. angela*). As such, the stratigraphic position of Walcott's types is uncertain.

The type material of *Blountia bristolensis* Resser, 1938 (pl. 5–7) is from the Nolichucky Formation at a reservoir on Mumpower Creek, 5.6 km north of Bristol, Virginia (USNM locality 36v; Resser, 1938, p. 65). Rasetti (1965, pl. 11. figs. 9–12) illustrated sclerites of this species from Russell Gap, Jefferson County, which is on the flanks of Shields Ridge. Here, it occurs in the upper 3.35 m of a massive limestone unit (collections cno/14, cnp/14, cnq/14; Rasetti, 1965, p. 17) in association with *Coosella perplexa* (Palmer, 1954), *Cheilocephalus brevilobus* (Walcott, 1916), *Glaphyraspis parva* (Walcott, 1889), *Aphelaspis* and *Tricrepicephalus* in the lowest collection, and with *A. minor* (Rasetti, 1965), *C. brevilobus* and *G. ornata* (Lochman, 1938) in the highest. This places *B. bristolensis* in the lowermost Steptoean. Rasetti also illustrated a nearly complete exoskeleton (pl. 5, figs. A–E) from a horizon at the top of a 5.5 m thick (18 feet) massive limestone unit (collection cnp/17; Rasetti, 1965, p. 20) that forms the base of his Hurricane Hollow section in Union County. The collection also includes *Aphelaspis transversa* Rasetti, 1965 and *C. brevilobus* and is about 1.5 m (5 feet) above a Marjuman (*Crepicephalus* Zone) collection with indeterminate species of *Coosia*,

Crepicephalus and *Tricrepicephalus*. *Blountia mimula* sensu Rasetti (= *B. angela* sp. nov.) (pl. 2) occurs about 11 m above *B. bristolensis* at Hurricane Hollow (collection cnr'/17; Rasetti, 1965, p. 20).

Rasetti (1965) reported *B. montanensis* Duncan, in Lochman and Duncan, 1944 from the Marjuman (Crepicephalus Zone) of the Nolichucky Formation, which were borrowed for study (pl. 12–13) as they are distinct from type material from Montana (pl. 11). They likely represent a new species, which occurs in the *Crepicephalus* Zone of the lower Nolichucky Formation, 1.6 miles east of Rogersville (collections cnk/1, cnm/2; Rasetti, 1965, p. 9), at the Big Creek section (collection cnn/1; Rasetti, 1965, p. 5) and at Crocket Creek (collection cnn/3; Rasetti, 1965, p. 9).

Montana.—The Pilgrim Formation of Montana spans the Marjuman–Steptoean boundary and includes several species of *Blountia* and related taxa (Lochman and Duncan, 1944). The original photographs of these species are so small that they are entirely unsuitable as coding sources for phylogenetic analysis, but we were able to borrow types from the U.S.N.M., and they are reillustrated and revised in this paper. *Blountia cora* Lochman, *Blountia janei* Lochman, *Blountina eleanora* Lochman and *Blountina triangularis* Lochman were collected from the Half Moon Pass section in the Big Snowy Mountains, although the detailed stratigraphic context of the samples (Lochman and Duncan, 1944, p. 20) is poorly documented and they cannot be placed in Deiss' (1936) measured section with any confidence. *Blountia montanensis* Duncan was collected from the Dry Wolf Creek section of Little Belt Mountains, where it co-occurs with *Blountina eleanora* and *Blountina triangularis* and species of *Crepicephalus* at Lochman horizons 4.5 and 4.5a, and Deiss horizon 38/4 (Lochman and Duncan, 1944,

p. 21). *Blountia nixonensis* is from the Nixon Gulch section, in the Horseshoe Hills, about 25 km west of Bozeman. It is part of a Steptoean assemblage that includes *Aphelaspis* and *Glaphyraspis* at horizon 2.5.

Nevada.—Palmer (1965, pl. 1, figs. 1, 2, 4; pl. 21, figs. D–J) assigned sclerites from the *Aphelaspis* Zone of the Mendha Formation, Highland Range, Lincoln County, Nevada (USGS loc. 2432-CO), to *B. bristolensis* Resser, 1938, but comparison with Resser's types (pl. 5, figs. F–H) shows that they represent a new species, *B. nevadensis*. He (1965, p. 29) also reported it from Yucca Flat, Nevada, and the House Range, Utah. A faunal list was not presented by Palmer, but the type material of *Glaphyraspis brevis* (Palmer, 1965; pl. 7, figs. 12, 13) is from USGS loc. 2432-CO; a cranidium from this collection (Palmer, 1965, pl. 7, fig. 22) attributed as *G. ornata* (Lochman, 1938) is misidentified and is better assigned to *G. brevis*. At Yucca Flat, *Blountia* is associated with *Cheilocephalus brevilobus* (Walcott, 1916) and *Aphelaspis subditus* Palmer, 1962 in collection USGS 3532-CO in the upper Bonanza King Formation (Palmer, 1965, pl. 23).

Québec.—Rasetti (1946) described two new species, *Blountia gaspensis* and *B. nasuta*, from beach exposures at Grosses-Roches, Gaspé Peninsula, eastern Québec, and these are revised in this paper. The trilobites are from boulders in debris flow conglomerates that are now assigned to the lower Grosses-Roches Formation (Bernstein et al., 1992). The two species do not co-occur, with *B. gaspensis* in boulder G-28 and *B. nasuta* in boulders G-29 and G–40 (Rasetti, 1946, table 1). *Blountia nasuta* is associated with *Catillicephala impressa* Rasetti, 1946 as revised by Westrop and Dengler (2014). *Catillicephala impressa* is also present in the Cow Head Group of western

Newfoundland, where it is part of a diverse assemblage of species that are correlative with the *Crepicephalus* Zone (Westrop and Dengler, 2014, p. 91 and fig. 1). *Blountia gaspensis* is associated with a different species of *Catillicephala*, *C. calva* Westrop and Dengler, 2014 (= *C. lata* of Rasetti, 1946), but the rest of fauna suggests that it is also from the *Crepicephalus* Zone (see Westrop and Dengler, 2014, p. 91 for discussion).

Newfoundland.—A new species, *Blountia newfoundlandensis*, is from the Cow Head Group of western Newfoundland. It occurs only in boulder CH 48, which is from conglomerates from the upper part (unit 5, bed 6) of the Downes Point Member of Shallow Bay Formation on the north shore of the Cow Head Peninsula (see Westrop and Eoff, 2012, figs. 1.2. and 2.2 for a locality map and a stratigraphic column). Boulder CH 48 includes *Aphelaspis* and is clearly from the lower part of the Steptoean; agnostoid arthropods that might provide better biostratigraphic resolution (Westrop and Eoff, 2012) are absent.

Phylogenetic Analysis

Since *Blountia* is a genus that managed to survive the extinction at the base of the Steptoean Stage before going extinct in the lower *Aphelaspis* Zone, the relationship between the pre- and post-extinction taxa are of interest, as well as the relationship with related genera. *Blountia*, *Maryvillia*, and *Blountina* have been discussed throughout the literature; Rasetti (1956) proposed that *Blountina* is synonymous with *Blountia*, and Pratt (1992) considered *Maryvillia* a junior synonym. A preliminary analysis of the relationship of select taxa of *Blountia* and its related genera are investigated using PAUP* (Swofford, 2013) and TNT (Goloboff et al., 2008).

Taxon Selection and Coding Sources

Species coded for phylogenetic analysis were evaluated from new images of type and archival specimens, and specimens collected from the field (*Blountia morgancreekensis* and *B. newfoundlandensis*). Twelve *Blountia* species were chosen from central Texas, northeastern Tennessee, central Montana, and western Newfoundland. *Blountia cora*, *B. janei*, *B. montanensis*, *B.* cf. *montanensis*, *B. gaspensis*, and *B. nasuta* are from the pre-extinction *Crepicephalus* Zone. *Blountia angela*, *B. bristolensis*, *B. nevadensis*, *B. newfoundlandensis*, *B. morgancreekensis* are from the post-extinction, *Aphelaspis* Zone. The type species of *Blountia*, *B. mimula* is from a mixed collection with trilobites from both zones. The type species of *Blountina*, *B. eleanora* and two species of *Maryvillia*, the type, *M. arion*, and *M. triangularis*, are included in the analysis, all from the *Crepicephalus* Zone. *Kingstonia gaspensis* from the *Crepicephalus* Zone was selected as the outgroup because of its featureless appearance, similar to the ingroup taxa.

Character Coding

The data matrix (Table 2) includes 15 ingroup species, plus the outgroup, five binary and four unordered multistate characters. See Appendix B for the character list. Parsimony uninformative characters, i.e. those that are autapomorphic or shared by all of the ingroup, were avoided and so branch collapsing rules were not utilized.

Results

Branch-and-Bound (implicit enumeration) search performed in PAUP* and TNT yielded the same strict consensus tree, though a different number of equally

parsimonious trees—54 in PAUP* and 3033 in TNT (length, 26; CI, 0.53; RI, 0.57; RC, 0.30). Support metrics are low, no nodes had a Bremer Support >1, and only one node had a Bootstrap Support >50%. Strict consensus tree is show in Figure 12 and character optimization performed in WinClada (Nixon, 2002) is in Figure 13.

The analysis is preliminary, but supports monophyly of *Maryvillia*, which includes *Blountina triangularis* (= *Maryvillia triangularis*), as suggested previously by Rasetti (1956). *Blountina* is monotypic and is the sister group to *Maryvillia*. However, recognition of these genera renders *Blountia* as paraphyletic, with a set of species, including *Blountia bristolensis*, *Blountia montanensis*, *Blountia nevadensis* and *Blountia morgancreekensis*, that is more closely related to *Maryvillia* and *Blountina* than they are to the type species, *Blountia mimula*. Species of the *Crepicephalus* Zone are mixed among the *Aphelaspis* Zone species, which does not support a monophyletic radiation of post-extinction species. Synonymy of all three genera under the senior name, *Blountia*, is a possible solution, but further work on the phylogeny should be performed before taking this step.

Systematic Paleontology

Illustrated material is housed at the National Museum of Natural History, Washington, D.C. (USNM), the National Invertebrate and Plant Type Fossil Collection, Geological Survey of Canada, Ottawa (GSC), and at the Oklahoma Museum of Natural History, University of Oklahoma (OU). Specimens from Quebec illustrated by Rasetti (1946) were housed at Laval University (LU) prior to their transfer to the GSC, and the original LU numbers cited in the paper are also included in the figure captions. To maximize

depth of field, all digital images were rendered from stacks of images focused at 100 micron intervals using Helicon Focus 4.0 for the Macintosh <http://www.heliconsoft.com>.

Family Kingstoniidae Kobayashi, 1933

Genus *Blountia* Walcott, 1916

Type species.—*Blountia mimula* Walcott, 1916, from the Nolichucky Formation, eastern Tennessee (by original designation).

Diagnosis.—Species of *Blountia* have a frontal area around one-third of the cranidial length with a rounded anterior margin, down-sloping preglabellar field, and flat to gently upturned anterior border. Glabella convex, raised above fixed cheeks, with straight, converging sides and rounded front; glabellar furrows absent on exoskeleton, may be perceivable on internal mold. Occipital ring short, about one-tenth of glabellar length (sag.). Combined fixed cheeks make up around 40% of cranidial width at the palpebral lobes. Palpebral lobes small, situated aside anterior half of glabella. Posterolateral projections large (tr.; exsag.), extend to pointed genal angle; posterior border furrow weakly defined. Thorax has seven to nine flat, transverse segments that deflect posteriorly at fulcrum, and downslope to small, pointed spines. Pleural furrow faint. Convex axis comprises about one-third width and is raised above pleural lobes. Pygidium semielliptical in outline, with border of even length around posterior and lateral margin and articulating facets on anterior corners. Axis tapers at border furrow; definition of border furrow varies. Typically, six to eight axial rings plus terminal piece.

Axial ring furrows and pleural and interpleural furrows weakly expressed on testate surface, more defined on internal mold.

Discussion.—Assignment of *Blountia* to Kingstoniidae, rather than Asaphiscidae (e.g., Rasetti, 1965), follows Westrop (1992), who drew attention to the structure of the occipital ring as a synapomorphy of the family. *Maryvillia* has been considered to be a junior synonym of *Blountia* by some authors (e.g., Pratt, 1992, p. 66). A preliminary phylogenetic analysis supports monophyly of *Maryvillia*, but also indicates that *Blountia* is paraphyletic. Pending further study, both genera are retained here, although the diagnosis of *Blountia* is descriptive in nature. *Blountia* is diagnosed as having a glabella that is more convex and raised above the fixed cheeks, a more rounded front end of the glabella, more impressed dorsal furrows, and a pyigidial axis that terminates at the border furrow, rather than on the border.

Two articulated specimens of *Blountia* are figured, *B. mimula* (pl. 1, figs. A–D) and *B. bristolensis* (pl. 5, figs. A–E), both of which have seven thoracic segments. Rasetti (1965, p. 58) reports an articulated specimen of an older, undescribed species of *Blountia* from the Murphy's Creek Formation in the Gaspé Peninsula, Quebec which had nine thoracic segments.

Blountia mimula Walcott, 1916

Plate 1, figs. A–J

1916 *Blountia mimula* Walcott, p. 399, pl. 61, figs. 4, 4a–c.

1938 *Blountia mimula* Walcott; Resser, p. 63, pl. 12, figs. 18–19.

non 1965 *Blountia mimula* Walcott; Rasetti, p. 59, pl. 10, figs. 3–7 [= *Blountia angela* sp. nov.].

Diagnosis.— Frontal area approximately one-third cranidial length, with gently sloping preglabellar field and flat anterior border nearly equal in length (sag.); anterior border furrow well-defined. Anterior margin rounded. Moderately convex glabella narrows anteriorly with outwardly convex lateral margin and well-rounded front. Seven thoracic segments. Pygidium is semielliptical in outline, posterior border approximately 15% total length, and border furrow very faint to entirely effaced.

Types.— The holotype is a nearly complete exoskeleton (USNM 62781; pl. 1, figs. A–D) from the Nolichucky Formation at Shields Ridge, Jefferson County, Tennessee (USNM loc. 120). Paratypes are a cranidium (USNM 62873; pl. 1, figs. E–G) and pygidium (USNM 62872; pl. 1, figs. H–J) from the Nolichucky Formation, 17.7 km (11 miles) northwest of Knoxville (USNM loc. 107c).

Occurrence.—Type specimen is from Shields Ridge (U.S.N.M. locality 120), Nolichucky Formation, Tennessee.

Description.—Cranidium exclusive of posterolateral projection subrectangular in outline, width at palpebral lobe equal to 75% of length, with evenly rounded anterior margin. Frontal area long, occupying about one-quarter cranidial length (27%; 25–29), preglabellar field comprises about 40% (39; 36–42); gently slopes down with subtle increase in slope anteriorly to flat anterior border; anterior border furrow shallow. Moderately convex glabella subtrapezoidal in outline, narrows slightly forward, with

well-rounded anterior margin. Glabellar width is about 75% (74; 70–78) its length at posterior end of palpebral lobe. Glabella surface smooth, lacking lateral glabellar furrows and only a hint of SO near axial furrow on some specimens (pl. 1, fig. A). Posterior margin of SO gently curved. Palpebral lobe short, about one-tenth (12%; 10–15) cranidial length, situated in front of glabellar mid-length. Anterior branches of facial suture diverge before curving along anterior cranidial margin; posterior branches extend about 45 degrees, increasing curvature posteriorly. Posterolateral projections extend laterally with backwardly curved posterior margins, tapering to a sharp point. Posterior border furrow weakly expressed across two-thirds of posterior margin, becoming entirely effaced beyond that point.

Thorax comprised of seven flat, transverse segments that taper to short, pleural spines, diverging posteriorly and sloping down. Pleural furrow very faint but expressed near fulcrum. Axis is convex and raised above pleural lobes, occupies about one-third (31%) thoracic width at anterior, narrowing (tr.) posteriorly. Axial furrows shallow but clearly defined grooves.

Pygidium subcircular in outline, maximum length around half its width. Axis convex, raised above pleural field, width one-third (32%; 21–33) maximum tail width (tr.). Axial furrows well-incised and shallow at axial tip. Faint axial ring furrows expressed at margin of axis in some individuals but effaced completely in others; at least seven axial rings present. Pleural field gently raised above down-sloping border, unfurrowed apart from barely perceptible pleural furrow at anterior. Lateral and posterior border furrows faint. Border length 15% maximum tail length. Entire exoskeleton smooth.

Discussion.—Considering Walcott's (1916) types (pl. 1) for *Blountia mimula*, there is variation in the glabellar width relative to the cranidial width (glabellar width 64% cranidial width at palpebral lobe in the holotype and 79% in the paratype), as well as the shape of the anterior margin—compared to the paratype, the holotype specimen has stronger curvature. The pygidia also have proportion variation; the holotype pygidium length is 50% of its width and the paratype is 64%.

Sclerites in Tennessee identified by Rasetti (1965, pl. 10, figs. 3–7) as *Blountia mimula* do not appear conspecific with the holotype and represent a new species, *B. angela* (pl. 2). The cranidium differs from the *B. mimula* holotype by having a slightly longer frontal area that is more rounded in outline, a preglabellar field that is gently sloped and consequently a shallower anterior border furrow. The glabella is slightly wider (width at palpebral lobes 75% of length, versus 70% in *B. mimula*) and has a more rounded outline. The pygidium of *B. angela* is more clearly distinguishable from the type specimen by having a better defined border furrow and pleural furrows; whereas *B. mimula* has deeper axial furrows. *B. mimula* types are testate, but an exfoliated pygidium shows that *B. angela* preserves fine pitting.

The holotype specimen of *Blountia montanensis* Duncan (pl. 11, fig. A–C) and the complete exoskeleton of *Blountia bristolensis* Resser illustrated by Rasetti (1965) (pl. 5, figs. A–E) differ from *B. mimula* by having facial sutures that extend straight from the palpebral lobe, whereas those of *B. mimula* are divergent (pl. 1, fig. E). The frontal area of *B. mimula* is longer than in both of these species (29% total cranidial length compared to 23% in *B. montanensis* and *B. bristolensis*), and the axial furrows on the cranidium of *B. mimula* and *B. cora* are more defined than those of *B. bristolensis*. The

pygidium of *B. bristolensis* differs from *B. mimula* by having a more rounded outline and has slightly shorter border with a far more clearly defined border furrow. The articulated specimens of both *B. mimula* and *B. bristolensis* have seven thoracic segments, but *B. bristolensis* has a wider axis (38% of thorax width versus 30% in *B. mimula*).

Blountia cora Lochman resembles the holotype of *B. mimula* by having shallow dorsal furrows and similar facial sutures —anterior branches that only slightly diverge forward and posterior branches that extend back at about 45 degrees. Both species also have a posterior cranidial margin that extends transversely then curves posteriorly at the genal angles. *Blountia cora* differs by having a much longer frontal area (35% total cranidial length) and a glabella that narrows (tr.) more anteriorly (pl. 8, figs. A, D). The pygidium of *B. cora* is wider (maximum length 64% width compared to 51% of *B. mimula*) and has a longer posterior border (21% versus 15% total length).

Blountia angela sp. nov.

Plate 2, figs. A–I

1965 *Blountia mimula* Walcott; Rasetti, p. 59, pl. 10, figs. 3–7.

Diagnosis.—Cranidia with well-rounded anterior margin, frontal area approximately one-third (sag.) cranidial length with down-sloping preglabellar field into flat border. Convex, subtrapezoidal glabella with rounded front. Pygidium semielliptical in outline, maximum length 65% its width. Down-sloping border long, around 13% tail length with well-defined border furrow. Around seven axial rings, plus a couple incorporated into terminal piece. Exoskeleton smooth, exfoliated surface preserves dense pitting.

Name.—For the author's mother, Angela Armstrong.

Types.—A holotype cranidium (USNM 144602, pl. 2, figs. A–C), paratype cranidium (USNM 144602, pl. 2, figs. D–E) and pygidia (USNM 144602, pl. 2, fig. F; USNM 144602 figs. G–I) from the *Aphelaspis* Zone, Nolichucky Formation, Hurricane Hollow (cnr/17) section (Rasetti, 1965), Union County, Tennessee.

Occurrence.— *Aphelaspis* Zone, Hurricane Hollow section (cnr/17) (Rasetti, 1965), Nolichucky Formation, Union County, Tennessee.

Description.—Cranidia subtrapezoidal in outline with a rounded anterior margin and constriction at palpebral lobes. Frontal area 30% cranidial length (sag.); preglabellar field about 40% of frontal area length, down-sloping into flat border separated by border furrow, which varies from well-defined to being faint medially (pl. 2, figs. A, D). Anterior border long, shortening slightly abaxially. Convex glabella subtrapezoidal in outline with well-rounded front, raised above fixed cheeks; axial and preglabellar furrows well-defined. Glabellar width at palpebral lobes three-fourths (72–78%) its sagittal length. Lateral glabellar furrows absent on testate surface. Occipital ring arcuate, SO not expressed on exoskeleton. Fixed cheeks down-sloping; combined fixed cheek width comprises 40% (41; 38–45) cranidial width at palpebral lobes. Palpebral lobes short, slightly curved bands, 15% glabellar length; positioned in front of glabellar mid-length. Anterior branches of facial sutures diverge slightly before curving towards anterior margin. Posterior branches extend obliquely back, deflecting posteriorly to genal angle. Posterior border furrow well impressed, nearly transverse across posterolateral projections. Posterior margin directed obliquely back, gently curved towards genal angle. Exoskeleton smooth.

Pygidium semielliptical in outline, sagittal length around 65% maximum width. Long lateral and posterior borders, 13% pygidial length (sag.), shortens somewhat anteriorly. Border down-sloping, separated from pleural field by well-incised border furrow that weakens slightly posteriorly. Anterior border furrow thick (exsag.), deep groove. Articulating facet present on anterior corners. Axis convex, raised above pleural field; comprises one-third (31%) of maximum pygidial width, tapering at border furrow. Articulating half-ring very short (3% axis length), slightly curved band; articulating furrow double the length of half-ring, both expressed on internal mold. Seven transverse axial rings plus two or three incorporated into terminal piece; defined on exfoliated surface, faintly expressed on exoskeleton. Rings decrease in width posteriorly with gently inflated bosses developed abaxially and subtle crest raised along sagittal line. Pleural field gently inflated, pleural furrows weakly defined on exfoliated surface and barely perceivable on exoskeleton. Testate surface smooth; dense pitting preserved on internal mold, with increased concentration on the pleural fields and absence on the anterior border furrow and articulating furrow.

Discussion.—These specimens were originally identified as *Blountia mimula* by Rasetti (1965) but as discussed above, they belong to a different, and completely new species. *Blountia angela* is comparable to *B. bristolensis* and differs by having a longer frontal area length (30% cranidial width compared to 23%), a gently sloping preglabellar field, and a shallow anterior border furrow. The pygidia resemble each other in their well-defined border furrow but *B. angela* has a longer relative to tail width (length 65% of width, versus 55%), a slightly longer border, and has a very faint axial ring furrows on

the exoskeleton. The cranidia of *B. angela* is also comparable to *B. janei*, which is discussed in that section.

Blountia bristolensis Resser, 1938

Plate 6, figs. A–H; Plate 7 figs. A–I

1938 *Blountia bristolensis* Resser, p. 65, pl. 12, fig. 24.

1938 *Maryvillia bristolensis* Resser, p. 87, pl. 12, fig. 38.

1944 *Blountia nixonensis* Lochman, in Lochman and Duncan, p. 43, pl. 4, figs. 7–12.

1965 *Blountia bristolensis* Resser; Rasetti, p. 58, pl. 10, figs. 1–2, pl. 11 figs. 9–12.

non 1965 *Blountia bristolensis* Resser; Palmer, pg. 29, pl. 1, figs. 1, 2, 4 [= *Blountia nevadensis* sp. nov.].

Diagnosis.—Frontal area approximately one-fifth cranidial length, with sharp slope change between preglabellar field and anterior border, and well-defined anterior border furrow. Seven thoracic segments. Pygidium semicircular in outline with inflated pleural field, well-defined border furrow, and down-sloping border approximately one-tenth maximum pygidial length.

Holotype.— A pygidium (USNM 94942, pl. 5, figs. F–H) from the Nolichucky Formation, reservoir on Mumpower Creek, 5.6 km north of Bristol, Virginia (USNM locality 36v).

Occurrence.—*Aphelaspis* Zone, Nolichucky Formation, Rasetti's (1965) collections cnp/17, cnp/14, and cnq/14 in Tennessee. Type locality is U.S.N.M. locality 36v near Bristol, Virginia (Resser, 1938).

Discussion.— Rasetti (1965, p. 58) noted that the pygidium and the cranidium that Resser (1938) named *Blountia bristolensis* and *Maryvillia bristolensis*, respectively, are from the same collection and he considered them to represent a single species; *B. bristolensis* has page priority and the pygidium (pl. 5, figs. F–H) is the holotype. The cranidium of *Blountia bristolensis* Resser (1938) has a relatively short frontal area in which the preglabellar field varies from slightly longer to slightly shorter than the anterior border, and there is an abrupt change in slope at border furrow. An exoskeleton assigned to the species by Rasetti (1965) (pl. 5, figs. A–E) has similar frontal area proportions to Resser's cranidia and appears to be conspecific.

Both Palmer (1965) and Rasetti (1965) considered *Blountia nixonensis* to be conspecific with *Blountia bristolensis*. After comparing new images of Lochman's *B. nixonensis* paratypes (pl. 6, figs. F–H; pl. 7, figs. 7, figs. A–I), it is almost certain they belong to the same species. Palmer (1965, pl. 1, figs. 2–3) also identified a pygidium and cranidium from the Mendha Formation in Nevada as *Blountia bristolensis*, but these sclerites represent a distinct species and are assigned to a new species, *Blountia nevadensis*. New images (pl. 21, figs. A–J) show that the pygidium somewhat resembles *B. bristolensis* but differs by being relatively narrower (maximum length 69% of width, versus 55% of *B. bristolensis*), having a longer border (17% of maximum tail length compared to 11% of *B. bristolensis*), and distinct axial rings that are inflated abaxially. The cranidia of both species are characterized by a strongly convex, subtrapezoidal glabella with a well-rounded front. The frontal area of the Nevadan species is clearly distinct, and more closely resembles *Blountia nasuta* Rasetti 1946 (pl. 20, figs. A–F) by having an anterior border that is longest medially and shortens abaxially, creating a

triangular outline. *Blountia nasuta* differs from *B. nevadensis* by having a longer frontal area (38% of total cranidial length verses 30%), a more defined anterior border furrow, and posterolateral projections that are narrow more abruptly and taper to a sharper point. The pygidium of *B. nasuta* has a distinctive subtriangular outline with a sagittal border length comprising one-fourth of the pygidium, compared to the subelliptical tail in *B. nevadensis*.

Blountia newfoundlandensis from the Cow Head Group, western Newfoundland, closely resembles *B. bristolensis* (pl. 25). Both species have broadly rounded anterior margins with steep preglabellar fields and preocular areas, deeply incised anterior border furrows. Strongly convex glabellae with sides that narrow (tr.) forward to well-rounded anterior margins are characteristic of both species, as well as pointed posterolateral projections that extend posteriorly. *Blountia newfoundlandensis* differs by having a narrower glabella (glabellar width is 69% of length verses 79% of *B. bristolensis*) and palpebral lobes situated slightly farther forward. Also, the pygidium of *B. newfoundlandensis* has a longer pygidial posterior border (18% of maximum tail length compared to *B. bristolensis*' 11%) and distinct axial rings with gently inflated distal ends.

Blountia cora Lochman, 1944

Plate 8, figs. A–J

1944 *Blountia cora* Lochman, in Lochman and Duncan, p. 51, pl. 8, figs 7–11.

non 2000 *Blountia cora* Lochman, in Lochman and Duncan; Stitt and Perfetta, p. 213, figs. 11.6–11.7 [= *Blountia* sp. indet.].

Diagnosis.—Anterior margin evenly rounded; very long frontal area, approximately one-third total cranidial length, roughly equally divided into preglabellar field and gently upturned anterior border; differentiated by shallow border furrow and change in slope. Wide fixigenae, about half cranidial width; glabella narrows (tr.) anteriorly. Semiellipitical pygidium, maximum length about two-thirds maximum width, with shallow border furrow, and distinct axial furrows.

Types.—A holotype cranidium (USNM 127151, pl. 8, figs. A–C), paratype cranidia (USNM 127153, pl. 8, figs. D–E) and pygidia (USNM 127153, pl. 8, figs. G–H; USNM 127152b, pl. 8, figs. I–J) from the Pilgrim Formation, Half Moon Pass section (Lochman and Duncan, 1944), Big Snowy Mountains, Montana.

Occurrence.—*Crepicephalus* Zone, Pilgrim Formation, Half Moon Pass section, Lochman and Duncan's (1944) horizons 9.1, 9.1x, and 9.2, Big Snowy Mountains, Montana.

Discussion.—A cranidium and pygidium from the lower Deadwood Formation of the Black Hills, North Dakota, were illustrated as *Blountia cora* by Stitt and Perfetta (2000, fig. 11.6, 11.7), but are almost certainly misidentified. The cranidium is too poorly preserved and illustrated for a comprehensive evaluation but appears to have an anterior border that is noticeably shorter than the preglabellar field, whereas they are subequal in length in the types of *B. cora* (pl. 8, figs. A–E). In addition, the anterior branches of the facial sutures appear to be subparallel, rather than conspicuously divergent, as in the types. The pygidium from the Deadwood Formation is relatively narrower than any of the types (pl. 8, figs. F–J) but, because it is illustrated in dorsal view only, additional comparisons are difficult.

Cranidia of *B. cora* and *B. angela* share evenly rounded anterior margin, moderately sloping strongly convex, subtrapezoidal glabellar with a well-rounded front end, deep axial furrows, and posterolateral projections that extend posteriorly at about 45 degrees with a posterior border margin that curves back towards the genal angle (pl. 8, fig. A, compared to pl. 2, fig. A). The latter is differentiated by having a slightly shorter preglabellar field (37% of frontal area versus 43% in *B. cora*) and narrower fixed cheek (41% of cranidial width compared to 48%). *Blountina eleanora* also has a glabella of similar morphology to *B. cora* but is relatively wider (glabellar width to length ratio of 81% compared to 72% in *Blountia cora*). *Blountina eleanora* has a much shorter frontal area with a transverse anterior margin, a preglabellar field that slopes steeply, and a better defined anterior border furrow compared to both *Blountia cora* and *B. angela*. The pygidium of *B. cora* has a weak to completely effaced border furrow like *Blountina eleanora*, and a longer posterior border than both *Blountina eleanora* and *Blountia angela* (21% of maximum tail length, verses 13% in both species).

Blountia alexas (Rasetti, 1965, pl. 9, figs. 9–12) has the same glabella width to length ratio as *B. cora* but differs by not narrowing (tr.) as much anteriorly. Both species have upturned anterior borders, but in *B. cora*, it is at a lesser degree relative to the preglabellar field. *Blountia alexas* has a longer posterior border of the pygidium (26% of maximum tail length, compared to 21%) and both species have a shallow border furrow.

Blountia janei Lochman, 1944

Plate 9, figs. A–G; Plate 10, figs. A–H

1944 *Blountia janei* Lochman, in Lochman and Duncan, p. 52, pl. 8, figs. 1–6.

non 2000 *Blountia janei* Lochman, in Lochman and Duncan; Stitt and Perfetta, p. 213, fig. 11.14–11.17 [=*Blountia* sp. indet].

Diagnosis.—Frontal area one-third cranidial length with broadly rounded front and shallow anterior border furrow; preglabellar field slightly longer than anterior border. Anteriorly rounded, subtrapezoidal glabellar outline with strong convexity. Elongate, semielliptical pygidium, length about three-fourths of maximum width, with faint border furrow and axial furrows that become effaced at axial tip in larger specimens; axis short, occupying nearly 80% (78%) of pygidial length; six axial rings, with three small segments incorporated into terminal piece (pl. 10, fig. F). Exfoliated cranidium preserves pitting, except on glabella and anterior border, with increased density on preglabellar field.

Types.—A holotype cranidium (USNM 127144, pl. 9, figs. E–G), paratype cranidia (USNM 127150, pl. 9, figs A–C: USNM 122149, pl. 9, fig D), and pygidia (USNM 127145a, pl. 10 figs. A–C; USNM 127149, pl. 10, fig. D; USNM 127146, pl. 10, fig. E; USNM 127145b, pl. 10, figs. F–H) from the Pilgrim formation, Half Moon Pass Section (Lochman and Duncan, 1944), Big Snowy Mountains, Montana.

Occurrence.—*Crepicephalus* Zone, Pilgrim formation, Half Moon Pass section, Lochman and Duncan's (1944) horizons 9.1, 9.1a, 9.1x, and 9.2, Big Snowy Mountains, Montana.

Discussion.—The cranidium of *Blountia janei* closely resembles *Blountia angela* (pl. 2, figs. A–E), in possessing an evenly rounded anterior cranidial margin and a preglabellar

field that slopes down at a somewhat shallow angle. Both species share a subtrapezoidal, anteriorly rounded glabella, although *B. janei* has slightly bowed sides, and posterolateral projections that curve posteriorly towards the genal angle. *Blountia janei* differs in having a down-sloping anterior border and a pygidium with a shorter axis (75% of sagittal pygidium length, compared to 85%) and a consequently longer border, six distinct axial rings compared to seven, plus three rings in the terminal piece in both species. The pleural field of *B. janei* is less inflated compared to *B. angela* and so the border furrow is less distinct. The pygidium of *B. janei* is closer to *B. minula* than of *B. angela*. *Blountia mimula* also lacks a distinct border furrow but the two species differ by *B. mimula* having better incised axial furrows while *B. janei's* weakens posteriorly, becoming effaced at the axial tip. The cranidia are less alike; width at palpebral lobe to maximum length ratio of *B. janei* is around 86% (81–89) and *B. mimula's* is 76% (73–78). The sides of the glabella of *B. mimula* also differ and are straight as in *B. angela* instead of bowed. All three species have anterior branches of the facial sutures that slightly diverge from the palpebral lobes.

Blountia montanensis Duncan, 1944

Plate 11, figs. A–L

1944 *Blountia montanensis* Duncan, in Lochman and Duncan, 1944, p. 53, pl. 8, figs. 29–34.

non 1965 *Blountia montanensis* Duncan, in Lochman and Duncan; Rasetti, p. 57, pl. 9, figs. 13–20.

Diagnosis.—Frontal area short, less than one-fifth cranidial length; entire frontal area down-sloping, with gently slope change between the preglabellar field and anterior border, anterior border furrow well-defined. Combined width of palpebral area occupies about 40% of cranidial width across the palpebral lobes.

Types.—A holotype cranidium (USNM 126836, pl. 11, figs A–C) and paratype cranidia (USNM 126837, pl. 11, figs. D–F; USNM 126838, pl. 11, fig. G, pl. 11, fig. K–L; USNM 126839, pl. 11, fig. H–J) from the Pilgrim Formation, Dry Wolf Creek section (Lochman and Duncan, 1944), Little Belt Mountains, Montana.

Occurrence.— *Crepicephalus* Zone, Pilgrim Formation, Dry Wolf Creek section (horizons 38/4, 4.5, and 4.5a) in Little Belt Mountains and Half-Moon Pass section (horizon 9.4) in Big Snowy Mountains, Montana (Lochman and Duncan, 1944).

Discussion.—Rasetti (1965) figured several cranidia and pygidia as *Blountia montanensis* (pl. 12–13) but there are several differences compared to Lochman and Duncan's types (pl. 11, fig. A–C) and it is likely they are not conspecific. The sides of the glabella of the types are not as rounded, the fixed cheeks are wider (40% total of cranidial width at the palpebral lobe compared to 30%), and the posterolateral projections are wider (tr.) and less pointed without the conspicuous backward deflection seen in Rasetti's specimens (pl. 12, fig. D). The species are, however, comparable in length of the frontal area and the preglabellar field, and the inflation of the anterior border.

Blountia mimula and *B. bristolensis* have similar glabellar morphology as the type of *B. montanensis*, but both species differ by having shallower cranidial furrows, sharply pointed posterolateral projections that extend back, and a flat-lying anterior

border (pl. 1, fig. B and pl. 5, fig. A, compared to pl. 11, fig. C). The type cranidia of *B. mimula* (pl. 1, fig. E) show variation in anterior margin shapes from elliptical to more evenly rounded like *B. montanensis* and *B. bristolensis*. *Blountia mimula* differs from both *B. montanensis* and *B. bristolensis* by the outward divergence of facial sutures as they extend anteriorly from the palpebral lobe.

Blountia cf. *montanensis* (Duncan, 1944)

Plate 12, figs. A–I; Plate 13, figs. A–I

1965 *Blountia montanensis* Duncan, in Lochman and Duncan; Rasetti, p. 57, pl. 9, figs. 13–20

Types.—Cranidia (USNM 144598, pl. 12, figs. A–C; USNM 144599, pl. 12, figs. D–F; USNM 144598, pl. 12, figs. G–H; USNM 144599, pl. 12, fig. I) and pygidia (USNM 144599, pl. 13, fig. A–C; USNM 144599, pl. 13, fig. D–F; USNM 144598, pl. 13, fig. G–I) from Rogersville and Big Creek sections in Hawkins County, Tennessee.

Occurrence.—*Crepicephalus* Zone, Nolichucky Formation, Hawkins County, Tennessee at Rasetti's (1965) localities cnk/1, cnm/2, cnn/1, and cnn/3.

Discussion.—Rasetti (1965) figures specimens from the *Crepicephalus* Zone of Tennessee as *Blountia montanensis*; as discussed above, there are several differences and they should be considered separate species. A new species from Newfoundland, *Blountia newfoundlandensis*, resembles the Tennessee species by having an evenly rounded anterior margin of the cranidium. *Blountia* cf. *montanensis* differs by having substantially narrower fixed cheeks (29% combined width of cranidium at palpebral lobes, versus 43%), slightly deeper axial furrows, palpebral lobes situated farther back

relative to the glabella, and posterolateral projections that extend to a sharper point. The pygidia are very similar; maximum length is 63% maximum width, border length (sag.) is 18% length, there are seven to eight axial rings faintly expressed on the testate surface. The pygidial border of *B. newfoundlandensis* lengthens a little adaxially in some specimens, whereas Rasetti's specimens have a border of consistent length, and the one exfoliated specimen from Tennessee has more incised furrows.

Blountia gaspensis Rasetti, 1946

Plate 18, figs. A–I; Plate 19, figs. A–G

1946 *Blountia gaspensis* Rasetti, p. 446, pl. 67, figs. 7–10.

Diagnosis.—Broadly rounded anterior cranidial margin. Frontal area occupies approximately 30% of cranidial length; down-sloping preglabellar field and slightly shorter, nearly flat anterior border differentiated by change in slope, and shallow but clearly defined anterior border furrow. Facial sutures diverge conspicuously anteriorly from palpebral lobes. Subtrapezoidal glabella with well-rounded front; shallow axial furrows. Subelliptical pygidium with border of even width approximately equal to 15% maximum pygidial length; separated from pleural field by strongly-incised border furrow. Shallow axial furrows. Internal mold with at least nine axial rings and terminal piece of two segments, and faint, straight pleural furrows.

Types.—A holotype cranidium (LU 1004a, pl. 18, figs. A–C) and paratype cranidia (LU 1004d, pl. 18, figs. D–F; LU 1006, pl. 18, figs. G–I) and pygidia (LU 1004c, pl. 19, figs. A–F; LU 1004e, pl. 19, fig. G) from Grosses-Roches, western Gaspé, Matane County, Quebec.

Occurrence.—*Crepicephalus* Zone, Grosses-Roches, western Gaspé, Matane County, Quebec, boulder G28 (Rasetti, 1946).

Discussion.— Like *Blountia morgancreekensis* (pl. 22, fig. A) from the Riley Formation of central Texas, *B. gaspensis* (pl. 18, fig. A) has a long frontal area (28% of cranidial length in both species) with facial sutures that diverge abaxially from the palpebral lobes, and glabellar width three-fourths its length. However, *B. morgancreekensis* differs by having a more rounded anterior cranidial margin and a shorter palpebral lobe (11% of cranidial length (sag.), versus 17% in *B. gaspensis*), and a shallower anterior border furrow. The pygidia are fairly similar; width about 70% its length, posterior border about 15% sagittal length, and around eight axial rings expressed on the exfoliated surface. However, *B. gaspensis* has a conspicuous pygidial border furrow marked in part by a sharp break in slope at the edge of the pleural field (pl. 19, figs. A–F).

The cranidia that Rasetti (1965; pl. 2, figs. A–E) identified as *Blountia mimula* have similar proportions to *B. gaspensis*, although the preglabellar field is slightly shorter (37% of frontal area, versus 43% in *B. gaspensis*) and the anterior cranidial margin is more rounded than in *B. gaspensis*. The pygidia of *B. gaspensis* have deeper border furrows and sharper breaks between the pleural field and the nearly flat border that contrast with the more down-sloping border in *B. angela* (pl. 2, figs. D–F vs. pl. 18, figs. G–I). In other respects, pygidial morphology of these species is similar.

Blountia nasuta Rasetti, 1946

Plate 20, figs. A–M

1946 *Blountia nasuta* Rasetti, p. 446, pl. 67, figs. 11–14.

Diagnosis.—Anterior border increases in length medially, producing roughly triangular outline; roughly equal in length to preglabellar field. Gradual slope change between down-sloping preglabellar field and nearly flat anterior border; shallow anterior border furrow. Strongly convex, subtrapezoidal glabella with well-rounded front; shallow axial furrows. Palpebral lobes situated more posteriorly, at about mid-length of glabella. Triangular pygidium with border occupying one-quarter of length (sag.) but narrowing abaxially. Border furrow faint; moderately incised axial furrows that weaken at axis tip. Pleural field gently inflated above border. Pitted sculpture and at least nine axial rings and terminal piece expressed on exfoliated surface.

Types.—A holotype cranidium (LU 1005a; pl. 20, figs. A–C) and paratype cranidia (LU 1105f, pl. 20, figs. D–F; LU 1005c, pl. 20, figs. G–I; LU 1005b, pl. 20, figs. J–L; LU 1005e, pl. 20, fig. M) from Grosses-Roches, western Gaspé, Matane County, Quebec (Rasetti, 1946).

Occurrence.— *Crepicephalus* Zone, Grosses-Roches, western Gaspé, Matane County, Quebec, boulder G-29 (Rasetti, 1946).

Discussion.— The cranidium of *B. nevadensis* n. sp. (pl. 21, figs. A–C, F) somewhat resembles *Blountia nasuta* (pl. 20, figs. A–F) by possessing a long, medially expanding, subtriangular anterior border, but it differs by having a shorter frontal area (30% cranidial length (sag.) versus 37% in *B. nasuta*) and an even shorter preglabellar field (36% of frontal area (sag.), versus 46%). The palpebral lobes in *B. nasuta* are more posteriorly positioned, so that the posterolateral projections are shorter (exsag.) and lack

the conspicuous posterior deflection of the tips that characterizes *B. nevadensis*. The pygidia (pl. 20, figs. G–M; pl. 21, figs. G–J) are very different; *B. nasuta* has a subtriangular outline and the axis has at least one more axial ring and is more raised above the pleural field. In contrast, *B. nevadensis* is semielliptical in outline and consequently has a more even border length around the margin (border is 17% sagittal length compared to 25%). The border furrow is also slightly more defined, and axial rings have subtly inflated knobs expressed on the testate, which *B. nasuta* preserves only on the exfoliated surface, and axial ring furrows are better defined on the internal mold.

The cranidium of *B. morgancreekensis* (pl. 22, 24) is similar to *B. nasuta*, except for its evenly rounded anterior margin and consequently shorter frontal area (28% of total cranidial length, versus 37% of *B. nasuta*). The pygidia are clearly different in outline, as *B. morgancreekensis* (pl. 23) is subcircular rather than triangular in outline, has at least one more axial ring, and has dense pitting preserved on the exfoliated surface. The border of *B. morgancreekensis* is more down-sloping, has a fairly even length along the lateral and posterior margins, and is shorter (14% of sagittal length) than in *B. nasuta*.

See below for comparisons with *Blountina triangularis*.

Blountia nevadensis sp. nov.

Plate 21, figs. A–J

1965 *Blountia bristolensis* Resser; Palmer, p. 29, pl. 1, figs. 1, 2, 4.

Diagnosis.— Frontal area long, about 30% cranidial length, with gently slope change between preglabellar field and anterior border; faint anterior border furrow. Anterior border expands medially with subtriangular outline. Preglabellar field shorter (sag.) than border Glabella subtrapezoidal in outline and moderately convex. Fixed cheeks one-third cranidial width with large (exsag.) posterolateral projections. Pygidium semielliptical in outline with length about two-thirds maximum width, posterior border 17% of total length. Posterior border furrow and axial furrows shallow but clearly defined, weaken towards axis tip. Axial rings inflated abaxially into low knobs on both external surface and internal mold.

Name.—Named for its occurrence in the Mendha Formation in Nevada.

Types.—A holotype cranidium (USNM 141505; pl. 21, figs. A–C), paratype free cheek (USNM 141504, pl. 21, figs. D–E), cranidium (USNM 141505, pl. 21, figs. F) and pygidia (USNM 141506, pl. 21, figs. H–J) from Highland Range, Nevada (Palmer, 1965).

Occurrence.—*Aphelaspis* Zone, House Range, Utah; Highland Range and Yucca Flat, Nevada.

Description.—Cranidia roughly subelliptical in outline with nasute anterior margin; width at palpebral lobes 80% sagittal length. Frontal area long, about one-third (31%) cranidial length; preglabellar and preocular fields even in length, anterior border subtriangular in outline decreasing in length (exsag.) abaxially. Preglabellar field occupies one-third of frontal area length (sag.) and gently down-sloping with gradual change into flat anterior border; weakly expressed anterior border furrow. Strongly convex glabella subtrapezoidal in outline with broadly rounded front; at mid-point,

glabellar width 70% of length. Occipital furrow faint and curved gently backward, LO gently curved, even in length across glabella; accounts for about one-tenth glabellar length (sag.). Fixed cheeks wide, combined with 40% (40–41) of cranidial width at palpebral lobes. Palpebral lobes slightly curved and oblique, equal to 11% maximum cranidial length. Facial sutures in front of palpebral lobes diverge slightly outward then curve towards anterior margin. Posterolateral projections curve backwards and taper to a point. Posterior border furrow shallow and disappears distally; posterior border directed obliquely back from glabella and conspicuously deflects back.

Free cheek narrow, extending into short, pointed genal spine. Shallow lateral border furrow separates narrow (tr.; exsag.), roughly triangular librigenal field from broad (tr.), convex lateral border. Eye small, globular; ocular suture absent. Conspicuous terrace ridges on margins of lateral border.

Pygidium semielliptical in outline, length (sag.) about 70% of maximum width. Axis convex, raised above pleural field, occupies about one-third of tail width at anterior. Axial furrows moderately incised, become faint at terminus of axis. Abaxially, axial rings gently inflated into low knobs. Posterior border 17% (16–17) of tail length (sag.), narrows slightly anteriorly. Border furrow shallow becoming indistinct towards axis. Pleural field smooth, no trace of pleural furrows on exoskeleton; raised above down-sloping border.

Discussion.— Palmer (1965, pl. 1, figs. 2–3) assigned a cranidium, librigena and pygidium from the Mendha Formation, Nevada, as *Blountia bristolensis*. New images (pl. 21, figs. A–J) of these and previously unfigured, associated specimens show that they are misidentified. The pygidium (pl. 21, figs. H–J) somewhat resembles *B.*

bristolensis (plates 5 and 7), but is longer (maximum length 69% maximum width, versus 58% in *B. bristolensis*) and the axial rings are inflated abaxially. The cranidia are clearly different (compare pl. 21, figs. A–G and pl. 5, figs. A–E; pl. 6, figs. A–H) and Palmer's specimens are more like *Blountia nasuta* Rasetti 1946 (pl. 20, figs. A–F) in having a border that narrows abaxially to produce a triangular outline. *Blountia nasuta* differs from *B. nevadensis* in having a longer preglabellar field, more slightly more rounded glabellar outline, and a triangular shaped pygidium with a faint border furrow (see discussion of *B. nasuta*, above), indicating that Palmer's specimens represent a new species, *B. nevadensis*.

Blountia cora (pl. 8), *B. gaspensis* (pl. 18) and *B. nevadensis* share a glabella that narrows more anteriorly than other species, and their glabellar width at the palpebral lobes is about 75% its sagittal length. However, both *B. cora* and *B. gaspensis* are differentiated clearly by possession of anterior cranidial margins that are evenly rounded whereas *B. nevadensis* is distinctly nasute. The subtriangular border of the latter contrasts with the more arcuate borders of the other two species. In addition, the preglabellar field of *B. cora* is longer than in *B. nevadensis* (43% of frontal area, versus 36%) and the anterior border is upturned rather than slightly down-sloping (compare pl. 8, fig. A–C and pl. 21, figs. B, F). *Blountia gaspensis* has similar frontal area length to *B. nevadensis* but has a steeply sloping preglabellar field (pl. 18, fig. E) and a better defined anterior border furrow than both *B. nevadensis* and *B. cora*. The posterolateral projections of *B. nevadensis* and *B. cora* are large and curved back distally whereas those of *B. gaspensis* are directed more transversely. *Blountia cora* has a slightly wider tail with a more circular outline and a weakly etched border furrow. In contrast, *B.*

gaspensis has a strongly incised border furrow that does not weaken towards the axis and has faint pleural furrows on the exoskeleton.

The pygidia of *B. nevadensis* and *B. newfoundlandensis* (pl. 26) share a well-defined border furrow and axial furrows that weakens adaxially, an axis that tapers at the border furrow, similar border length (about one-fifth of maximum tail length), and the presence of inflated knobs on the axial rings of the exoskeleton. However, these species are quite distinct in cranidial morphology. *Blountia newfoundlandensis* (pl. 25) has a much shorter frontal area with a steeply sloping preglabellar field and an arcuate, rather than subtriangular, anterior border.

Blountia morgancreekensis sp. nov.

Plate 22, figs. A–J; Plate 23, figs. A–J; Plate 24, figs. A–G

1942 *Maryvillia hybrida* Resser, p. 71, pl. 13, figs. 14, 15 (only; figs. 16, 17, which is the holotype pygidium, may belong to *Coosella* Lochman, 1936; see Palmer, 1954, p. 722, and Rasetti, 1956, p. 1268).

1954 *Blountia nixonensis* Lochman, in Lochman and Duncan; Palmer, p. 722, pl. 79, fig. 4.

Diagnosis.—Frontal area long, equal to about 30% of cranidial length; anterior border furrow indistinct with preglabellar field and anterior border separated primarily by a gradual change in slope. On internal mold, border lacks caecal network present on

preglabellar field. Pygidium with gently inflated pleural field and down-sloping borders. Eight to nine axial rings expressed on exfoliated surface. External surfaces of cranidia and pygidia smooth; pitted sculpture well-developed on internal molds of fixigenae and pleural fields but absent on glabella.

Holotype.—A nearly complete cranidium from the Cap Mountain Limestone, Riley Formation, Burnett County, Texas (OU 238142).

Name.— For the type locality at Morgan Creek, Burnet County, Texas.

Description.—Cranidium roughly trapezoidal in outline, with rounded anterior margin and constriction at palpebral lobe; width at palpebral lobe about 90% of length (88; 80–93). Frontal area long, accounting for about 30% cranidial length (29; 24–33). Anterior border furrow very shallow; barely perceptible on some specimens (e.g., pl. 25, 1G). Preglabellar field differentiated largely from anterior border by slope change; on internal mold, border lacks caecal network present on preglabellar field. Preglabellar field steeply slopes towards the anterior border and makes up on average 40% (37; 28–52) of the frontal area length. Anterior border is nearly flat. Glabella convex and lateral profile curves down anteriorly. Axial furrow faint on external surfaces of exoskeleton with slightly deeper preglabellar furrow; all furrows better expressed on internal mold. Glabella narrows slightly anteriorly to broadly rounded front; width at the posterior end of the palpebral lobes is three-quarters its length (75%; 69–81) and lacks furrows. SO and LO indistinct on exoskeleton but better defined on internal mold. On external surface, SO expressed only medially as finely-etched groove; on external mold, shallow but extends across full width of glabella; LO very short, makes up one-tenth of the glabellar length (sag.) (9%; 7–11). Lateral glabellar furrows absent on external surface,

with up to four pairs barely perceptible on internal mold (e.g., pl. 25, figs G, H). Palpebral lobe very short, approximately one-tenth total cranidial length (11%; 8–13), gently arcuate band, positioned in front of glabellar mid-length; convex palpebral ridge best expressed on internal mold, extending obliquely forward to reach axial furrow near anterior corner of glabella. Anterior branches of facial sutures diverge forward from palpebral lobes before curving evenly inward along anterior cranidial margin. Posterior branches diverge backward along curved path; curvature increases posteriorly, with sutures nearly parallel near posterior corners of cranidium. Palpebral areas of the fixed cheeks make up a combined two-fifths (39%; 36–45) of total width at cranidial mid-length; slope downward away from axial furrow. Posterior margin of posterior area deflected backward at about 15 degrees from transverse plane; smaller individuals (e.g., Fig 1I) have more strongly deflected margins. Postocular area curved steeply downward; extended into large, triangular posterolateral projection with pointed corners; smaller individuals (e.g., pl. 25, fig. I) tend to have rounded corners. Posterior border furrow faint on external surface but better defined on internal mold; shallows abaxially, disappearing at middle of posterolateral projection. Entire exoskeleton is smooth; apart from furrows, fixigenae of external mold densely pitted, with scattered pits on glabella; network of caecal markings on preglabellar and preocular fields.

Pygidium semicircular in outline; length approximately 70% (71; 66–76) of maximum width; conspicuous articulating facet on anterior corners. Articulating half-ring very short, gently curved, distinguishable only on internal mold. Articulating furrow about twice the length of half-ring; deep and visible on internal mold. Axis moderately convex and raised above pleural field; length (sag,) approximately 80% (83; 76–88) of pygidial

length. Maximum axis width approximately one-third (33%; 27–38) pygidium width; tapers posteriorly. Eight (pl. 26, fig. D) or nine (pl. 26, fig. J) axial rings decrease in length (sag.) posteriorly, usually with low inflated bosses developed abaxially; additional terminal piece small and rounded, so that axis comprises at least nine to ten segments. Axial ring furrows effaced on external surface but well-defined, transverse on internal mold; anterior furrows connected across crest of axis, but posterior-most furrows effaced medially. Anterior-most pleural furrow shallow on external surface, but deeper on internal mold; remainder of furrows effaced on external surface and weakly expressed on internal mold. Lateral and posterior borders down-sloping, separated from gently inflated pleural field by shallow border furrow (more firmly impressed on internal mold) that weakens towards posterior tip of axis (e.g., Fig, 2A, B); length (sag.) equal to approximately 15% (14; 10–17) maximum length of the pygidium but shortens towards anterior corners of pygidium. External surface of entire pygidium smooth; well preserved internal molds show closely spaced pits on pleural field, with reduced density on axis border.

Material.—One holotype cranidium (OU 238142), seven paratype cranidia (OU 238142–238158, OU 238151–238152), five paratype pygidia (OU 238146–238150), and several unfigured cranidia and pygidia from the Cap Mountain Limestone, Riley Formation, central Texas.

Occurrence.—*Aphelaspis spinosa* Zone, Cap Mountain Limestone, Burnet County, Riley Formation, Texas in collections MCNe1 2.1, LB -0.15, LB 0.2, and MCNe1 7.1.

Discussion.—Palmer (1954) recognized that the paratype cranidium of *Maryvillia hybrida* Resser, 1942 (pl. 24, figs. E–G) from the Cap Mountain Member was a species

of *Blountia*, but assigned it to *B. nixonsensis* Lochman, in Lochman and Duncan, 1944. Numerous new sclerites from the Cap Mountain Member at the Morgan Creek and Lake Buchanan sections now demonstrate that Resser's specimen records a distinct species that differs from *B. nixonensis*; the species are compared above.

Blountia morgancreekensis resembles *B. angela* (pl. 2) in morphology of the pygidium, including the expression of the axis and pitted sculpture on the internal mold, but is slightly narrower and longer in outline. Cranidia are similar in glabellar outline, although *B. morgancreekensis* is less convex (compare pl. 22, fig. H and pl. 2, fig. B); in addition, the anterior border furrow is shallower in *B. morgancreekensis*, the border is relatively narrower and the palpebral area of the fixigena is narrower (tr.). The holotype of *Blountia mimula* Walcott (1916; pl. 1, fig. A–D) is a nearly complete exoskeleton that differs from those of both *B. morgancreekensis* (pl. 22, fig. A) and *B. angela* (pl. 2, fig. A) in having a relatively shorter anterior cranidial border and, consequently, a shorter frontal area (see also the paratype cranidium, pl. 1, figs. E–G). The pygidium of the holotype and a paratype pygidium (pl. 1, H–J) are both relatively longer and thus more elliptical in outline, and the border furrow is very faint to entirely effaced.

In comparison to *B. bristolensis*, the cranidium of *B. morgancreekensis* has a longer frontal area that lacks a well-defined anterior border furrow, and a gentle change in slope between the preglabellar field and border. The pygidium of *B. bristolensis* (pl. 5, F–H; pl. 7) has a proportionately longer axis (90% of sagittal length, versus 83% in *B. morgancreekensis*) and more inflated pleural field that is bounded abaxially by a more firmly impressed border furrow.

Blountia morgancreekensis closely resembles *B. janei* (pl. 9) in that they both have a well-rounded anterior cranidial margins and subtrapezoidal glabellae with slightly rounded sides and rounded front ends. The pygidia lack defined features with faint border and axial furrows, with the border furrow of *B. janei* being more indistinct. The posterolateral projections of *B. morgancreekensis* are more triangular with straight edges, and the facial sutures diverge out from the palpebral lobes more before curving into the anterior margin. However, the pygidia provide clear separation of the species. *Blountia janei* has a distinctly shorter axis (77% of pygidial length versus 86% in *B. morgancreekensis*) with no more than seven distinct rings in front of the terminal piece (pl. 10, fig. F), rather than eight or nine as in *B. morgancreekensis* (pl. 23, fig. J). *Blountia mogancreekensis* also has a well-defined border furrow on both external surfaces and internal molds (pl. 23, fig. A, D, J), whereas the furrow is much weaker, even on internal molds of *B. janei* (pl. 10, fig. F).

Blountia newfoundlandensis sp. nov.

Plate 25, figs. A–N; Plate 26, figs. A–L

Diagnosis.—Frontal area 25% cranidial length, steep preglabellar field, flat anterior border, and well-incised anterior border furrow. Pygidium subcircular in outline, pleural field raised above border, and well-defined border furrow that weaken posteriorly towards axis tip. Gently inflated knobs on axial rings present on exoskeleton. Entire exoskeleton smooth, internal mold preserves pleural field and seven to eight axial rings.

Material.—One holotype cranidium (Figs. pl. 25, figs. A–C), four figured cranidia (pl. 25, figs. D–L), one figured free cheek (pl. 25, fig. M), five figured pygidia (pl. 26, figs.

A–L), 17 unfigured cranidia, and 13 unfigured pygidia from the Cow Head Group in western Newfoundland.

Occurrence.—*Aphelaspis* Zone, Cow Head Group, western Newfoundland.

Discussion.— Compared to *Blountia morgancreekensis*, *B. newfoundlandensis* has a steeply sloping preglabellar field while the anterior border is nearly flat, resulting in a sharp change in slope; the anterior border furrow is well-defined. The preglabellar field dips forward at a lower angle in *B. morgancreekensis* (pl. 24, fig. C), and there is a gradual change in slope at the relatively longer anterior border; the border furrow is faint. Other differences between cranidia include a more firmly impressed posterior border furrow and a less rounded anterior cranidial margin in *B. newfoundlandensis*. The posterior border of the latter narrows (exsag.) abaxially from the posterior corner of the cranidium, whereas it maintains a more even length in *B. morgancreekensis*. The pygidium of *B. newfoundlandensis* has a longer posterior border, with more conspicuous narrowing towards the anterior corners, and consequently a shorter axis and fewer axial rings (6–7 versus 8–9); axial and border furrows are more firmly impressed than in *B. morgancreekensis*, and the pleural furrows are expressed on the external surface, albeit faintly. Finally, the pitted sculpture of the internal mold of *B. morgancreekensis* is not expressed in *B. newfoundlandensis*.

Blountia angela differs from *B. newfoundlandensis* by having a longer frontal area (30% versus 23%; 14–28), broader anterior margin of the cranidium, a somewhat more rounded glabellar front, and a shallower anterior border furrow. The preglabellar field of *B. newfoundlandensis* dips down at a steeper slope than that of *B. angela*, and the anterior border is flatter. Both species have the similar length proportions of the

preglabellar field and the anterior border compared to the total frontal area length, and both have deep axial furrows on both the cranidium and pygidium. The posterior margin of the occipital ring is more strongly curved in *B. angela*, and the posterior branches of the facial sutures have more curvature. The pygidia of *B. angela* differs by having a slightly shorter posterior border, faint definition of the axial rings on the testate surface, and by the presence of pitting on the internal mold.

Blountia newfoundlandensis resembles *B. bristolensis* by having a short frontal area around 23% of cranidial length (sag.), steeply sloping preglabellar field, and posterior branches of the facial sutures that extend nearly straight with little curvature as seen in many other *Blountia* species (e.g., *B. mimula*). The cranidium differs from *B. bristolensis* by its glabella with near parallel sides and greater convexity, so that it is raised well above the fixed cheeks. The pygidiun of *B. bristolensis* has a shorter posterior border (11% of sagittal length versus 18%) and no definition of axial rings on the exoskeleton.

Genus *Maryvillia* Walcott, 1916

Type species.—*Maryvillia arion* Walcott, 1916, from the Nolichucky Formation, eastern Tennessee (by original designation).

Diagnosis.—Subtrapezoidal cranidium with long frontal area, around one-third total length. Preglabellar field downslopes into flat to concave border; border furrow broad (sag.), but shallow. Glabella subtrapezoidal in outline with truncated front. Glabella very weakly convex, barely inflated above down-sloping fixed cheeks. Pygidium

semielliptical in outline with weak dorsal furrows. Axis terminates beyond the border furrow. Border down-sloping and slightly inflated.

Discussion.—Rasetti (1956) considered *Maryvillia* to be separated from *Blountia* by the shallower dorsal furrows, the greatly reduced glabella and fixed cheeks, less divergent anterior branches of the facial sutures, and a convex pygidial border. Pratt (1992) preferred to treat *Maryvillia* as a junior subjective synonym of *Blountia* because he believed that characters identified by Rasetti were in fact gradational between the genera.

Maryvillia arion Walcott, 1916

Plate 3, figs. A–K; Plate 4, figs. A–G; Plate 19, figs. H–K

1916b *Maryvillia arion* Walcott, p. 400, pl. 64, figs. 4–4c.

1942a *Blountia arguta* Walcott; Resser, p. 8.

1956 *Maryvillia arion* Walcott; Rasetti, p. 1267 (includes complete synonymy).

1961 *Maryvillia arion* Walcott; Rasetti, p. 116, pl. 21, figs. 14–15.

1965 *Maryvillia arion* Walcott; Rasetti, p. 59, pl. 9, figs. 22–26.

Diagnosis.—Well-rounded anterior margin of cranidium. Frontal area one-third cranidial length. Steeply sloping preglabellar field grades into flat anterior border across broad, very shallow border furrow. Subtrapezoidal glabella barely elevated above fixigenae. Pygidium subelliptical with smooth external surface, shallow furrows. Axis extends past border furrow onto down-sloping border. Pitting on exfoliated surface is variable in size.

Types.—A holotype cranidium (USNM 62826; pl. 3, figs. A–C), paratype cranidia (USNM 62826, pl. 3, figs. D–G; USNM 144603, pl. 3, figs. H–K) and pygidia (USNM 144604, pl. 4, figs. A–C; USNM 144603, pl. 4, figs. D–E; USNM 144603, pl. 4, figs. F–G) from the Nolichucky Formation, Rogersville, Hawkins County, Tennessee (Walcott, 1916).

Occurrence.—*Crepicephalus* Zone. Type locality is U.S.N.M locality 123b, 0.5 mile east of Rogersville, Nolichucky Formation, Tennessee. Rasetti's (1965) localities (cnm/2, cnn/1, cnn/2, cnn/3, cnn/4, cnn/14), Nolichucky Formation at the Big Creek and Rogersville sections in Hawkins County, and Lost Creek and Russell Gap sections in Jefferson County, Tennessee.

Description.—Cranidium subtrapezoidal in outline; width at palpebral lobe is 97% of length. Anterior margin is evenly rounded, frontal area is one-third total cranidial length; two-thirds of frontal area consists of anterior border. Preglabellar and preocular field steeply sloped, then gradually merges with flat anterior border. Anterior border furrow is gently incised on the internal mold. Glabella subtrapezoidal in outline with gently rounded front end, three pairs of furrows barely perceptible only on exfoliated surface. Glabellar width at palpebral lobe is 85% (83–86%) of length; convexity is low, subtly raised above fixed cheeks. LO short, less than one-tenth (7%; 6–8) of glabellar length; crescent-shaped, tapers (tr.) before reaching edge of glabella. SO and axial furrows well-incised on internal mold. Combined width of both fixed cheeks makes up about 40% of cranidial width at palpebral lobe. Palpebral lobes situated in front of mid-glabella length; moderately curved, short, about 15% of cranidial length. Raised palpebral ridge from lobe to anterior corner of glabella expressed on internal mold.

Anterior branches of facial suture extend forward, nearly parallel, then curve into anterior margin. Posterolateral projections extend transversely and slightly back, increasing curvature to a tapered point. Posterior border furrow well-defined on exfoliated surface, extending over three-quarters across (tr.) posterolateral projection. Dense pitting with bimodal size distribution preserved on internal mold.

Pygidium semi-subelliptical in outline, maximum length 70% (68–74) width. Very short articulating half-ring; articulating furrow slightly longer and well-incised only on exfoliated surface. Maximum axis width about one-third (36%; 34–38) of total width, tapers posteriorly and extends past border furrow. About twelve axial rings plus the terminal piece expressed on internal mold. Axial furrows shallow, weakening towards terminal piece. Axis raised slightly above pleural field. Pleural furrows weakly preserved on internal mold, indistinct on exoskeleton. Border is down-sloping; approximately one-tenth maximum tail length (sag.); differentiated from pleural field by shallow border furrow which weakens posteriorly, becoming indistinct at axis tip. External surface smooth, except for terrace ridges along posterior margin. Exfoliated surface preserve densely pitted sculpture with bimodal size distribution.

Discussion.— The types of *Maryvillia arion* consists of two exfoliated cranidia from the Nolichucky Formation near Rogersville, Tennessee. The pygidium attributed to *M. arion* by Walcott (1916) was considered by Resser (1942a) as having been incorrectly associated with the cranidia, and assigned it to a new species, *Blountia arguta*. Rasetti (1956) later suggested that Resser was incorrect naming a new species for this the pygidium, and returned it to *Maryvillia arion*, which is followed here. The pygidium of *M. arion* is similar to *B. mimula*, the type species of *Blountia*, but differs by having a

more elliptical outline, a more clearly defined border furrow, shallower axial furrows, and more axial rings (around 12 rings compared to 7–8 in *B. mimula*). The cranidium of *B. mimula* differs by having a far more elevated, convex glabella, anterior branches of facial sutures diverging outwards from palpebral lobes rather than straight forward, more constriction at palpebral lobes, and posterolateral projections with more curved edges that extend back.

Rasetti (1956) also considers *Blountina triangularis* to be conspecific with *M. arion*. The two species share several characteristics supporting assignment of the former to *Maryvillia*, such as cranidial width to length ratios close to one, a glabella that is just slightly raised above the fixed cheeks, triangular posterolateral projections, and facial sutures that extend nearly straight forward from palpebral lobes. Differences in other characters indicate that they are, however, distinct species. *Maryvillia triangularis* differs most obviously by a triangular shaped anterior margin with an anterior border that is longest medially (sag.) rather than having an even length along the anterior cranidial margin, posterolateral projections that are directed posteriorly rather than transversely, and a pygidium that is narrower and distinctly subtriangular in outline. In the phylogenetic analysis, *M. arion* and *M. triangularis* form a distinct clade (Fig. 10).

Maryvillia triangularis (Lochman, 1944)

Plate 16, figs. A–K

1944 *Blountina triangularis* Lochman, in Lochman and Duncan, p. 57, pl. 8, figs. 12–18.

1956 *Blountina triangularis* Lochman; Rasetti, p. 1268 [included in list of species that Rasetti considered to be synonyms of *Maryvillia arion* Walcott].

Diagnosis.—Anterior border flat to concave, narrows laterally with well-incised border furrow; steeply sloping preglabellar field. Moderately convex glabella that narrows (tr.) anteriorly to a broadly rounded front, and very shallow axial furrows. Posterolateral projections long and triangular. Pygidium subtriangular in outline with faint border, axial, and pleural furrows that all weaken posteriorly. Pitting preserved on internal mold.

Types.—A holotype cranidia (USNM 127159; pl. 16, figs. A–C), paratype cranidia (USNM 127161, pl. 16, figs. D–K), and pygidia (USNM 127160c, pl. 17, figs. A–E; USNM 127160d, pl. 17, fig. F; USNM 127161, pl. 17, figs. G–J) from the Pilgrim Formation, Half Moon Pass section (Lochman and Duncan, 1944), Big Snowy Mountains, Montana.

Occurrence.— *Crepicephalus* Zone, Pilgrim Formation, Half Moon Pass section, Lochman and Duncan's (1944) horizon 9.2, Big Snowy Mountains, Montana.

Discussion.—Rasetti (1956) considers *Blountina triangularis* and *Maryvillia arion* (pl. 3, 4) to be indistinguishable. While they are certainly related, they are distinct species; *B. triangularis* has a more strongly curved anterior margin with an anterior that is longest medially (tr.) while *M. arion* has a more evenly rounded margin and an anterior border that maintains a more even length. The pygidia of *B. triangularis* are also more triangular in outline. See the discussion below for comparison of *B. triangularis* with *Blountina eleanora*.

The cranidium of *Blountia nasuta* resembles *Blountina triangularis* (= *Maryvillia triangularis*) by having a roughly triangular anterior margin and a glabella width about four-fifths its length, but it differs by having a longer frontal area (37% cranidial length, versus 28% in *Blountina triangularis*) with a longer preglabellar field (46% of frontal area, versus 30%) that slopes down at a gentler angle. The facial sutures of *Blountia nasuta* diverge abaxially from the palpebral lobes, whereas those of *Blountina triangularis* are nearly parallel. In addition, the glabella is more rounded anteriorly, more convex, and the posterolateral projections have curved sutural margins compared to the straight ones of *Blountina triangularis*. The pygidia of both *Blountia nasuta* and *Blountina triangularis* have triangular outlines with similar length-to-width proportions, and faint border furrows. The former species differs by having a border length of 25% of maximum tail length (sag.), compared to 15% in *Blountina triangularis* and fewer axial rings preserved on the internal mold (7–8, versus 10–11).

Genus *Blountina* Lochman, 1944

Type species.—*Blountina eleanora* Lochman, in Lochman and Duncan, 1944 from the Pilgrim Formation, Half Moon Pass, Big Snowy Mountains, Montana (by original designation).

Diagnosis.—Cranidia subtrapezoidal in outline. Frontal area around one-quarter cranidial length with down-sloping preglabellar field and flat to slightly down-sloping anterior border; separated by anterior border furrow. Glabella nearly parallel-sided with well-rounded front; convex and raised above down-sloping fixed cheeks. Pygidia semielliptical in outline, mostly effaced with weak axial furrows. Pleural furrows and at

least six axial rings plus the terminal piece expressed on the exfoliated surface. Exoskeleton smooth with pitting preserved on internal mold.

Discussion.— Shaw (1952) considered *Blountina* to be a junior synonym of *Protillaenus* Raymond (1937) and believed differences between them are due to the type species, *Proteillaenus marginatus*, being older than most species assigned to *Blountina*. Later, Rasetti (1956) treated both *Blountina* and *Proteillaenus* as synonyms of *Maryvillia*. New images of the type species, *Blountina eleanora*, (pl. 14) show that it is distinct from *Maryvillia*; *Blountina triangularis*, however, does appear congeneric with *Maryvillia arion*, and Rasetti's assignment of this species has been retained (see discussion above). *Protellaenus* is based on poorly preserved material, and the name is best restricted to the types.

Although the cranidia are very different, the pygidium of *Blountina eleanora* is more like that of *Kingstonia* than of *Maryvillia*. Both *Blountina eleanora* and *Kingstonia* (for examples see *K. gaspensis* in Rasetti, 1946, pl. 69, figs. 17–22; *K. peltata* in Westrop, 1992, fig. 14.1–14.13) have semi-subelliptical pygidia with a border that slopes down steeply and is a little under-folded. *Kingstonia* is more effaced on both the testate and exfoliated surfaces, but both taxa lack a defined border furrow as seen in *Maryvillia arion*. See discussion of *B. eleanora* for a more detailed comparison with *M. arion*.

Blountina eleanora Lochman, 1944

Plate 14, figs. A–J; Plate 15, figs. A–I

1944 *Blountina eleanora* Lochman, in Lochman and Duncan, p. 56, pl. 8, figs. 35–40.

non 2000 *Blountia eleanora* Lochman, in Lochman and Duncan; Stitt and Perfetta, p. 213, figs. 11.8–11.13 [=*Blountina* sp. indet].

Diagnosis.—Frontal area about one-quarter total cranidial length with steeply sloping preglabellar field. Cranidium is slightly wider than it is long with evenly rounded anterior margin. Strongly convex glabella has nearly parallel sides, well-rounded front end, and a shallow occipital furrow expressed on the exoskeleton. Posterolateral projections long, extend to a narrow, tapered point. Semi-subelliptical pygidium has well-incised axial furrows that shallow at the terminal piece, faint pleural and interpleural furrows, and a weak border furrow on the external surface. Internal mold preserves pitted sculpture.

Types.—A holotype cranidium (USNM 127156, pl. 14, figs. A–C), paratype cranidia (USNM 127158; pl. 14, figs. D–H), free cheek (USNM 127157a; pl. 14, fig. I), and pygidia (USNM 127158, pl. 14, figs. J, D–E, I; USNM 127157b, pl. 15, figs. A–C; USNM 127157c; pl. 15, figs. G–H) from the Pilgrim Formation, Half Moon Pass section (Lochman and Duncan, 1944), Big Snowy Mountains, Montana.

Occurrence.— *Crepicephalus* Zone, Pilgrim Formation, Half Moon Pass section, Lochman and Duncan's (1944) horizon 9.2, Big Snowy Mountains, Montana.

Discussion.—*Blountina eleanora* is the type species of the genus. *Blountina triangularis* (pl. 16, 17) was later reassigned to *Maryvillia* by Rasetti (1956). *Blountina eleanora* differs from *B. triangularis* by having a gently rounded anterior margin, a slightly shorter frontal area (24% of cranidial length verses 28% in *B. triangularis*) with an anterior border that is more even in length rather than longest medially, and a far

more convex glabella with a well-rounded rather than truncate front. The triangular pygidium of *B. triangularis* is very different from the semielliptical pygidium of *B. eleanora*, with a length to width ratio of 132% versus 62% in *B. eleanora*, a faint border furrow, and weakly incised axial furrows. Both species have pitted sculpture preserved on the internal mold and terrace ridges along the margins of the exoskeleton.

Rasetti also assigned *B. eleanora* to *Maryvillia* but there are several characteristics suggesting that they belong to separate genera. The cranidia of *B. eleanora* has a slightly inflated anterior border, a more strongly convex glabella with a well-rounded front, compared to the more truncated front in *M. arion*, and it has more defined axial furrows. The pygidia, as mentioned above, are more dissimilar; *M. arion* has around twelve axial rings plus the terminal piece, and *B. eleanora* has seven plus the terminal piece. The border furrow on *B. eleanora* is effaced and barely distinguishable on the internal mold, whereas *M. arion* has well-defined border furrow that weakens posteriorly, and the axis of *B. eleanora* terminates at the border while that of *M. arion* extends past the border furrow and ends mid-border.

References

Goloboff, P., Farris, J., and Nixon, K., 2008, TNT: a free program for phylogenetic analysis, Cladistics 24:774–786.

Lochman, C., and Duncan, D., 1944, Early Upper Cambrian Faunas of Central Montana: Geological Society of America Special Papers, v. 54, p. 1–172, doi: 10.1130/spe54-p1.

Nixon, K.C., 2002, WinClada ver. 1.00.08, published by the author, Ithaca, NY, U.S.A.

Palmer, A.R., 1954, The faunas of the Riley Formation in central Texas: Journal of Paleontology, v. 28, p. 709–786.

Palmer, A.R., 1962, *Glyptagnostus* and associated trilobites in the United States: U.S. Geological Survey Professional Paper, no. 374-F.

Palmer, A.R., 1965, Trilobites of the late Cambrian Pterocephaliid biomere in the Great Basin, United States: U.S. Geological Survey Professional Papers, no. 493.

Pratt, B.R., 1992, Trilobites of the Marjuman and Steptoean stages (Upper Cambrian), Rabbitkettle Formation, southern MacKenzie Mountains, northwest Canada: Calgary, Alta., Canadian Society of Petroleum Geologists.

Rasetti, F., 1946, Early Upper Cambrian trilobites from western Gaspé: Journal of Paleontology, v, 20., p. 442–462.

Rasetti, F., 1956, Revision of the trilobite genus *Maryvillia* Walcott: Journal of Paleontology, v. 30, p. 1266–1269.

Rasetti, F., 1961, Dresbachian and Franconian trilobites of the Conococheague and Frederick limestones of the central Appalachians: Journal of Paleontology, v. 35, p. 104–124.

Rasetti, F., 1965, Upper Cambrian trilobite faunas of northeastern Tennessee: Washington D.C., The Smithsonian Institution, The Smithsonian Miscellaneous Collections, v. 148, 128 p.

Resser, C.E., and Howell, B.F., 1938, Lower Cambrian *Olenellus* Zone of the Appalachians: Geological Society of America Bulletin, v. 49, p. 195–248, doi: 10.1130/GSAB-49-195.

Resser, C.E., 1942a, Fifth contribution to nomenclature of Cambrian fossils: Washington D.C., The Smithsonian Institution, The Smithsonian Miscellaneous Collections, v. 101.

Resser, C.E., 1942b, New Upper Cambrian trilobites: Washington D.C., The Smithsonian Institution, The Smithsonian Miscellaneous Collections, v. 103.

Shaw, A.B., 1952, Paleontology of Northwestern Vermont: II. Fauna of the Upper Cambrian Rockledge Conglomerate near St. Albans: Journal of Paleontology, v. 26, p. 458–483, doi:

Swofford, D., 2003, PAUP*: Phylogenetic Analysis Using Parsimony (* and Other Methods) Version 4, Sinauer Associates, Sunderland, MA, U.S.A.

Walcott, C.D., 1916, The Cambrian Fauna of Eastern Asia: Washington D.C., The Smithsonian Institution, The Smithsonian Miscellaneous Collections, v. 3.

Westrop, S.R., 1992, Upper Cambrian (Marjuman–Steptoean) Trilobites from the Port au Port Group, Western Newfoundland: Journal of Paleontology v. 66, p. 228–255, doi: 10.1017/s0022336000033758.

Table 2: Data matrix used in phylogenetic analysis. See Appendix B for characters.

Character	1	2	3	4	5	6	7	8	9
Kingstonia gaspensis	0	0	0	0	0	0	0	0	0
Blountia mimula	2	1	0	1	1	1	0	0	1
Blountia angela	2	2	0	1	1	1	1	0	1
Blountia bristolensis	1	2	0	1	1	1	1	0	1
Blountia cora	3	1	0	1	2	1	0	0	1
Blountia janei	3	1	0	1	2	1	0	0	1
Blountia montanensis	1	2	0	?	?	1	?	?	1
Blountia cf. *montanensis*	1	2	0	1	1	1	0	0	1
Blountia gaspensis	2	1	0	1	1	1	1	0	1
Blountia nasuta	3	1	0	0	2	1	0	0	1
Blountia nevadensis	2	2	0	1	1	1	1	0	1
Blountia morgancreekensis	2	1	0	1	1	1	1	0	1
Blountia newfoundlandensis	1	1	0	1	1	1	1	0	1
Maryvillia arion	3	2	1	1	1	0	0	1	2
Maryvillia triangularis	2	2	1	0	1	0	0	1	2
Blountina eleanora	1	2	1	1	1	1	0	0	1

Figure 12: Strict consensus of 3033 equally parsimonious trees computed from Branch-and-Bound (implicit enumeration) search. Number indicates node with a G.C. Bootstrap Support >50% (computed in WinClada; Nixon, 2002).

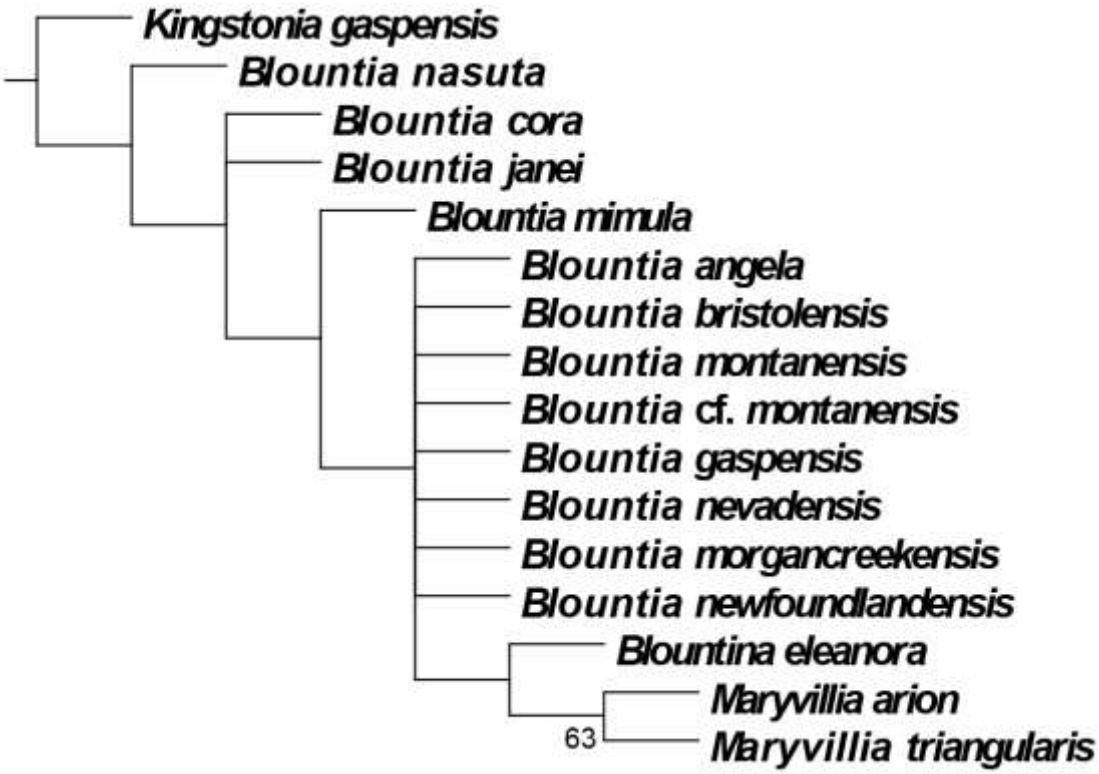
Kingstonia gaspensis
Blountia nasuta
Blountia cora
Blountia janei
Blountia mimula
Blountia angela
Blountia bristolensis
Blountia montanensis
Blountia cf. montanensis
Blountia gaspensis
Blountia nevadensis
Blountia morgancreekensis
Blountia newfoundlandensis
Blountina eleanora
Maryvillia arion
63
Maryvillia triangularis

Figure 13: Optimized character distribution with only unambiguous state changes (i.e. characters whose optimization does not differ between ACCTRAN and DELTRAN). Filled circles are states that optimize to one node and open circles are states that show homoplasy. The upper number is the character; the lower number is the character state (computed in WinClada; Nixon, 2002).

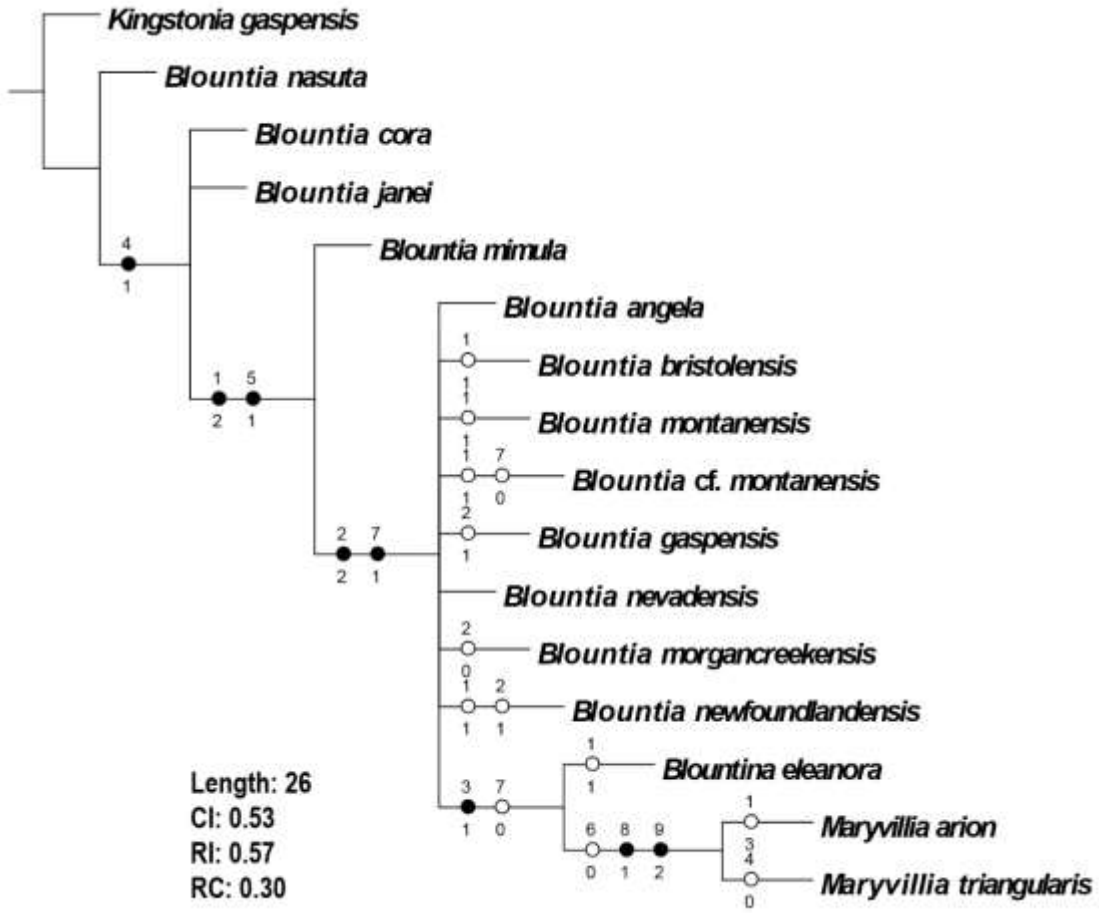
Kingstonia gaspensis
Blountia nasuta
Blountia cora
Blountia janei
Blountia mimula
Blountia angela
Blountia bristolensis
Blountia montanensis
Blountia cf. montanensis
Blountia gaspensis
Blountia nevadensis
Blountia morgancreekensis
Blountia newfoundlandensis
Blountina eleanora
Maryvillia arion
Maryvillia triangularis
Length: 26
CI: 0.53
RI: 0.57
RC: 0.30

Chapter IV: Genus *Aphelaspis*

Introduction

Although the base of the international Paibian Stage is defined by the first occurrence of the agnostoid arthropod, *Glyptagnostus recticulatus* (Angelin) (Peng et al., 2004), across most of Laurentian North America, it is approximated by the base of the Steptoean Stage (Ludvigsen and Westrop, 1985; Palmer, 1998). The appearance of species of *Aphelaspis* Resser, 1935 near the base of the Steptoean is a characteristic feature of Laurentian trilobite faunas (e.g., Palmer, 1984, fig. 5), so that this genus is of considerable biostratigraphic significance. Modern studies of the succession of *Aphelaspis* species began with the pioneering work of Palmer (1954) on the Riley Formation of central Texas, which is now 60 years old. Here *Aphelaspis* from Texas is revised for the upper Cap Mountain and lower Lion Mountain members of the Riley Formation. Some species named by Palmer (1954) are known from only single specimens (e.g., *A. spinosa*; *A. constricta*), and new material adds significantly to knowledge of variability.

Stratigraphic Setting

Texas.—Palmer (1954) recognizes four species of *Aphelaspis* in the Riley Formation of central Texas. He assigned specimens from the *Aphelaspis* Zone of the Cap Mountain Limestone and Lion Mountain Sandstone members to *A. walcotti* Resser 1938a, which Rasetti (1965) pointed out is likely a misidentification. Material here reveals those

similar to *A. walcotti* likely represents more than one new species and is given open nomenclature of *A.* cf. *walcotti*; it ranges throughout the *Aphelaspis* Zone (*Aphelaspis spinosa* zone and *Aphelaspis longifrons* Zone). *Aphelaspis spinosa* Palmer 1954 is exclusive to central Texas and ranges through the *Aphelaspis spinosa* zone in the Cap Mountain member. *Aphelaspis constricta* Palmer 1954 and *A. longifrons* Palmer 1954 are also only found in the Riley Formation and are restricted to the *Aphelaspis longifrons* Zone in the upper Cap Mountain Limestone.

Tennessee and Virginia.— *Aphelaspis walcotti* Resser 1938a is documented from the Nolichucky Formation in Tennessee as well as in Virginia. Rasetti (1965) documents several species of *Aphelaspis* from the Appalachian region. *Aphelaspis tarda* Rasetti 1965 is recorded in the upper *Aphelaspis* Zone in Virginia. *Aphelaspis buttsi* (Kobayashi) 1936 and *Aphelaspis lata* Rasetti 1965 are both found in the lower *Aphelaspis* Zone in Tennessse. *Aphelaspis camiro* (Walcott) 1916 is documented at Shield's Ridge in the lower mid-*Aphelaspis* Zone. Higher stratigraphically, *Aphelaspis arses* Rasetti 1965 is documented near Maryville, and above that *Aphelaspis arsoides* Rasetti 1965 is documented in the middle *Aphelaspis* Zone in Tennessee.

Systematic Paleontology

Family Pterocephaliidae Kobayashi, 1935

Subfamily Aphelaspidinae Palmer, 1960

Genus *Aphelaspis* Resser, 1935

Type species.—*Aphelaspis walcotti* Resser 1938 Upper Cambrian, Nolichucky Formation, Virginia (proposed as a replacement for *Conocephalites depressus* Shumard by Palmer, 1953).

Discussion.— The nomenclatural history of the type species of *Aphelaspis* is complicated, and a previous suggestion that *Aphelaspis walcotti* Resser occurs in Texas (Palmer, 1953, 1954) is doubtful (Rasetti, 1965, p. 77; see also following discussion). Shumard (1861) named *Conocephalites depressus* for material from what is now the Cap Mountain Member of the Riley Formation in central Texas. He provided a written description but no illustration, and the types were apparently destroyed in a fire (Resser, 1935). Nonetheless, Resser (1935, pp. 11, 12) designated *C. depressus* as the type species of a new genus, *Aphelaspis*, and noted that "Walcott long ago set aside specimens as the species, and since they agree with Shumard's description, little doubt of their identity remains." This implies that Walcott's intended to propose a neotype prior to his death in 1928. Bridge and Girty (1937, pl. 69, figs. 25, 26) subsequently illustrated some of Walcott's specimens under the name of *A. depressa* (Shumard). However, Palmer (1953) asserted that Bridge and Girty's specimens did not in fact match Shumard's description (although he did not specify how they differed), and claimed instead that these specimens were conspecific with *A. walcotti* Resser, 1938 from the Nolichucky Formation of Tennessee. Palmer also indicated that he would request that the International Commission on Zoological Nomenclature (ICZN) establish *A. walcotti* as type species and add *Aphelaspis* to the official list of names in zoology. However, the list of names as updated in 2012 does not include *Aphelaspis*,

and there is no numbered opinion on the status of *A. walcotti*; apparently no petition was ever made to the ICZN on this matter. The ICZN allows authors to preserve established usage of the type species of a genus in the interests of stability without making an application to the Commission. Palmer's proposed designation of *Aphelaspis walcotti* has been followed in all subsequent studies that indicate the type species (e.g., Palmer 1962, 1965; Jago, 1987; Pratt, 1992; Cooper et al., 1996; Lee and Chatterton, 2005), even when the occurrence of the species in Texas has been questioned (Rasetti, 1965). It certainly meets the criteria for preserved usage under the ICZN.

Aphelaspis cf. *walcotti* (Resser, 1938a)

Plate 27, figs. A–J; Plate 28, figs. A–H

cf. 1938a *Aphelaspis walcotti* Resser, p. 59, pl. 13, fig. 14.

cf. 1954 *Aphelaspis walcotti* Resser, in Palmer, p. 746, pl. 84, figs. 2, 4–7 (only; fig. 8 is a pygidium that does not seem conspecific with *A. walcotti*; see for synonymy).

cf. 1962 *Aphelaspis walcotti* Resser, in Palmer, pl. 4, figs. 24, 28, 33.

cf. 1965 *Aphelaspis walcotti* Resser, in Rasetti, p. 76, pl. 18, figs. 10–20 (see for synonymy).

Diagnosis.—Long frontal area, approximately 35% of cranidial length, with steeply sloping, slightly concave preglabellar field and a flat to gently upturned anterior border; border furrow shallow. Free cheek extends to pointed spine and is truncated anteriorly by anterior branch of facial suture; lateral border comprises one-third of free cheek width. Pygidium over twice as wide as is long. Axis width nearly equal to its length,

comprising one-third of pygidial width. Axis has three axial rings plus terminal piece. Pleural furrows shallow. External surface smooth, internal mold may preserve fine, dense pitting.

Holotype.—Cranidium from the Nolichucky Shale, Virginia (Resser 1938a, p. 59, pl. 13, fig. 14)

Material.—Cranidia (OU 238054–238056, OU 238059–238062), a free cheek (OU 238058), a pygidium (OU 238057), and several unfigured sclerites from the Riley Formation, Texas.

Occurrence.—*Aphelaspis spinosa* and *Aphelaspis longifrons* Zones, Cap Mountain Member, Riley Formation, Burnet County, Texas, Lake Buchanan (LB) and Morgan Creek North (MCN and MCNe1) sections, collections MCNe1 2.1, LB -0.15, LB 0.30, MCNe1 5.8–5.9, LB 0.50–0.70, LB 0.80, LB 0.90–0.10, LB 1.40, MCNe1 7.10, LB 2.10, LB 2.15, LB 3.40.

Description.—Cranidium exclusive of posterolateral projection rectangular in outline with a rounded anterior margin, cranidial width at posterior end of palpebral lobe is 80% its length (81; 66–94). Anterior border flat to gently upturned, varies from having near-equal length across (pl. 28, fig. C) to having greatest length medially and shortening abaxially (pl. 27, fig. A). Frontal area about one-third (35%; 30–40) cranidial length. Preglabellar field slightly convex and steeply sloping, differentiated from anterior border by slope change; border furrow shallow on exoskeleton, better defined on internal mold. Axial and preglabellar furrows moderately incised. Glabella subtrapezoidal in outline, narrowing anteriorly to a slightly rounded front; gently

convex and raised above fixed cheeks. Three pairs of glabellar furrows weakly expressed only on internal mold; furrows straight to gently curved, increasing angularity from near transverse at S3 to 45 degrees backward at S1. SO shallow, becoming indistinguishable adaxially; moderately impressed on exfoliated surface. LO length less than one-fifth (sag.) (17%; 12–20) of the total glabellar length; small, gently raised median node may be present. Palpebral area is flat to slightly down-sloping; total fixed cheek width at the palpebral area vary in width, but average 40% (39; 30–47) of cranidial width. Palpebral lobe is crescent-shaped band, approximately one-fourth (27%; 23–33) cranidial length, with gently incised furrow. Convex ocular ridges extending obliquely from anterior end of palpebral lobe to anterolateral corner of glabella faintly expressed on exoskeleton, but typically well-defined on internal mold. Anterior branches of facial sutures diverge from palpebral lobes then sharply curve in at anterior border to a rounded margin. Posterior branches extend backward along a curved path. Posterior border furrow well-incised, shallowing adaxially. Postocular areas slope down steeply into tapered posterolateral projections. Entire exoskeleton smooth. Except for furrows and glabella, internal mold often preserves fine, dense pitting.

Free cheek extends into long, pointed genal spine. Border flat, about one-third (33%; 27–39) total cheek width at anterior margin; differentiated from moderately convex librigenal field by slope change; lateral border furrow shallow. Posterior border furrow meets lateral furrow, extending halfway down spine, shallowing posteriorly. Anteriorly the border is cut by facial suture, narrowing into long projection. Eye socle raised above well above cheek field. Genal spine may have caecal markings on

exoskeleton. Exfoliated cheek preserves fine pitting, increasing in density towards border.

Pygidium over twice as wide as it is long, (length 44% of width; 43–45). Pleural band transverse from axis, then curves back about 30 degrees until reaching maximum pygidial width about mid-length, then gently curves towards the axis. Articulating half-ring similar length as axial rings, gently curved, tapering before reaching either end of the axis. Articulating furrow well-incised, about half the length of half-ring. Axis strongly convex above pleural field. Maximum axis width about one-third (36%; 34–39) maximum pygidium width; axis length 85% (81–88) pygidial length (sag.). Maximum axis width is approximately that of the axis length (100%; 93–108). Two or three axial rings, plus terminal piece; axial rings shorten adaxially and well-defined furrows expand between, becoming successively shallower towards rear of axis. Lateral and posterior fields down-sloping, increasing steepness towards border; convex median peak on posterior border. Two or three pairs of pleural and interpleural furrows expressed on exfoliated surface; anterior-most furrows deepest and are gently expressed on exoskeleton. Outer surface smooth, internal mold preserves fine pitting with decreased density on furrows.

Discussion.— Palmer assigned cranidia with variable features from the Riley Formation (1954, pl. 84, figs. 2, 4–8) to *Aphelaspis walcotti*. Rasetti (1965) expressed doubt that *Aphelaspis walcotti* was present in Texas due to the variability in Palmer's figured specimens. The pygidium Palmer assigned (1954, pl. 84, fig. 8) to *A. walcotti* is undoubtedly misidentified; it has a posterior margin that is nearly transverse rather than semielliptical and is not as wide compared to specimens in the type collection from

Virginia (Palmer, 1962, pl. 4, fig. 33). A figured cranidia from the type collection of *A. walcotti* (Palmer, 1962, pl. 4, fig. 24) has a frontal area of 37%, which is similar to the Riley Formation specimens (35%; 30–39); but the anterior border comprises half of the frontal area, compared to an average of 41% (32–46%) in Texas. Rasetti (1965, pl. 18. figs. 10–20) identifies specimens in Tennessee as *A. walcotti* and describes them as having a frontal area 60% the glabellar length; the type material in Palmer (1962) is 65% and the Texas specimens have a frontal area averaging 50% (53; 42–65). Rasetti (1965) notes that the relative proportion of the anterior border and preglabellar field, as well as the slope of the preglabellar field, is often are variable within a population, which is observed in Texas (anterior border comprises 41%; 32–50 of frontal area). This proportional variation, in addition to variation in pygidia of the Texas specimens leads to speculation that there is more than one species, of which none may be conspecific with *A. walcotti*. Further review with type specimens is needed, so here the Texas specimens are placed in open nomenclature of *Aphelaspis* cf. *walcotti*.

Aphelaspis cf. *walcotti* in Texas closely resembles *Aphelaspis tarda* Rasetti (1965; pl. 20, figs. 1–18). Relative proportions of the cranidia are nearly the same. The glabella of *A. tarda* narrows slightly more anteriorly and the palpebral areas of *A. walcotti* are typically flat, whereas *A. tarda* tend to be upsloping. Furrows on the free cheek of *A. tarda* are more defined and seem to extend into a longer genal spine. The maximum pygidial width of *A. tarda* is less than twice its length (width 1.8 times length, compared to 2.3 in *A.* cf. *walcotti*), and the border along the sagittal line is longer (27% pygidial length, compared to 14%). The articulating half-ring of *A.* cf. *walcotti* narrows abaxially

and is longer medially than in *A. tarda* (18% of axis length, compared to 10%) (Rasetti, 1965, pl. 20, fig. 16), which has an even length.

Aphelaspis constricta Palmer, 1954

Plate 29, figs. A–H; Plate 30, figs. A–I; Plate 31, figs. A–I.

1954 *Aphelaspis constricta* Palmer, p. 745, pl. 84, fig. 11.

Diagnosis.—Evenly rounded anterior margin, frontal area less than one-third cranidial length; very short anterior border (30%; 23–41 of frontal area) separated from long preglabellar field by shallow border furrow. Anterior border upturned and gently arched. Anterior branches of facial sutures extend straight forward or slightly diverge from palpebral lobes.

Holotype.—Cranidium from the *Aphelaspis* Zone, Lion Mountain Member, Riley Formation, Lion Mountain section (now flooded by Lake Buchanan; Palmer, 1954, p. 782), Burnet County, (USGS collection 8, 60.96 m [200 feet]—62.48m [205 feet] above the base of the section; Palmer, 1954, p. 786) Texas (Palmer 1954, p. 745, pl. 84, fig. 11).

Material.—Cranidia (OU 238063–238074) and additional, unfigured cranidia from the Riley Formation, Texas.

Occurrence.—*Aphelaspis longifrons* Zone, Cap Mountain Member (collections HP 2.5 Pulloff and HP 2.6 Pulloff) and Lion Mountain Member (Palmer, 1954, U.S.G.S. collections 8), Riley Formation, Texas.

Discussion.—*Aphelaspis constricta* is an uncommon species associated with *A. longifrons*. It is distinguished from the other Texas species by a frontal area less than one-third (30%; 22–32) of total cranidial length, a short anterior border (31%; 23–43; smaller individuals have longer borders), and by the anterior branches of the facial sutures which extend straight forward or slightly diverge out from the palpebral lobes, as opposed to the greater divergence expressed in the other species. The width of the cranidium of *A. constricta* at the palpebral area is a little less than its sagittal length (94%; 88–97). This is greater than that of *A.* cf. *walcotti* (80%; 66–87), *A. longifrons* (74%; 65–85), and *A. spinosa* (74%). It most closely resembles *A.* cf. *walcotti* in general morphology, including the presence of a small, slightly raised median occipital node. The anterior border of *A.* cf. *walcotti* is typically flat, whereas *A. constricta* is gently arched in anterior view. Like *A. spinosa*, the external surface may be finely pitted (pl. 29, fig. A) but can also be smooth like the other species.

Aphelaspis constricta is comparable to *A. buttsi* Kobayashi from Tennessee (Rasetti, 1965, pl. 16, figs. 1–7) and Alabama (Palmer, 1962, pl. 4, figs. 23, 26, 31, 32) as both have a short frontal area less than one-third of cranidial length with a short anterior border comprising one-third of frontal area. *Aphelaspis buttsi* has a more defined anterior border furrow and more impressed lateral glabellar furrows on the exfoliated surface. *Aphelaspis lata* (Rasetti, 1965, pl. 16, figs. 8–20) from Tennessee also has a short anterior border, one-third of the frontal area, but has a slightly longer frontal area, 33% of cranidial length (sag.) and deeper dorsal furrows on the cranidium.

Aphelaspis longifrons Palmer, 1954

Plate 32, figs. A–G; Plate 33, figs. A–G; Plate 34, figs. A–G

1954 *Aphelaspis longifrons* Palmer, p. 745, pl. 84, figs. 9, 12, pl. 85, figs. 2, 3.

Diagnosis.— Differentiated from other *Aphelaspis* species by very long frontal area, about 40% of cranidium length. Anterior margin well-rounded. Preglabellar field moderately down-sloping into flat anterior border; border furrow shallow. Anterior border often longest medially, comprising half (55; 37–67) of the frontal area. Free cheek border makes up half of cheek width on lateral margin; long genal spine and anterior projection present. Pygidium up to twice as wide as it is long, border well-rounded. Two to three axial rings. Furrows faint on external surface. Entire surface smooth, internal mold preserves fine pitting, with increased density and caecal venation on the preglabellar field.

Holotype.—Cranidium from *Aphelaspis* Zone, Riley Formation, Texas (Palmer 1954, p. 745, pl 85, fig. 2).

Material.—Cranidia (OU 238076–238078, OU 238082–238085), free cheeks (OU 238075, OU 238080), pygidia (OU 238079, OU 238081, OU 238086), and additional, unfigured sclerites from the Riley Formation, Texas.

Occurrence.—*Aphelaspis longifrons* Zone, Cap Mountain Limestone, Riley Formation, Hoover Point section, collections HP 2.5 Pulloff, HP 2.6 Pulloff, LB 2.10, LB 2.15, and LB 4.45.

Discussion.—*Aphelaspis longifrons* is differentiated from other species of the genus by its long, well-rounded frontal area that is approximately 40% (34–44) of total cranidium

length (sag.), long anterior border (55%; 37–67 of frontal area), and the lack of a median node or spine on its occipital ring. Among species that also occur in the Riley Formation, *A.* cf. *walcotti* and *A. spinosa* both have a frontal area comprising an average of 35% cranidium length, and *A. constricta* is less than one-third. The anterior border of *A. longifrons* makes up over half of the frontal area (sag.), which is on average greater than that of *A.* cf. *walcotti* (41%; 41–50), *A. constricta* (43%; 42–44), and *A. spinosa* (43%; 41–45). The preglabellar field slopes down at a shallower angle and often preserves caecal markings on the exfoliated surface, which is not seen in the other Texas species. The free cheek of *A. longifrons* is similar to that of *A.* cf. *walcotti*, but has a longer border, comprising half (48%; 47–52) of the cheek width at the anterior margin.

Aphelaspis longifrons is most similar to *A. camiro* Walcott (Rasetti 1965, pl. 12, figs. 1–17), both of which have a long frontal area, approximately 40% of the cranidial length (sag.). The anterior border comprises a larger portion of the frontal area in *A. longifrons* (55% versus 42% in *A. camiro*), and the preglabellar field slopes somewhat more gently. Due to a sharper slope, the anterior border furrow in *A. camiro* is more defined. The palpebral areas are upsloping in *A. camiro* (Rasetti, 1965, pl. 12, fig. 5) whereas they are flat in *A. longifrons* (pl. 34, fig. F). Both species have unusual pygidia that are well-rounded and not as wide as the other Texas *Aphelaspis* species (width 1.5 times the length in *A. longifrons*; 1.8 times in *A. camiro*). The furrows on *A. camiro* are more strongly incised, including the anteriormost set of pleural furrows, which are effaced on *A. longifrons*. *Aphelaspis camiro* has three or four axial rings compared to two in *A. longifrons*.

Aphelaspis spinosa Palmer, 1954

Plate 35, figs. A–J; Plate 36, figs. A–H; Plate 37, figs. A–J

1954 *Aphelaspis spinosa* Palmer, p. 746, pl. 84, fig. 10.

Diagnosis.— *Aphelaspis* with long occipital spine and conspicuous pitted sculpture on the testate surface; anterior border maintains nearly constant width (sag., exsag.).

Holotype.—Cranidium from *Aphelaspis* Zone, Riley Formation, Texas (Palmer 1954, pg. 746, pl. 84, fig. 10).

Material.—Cranidia (OU 238087–238088, OU 238091–238092, OU 238094–238095), a free cheek (OU 238097), pygidia (OU 238089–238090, OU 238093, OU 238096), and additional sclerites from the Riley Formation, Texas.

Occurrence.—*Aphelaspis longifrons* Zone, Cap Mountain Limestone, Riley Formation, Morgan Creek North (MCN) and Lake Buchanan (LB) sections, collections MCNe1 2.10, LB -0.15, MCNe1 5.80–5.90, LB 0.90–1.0.

Discussion.—*Aphelaspis spinosa* has a cranidium similar to *A.* cf. *walcotti*, including the frontal area length, rounded anterior margin, but primarily differs by the presence of a median spine on the occipital ring and having dense pitting on the exoskeleton. The anterior border of *A. spinosa* is also slightly longer (45% of frontal area (sag.), compared to 40% in *A.* cf. *walcotti*). Many individuals of *A.* cf. *walcotti*, as well as *A. constricta*, bear a small, median occipital node, which could be a homologous feature. Palmer (1954) suggested *A.* cf. *walcotti* and *A. spinosa* could be dimorphs of a single species, but the former extends through a thicker stratigraphic interval.

Aphelaspis spinosa resembles *A. arses* Walcott (Rasetti 1965, pl. 13, figs. 16–22) from the Nolichucky Formation, Tennessee, which also has an occipital spine. *Aphelaspis arses* differs by having more divergent anterior branches of the facial sutures and the preglabellar field is proportionately longer, occupying nearly three-quarters of the frontal area (73%, versus less than 60% [57%] in *A. spinosa*), and the anterior border correspondingly shorter. The occipital furrow of *A. arses* is also more incised medially than *A. spinosa*, but the furrow shallows abaxially in both species. The posterior border furrow is less defined in *A. spinosa* and its posterolateral projections do not extend as far. Palpebral lobe length in *A. arses* is about one-quarter the sagittal cranidial length, compared to about one-fifth on *A. spinosa* (Palmer 1954, pl. 84, fig. 10). *Aphelaspis arsoides* Rasetti (1965; pl. 11, figs. 15–21), also from the Nolichucky Formation, is another similar species, differing from both *A. spinosa* and *A. arses* by possessing more prominent ocular ridges, anterior branches of facial sutures that diverge more, and the presence of dense pitting in the furrows.

References

Bridge, J., and Girty, G.H., 1937, A redescription of Ferdinand Roemer's Paleozoic types from Texas: U.S. Geological Survey Professional Paper, no. 186-M.

Cooper, R.A., Jago, J.B., and Begg, J.G., 1996, Cambrian trilobites from Northern Victoria Land, Antarctica, and their stratigraphic implications: New Zealand Journal of Geology and Geophysics, v. 39, p. 363–387, doi: 10.1080/00288306.1996.9514720.

Jago, J.B., 1987, Idamean (Late Cambrian) trilobites from the Denison Range, south-west Tasmania: Palaeontology, v. 30, p. 207–231.

Lee, D.C., and Chatterton, B.D., 2005, Protaspides of Upper Cambrian *Aphelaspis* (Ptychopariida, Trilobita) and related species with their taxonomic implications: Palaeontology, v. 48, p. 1351–1375, doi: 10.1111/j.1475-4983.2005.00509.x.

Ludvigsen, R., and Westrop, S.R., 1985, Three new Upper Cambrian stages for North America: Geology, v. 13, p. 139–143, doi: 10.1130/0091-7613(1985)13<139:tnucsf>2.0.CO;2.

Palmer, A.R., 1953, *Aphelaspis* Resser and its genotype: Journal of Paleontology, v. 27. p. 157–157.

Palmer, A.R., 1954, The faunas of the Riley Formation in central Texas: Journal of Paleontology, v. 28, p. 709–786.

Palmer, A.R., 1962, *Glyptagnostus* and associated trilobites in the United States: U.S. Geological Survey Professional Paper, no. 374-F.

Palmer, A.R., 1965, Trilobites of the late Cambrian Pterocephaliid biomere in the Great Basin, United States: U.S. Geological Survey Professional Papers, no. 493.

Palmer, A.R., 1984, The biomere problem: evolution of an idea: Journal of Paleontology, v. 58, p. 599–611.

Palmer, A.R., 1998, A proposed nomenclature for stages and series for the Cambrian of Laurentia: Canadian Journal of Earth Sciences, v. 35 p. 323–238, doi: 10.1139/e97-098.

Peng, S.C., Babcock, L.E., Robison, R.A., Lin, H., Rees, M.N., and Saltzman, M.R., 2004, Global Standard Stratotype-section and Point (GSSP) of the Furongian Series and Paibian Stage (Cambrian): Lethaia, v. 37, p. 365–379, doi: 10.1080/00241160410002081.

Pratt, B.R., 1992, Trilobites of the Marjuman and Steptoean stages (Upper Cambrian), Rabbitkettle Formation, southern MacKenzie Mountains, northwest Canada: Calgary, Alta., Canadian Society of Petroleum Geologists.

Rasetti, F., 1965, Upper Cambrian trilobite faunas of northeastern Tennessee: Washington D.C., The Smithsonian Institution, The Smithsonian Miscellaneous Collections, v. 148, 128 p.

Resser, C.E., 1935, Nomenclature of some Cambrian trilobites: Washington D.C., The Smithsonian Institution, The Smithsonian Miscellaneous Collections, v. 93, 46 p.

Resser, C. E., 1938, Cambrian System (restricted) of the southern Appalachians: Geological Society of America, Special Paper no. 15.

Shumard, B.F., 1861, The primordial zone of Texas, with descriptions of new fossils: American Journal of Science, v. 32, p. 213–221, doi: 10.2475/ajs.s2-32.95.213.

Chapter V: Other Genera in the Riley Formation

Systematic Paleontology

Illustrated material is kept at the National Museum of Natural History, Washington, D.C. (USNM) and at the Oklahoma Museum of Natural History, University of Oklahoma (OU). The images were rendered from stacks of images focused at 100 micron intervals using Helicon Focus 4.0 for the Macintosh <http://www.heliconsoft.com>.

Family Cheilocephalidae Shaw, 1956

Genus *Cheilocephalus* Berkey, 1898

Type species.—*Cheilocephalus st. croixensis* Berkey, 1898, Upper Cambrian, Minnesota (by original designation).

Discussion.—*Cheilocephalus* was revised by Westrop et al. (2008), and their diagnosis is used in this paper.

Cheilocephalus brevilobus Walcott, 1916

Plate 38, figs A–F

1916 *Lisania*? *breviloba* Walcott, p. 404, pl. 66, figs. 3–3c.

1954 *Cheilocephalus breviloba* (Walcott); Palmer, p. 759, pl. 88, figs. 1–4.

2008 *Cheilocephalus brevilobus* (Walcott); Westrop et al., p. 734, figs. 5a–i (see for synonymy).

Holotype.—An articulated cranidium and thorax (USNM 62852) from the Nolichucky Formation, Greene County, Tennessee (Westrop et al., 2008, figs. 5a–d).

Material.—Two cranidia (OU 238103–238104) from the Lion Mountain Sandstone, Riley Formation, Texas.

Occurrence.— *Blandicephalus texanus* Zone, Lion Mountain Sandstone, Riley Formation, Burnett County, central Texas, collections HP 3.70, HP 4.50.

Diagnosis.—See Westrop et al., 2008, p. 734.

Description.—Cranidium subtrapezoidal in outline, width nearly equal to sagittal length at posterior end of palpebral lobes. Anterior margin broad, evenly rounded. Frontal area around 15% cranidial length. Axial furrows narrow, shallow groove. Glabella gently convex, raised above down-sloping fixed cheeks; subtrapezoidal in outline, narrowing anteriorly; width about two-thirds its length at posterior end of palpebral lobe. Glabella comprises at least half of cranidial width at palpebral lobes. Glabellar furrows effaced on exoskeleton, three faint pairs preserved on internal mold. LO expands medially, about 15% of glabellar length (sag.). SO weakly impressed medially; deepens and narrows abaxially. Palpebral lobe located anteriorly of mid-glabellar length; small curved band, about one-tenth cranidial length. Palpebral ridge gently raised, directed obliquely from palpebral lobe to anterolateral corner of glabella. Anterior branches of facial sutures diverge slightly from palpebral area, then curve in sharply along anterior margin. Posterior branches extend about 20 degrees from transverse plane, then sharply curve back to rounded corner. Posterior border furrow well-incised groove, weakening towards genal angle; follows gently curved path across posterolateral projection.

Subtriangular flange present mid-way along posterior margin. Exoskeleton smooth with fine, sparse pitting and caecae along margins.

Pygidium semi-subelliptical in outline, sagittal length more than half maximum width. Small flange on anterior margin, halfway between axis and lateral margin. Articulating half-ring very short, less than half the length of axial rings. Axis convex, raised well above pleural field; anterior width comprises about one-third pygidial width. Six to seven axial rings, terminal piece small. Axial ring furrows nearly transverse, slightly curved medially; furrows moderately impressed, weakening posteriorly, last one or two indistinct on internal mold. Pleural and interpleural furrows faintly expressed on exoskeleton, better defined on exfoliated surface. Pleural field down-sloping into slightly concave border. Border about 15% pygidial length along sagittal axis; border furrow moderately incised. Anterior pleural furrow deep groove, directed obliquely back from axis to border furrow, then weakening and extending nearly transverse across border. Exoskeleton smooth except fine pitting along margin of pygidium.

Discussion.—Palmer (1954) identified two species of *Cheilocephalus* in the Riley Formation: *C. brevilobus* and *C. minutus* Palmer (1954; pl. 88, figs. 5–6, 8). Lochman and Hu (1962) considered that Palmer's holotype cranidium of *C. minutus* to belong to *C. brevilobus* and the paratype pygidia to *Maryvillia*. Compared to *C. brevilobus*, the cranidium (Palmer, 1954, pl. 88, fig. 5) of *C. minutus* differs in having a more rounded anterior margin of the cranidium, and the posterior branches of the facial sutures are less divergent. The paratype pygidia (Palmer, 1954, pl. 88, figs. 6, 8) of *C. minutus* differ unequivocally from the type species of *Maryvillia, M. arion* Walcott (see Chapter

III), in having far fewer segments (five distinct axial rings versus nine to ten in *M. arion*). The pygidium of *C. brevilobus* differs from *C. minutus* by having better defined pleural furrows and shorter, deeper axial ring furrows on the exfoliated surface, and a noticeably longer border (equal to 18% of pygidial length) that is distinctly concave, rather than down-sloping. Although the types of *C. minutus* are small specimens, similarly sized sclerites of *C. brevilobus* (Palmer, 1954; pl. 88, fig. 3–4) still display differences in morphology outlined above. According to Palmer's (1954, p, 759) occurrence data, *C. minutus* has a shorter stratigraphic range than *C. brevilobus*, and is confined to the lower *Aphelaspis* Zone, rather than extending throughout the zone. There is ample evidence to consider *C. minutus* to be a distinct species.

The pygidium of *C. brevilobus* from MCS 4.5 has shallower furrows and is longer (length equal to 70% of width) relative to Palmer's (1954, pl. 88, figs. 2, 4) figured specimens (65%) and the paratype (Westrop et al., 2008, fig. 5e) from Tennessee (58%). These differences seem to be size-related and may be ontogenetic in nature. There is evidence for other, size-related, possibly ontogenetic variation in *Cheilocephalus* pygidia. For example, Rasetti (1965, pl. 17, fig. 1) figured a large pygidium of *C. brevilobus* with about seven axial rings and an appreciably longer than border (32% sagittal length compared to around 15% in smaller specimens). Similarly, the *Cheilocephalus* pygidia illustrated by Lochman and Hu (1962, pl. 69, figs. 16–17, 19–24) and of *C. hisingeri* Billings (1965) from the Shallow Bay Formation in western Newfoundland (Westrop et al., 2008; fig. 4a–h) show a trend of increased border length with increasing specimen size, supporting this interpretation.

Cheilocephalus cf. *granulosus* (Palmer, 1965)

Plate 39, figs. A–G

cf. 1962 *Cheilocephalus breviloba* Walcott; in Lochman and Hu, p. 436, pl. 69, figs. 1–24.

cf. 1965 *Cheilocephalus granulosus* Palmer, p. 31, pl. 1, figs. 6–8.

?1992 *Cheilocephalus granulosus* Palmer; in Pratt, p. 69, pl. 24, fig. 7.

non 2008 *Cheilocephalus* cf. *granulosus* Palmer; in Westrop et al., 2008, p. 736, figs. 6a–k, 7a–g.

Material.—Two cranidia (OU 238105–238106) and additional, unfigured sclerites from the Cap Mountain Limestone, Riley Formation, Texas.

Occurrence.—*Aphelaspis spinosa* Zone, Cap Mountain Limestone, Riley Formation, Burnet County, Texas, collections MCNe1 2.10, LB -0.15, MCNe1 5.80–5.90.

Discussion.—The holotype cranidium of *C. granulosus* Palmer (1965, pl. 1, fig. 6) is an incomplete specimen, making it difficult to give a confident identification. Lochman and Hu (1962) identify specimens (1962, pl. 69, fig. 1–24) from Montana as *C. brevilobus* and describe them as having fine granulated sculpture. However, among Walcott's types of *C. brevilobus*, cranidia that retain the exoskeleton are characterized by smooth surfaces (Westrop et al., 2008, fig. 5h), and Palmer suggested that the Montana specimens may in fact be conspecific with *C. granulosus*. *Cheilocephalus* cranidia collected from the upper *Aphelaspis* Zone in Texas are similar to the Montana specimens by having long frontal areas and subtrapezoidal glabellas. They also resemble the *C. granulosus* type specimen by having a long frontal area and granulated surface. Pratt (1992, pl. 24, fig. 17) figures a fragmented pygidium as *C. granulosa*, but

its condition prevents a confident identification. *C. brachyops* Palmer (1965, pl. 1, fig. 12–15, 17) is another granulose species, but differs from the Texas specimens by having a very short frontal area and more rectangular glabella.

Family Elviniidae Kobayashi, 1935

Genus *Dunderbergia* Walcott, 1924

Type species.—*Crepicephalus* (*Loganellus*) *nitidus* Hall and Whitfield, 1877, Dunderberg Formation, Nevada (by original designation).

Dunderbergia cf. *variagranula* (Palmer, 1954)

Plate 40, figs. A–I

cf. 1954 *Dunderbergia variagranula* Palmer, p. 761, pl. 88, figs. 7, 9–10; pl. 89, fig. 1.

Material.—Two cranidia (OU 238114–238115), two pygidia (OU 238116–238117), and additional, unfigured sclerite from the Riley Formation, Texas.

Occurrence.—*Blandicephalus texanus* Zone, Lion Mountain Sandstone, Riley Formation, Burnet County, Texas, collections HP 3.10, 3.65, 3.70, 3.75, and MCS 4.50.

Discussion.—Palmer (1954) named *D. variagranula* and diagnosed it as a variable species with either an exoskeleton covered in granules of various coarseness and density (Palmer, 1954; pl. 88. figs. 7, 9, 10) or a smooth surface (Palmer, 1954; pl. 89, fig. 1); granulose specimens were more abundant in Palmer's collections. In a subsequent work that included observations on variability of samples from Nevada and Utah, he (Palmer, 1960, p. 68) concluded that the material from Texas represented two distinct species, and he restricted *D. variagranula* to the granulose holotype. Specimens with a smooth

exoskeleton may represent a new species, but time did not permit more than a cursory evaluation of *Dunderbergia* sclerites collected during this study, and open nomenclature is used here. However, the new specimens (e.g., pl. 40, figs. A–C, H–I) may provide a large enough sample size to revise the genus as it occurs in the Lion Mountain Member through most of the *Blandicephalus texanus* Zone.

Family Lonchocephalidae Hupé, 1955

Genus *Glaphyraspis* Resser, 1937

Type species.—*Liostracus parvus* Walcott 1899, Upper Cambrian strata, Pebble Creek area, Yellowstone National Park, Wyoming (by original designation).

Glaphyraspis parva (Walcott, 1899)

Plate 41, figs. A–P

1899 *Liostracus parvus* Walcott, p. 463, pl. 65, fig. 6.

1937 *Glaphyraspis parva* (Walcott); Resser, p. 12.

1938 *Raaschella ornata* Lochman, p. 82, pl. 18, figs. 6–10.

1954 *Raaschella ornata* Lochman; Palmer, p. 764, pl. 89, figs. 7–9.

1965 *Glaphyraspis parva* (Walcott); Rasetti, p. 40, pl. 10, figs. 9–17.

1965 *Glaphyraspis ornata* (Lochman); Rasetti, p. 41, pl. 10, fig. 8; pl. 11, figs. 13–14.

non 1968 *Glaphyraspis ornata* (Lochman); Lochman, p. 1157, pl. 149, figs. 12–19, 22.

1992 *Glaphyraspis parva* (Walcott); Pratt, p. 71, pl. 26, figs. 13–22 (see for full synonymy).

Diagnosis.—Subtrapezoidal cranidium with moderately to strongly convex subtrapezoidal glabella bearing two to three pairs of deeply incised, gently curved glabellar furrows directed obliquely back. Down-sloping frontal area one-fifth cranidial length; border furrow deeply incised, preglabellar furrow deepest medially. Large occipital ring, greatest length medially; occipital spine absent. Semicircular pygidium with three to four axial rings, well-defined pleural furrows, and ridge on pleural bands at transition from flat pleural field to down-sloping border. Exoskeleton texture varies from smooth, granulated, to tuberculate; internal mold preserves granulation.

Holotype.—Cranidium in Upper Cambrian strata, Yellowstone National Park, Wyoming (Walcott, in Hague, 1899, pl. 65, fig. 4).

Material.—Cranidia (OU 238127–238129, OU 238131, OU 238133), pygidia (OU 238130, OU 238132), and additional sclerites from the Cap Mountain Limestone, Riley Formation, Texas.

Occurrence.—*Aphelaspis spinosa* Zone, Cap Mountain Limestone, Riley Formation, Burnet County, Texas, collections MCNe1 2.10, MCNe1 5.80–5.90, MCNe1 7.10.

Description.—Cranidia subrectangular in outline with rounded anterior margin; width at posterior end of palpebral lobes slightly greater than sagittal length. Frontal area and post-ocular areas steeply down-sloping, moderately arched in anterior view. Frontal area about one-fifth (22%; 19–25) of cranidial length (sag.). Anterior border greatest length medially, tapering towards lateral margin; border furrow well-defined groove. Preglabellar field comprises 60% (57–66) frontal area. Axial furrows deep; preglabellar furrow shallower, deepening medially. Glabella subtrapezoidal in outline, truncate anteriorly, with variable convexity, moderately to strongly convex above fixed cheeks.

Two to three pairs of slightly curved furrows directed obliquely back, S1 and S2 deep grooves, S3 faint when expressed. S0 transverse, deeply incised. Occipital ring thick arcuate band, longest medially, 22% (21–24) of glabellar length, tapering towards corners of glabella; occipital spine absent. Glabella makes up half (51%; 48–55) of cranidial width at posterior end of palpebral lobes. Small palpebral lobes positioned at glabellar mid-length; about 16% (15–17) cranidial length. Raised palpebral ridges extend transversely from palpebral lobe to about one-quarter distance behind anterior corner of glabella. Anterior branches of facial sutures follow curved path towards anterior margin. Posterior branches extend obliquely back from palpebral lobe, increasing curvature towards posterior corner of cranidium. Cranidial posterior margin deflects back; posterior border furrow conspicuous, deep groove. Fixed cheeks flat to gently down-sloping, increasing steepness at posterolateral projections. Exoskeleton ornamentation variable; may be granulated or tuberculate. Exfoliated surface preserves granulated texture.

Pygidium semicircular in outline; width twice its sagittal length. Axis raised above pleural field, tapering posteriorly; maximum axis width comprises one-third pygidial width. Articulating half-ring subelliptical, slightly shorter than first axial ring, about 10% axis length; articulating furrow deep groove. Three or four axial rings separated by well-incised, transverse axial ring furrows and deep pits at the axial furrows, plus one or two segments incorporated into the terminal piece indicated by shallow furrows. Pleural field flat, down-sloping at border; posterior border short, about 10% pygidial length (sag.). Three or four pairs of well-expressed pleural furrows weaken posteriorly; interpleural furrows faint. Pleural bands transverse, then curve

posteriorly at border slope change, marked by raised ridge. Exoskeleton is finely granulated.

Discussion.— *Raaschella ornata* Lochman (1938; p. 82, pl. 18, figs. 6–10) described from the Cap Mountain Limestone in Mason County, Texas, was reassigned to *Glaphyraspis* Resser (1937) and was later reported from Tennessee by Rasetti (1965). However, Pratt (1992) followed Lochman and Hu (1962) in treating *G. occidentallis* (Lochman, in Lochman and Duncan, 1944) as a junior synonym of the type species, *G. parva* (Walcott), and also included *G. ornata* as an additional synonym. This is followed here. Pratt considered *G. parva* to show considerable intraspecific variation, including glabella outline (subrectangular to subtrapezoidal) and convexity, and sculpture of the exoskeleton. Some of this variability is ontogenetic, in which larger specimens often have weaker glabellar furrows and a slightly longer frontal area which slopes down at a shallower angle (pl. 41, figs. J, K). Specimens collected in Burnet County as part of this study were collected about 75 miles (120 km) west of the type locality of *G. ornata*. Cranidia differ minimally from Lochman's types in having a slightly narrower glabella (width 70% of length compared to 77% in Lochman's specimens) and the pygidium has three well-defined axial rings instead of four.

Glaphyraspis dianae sp. nov.

Plate 42, figs. A–F; Plate 43, figs. A–P

1968 *Glaphyraspis ornata* Lochman, p. 1157, pl. 149, figs. 12–19, 22.

Diagnosis.—*Glaphyraspis* species with subtrapezoidal glabella with two pairs of deeply-incised lateral furrows and a faint to effaced third pair; occipital spine present. Pygidium has four or five axial rings plus two or three segments in the terminal piece.

Holotype.—A cranidium (pl. 42, figs. A–C, OU 238118) from the *Aphelaspis spinosa* Zone, Cap Mountain Limestone, Riley Formation, collection LB 0.8.

Name. —For the author's grandmother, Carla Diane Armstrong.

Material.—Holotype cranidium (OU 238118), paratype cranidia (OU 238120, OU 238124), free cheeks (OU 238123, OU 238125), pygidia (OU 238119, OU 238121–238122, OU 238126), and additional sclerites from the Cap Mountain Limestone, Riley Formation, Texas.

Occurrence.—*Aphelaspis spinosa* Zone, Cap Mountain Limestone, Riley Formation, Texas, collections LB 0.80, MCNe1 7.10.

Discussion.—*Glaphyraspis dianae* is generally similar to *G. parva* but differs by the presence of a occipital spine and the pygidia have at least four defined axial rings plus two or three incorporated into the terminal piece. Lochman (1968; pl. 149, figs. 12–19, 22) assigned specimens from the *Crepicephalus* Zone of Missouri to *G. ornata* which display tuberculate testate, an occipital spine, and five axial rings on the pygidium. The type specimens of *G. ornata*, considered synonymous (Pratt, 1992) with *G. parva*, lacks an occipital spine, and as Pratt suggested, the Missouri species should be considered new. Specimens of *G. ornata* figured by Rasetti (1965, pl. 11, figs. 13–14), including an articulated thorax, have four pairs of deeply incised glabellar furrows, lack an occipital spine, have five pygidial axial rings, and tubercles on the entire exoskeleton. Compared *G. dianae* in Texas, the Missouri specimens have a somewhat wider glabella (width

75% length compared to 68%), a slightly longer anterior border (47% of frontal area, versus 40%), and tubercles on the cranidium and free cheek exoskeleton, which are variable in size but larger than those present on the Texas specimens. Specimens from both localities have subtrapezoidal glabellas, two pairs of deep glabellar furrows and a faint to effaced third pair, an occipital ring, and pygidia with four to five defined axial rings and a granulated surface. However, cranidia collected display a range from smooth to fine granules. The granulated specimens (pl. 43) could prove to represent a distinct species, but more samples are needed to further evaluate this, and a broad diagnosis is used here. *Glaphyraspis parva* as revised by Pratt (1992) varies in several characters, including surface sculpture, both within the same section and across different localities (Rasetti, 1965, Pratt, 1992). It is therefore reasonable to attribute the differences between the Missouri and Texas specimens as intraspecific variation and assign the Missouri sclerites to *G. dianae*.

Glaphyraspis davidis Pratt (1992; p. 71, pl. 26, figs. 5–12), from the *Cedaria* Zone in the Rabbitkettle Formation in northwest Canada, has an occipital spine but differs from *G. dianae* by having a rectangular glabellar rather than subtrapezoidal, much shallower glabellar furrows, and a short anterior border. The pygidium associated with *G. davidis* differs by a more convex axis and deeper axial rings furrows. *Glaphyraspis newtoni* Perfetta, in Stitt and Perfetta (2000; p. 214, pl. 10, figs. 30–31), known from two small cranidia in the Upper Cambrian Deadwood Formation in the Black Hills, South Dakota, also has an occipital spine, but differs from *G. dianae* in having a forwardly expanding glabella, two pairs of short lateral glabellar furrows, and a very short anterior border.

Glaphyraspis richardi sp. nov.

Plate 44, figs. A–G

Diagnosis.—*Glaphyraspis* species with smooth exoskeleton, subtrapezoidal glabella lacking lateral glabellar furrows, and baring an occipital spine. Pygidium with four defined axial rings, plus two or three incorporated in the terminal piece, and well-defined pleural furrows.

Holotype.—A cranidium (pl. 44, figs. A–C, OU 238134) from the *Aphelaspis spinosa* Zone, Cap Mountain Limestone, Riley Formation, collections LB 0.9–1.0.

Name.—For the author's grandfather, Richard Armstrong.

Material.—Holotype cranidium (OU 238134), paratype cranidium (OU 238135), pygidia (OU 238136–238137), and additional unfigured sclerites from the Cap Mountain Limestone, Riley Formation, Texas.

Occurrence.—*Aphelaspis spinosa* Zone, Cap Mountain Limestone, Riley Formation, Burnet County, Texas, collections LB 0.90–1.0.

Discussion.— Compared to the other species from the Cap Mountain Member, *G. parva* and *G. dianae*, *G. richardi* differs by lacking glabellar furrows and has a shorter anterior border (33% frontal area, compared to 40% in the other species). Like *G. dianae*, *G. richardi* has an occipital spine, but clearly differs from the latter in the effacement of the lateral glabellar furrows. *Glaphyraspis richardi* resembles *G. declivis* Rasetti (1965; p. 42, pl. 14, figs. 20–24), from the Nolichucky Formation of Tennessee, in the absence of both lateral glabellar furrows and surface sculpture, but differs by having an occipital spine rather than a subtle node, a less rounded anterior margin with a conspicuous anterior border, and wider (tr.) posterolateral projections. *Glaphyraspis*

ovata Rasetti (1961; p. 113, pl. 22, figs. 19–24), from the lower Conococheague Formation of Virginia, is another smooth species but is distinguished from *G. richardi* by the presence of weakly incised glabellar furrows, a strongly convex glabella, deeper axial furrows, and like *G. declivis*, has a more rounded anterior margin, and lacks and occipital spine. *Glaphyraspis oderi* Rasetti (1965, p. 41, pl. 10, figs. 18–22), from the Nolichucky Formation of Tennessee, also has faint glabellar furrows and lacks an occipital spine.

Family Crepicephalidae Kobayashi, 1935

Genus *Coosella* Lochman, 1936

Type species.—*Coosella prolifica* Lochman, 1936, from the Bonneterre Dolomite, upper Cambrian, Missouri (by original designation).

Coosella cf. *perplexa* (Palmer, 1954)

Plate 46, figs. A–K

cf. 1954 *Crepicephalus*? *perplexus* Palmer, p. 733, pl. 77, figs. 1, 2, 4.

cf. 1965 *Coosella perplexa* (Palmer), in Rasetti, p. 50, pl. 15, figs. 19–26.

Material.—Incomplete cranidium (OU 238107) and two pygidia (OU 238108–238109) from the Cap Mountain Limestone, Riley Formation, Texas.

Occurrence.—*Coosella perplexa* Zone, Cap Mountain Limestone, Riley Formation, Texas, Burnet County, Texas, collections MCNe2 3.90.

Discussion.—Palmer (1954) assigned a *Coosella*-like species to *Crepicephalus*? *perplexus* in part from its stratigraphic position above an apparent discontinuity

between the *Coosella* Zone and its occurrence in the base of the *Aphelaspis* Zone. *Crepicephalus* is characterized by long pygidial spines that are not present in *C.*? *perplexus* but instead has a *Coosella*-like pygidium with a smooth margin with a median notch. Accordingly, Rasetti (1965) reassigned *C.*? *perplexus* to *Coosella*. An incomplete cranidium (pl. 46, fig. A) and two pygidia, one small (pl. 46, fig, B–D) and one large (pl. 46, fig. E–F), were collected from the basal beds of the Morgan Creek extended section (MCNe2 3.9). The cranidium and smaller pygidia resemble *Coosella perplexa*, but the large tail has a longer border (45% of sagittal width, compared to 36% in the smaller), which could be an ontogenetic difference. A larger sample size and review of type specimens is needed to determine any ontogenetic variation and to make a confident identification.

Genus *Coosina* Rasetti, 1956

Type species.—*Maryvillia ariston* (part) Walcott, 1916, from the Nolichucky Formation, Tennessee.

Coosina cf. *ariston* (Walcott, 1916)

Plate 46, figs. A–E

cf. 1916 *Maryvillia ariston* Walcott (part), p. 401, pl. 64, fig. 5.

cf. 1954 *Maryvillia ariston* Walcott, in Palmer, p. 723.

cf. 1956 *Coosina ariston* (Walcott), in Rasetti, p. 1267 (includes complete synonymy).

cf. 1961 *Coosina ariston* (Walcott), in Rasetti, p. 111, pl. 21, figs. 12–13.

Material.—Incomplete cranidium (OU 238110) and pygidium (OU 238111) from the Cap Mountain Limestone, Riley Formation, Texas.

Occurrence.—*Coosella perplexa* Zone, Cap Mountain Limestone, Riley Formation, Burnet County, Texas, collections MCNe2 3.90.

Discussion.—The type material of *Maryvillia ariston* Walcott (1916) has a tangled nomenclatural history that has been summarized by Rasetti (1956). The holotype cranidium (Walcott, 1916, pl. 64. fig. 5) was the basis for *Coosina* Rasetti, 1956, but the paratype pygidium was correctly assigned to *Maryvillia*. An exfoliated pygidium and cranidium (pl. 45, figs. A–E) collected from the Morgan Creek collection MCNe2 3.9 (Fig. 3) resembles the species that Palmer (1954, p. 723, pl. 79, fig. 6–9) identified as *Maryvillia* cf. *ariston*. These sclerites may record an undescribed species of *Coosina*, but more material is needed for a confident evaluation, and open nomenclature is used here.

Family Llanoaspididae Lochman, in Lochman and Duncan, 1944

Genus *Llanoaspis* Lochman, 1938

Type species.—*Llanoaspis modesta* Lochman, 1938, Riley Formation, upper Cambrian, Texas (by original designation).

Llanoaspis cf. *peculiaris* (Resser, 1938a)

Plate 45, figs. F–I

cf. 1938a *Genevievella peculiaris* Resser, p. 78, pl. 15 figs. 6–7.

cf. 1954 *Llanoaspis peculiaris* (Resser), in Palmer, p. 737, pl. 82, fig. 5

Material.—Two incomplete cranidia (OU 238112–238113) from the Cap Mountain Limestone, Riley Formation, Texas.

Occurrence.—*Coosella perplexa* Zone, Cap Mountain Limestone, Riley Formation, Burnet County, Texas, collections MCNe2 3.90.

Discussion.—Palmer (1954) notes that *Llanoaspis peculiaris* is characterized by its strongly arched cranidium and a shorter (sag.) glabella. Two cranidia, which were collected from the lower part of the Morgan Creek composite section, are strongly convex and have glabellar width three-fourths its length (sag.), and are similar to Palmer's figured specimens identified as *L. peculiaris* (1954; pl. 82, fig. 5). The holotype cranidium (Resser, 1938; pl. 15, fig. 6) shows a longer, more rectangular glabella and from a preliminary assessment may not be conspecific with the specimens in central Texas. Type and other specimens will need to be studied to revise *Llanoaspis*, and open nomenclature is used here.

Family Pterocephaliidae Kobayashi, 1935

Genus *Blandicephalus* Palmer, 1954

Type species.—*Blandicephalus texanus* Palmer, 1954, from the Riley Formation, Texas (by original designation).

Blandicephalus texanus Palmer, 1954

Plate 47, figs. A–I

1954 *Blandicephalus texanus* Palmer, p. 749, pl. 85, figs. 7–10.

Material.—Three cranidia (OU 238098–238100), a free cheek (OU 238101), a pygidium (OU 238102), and additional, unfigured sclerites from the Lion Mountain Sandstone, Riley Formation, Texas.

Occurrence.—*Blandicephalus texanus* Zone, Lion Mountain Sandstone, Riley Formation, Burnet County, Texas, collections HP 3.10, 3.65, 3.70, 3.75.

Discussion.—*Blandicephalus texanus* is the sole species assigned to the genus and it occurs only in central Texas. It is characterized by an effaced surface, long frontal area with a semicircular outline of the anterior margin, and a wide, subelliptical-shaped tail. The exfoliated cranidium preserves weak impressions of lateral glabellar furrows and caecae markings on the preglabellar field and palpebral lobes. Palmer (1954) only identified this species from one collection, noting that it is rare. However, collections made during this study show that *B. texanus* is locally abundant, and first occurs at the base of Palmer's post-*Aphelaspis* zone, then persists through part of the Lion Mountain Sandstone (HP 3.1, 3.65, 3.7, 3.75). In the revised zonation established in this thesis, *Blandicephalus texanus* is the name-bearing species of the youngest zone that replaces Palmer's post-*Aphelaspis* Zone.

Genus *Labiostria* Palmer, 1954

Type species.—*Labiostria conveximarginata* Palmer, 1954, from the Riley Formation, Texas (by original designation).

Labiostria conveximarginata Palmer, 1954

Plate 48, figs. A–C; Plate 49, figs. A–B; Plate 50, figs. A–E

1954 *Labiostria conveximarginata* Palmer, p. 751, pl. 86, figs. 1–4.

Material.—One cranidium (OU 238153), one pygidium (OU 238154), and additional sclerites from the Lion Mountain Sandstone, Riley Formation, Texas.

Occurrence.—*Blandicephalus texanus* Zone, Lion Mountain Sandstone, Riley Formation, Burnet County, Texas, collections, HP 3.65, HP 3.70, MCS 4.50.

Discussion.— *Labiostria* is a common species throughout the Steptoean in central Texas that Palmer (1954) diagnosed as very similar to *Aphelaspis*, differing by a narrow border furrow on the frontal area of the cranidium. Palmer (1962) later suppressed the genus as a junior synonym of *Aphelaspis*, however, as Pratt (1992) pointed out, *Labiostria* has a median suture (see Pratt, 1992, pl. 14, fig. 20), whereas *Aphelaspis* has a rostral plate, and he removed it from synonymy. *Labiostria conveximarginata* is also distinguished by a gently convex border and median plectrum of the anterior border (pl. 50, figs. A–C). Specimens were recovered from the upper *Blandicephalus texanus* Zone (HP 4.5).

Labiostria sigmoidalis Palmer, 1954

Plate 48, figs. G–I; Plate 50, figs. F–G

1954 *Labiostria sigmoidalis* Palmer, p. 751, pl. 86, fig. 5.

Material.—One cranidium (OU 238155) and additional, unfigured sclerites from the Lion Mountain Sandstone, Riley Formation, Texas.

Occurrence.— *Blandicephalus texanus* Zone, Lion Mountain Sandstone, Riley Formation, Burnet County, Texas, collections, HP 3.65, HP 3.70, MCS 4.50.

Discussion.—*Labiostria sigmoidalis* is distinguished from the other species occurring in the Riley Formation by posterior pair of glabellar furrows which fork adaxially, and its sigmoidal shape of the frontal area in lateral view (pl. 48, fig. I), caused by a convex preglabellar field and border separated by a concave border furrow. Pygidium and free cheek are not known. Palmer (1954) only collected this species from one section in the *Blandicephalus texanus* Zone (his post-*Aphelaspis* Zone). In this study, specimens were recovered from the upper *Blandicephalus texanus* Zone (MCS 4.5).

Labiostria platifrons Palmer, 1954

Plate 48, figs. D–E; Plate 49, figs. D–G

1954, *Labiostria platifrons* Palmer, 1954, p. 751, pl. 86, figs. 6–8.

Occurrence.— *Blandicephalus texanus* Zone, Lion Mountain Sandstone, Riley Formation, Burnet County, Texas, collections, LB 5.75, HP 3.10, HP 3.65, MCS 4.50.

Discussion.—*Labiostria platifrons* has a flat anterior border of the cranidium, unlike *L. conveximarginata* and *L. sigmoidalis*, whose borders are convex. Specimens were recovered throughout the *Blandicephalus texanus* Zone (LB 5.75, MCS 4.5).

Gen. nov. aff. *Dunderbergia*

Plate 51, figs A–I

Material.—Three cranidia (OU 238138–238140), a free cheek (OU 238141), and additional, unfigured sclerites from the Lion Mountain Sandstone, Riley Formation, Texas.

Occurrence.—*Blandicephalus texanus* Zone, Lion Mountain Sandstone, Riley Formation, Burnet County, Texas, collections HP 3.10, HP 3.65, HP 3.75, MCS 4.50.

Discussion.—Sclerites occurring throughout the *Blandicephalus texanus* Zone (HP 3.1, HP 3.65, HP 3.7, MCS 4.5) in the Riley Formation in Texas represents a new species, and likely a new genus. It somewhat resembles *Aphelaspis* by its long frontal area, gently inflated preglabellar field and long, upturned border, and a subtrapezoidal glabella with a truncate front (pl. 27, fig. A); but it has a densely tuberculated surface, indicating possible relation to *Dunderbergia* (pl. 40) which occurs in the same assemblage. Further work needs to be done to address the identification of this taxon and its occurrence throughout the Lion Mountain Sandstone.

References

Lochman, C., and Hu, C.H., 1962, An *Aphelaspis* Zone faunule from Logan, Montana: Journal of Paleontology, v. 36, p. 431–441.

Palmer, A.R., 1954, The faunas of the Riley Formation in central Texas: Journal of Paleontology, v. 28, p. 709–786.

Palmer, A.R., 1960, Trilobites of the Upper Cambrian Dunderberg Shale, Eureka District, Nevada: U.S. Geological Survey Professional Paper, no. 334–C, p. 53–109.

Palmer, A.R., 1962, *Glyptagnostus* and associated trilobites in the United States: U.S. Geological Survey Professional Paper, no. 374-F.

Pratt, B.R., 1992, Trilobites of the Marjuman and Steptoean stages (Upper Cambrian), Rabbitkettle Formation, southern MacKenzie Mountains, northwest Canada: Calgary, Alta., Canadian Society of Petroleum Geologists.

Rasetti, F., 1956, Revision of the trilobite genus *Maryvillia* Walcott: Journal of Paleontology, v. 30, p. 1266–1269.

Rasetti, F., 1965, Upper Cambrian trilobite faunas of northeastern Tennessee: Washington D.C., The Smithsonian Institution, The Smithsonian Miscellaneous Collections, v. 148, 128 p.

Resser, C. E., 1938, Cambrian System (restricted) of the southern Appalachians: Geological Society of America, Special Paper no. 15.

Resser, C.E., 1942a, Fifth contribution to nomenclature of Cambrian fossils: Washington D.C., The Smithsonian Institution, The Smithsonian Miscellaneous Collections, v. 101.

Resser, C.E., 1942b, New Upper Cambrian trilobites: Washington D.C., The Smithsonian Institution, The Smithsonian Miscellaneous Collections, v. 103.

Walcott, C.D., 1916, The Cambrian Fauna of Eastern Asia: Washington D.C., The Smithsonian Institution, The Smithsonian Miscellaneous Collections, v. 3.

Westrop, S.R., Eoff, J.D., Ng, T.W., Dengler, A.A., and Adrain, J.M., 2008, Classification of the Late Cambrian (Steptoean) trilobite genera *Cheilocephalus* Berkey, 1898 and *Oligometopus* Resser, 1936 from Laurentia: Canadian Journal of Earth Sciences, v. 45, p. 725–744, doi: 10.1139/e08-026.

APPENDIX A: Abundances and Distributions

Table 3: Individuals of Species by Section

	Aphelaspis constricta	*Aphelaspis longifrons*	*Aphelaspis spinosa*	*Aphleaspis* cf. *walcotti*	*Blandicephalus texanus*	*Blountia morgancreekensis*	*Cheilocephalus brevilobus*	*Cheilocephalus* cf. *granulosa*	*Coosella* cf. *perplexa*	*Coosina* cf. *ariston*	*Dunderbergia* cf. *variagranula*	*Glaphyraspis dianae*	*Glaphyraspis parva*	*Glaphyraspis richardi*	*Labiostria convexiimarginata*	*Labiostria platifrons*	*Labiostria sigmoidalis*	*Llanoaspis* cf. *peculiaris*	Gen. nov. aff. *Dunderbergia*
MCNe2 3.90									2	1								2	
MCNe1 2.10			6	48				3					9						
LB -0.15			1	4		1		1											
LB 0.30				5															
MCNe1 5.8–5.9			26	29		4		6					34						
LB 0.50–0.70				3															
LB 0.80				101		4						4							
LB 0.90–1.00			4	7										3					
LB 1.40				1															
MCNe1 7.10				90		42						2	1						
HP 2.6 Pulloff	11	11																	
HP 2.5 Pulloff	17	49																	
LB 2.10		2		8															
LB 2.15		2		15															
LB 3.40				8															
LB 4.45		4																	
LB 5.75																2			
HP 3.10					7						5					2			7
HP 3.65					14						31				8	2	1		10
HP 3.70					23		1				36				4		4		
HP 3.75					19						10								1
MCS 4.50							1				4				2	12	9		5
Total	28	68	37	319	63	51	2	10	2	1	86	6	44	3	14	18	14	2	23

Table 4: Genera Abundance by Biozone

	***Coosella perplexa* Zone**	***Aphelaspis spinosa* Zone**	***Aphelaspis longifrons* Zone**	***Blandicephalus texanus* Zone**
Aphelaspis		333	123	
Blandicephalus				63
Blountia		47		
Cheilocephalus		10		2
Coosella	2			
Coosina	1			
Dunderbergia				86
Glaphyraspis		61		
Labiostria			2	58
Llanoaspis	2			
Gen. nov. aff. *Dunderbergia*				23
Total	5	451	125	232

Table 5: Species Abundance by Biozone

	***Coosella perplexa* Zone**	***Aphelaspis spinosa* Zone**	***Aphelaspis longifrons* Zone**	***Blandicephalus texanus* Zone**
Aphelaspis constricta			28	
Aphelaspis longifrons			68	
Aphelaspis spinosa		37		
Aphleaspis* cf. *walcotti		288	20	
Blandicephalus texanus				63
Blountia morgancreekensis		48		
Cheilocephalus brevilobus				2
Cheilocephalus* cf. *granulosa		10		
Coosella* cf. *perplexa	2			
Coosina* cf. *ariston	1			
Dunderbergia* cf. *variagranula				86
Glaphyraspis dianae		6		
Glaphyraspis parva		46		
Glaphyraspis richardi		3		
Labiostria conveximarginata				14
Labiostria platifrons			2	16
Labiostria sigmoidalis				14
Llanoaspis* cf. *peculiaris	2			
Gen. nov. aff. *Dunderbergia*				16

Table 6: Species and Sclerite Distribution by Section

MCNe2 3.90	**Cranidia**	**Pygidia**	**Librigenae**	**Hypostomes**	**Individuals**
Coosella cf. *perplexa*	1	2			2
Coosina cf. *ariston*	1	1			1
Llanoaspis cf. *peculiaris*	2				2
				Total:	5
MCNe1 2.10					
Aphelaspis cf. *walcotti*	48	1	6		48
Aphelaspis spinosa	6				6
Aphleaspis sp.		2		1	2
Cheilocephalus cf. *granulosa*	2	3			3
Glaphyraspis parva	9	2			9
				Total:	68
LB -0.15					
Aphelaspis spinosa		1			1
Aphelaspis cf. *walcotti*	4				4
Aphelaspis sp.	2				2
Blountia morgancreekensis	1				1
Cheilocephalus cf. *granulosa*	1				1
				Total:	9
LB 0.30					
Aphelaspis cf. *walcotti*	4	5	4		5
Glaphyraspis parva	2	1			2
				Total:	7
MCNe1 5.80–5.90					
Aphelaspis cf. *walcotti*	29	5	4		29
Aphelaspis spinosa	26	2	6		26
Aphelaspis sp.				4	4
Blountia morgancreekensis		1			1
Cheilocephalus cf. *granulosa*	1	6			6
Glaphyraspis parva	34	11	3		34
				Total:	100
LB 0.50–0.70					
Aphelaspis cf. *walcotti*	3	1	2		3
Glaphyraspis sp.	1				1
Gen. sp. unknown			1		1
				Total:	5

LB 0.80	Cranidia	Pygidia	Librigenae	Hypostomes	Individuals
Aphelaspis cf. *walcotti*	101	1	5	1	101
Blountia morgancreekensis	4	4			4
Glaphyraspis dianae	4	3	2		4
				Total:	109
LB 0.90–1.00					
Aphelaspis spinosa	4	2	3		4
Aphelaspis cf. *walcotti*	7				7
Glaphyraspis richardi	3				3
Glaphyraspis sp.	2	4	1		4
Gen. sp. unknown		1	1		1
				Total:	18
LB 1.40					
Aphelaspis cf. *walcotti*	1				1
Gen. sp. unknown			1		1
				Total:	2
MCNe1 7.10					
Aphelaspis cf. *walcotti*	90	15	8		90
Blountia morgancreekensis	42	32			42
Glaphyraspis dianae	2				2
Glaphyraspis parva	1				1
Glaphyraspis sp.		1			1
				Total:	136
HP 2.60 Pulloff					
Aphelaspis constricta	11				11
Aphelaspis longifrons	11	2	4		11
				Total:	22
HP 2.50 Pulloff					
Aphelaspis constricta	17		1		17
Aphelaspis longifrons	49	4	11		49
Aphelaspis sp.	7			2	7
				Total:	73
LB 2.10					
Aphelaspis longifrons	2				2
Aphelaspis cf. *walcotti*	8		1		8
				Total:	10
LB 2.15					
Aphelaspis longifrons	2				2
Aphelaspis cf. *walcotti*	4				4
				Total:	6

LB 3.40	Cranidia	Pygidia	Librigenae	Hypostomes	Individuals
Aphelaspis cf. *walcotti*	8		3		8
				Total:	8
LB 4.45					
Aphelaspis longifrons	4		1		4
Gen. sp. unknown	1				1
				Total:	5
LB 4.50					
Gen. sp. unknown	1				1
				Total:	1
LB 5.75					
Labiostria platifrons	2				2
				Total:	2
HP 3.10					
Blandicephalus texanus	7		1		7
Dunderbergia cf. *variagranula*	5	2		1	5
Labiostria platifrons	2	1			2
Gen. nov. aff. *Dunderbergia*	7	2			7
				Total:	21
HP 3.65					
Blandicephalus texanus	14	1	2		14
Dunderbergia cf. *variagranula*	31	16		2	31
Labiostria convexiimarginata	8				8
Labiostria platifrons	2				2
Labiostria sigmoidalis	1				1
Labiostria sp.	6	3			6
Gen. nov. aff. *Dunderbergia*	10				10
Gen. sp. unknown			2	2	2
				Total:	74
HP 3.70					
Blandicephalus texanus	23	3			23
Cheilocephalus brevilobus	1				1
Dunderbergia cf. *variagranula*	36	6			36
Labiostria convexiimarginata	4				4
Labiostria sigmoidalis	4				4
Labiostria sp.	4	2	1		4
Gen. sp. unknown			1	2	2
				Total:	74

HP 3.75	**Cranidia**	**Pygidia**	**Librigenae**	**Hypostomes**	**Individuals**
Blandicephalus texanus	19	2	1		19
Dunderbergia cf. *variagranula*	10	1			10
Labiostria sp.	7	1			7
Gen. nov. aff. *Dunderbergia*	1				1
Gen. sp. unknown	2		2		2
				Total:	39
MCS 4.50					
Cheilocephalus brevilobus		1			1
Dunderbergia cf. *variagranula*	4				4
Labiostria conveximarginata	2				2
Labiostria platifrons	12				12
Labiostria sigmoidalis	9				9
Labiostria sp.	5		2		5
Gen. nov. aff. *Dunderbergia*	5				5
				Total:	38

APPENDIX B: Phylogenetic Analysis Character List

1. Frontal area length/total cranidial length: 0, <20% (e.g., see *Kingstonia gaspensis* in Rasetti, 1946, pl. 69, figs. 18–19); 1, 21–24% (e.g., see pl. 5, fig. C); 2, 26–30% (e.g. see pl. 2, fig. A); 3, >30% (e.g., pl. 20, fig. A).
2. Anterior border length/frontal area length: 0, <50% (e.g., see *Kingstonia gaspensis* in Rasetti, 1946, pl. 69, figs. 17–22); 1, 54–60% (e.g., pl. 25, fig. A); 2, 63+% (e.g., pl. 16, A).
3. Glabella width/length: 0, 70–75% (e.g., pl. 8, fig. A); 1, 80+% (e.g., pl. 14, fig. A).
4. Pygidium outline: 0, subtriangular (e.g., pl. 20, fig. J); 1, semicircular (e.g., pl. 13, fig. J).
5. Pygidial border length/pygidium length: 0, <10% (e.g., see *Kingstonia gaspensis* in Rasetti, 1946, pl. 69, fig. 20); 1, 13–18% (e.g., pl. 5, fig. F); 2, >20% (e.g., pl. 8, fig. G).
6. Glabella inflated above fixed cheeks: 0, absent (e.g., pl. 3, figs. B–K); 1, present (e.g., pl. 1, figs. D, F).
7. Pygidial border furrow incision: 0, faint (e.g., pl. 15, figs. A–F); 1, defined (e.g., pl. 19, figs. A–G).
8. Axis extends beyond pygidial border furrow: 0, absent (e.g., pl. 2, figs. F–G); 1, present (e.g., pl. 19, fig. H–K).
9. Pygidial border slope: 0, strongly down-sloping (e.g., see *Kingstonia gaspensis* in Rasetti, 1946, pl. 69, fig. 21); 1, flat to gently down-sloping (e.g., pl. 1, fig. B); 2, convex (e.g., pl. 17, fig. E)

APPENDIX C: Plates

Plate 1

Blountia mimula Walcott, 1916 from the Nolichucky Formation, Knoxville region, Tennessee (all previously figured by Walcott 1916, pl. 61, fig. 4, 4a–b).

A–D, articulated exoskeleton lacking free cheeks (USNM 62781; holotype), dorsal, lateral, posterior, anterior views, x14.

E–G, cranidium (USNM 62783), dorsal, anterior, lateral views, x14.

H–**J**, pygidium (USNM 62782), dorsal, lateral, posterior views, x14.

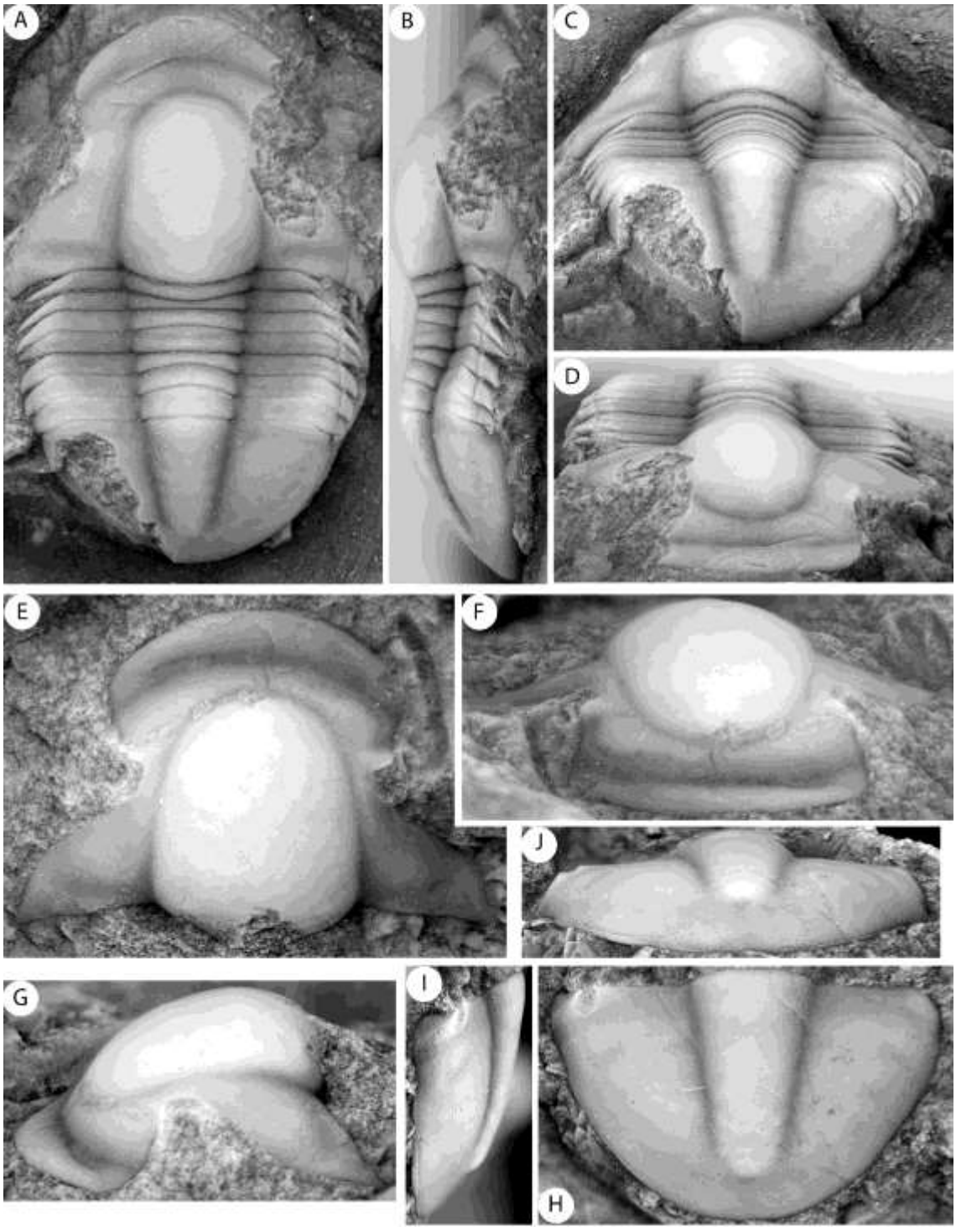
A
B
C
D
E
F
J
G
I
H

Plate 2

Blountia angela n. sp. from the Nolichucky Formation, Tennessee (all previously figured in Rasetti 1965, pl. 10, figs. 3–7).

A–C, cranidium (USNM 144602; holotype), dorsal, anterior, lateral views, x10.5.

D–E, cranidium (USNM 144602) dorsal, lateral views, x9.7.

F, pygidium (USNM 144602), dorsal view, x7.9.

G–I, exfoliated pygidium (USNM 144602), x7.9.

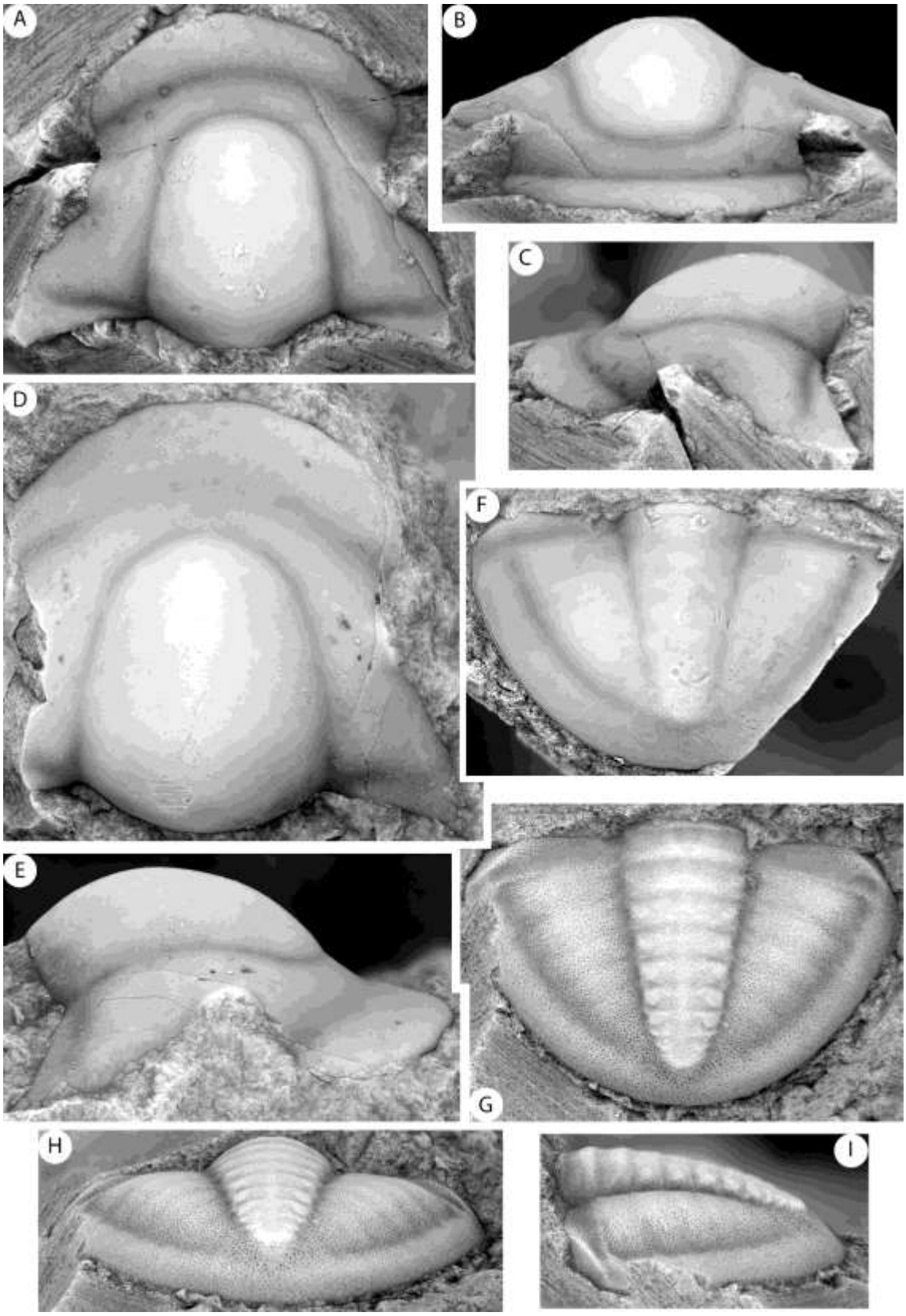
A
B
C
D
F
E
G
H
I

Plate 3

Maryvillia arion Walcott, 1916 from the Nolichucky Formation, Rogersville, Hawkins County, Tennessee.

A–C, exfoliated cranidium (USNM 62826; holotype), dorsal, anterior, lateral views, x6.6 (previously figured by Walcott 1916, pl. 64, figs. 4, 4b).

D–G, exfoliated cranidium (USNM 62826), dorsal, anterior, lateral, posterior views, x4.4.

H–K, exfoliated cranidium (USNM 144603), dorsal, posterior, lateral, anterior views, x3.5 (previously figured by Rasetti 1965, pl. 9, figs. 22–23).

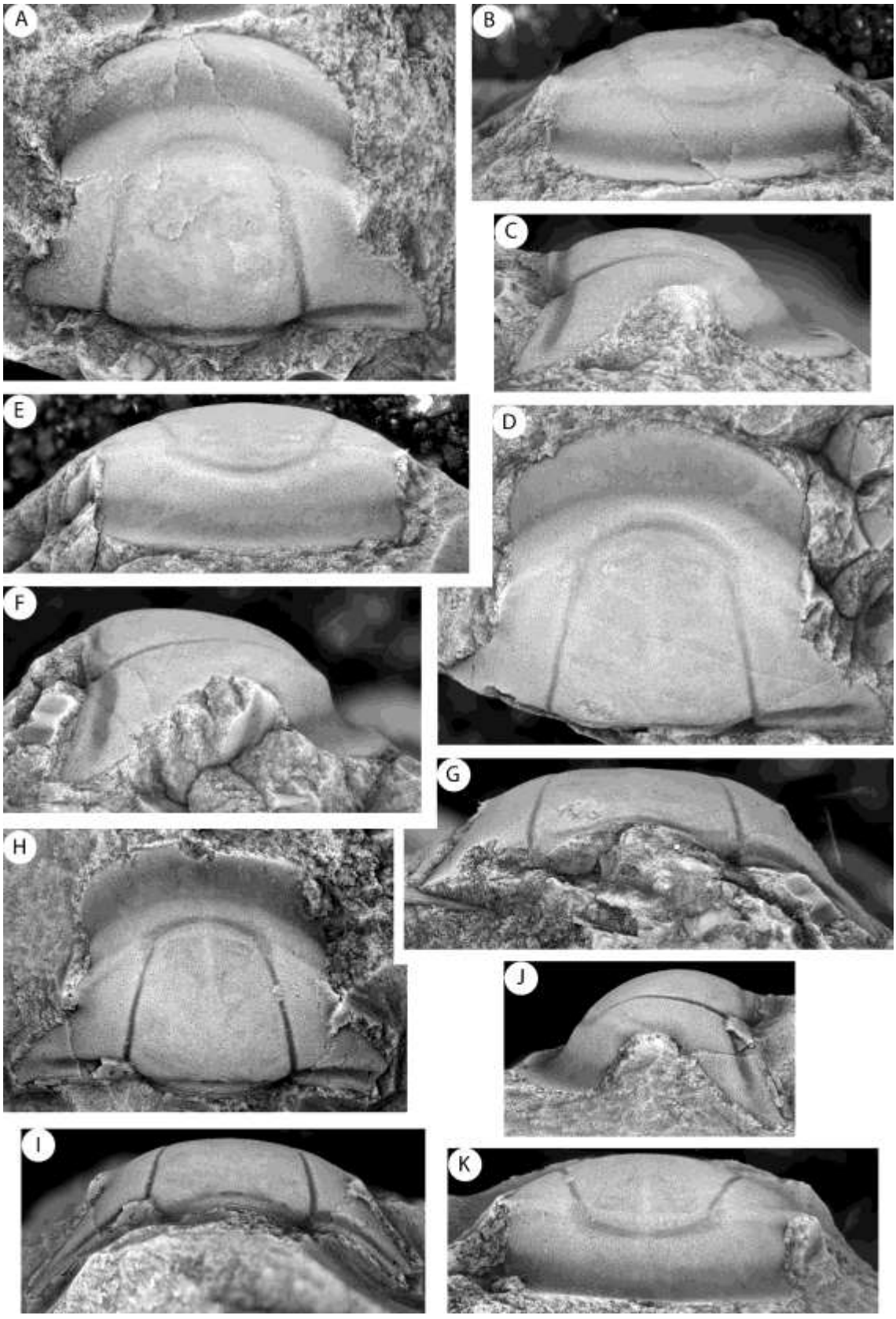
A
B
C
E
D
F
G
H
J
I
K

Plate 4

Maryvillia arion Walcott, 1916 from the Nolichucky Formation, Rogersville, Hawkins County, Tennessee (all previously illustrated by Rasetti 1965, pl. 9, figs. 22–26)

A–C, partially exfoliated pygidium (USNM 144604), dorsal, posterior, lateral views, x6.

D–E, pygidium (USNM 144603), dorsal, posterior views, x3.

F–G, exfoliated pygidium (USNM 144603), dorsal, posterior views, x3.

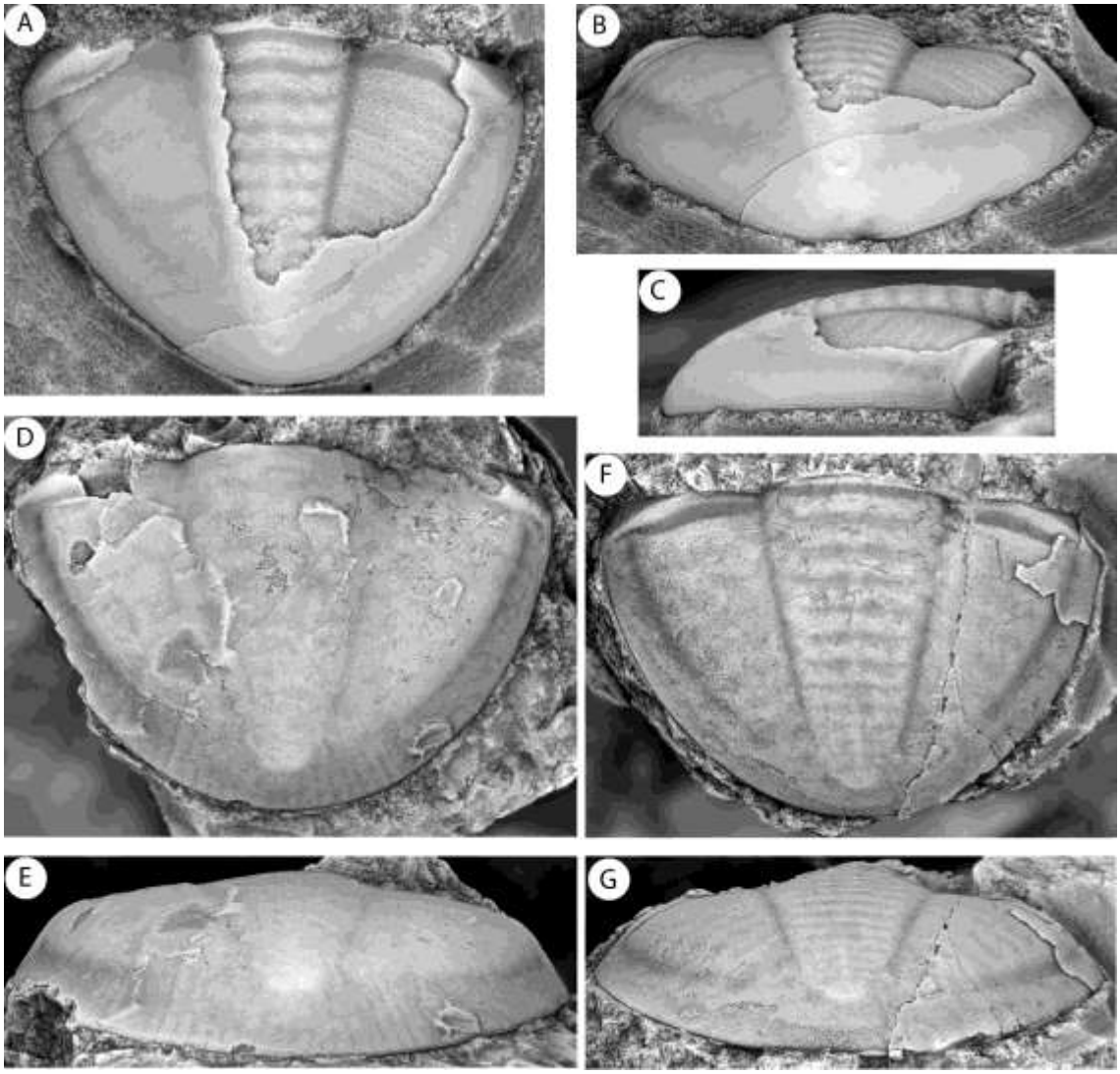
A
B
C
D
F
E
G

Plate 5

Blountia bristolensis Resser, 1938 from the Nolichucky Formation in Tennessee and Virginia.

A–E, exoskeleton lacking free cheeks (USNM 144600), lateral, dorsal, cranidium dorsal, anterior, posterior views, x6 (previously illustrated in Rasetti 1965, pl. 10, figs. 1–2).

F–H, pygidium (USNM 9492; holotype), dorsal, posterior, lateral views, x14 (previously illustrated in Resser 1938, pl. 12, fig. 24).

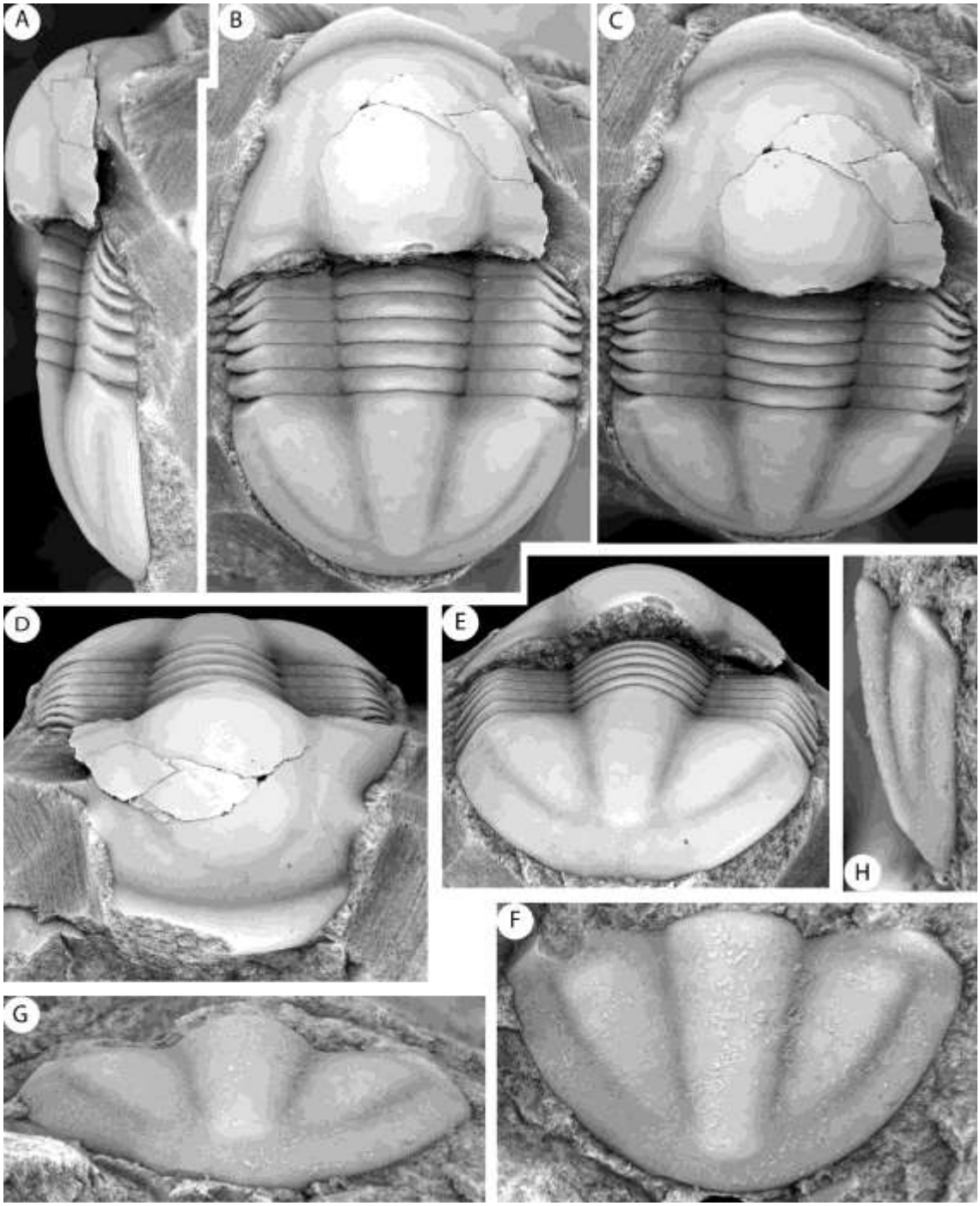
A
B
C
D
E
H
F
G

Plate 6

Blountia bristolensis Resser, 1938 from the Nolichucky Formation in Virginia.

A–C, cranidium (USNM 94963, holotype), dorsal, anterior, lateral views, x10.2 (previously figured in Resser, 1938, pl. 12, fig. 38).

D–E, cranidium (USNM 94963), dorsal, lateral views, x10.2.

F–H, cranidium (USNM 511430), dorsal, anterior, lateral views, x8.5.

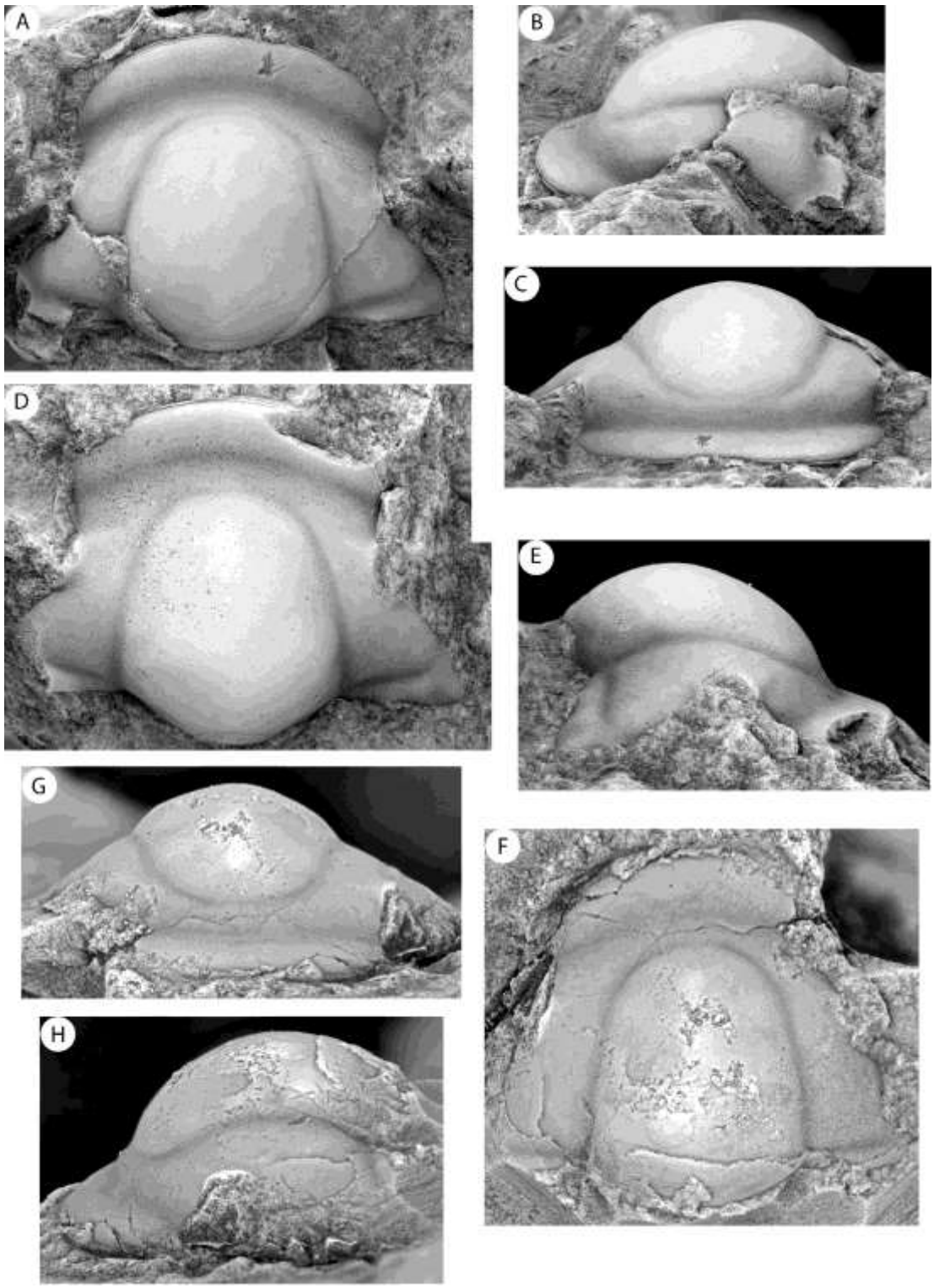
A
B
C
D
E
F
G
H

Plate 7

Blountia bristolensis Lochman, 1944 from the Pilgrim Formation, Nixon Gulch section, Montana.

A–C, pygidium (USNM 511427), dorsal, posterior, lateral views, x8.

D–E, pygidium (USNM 511428), dorsal, lateral views, x17.

F–H, pygidium (USNM 511434), dorsal, posterior, lateral views, x8.

I, pygidium (USNM 511434), dorsal view, x6.5.

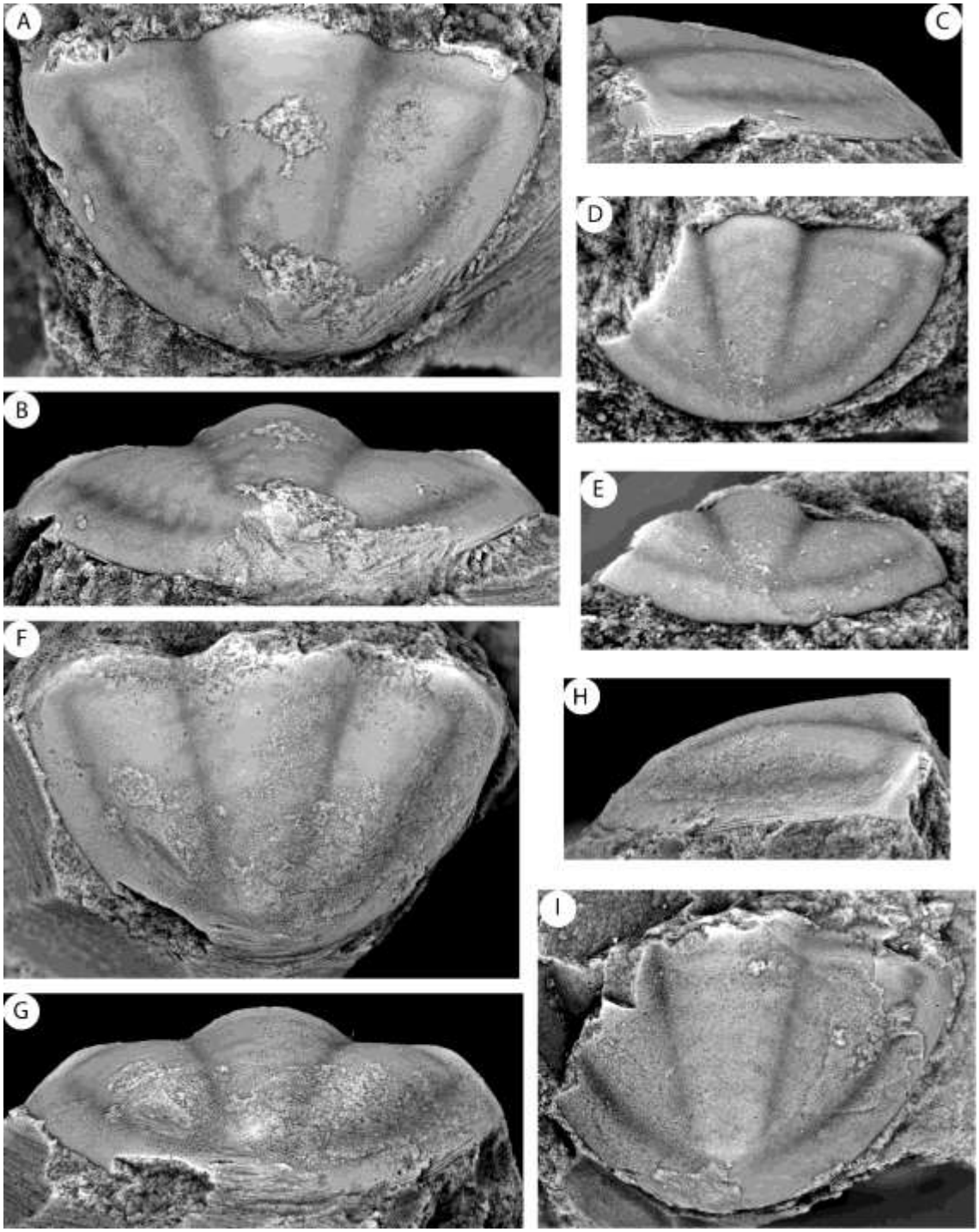
A
C
D
B
E
F
H
I
G

Plate 8

Blountia cora Lochman, 1944 from the Pilgrim Formation, Half Moon Pass section, Big Snowy Mountains, Montana.

A–C, exfoliated cranidium (USNM 127151; holotype), dorsal, anterior, lateral views, x10.8 (previously figured in Lochman and Duncan 1944, pl. 8, fig. 7–8).

D–E, exfoliated cranidium (USNM 127153), dorsal, anterior views, x13.5.

F, pygidium (USNM 127153), dorsal view, x18.

G–H, pygidium (USNM 127153), dorsal, posterior views, x18.

I–J, pygidium (USNM 127152b), dorsal, lateral views, x12.6 (previously figured in Lochman and Duncan 1944, pl. 8, figs. 9–10).

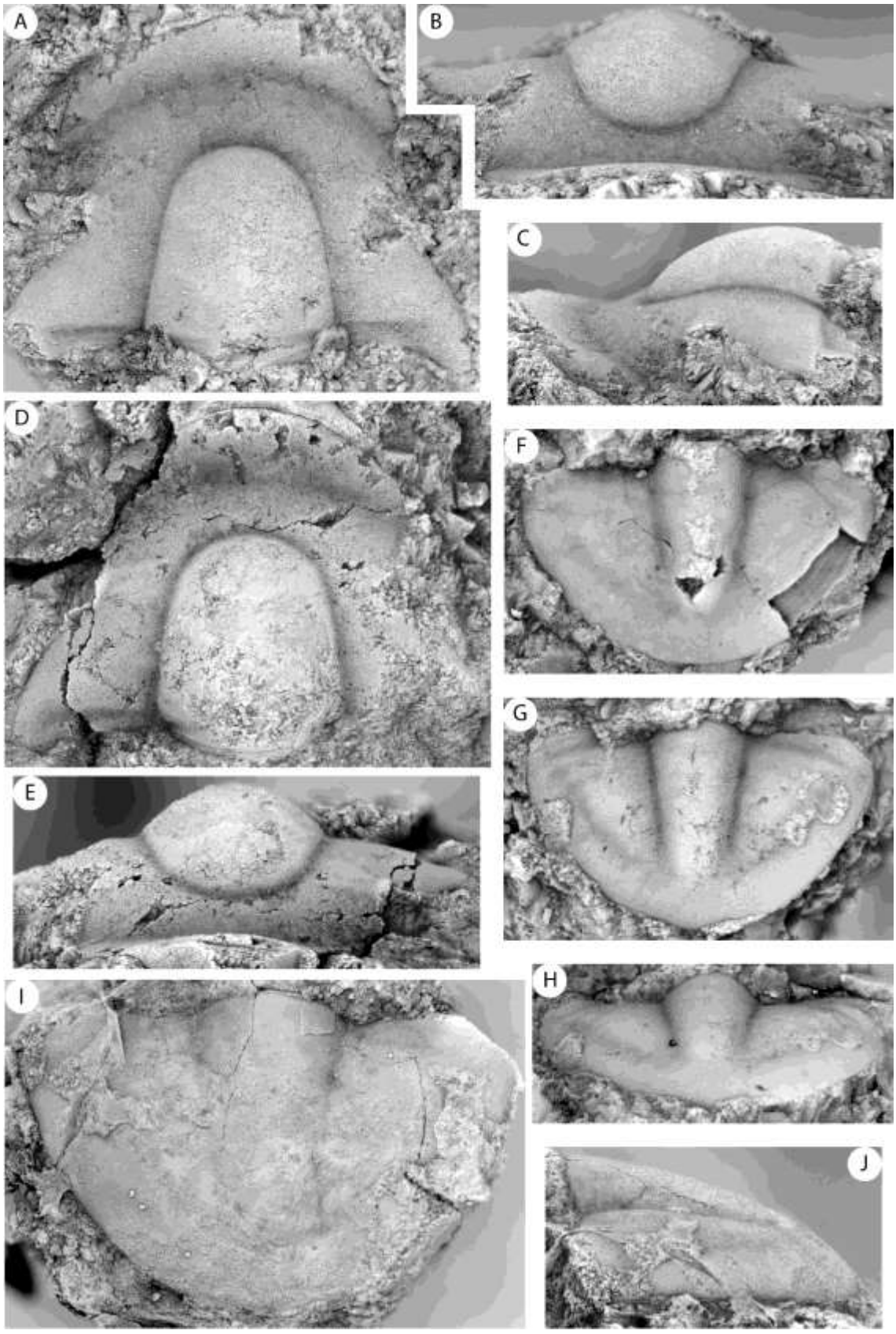
A
B
C
D
F
G
E
H
I
J

Plate 9

Blountia janei Lochman, 1944 from the Pilgrim Formation, Half Moon Pass section, Big Snowy Mountains, Montana.

A–C, cranidium (USNM 127150), dorsal, lateral, anterior view, x13.4.

D, cranidium (USNM 122149), dorsal view, x13.4.

E–G, cranidium (USNM 127144; holotype), dorsal, lateral, anterior views, x14.2 (previously figured in Lochman and Duncan 1944, pl. 8, figs. 2, 5).

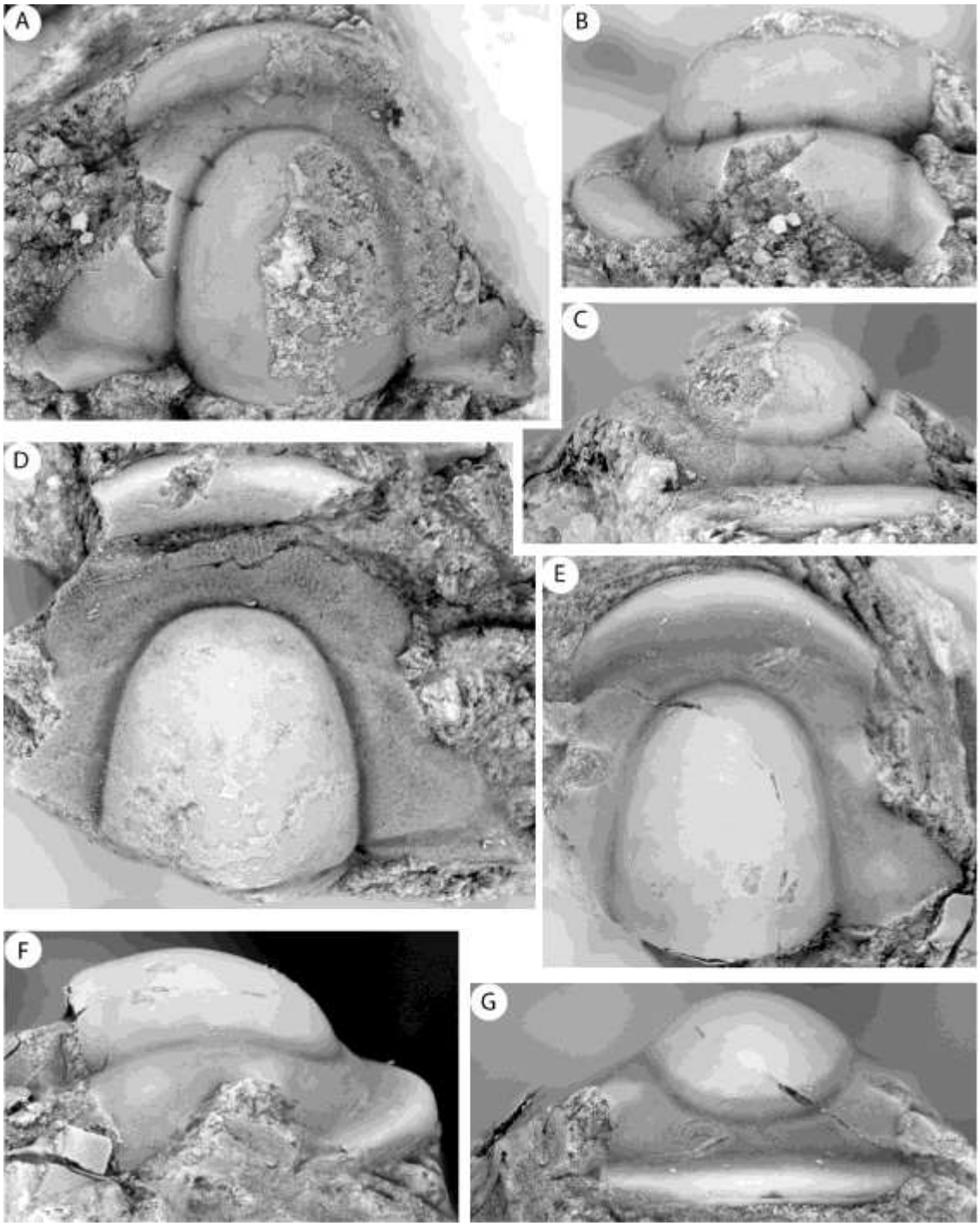
A
B
C
D
E
F
G

Plate 10

Blountia janei Lochman, 1944 from the Pilgrim Formation, Half Moon Pass section, Big Snowy Mountains, Montana.

A–C, pygidium (USNM 127145a), dorsal, lateral, posterior views, x15 (previously figured in Lochman and Duncan, 1944, pl. 8, figs. 3, 6).

D, pygidium (USNM 127149), dorsal view, x17.6.

E, pygidium (USNM 127146), dorsal view, x17.6.

F–H, partly exfoliated pygidium (USNM 127145b), dorsal, lateral, posterior views, x15 (previously figured in Lochman and Duncan 1944. pl. 8, fig. 4).

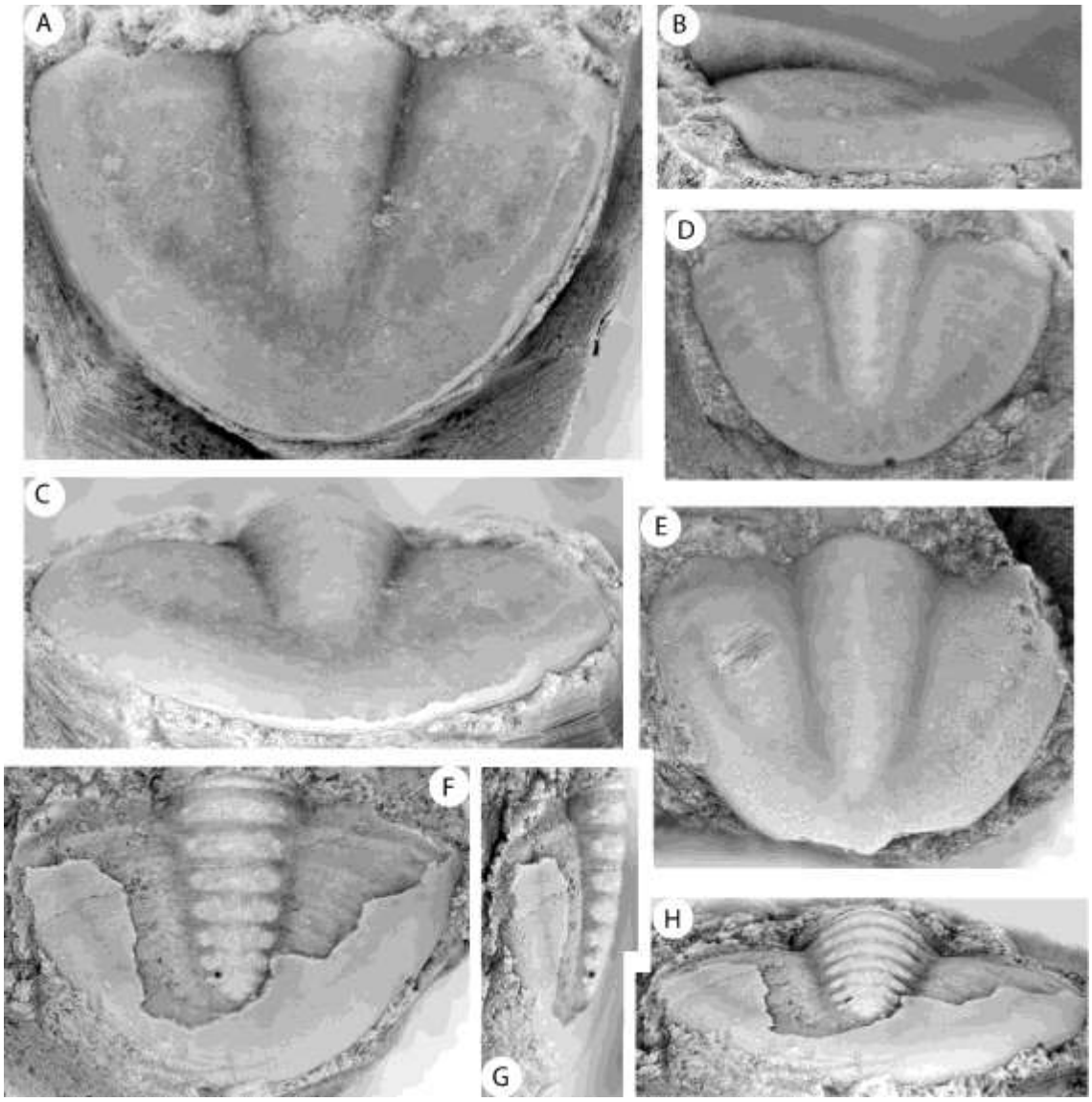
A
B
D
C
E
F
G
H

Plate 11

Blountia montanensis Duncan, 1944 from the Pilgrim Formation, Dry Wolf Creek section, Little Belt Mountains, Montana.

A–C, cranidium (USNM 126836; holotype), dorsal, anterior, lateral views, x18 (previously figured in Lochman and Duncan 1944, pl. 8, figs. 33–34)

D–F, cranidium (USNM 126837), dorsal, lateral, anterior views, x13.5 (A–F previously illustrated in Lochman and Duncan 1944, pl. 8, figs. 29–30).

G, cranidium (USNM 126838), dorsal view, x18.

H–J, cranidium (USNM 126839), dorsal, anterior, lateral views, x18.

K–L, cranidium (USNM 126838), dorsal, lateral views, x18.

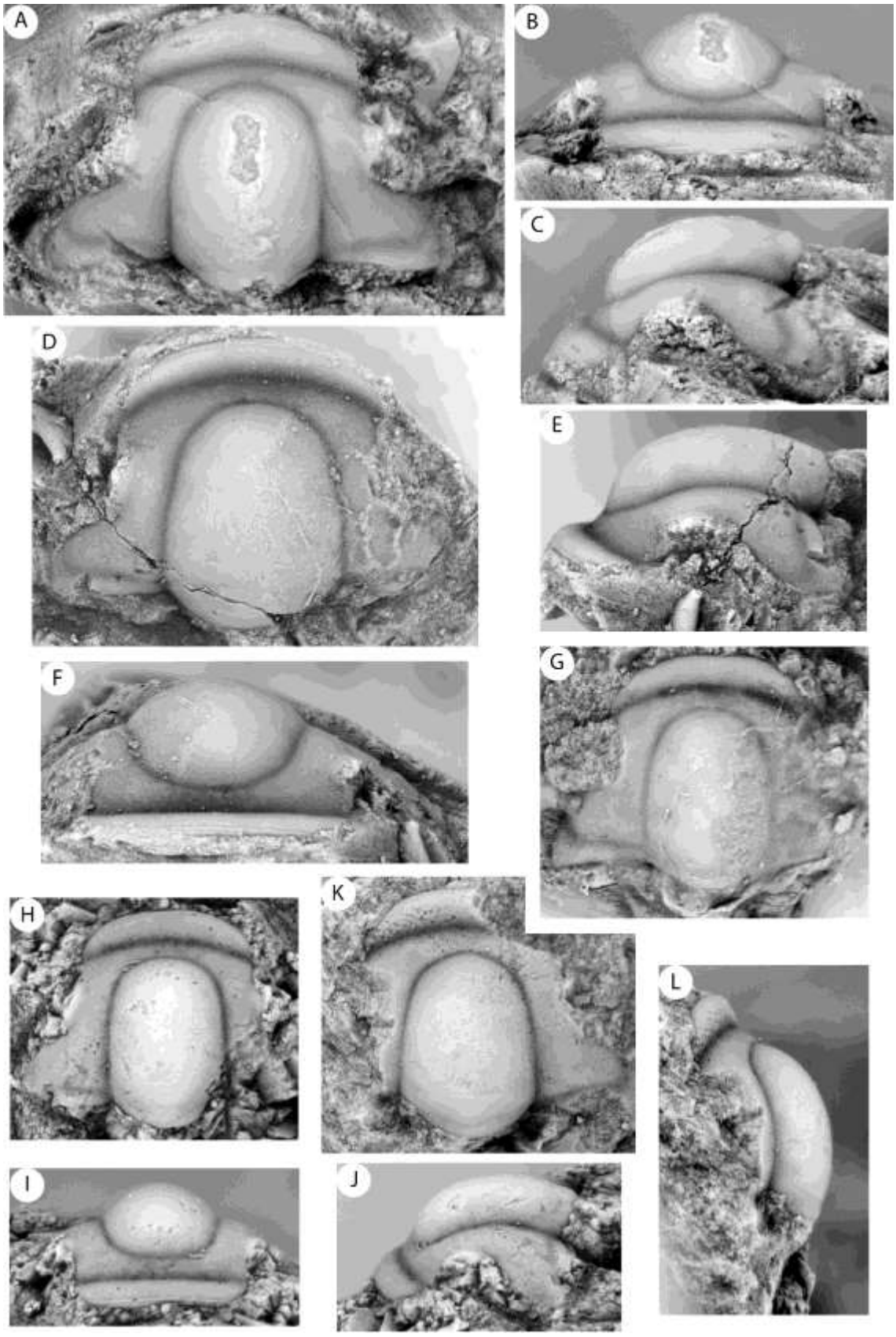
A
B
C
D
E
F
G
H
K
L
I
J

Plate 12

Blountia* cf. *montanensis (Duncan, 1944) from Rogersville and Big Creek sections, Hawkins County, Tennessee (all previously illustrated in Rasetti 1965, pl. 9, figs. 13–17).

A–C, cranidium (USNM 144598), dorsal, anterior, lateral views, x13.7.

D–F, cranidium (USNM 144599), dorsal, lateral, anterior views, x14.5.

G–H, free cheek (USNM 144598), dorsal, lateral views, x13.7.

I, cranidium (USNM 144599), dorsal view, x8.

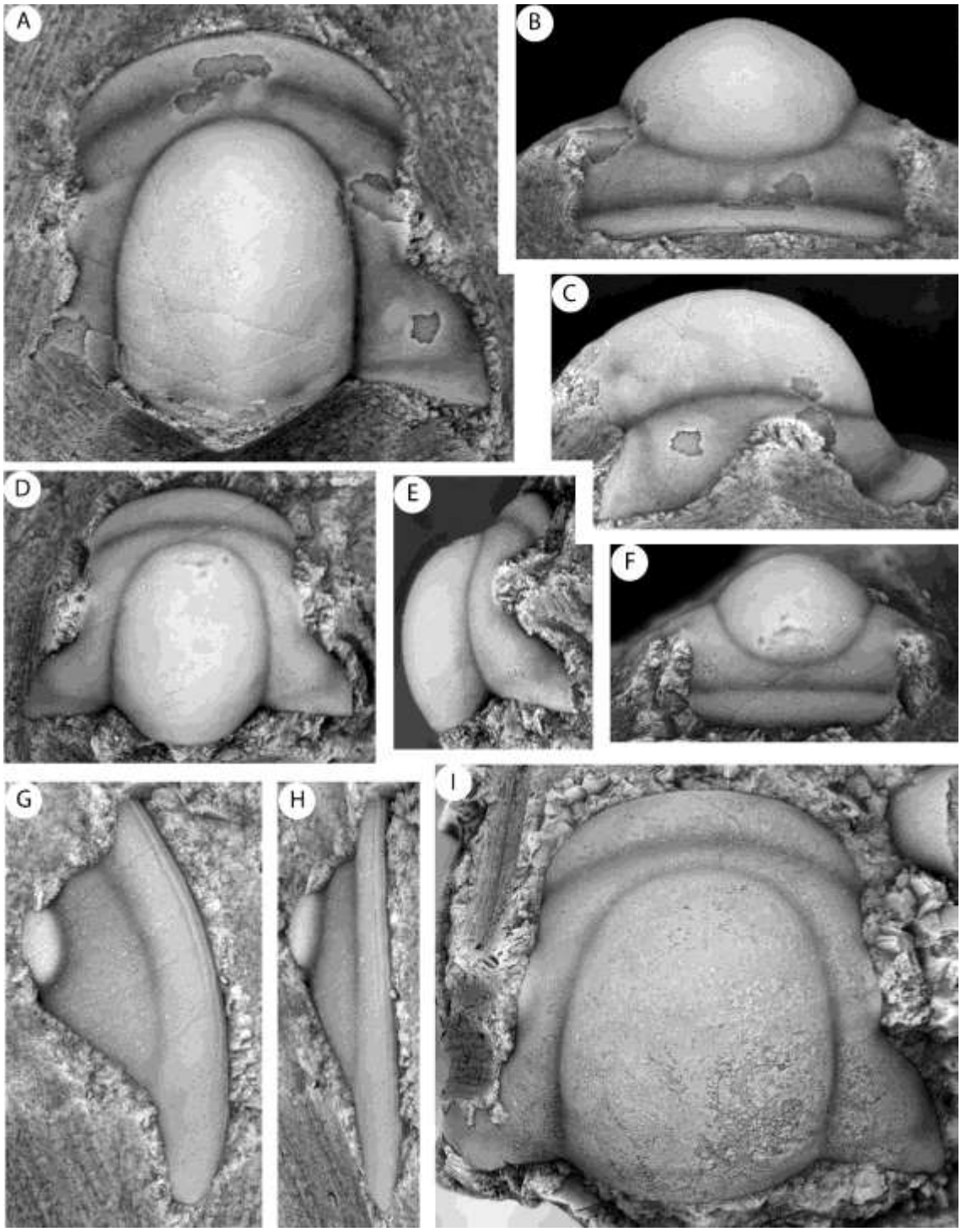
A
B
C
D
E
F
G
H
I

Plate 13

Blountia* cf. *montanensis (Duncan, 1944) from Rogersville and Big Creek sections, Hawkins County, Tennessee (all previously illustrated in Rasetti 1965, pl. 9, figs. 15, 18, 19).

A–C, exfoliated pygidium (USNM 144599), dorsal, lateral, posterior views, x9.

D–F, pygidium (USNM 144599), dorsal, posterior, lateral views, x12.5.

G–I, pygidium (USNM 144598), dorsal, lateral, posterior views, x12.5.

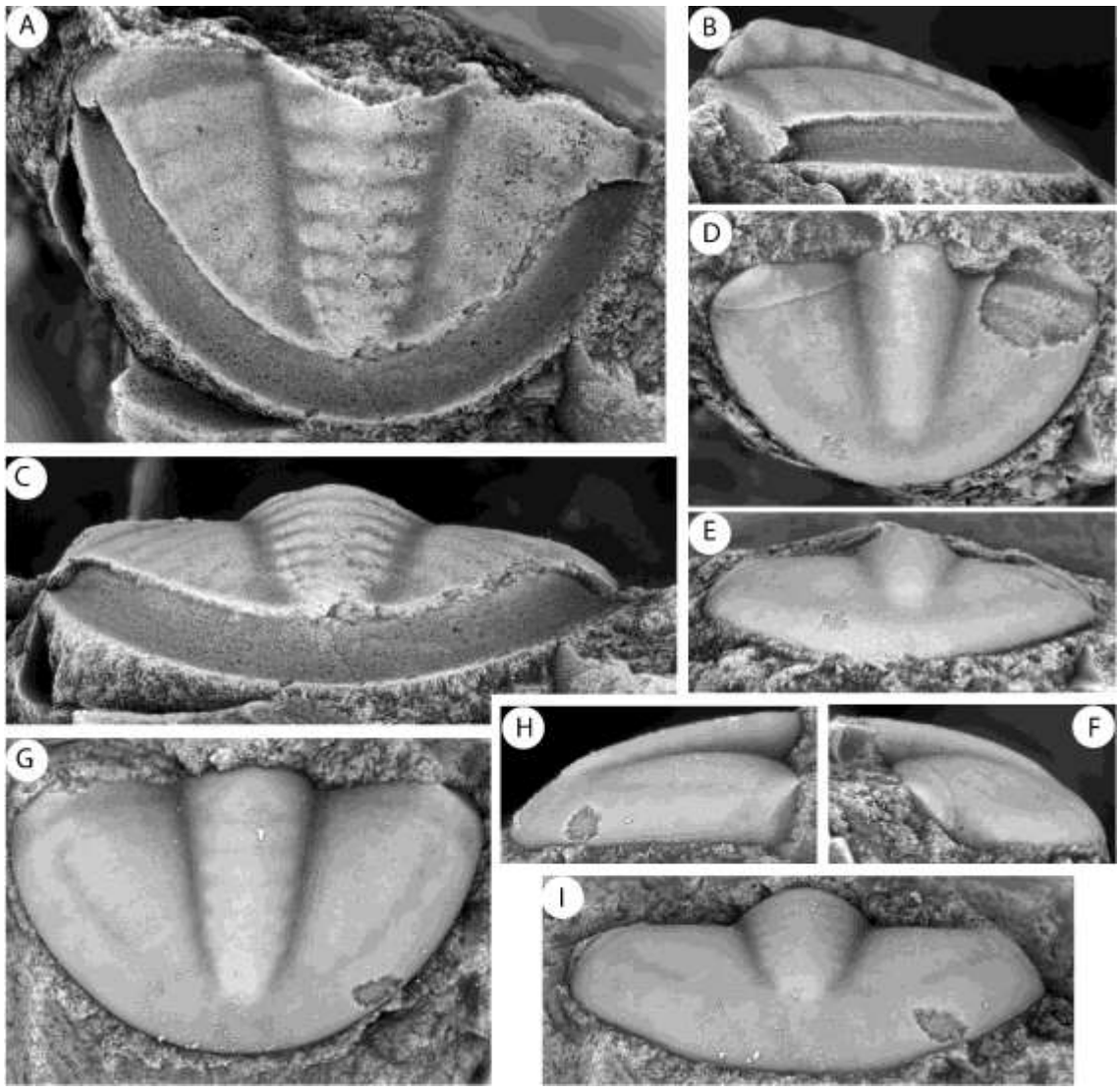
A
B
D
C
E
H
F
G
I

Plate 14

Blountina eleanora Lochman, 1944 from the Pilgrim Formation, Half Moon Pass section, Big Snowy Mountains, Montana.

A–C, exfoliated cranidium (USNM 127156; holotype), dorsal, anterior, lateral views, x11.7 (previously illustrated in Lochman and Duncan 1944, pl. 8, figs. 37, 40).

D–E, cranidium (USNM 127158), dorsal, anterior views, x11.7.

F–H, cranidium (USNM 127158), dorsal, anterior, lateral views, x13.5.

I, free cheek (USNM 127157a), dorsal view, x15.3 (previously illustrated in Lochman and Duncan, 1944, pl. 8, fig. 36).

J, exfoliated pygidium (USNM 127158), dorsal view, x18.

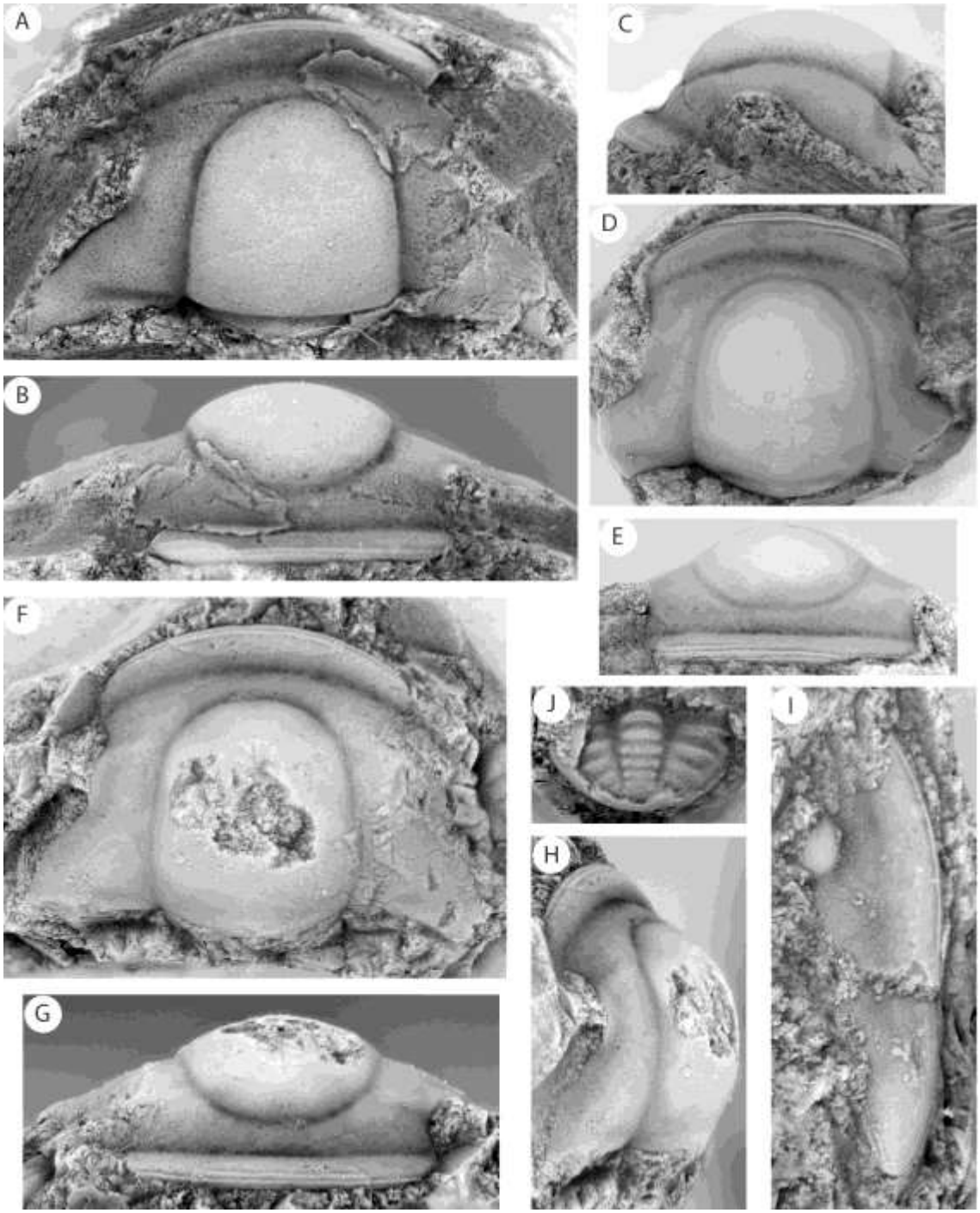
A
C
D
B
E
F
J
I
H
G

Plate 15

Blountina eleanora Lochman, 1944 from the Pilgrim Formation, Half Moon Pass section, Big Snowy Mountains, Montana.

A–C, pygidium (USNM 127157b), dorsal, posterior, lateral views, x10.7 (previously illustrated in Lochman and Duncan 1944, pl. 8, figs. 38–39).

D–E, pygidium (USNM 127158), dorsal, posterior views, x14.2.

F, pygidium (USNM 127158), dorsal view, x13.3.

G–H, exfoliated pygidium (USNM 127157c), dorsal, posterior views, x16.5 (previously illustrated in Lochman and Duncan 1944, pl. 8, fig. 35).

I, exfoliated pygidium (USNM 127158), dorsal view, x13.3.

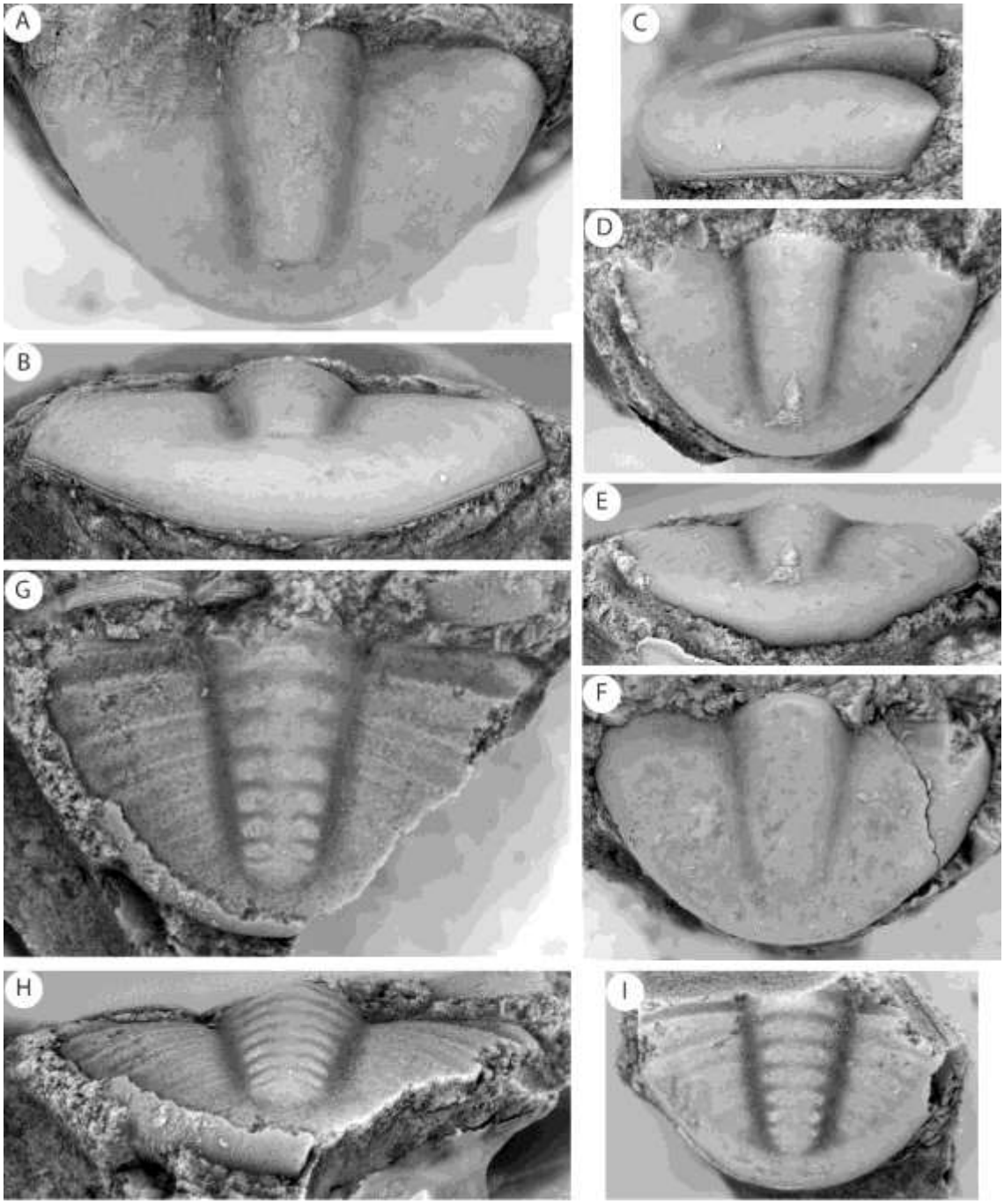
A
C
D
B
E
G
F
H
I

Plate 16

Maryvillia triangularis (Lochman, 1944) from the Pilgrim Formation, Half Moon Pass Section, Big Snowy Mountains, Montana.

A–C, cranidium (USNM 127159; holotype), dorsal, lateral, anterior views, x16.4 (previously figured in Lochman and Duncan 1944, pl. 8, figs. 16–17).

D–F, cranidium (USNM 127161), dorsal, lateral, anterior views, x13.7.

G, exfoliated cranidium (USNM 127161), dorsal view, x6.4.

H, exfoliated cranidium (USNM 127161), dorsal view, x4.

I–K, exfoliated cranidium (USNM 127161), dorsal, anterior, lateral views, x5.5.

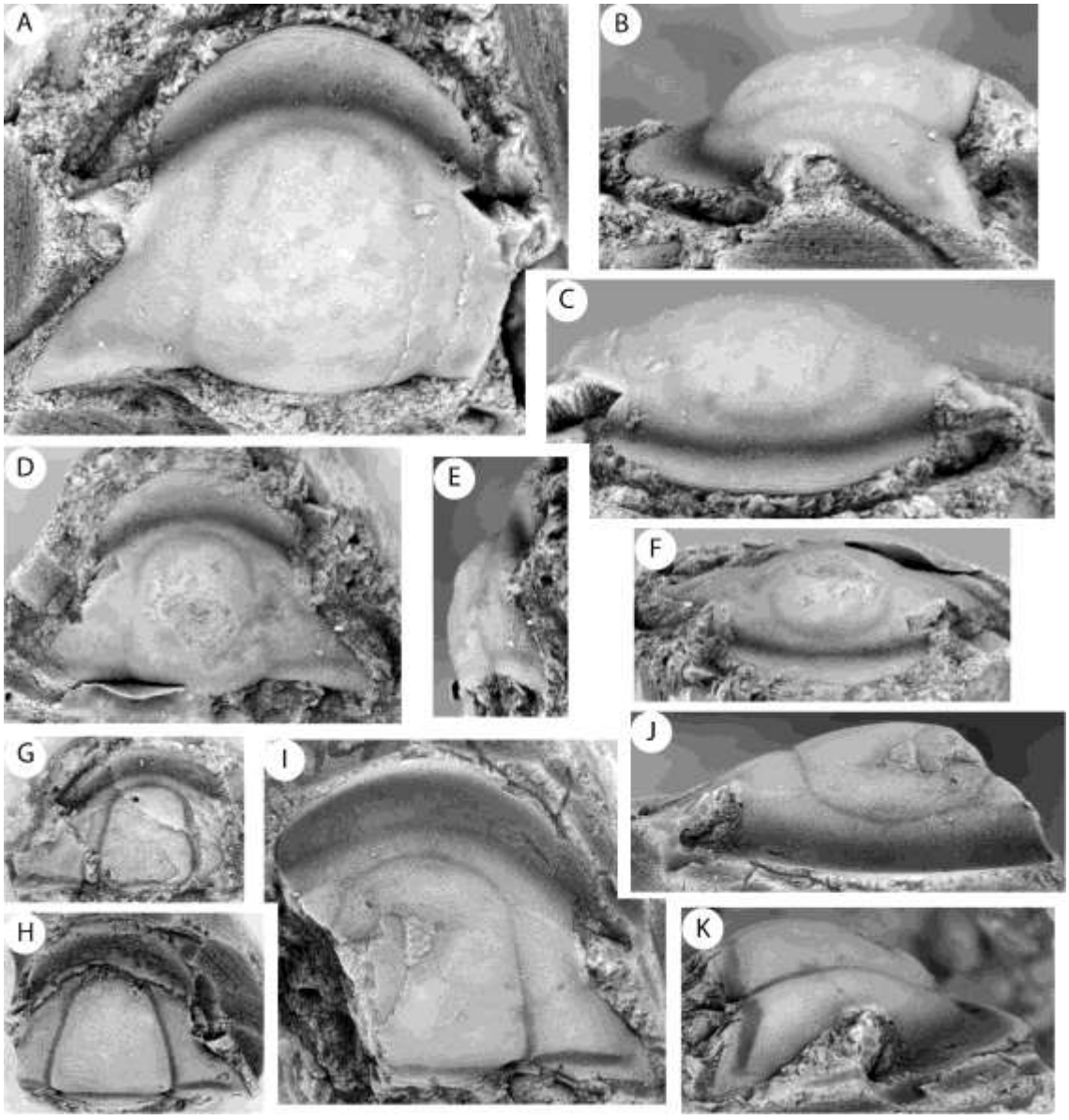
A
B
C
D
E
F
G
I
J
H
K

Plate 17

Maryvillia triangularis (Lochman, 1944) from the Pilgrim Formation, Half Moon Pass Section, Big Snowy Mountains, Montana.

A–B, pygidium (USNM 127160c), dorsal, posterior views, x12.3 (previously illustrated in Lochman and Duncan 1944, pl. 8, fig. 15).

C–E, exfoliated pygidium (USNM 127160b), dorsal, posterior, lateral views, x8 (previously illustrated in Lochman and Duncan 1944, pl. 8, figs. 12–13).

F, exfoliated pygidium (USNM 127160d), dorsal view, x13.2 (previously illustrated in Lochman and Duncan 1944, pl. 8, fig. 18).

G, pygidium (USNM 127161), dorsal view, x17.6.

H, pygidium (USNM 127161), dorsal view, x17.6. **I–J**, pygidium (USNM 127161), dorsal, posterior views, x13.2.

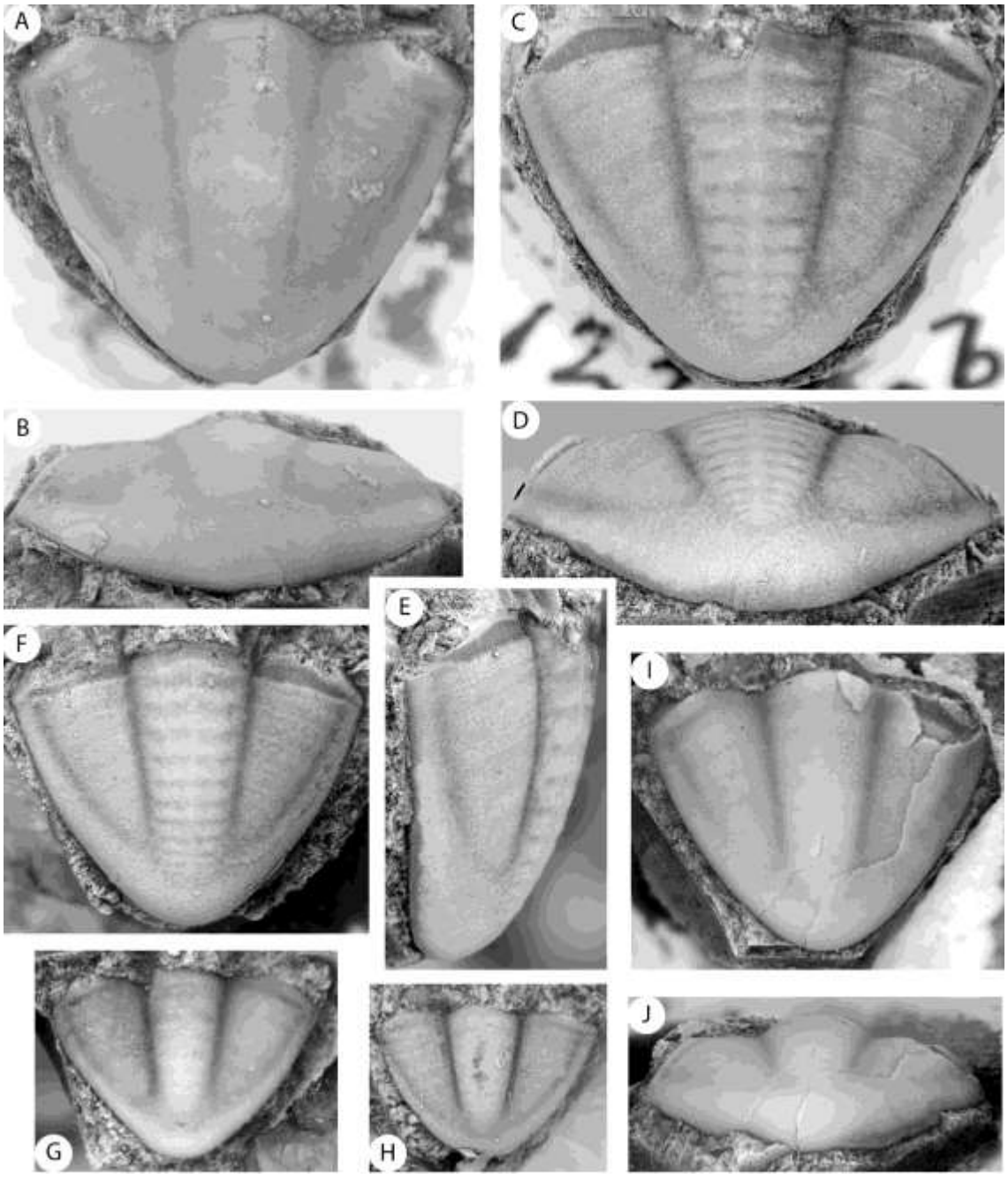
A
C
B
D
E
F
I
G
H
J

Plate 18

Blountia gaspensis Rasetti, 1946 from Grosses-Roches, Quebec.

A–C, cranidium (LU 1004a; holotype), lateral, dorsal, anterior views, x8.8 (previously illustrated in Rasetti 1946, pl. 67, figs. 7–8).

D–F, partially exfoliated cranidium (LU 1004d), dorsal, lateral, anterior views, x6.6.

G–I, cranidium, missing anterior border (LU 1006), anterior, lateral, dorsal views, x11.5.

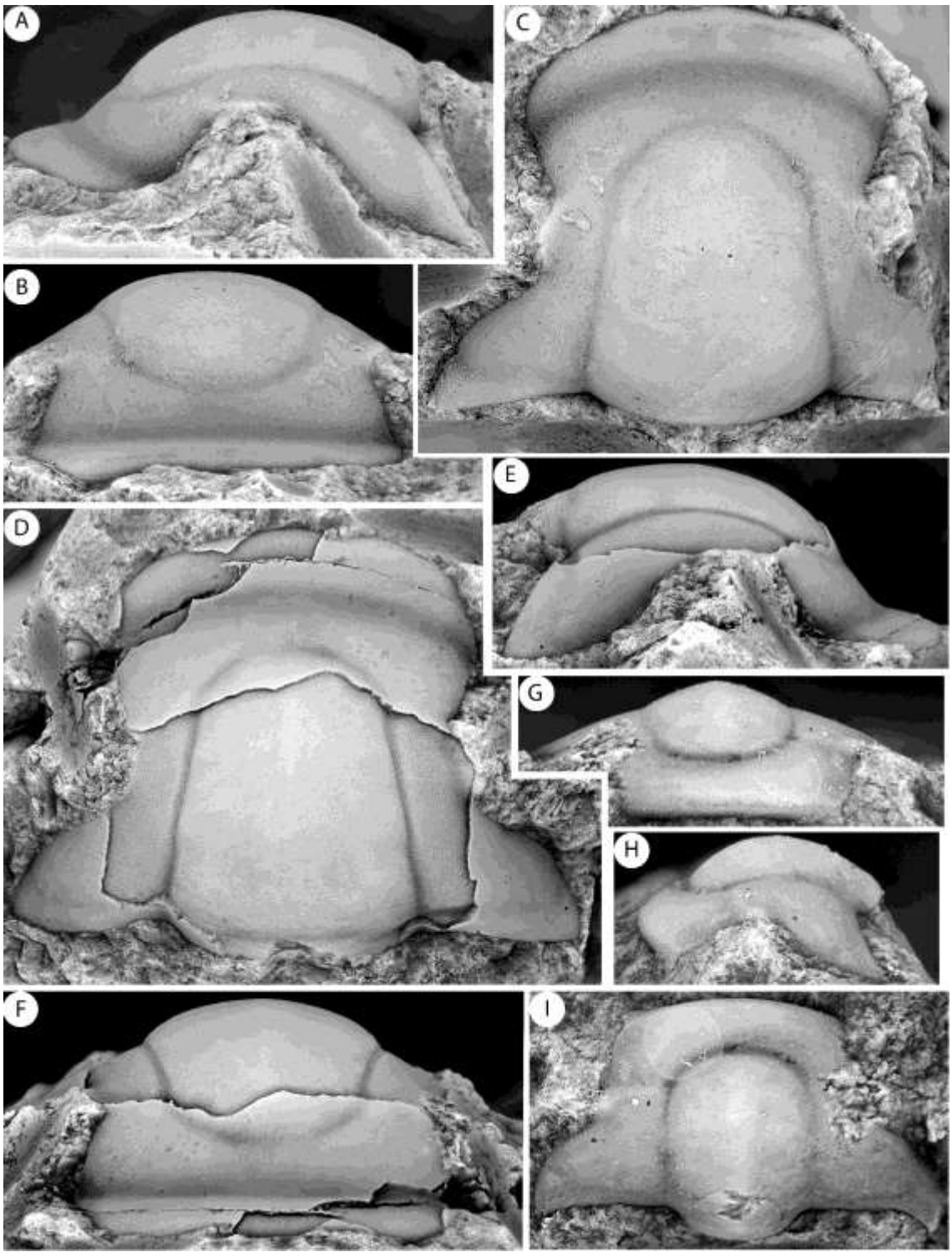
A
C
B
E
D
G
H
F
I

Plate 19

Blountia gaspensis Rasetti, 1946 from Grosses-Roches, Quebec.

A–C, pygidium (LU 1004c), dorsal, posterior, and lateral views, x5.5.

D–F, partially exfoliated pygidium (LU 1004c), dorsal, posterior, and lateral views, x5.5 (A–F previously illustrated in Rasetti 1946, pl. 67, figs. 9–10).

G, exfoliated pygidium (LU 1004e), dorsal view, x5.5.

Maryvillia arion Walcott 1916 from the Nolichucky Formation, one-half mile east of Rogersville, Tennessee; previously unfigured.

H–J, exfoliated pygidium (USNM 62827; holotype), dorsal, lateral, and posterior views, x6.5.

K, exfoliated pygidium, dorsal view, x3.6.

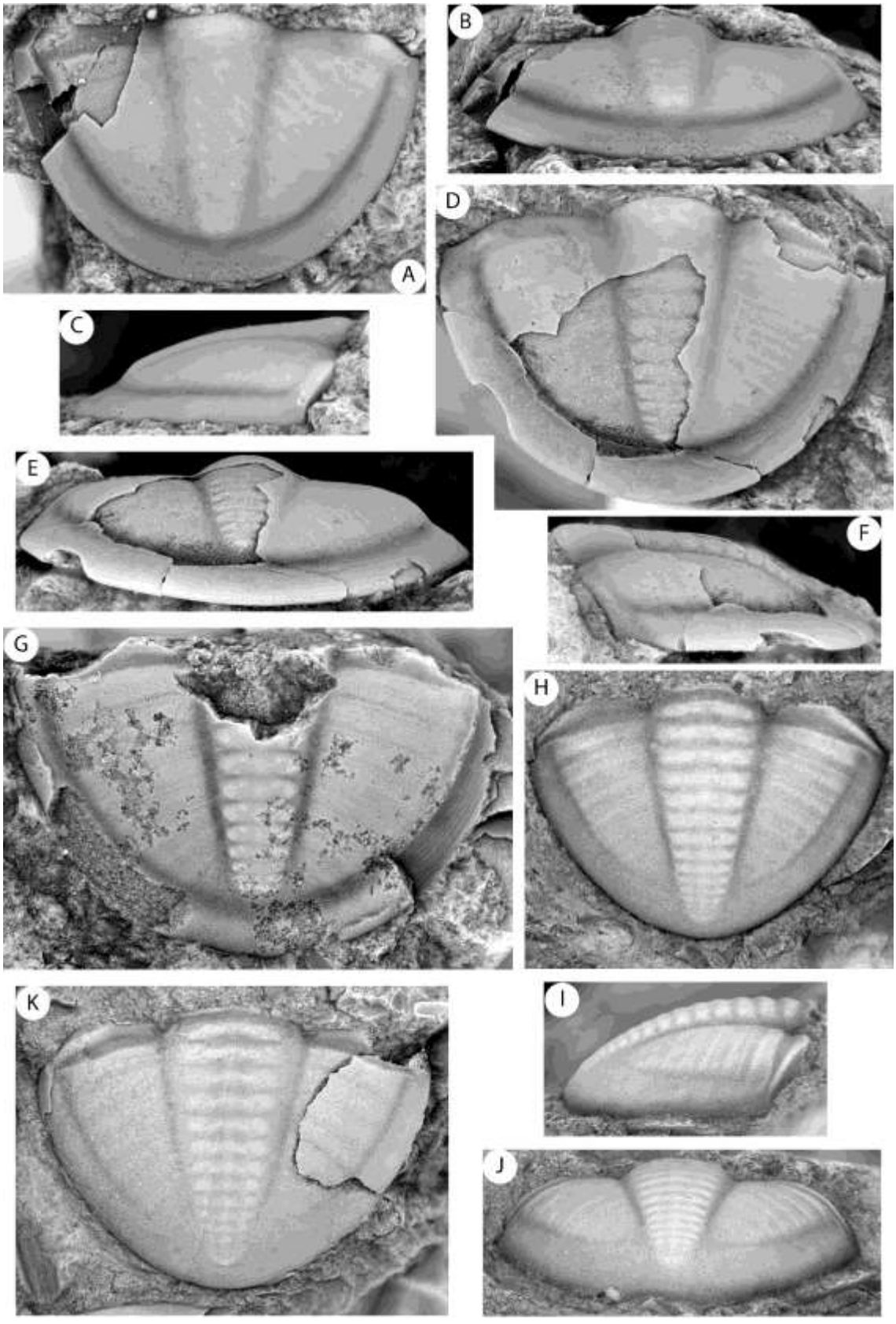
A
B
C
D
E
F
G
H
I
J
K

Plate 20

Blountia nasuta Rasetti, 1946 from Grosses-Roches, Quebec.

A–C, partially exfoliated cranidium (LU 1005a; holotype), dorsal, anterior, lateral views, x9.3 (previously figured in Rasetti 1946, pl. 67, figs. 11–12).

D–F, cranidium (LU 1005f), dorsal, lateral, anterior views, x14.

G–I, pygidium (LU 1005c), dorsal, lateral, posterior views, x7.5 (previously figured in Rasetti 1946, pl. 67, fig. 13).

J–L, pygidium (LU 1005b), dorsal, posterior, lateral views, x7.5 (previously figured in Rasetti 1946, pl. 67, fig. 14).

M, exfoliated pygidium (LU 1005e), dorsal view, x5.6.

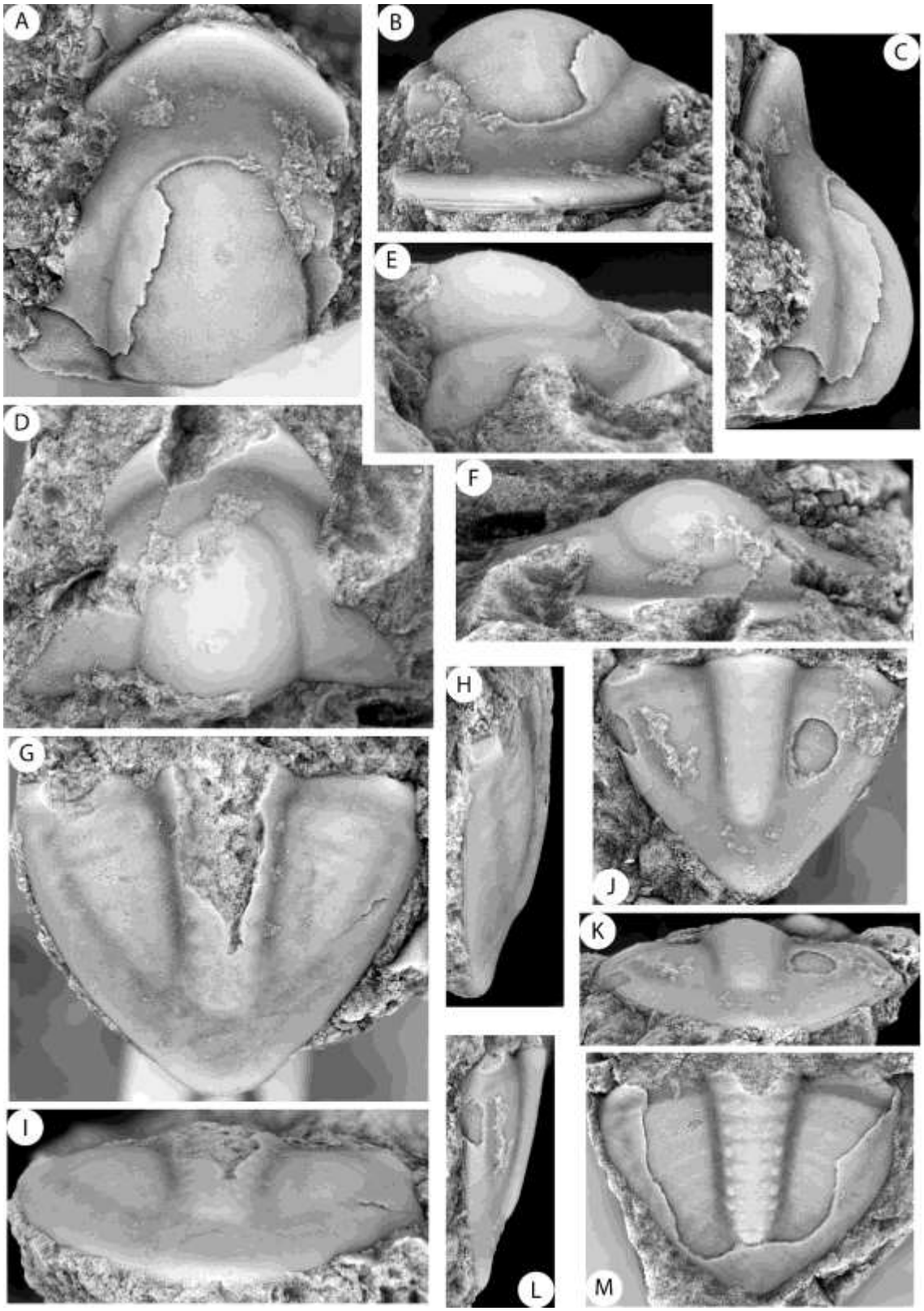
A
B
C
E
D
F
H
J
G
K
I
L
M

Plate 21

Blountia nevadensis n. sp. from House Range, Utah and Yucca Flat, Nevada.

A–C, cranidium (holotype; USNM 141505), anterior, lateral, dorsal views, x13.8.

D–E, free cheek (USNM 141504), dorsal, lateral views, x9.2 (previously figured in Palmer 1965, pl. 1, fig. 1)

F, cranidium (USNM 141505), dorsal view, x9.2 (previously figured in Palmer 1965, pl. 1, fig. 2)

G, pygidium (USNM 141506), dorsal view, x13.8.

H–J, pygidium (USNM 141506), dorsal, anterior, lateral views, x18.4 (previously figured in Palmer 1965, pl. 1, fig. 4).

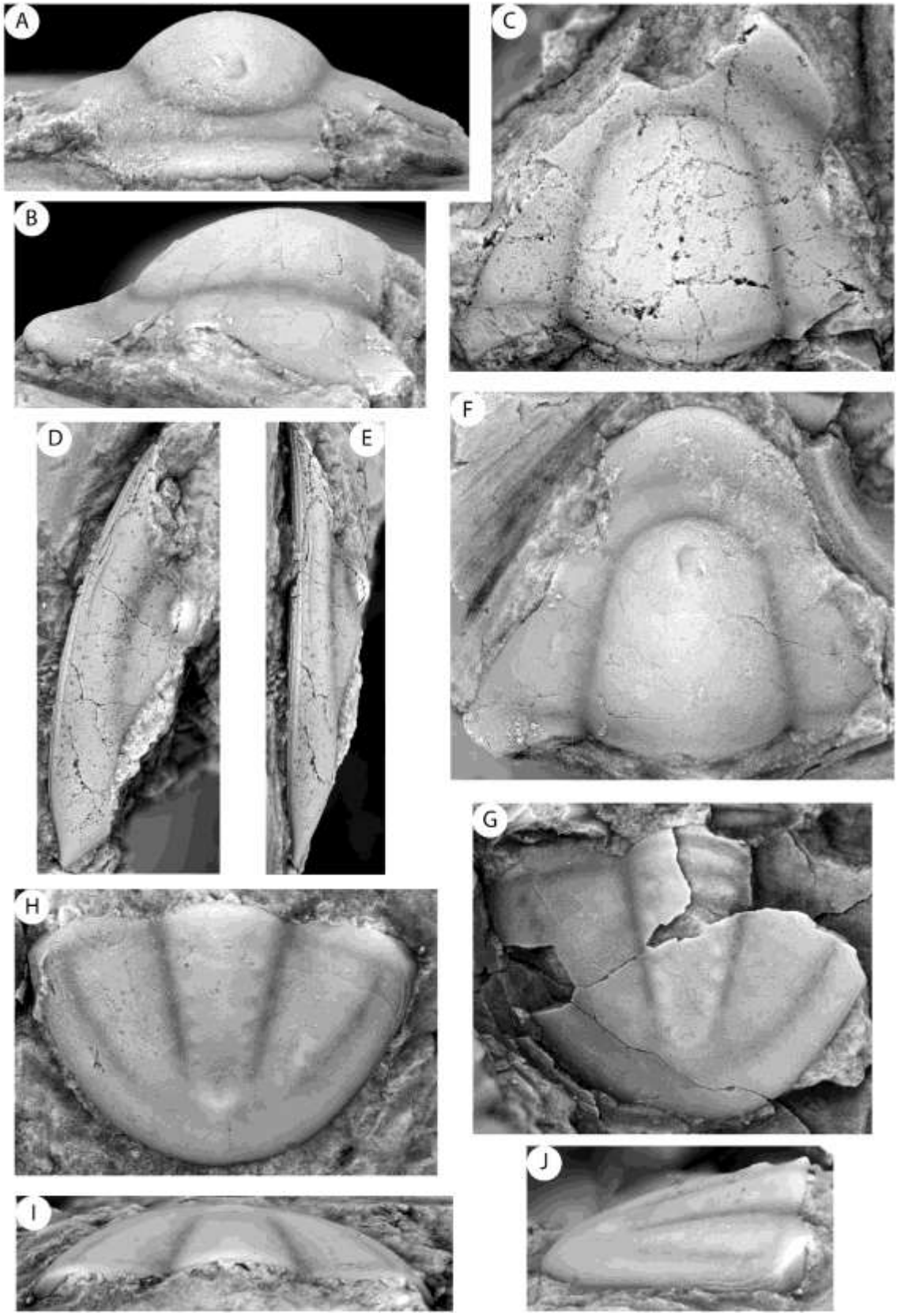
A
B
C
D
E
F
G
H
I
J

Plate 22

Blountia morgancreekensis n. sp. from the Cap Mountain Limestone, Burnet County, Texas (MCNe1 7.1).

A–C, holotype cranidium (OU 238142), dorsal, lateral, anterior views, x6.2.

D–F, exfoliated cranidium (OU 238143), dorsal, lateral, anterior views, x7.

G–H, exfoliated cranidium (OU 238144), dorsal, anterior views, x5.3.

I–J, cranidium (OU 238145), dorsal, lateral views, x9.

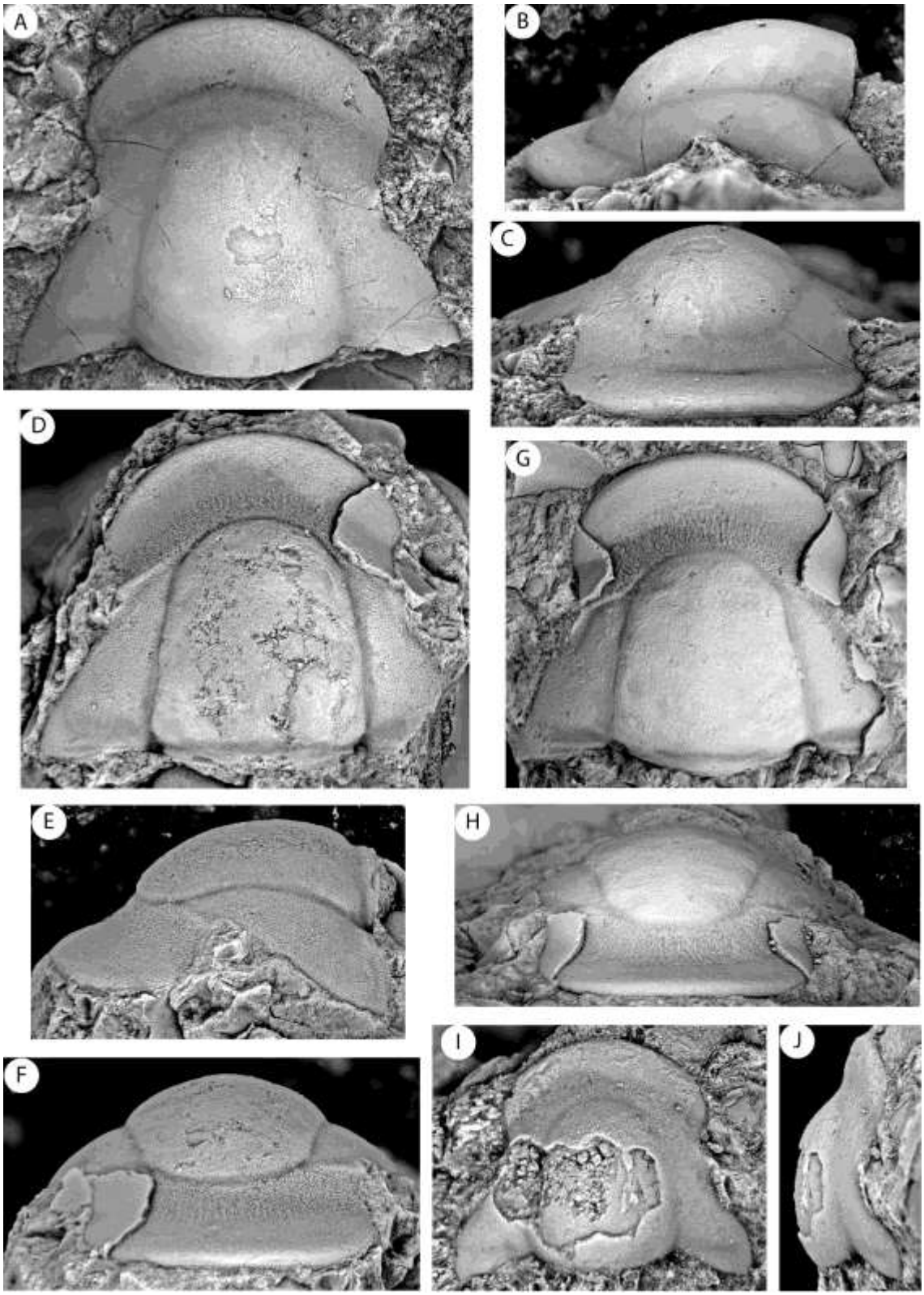
A
B
C
D
G
E
H
F
I
J

Plate 23

Blountia morgancreekensis n. sp. from Cap Mountain Limestone, Burnet County, Texas (MCNe1 7.1).

A–B, partially exfoliated pygidium (OU 238146), dorsal, posterior views, x6.

C, pygidium (OU 238149), dorsal view, x10.5.

D–F, exfoliated pygidium (OU 238147), dorsal, posterior, lateral, x9.

G–I, pygidium (OU 238148), dorsal, lateral posterior views, x13.

J, exfoliated pygidium (OU 238150), dorsal view, x9.

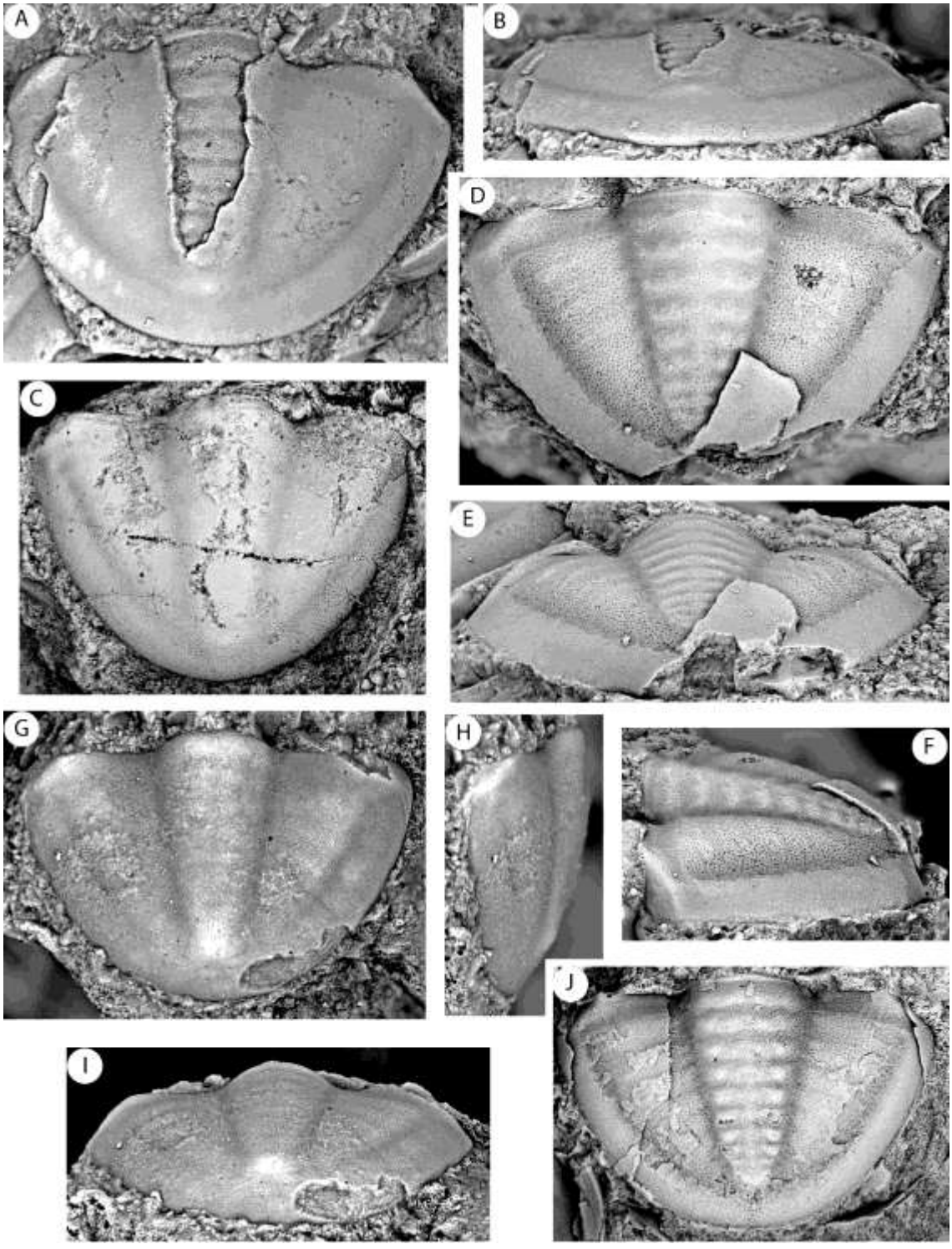
A
B
D
C
E
G
H
F
J
I

Plate 24

Blountia morgancreekensis n. sp. from Cap Mountain Limestone, Burnet County, Texas (Figs. A–D from section MCNe1 7.1).

A–C, exfoliated cranidium (OU 238151), dorsal, anterior, lateral views, x8.

D, partially exfoliated cranidium (OU 238152), dorsal view, x7.

E–G, exfoliated cranidium (USNM 108765b), dorsal, lateral, anterior views, x4.5 (previously illustrated in Palmer 1954, pl. 79, fig. 4).

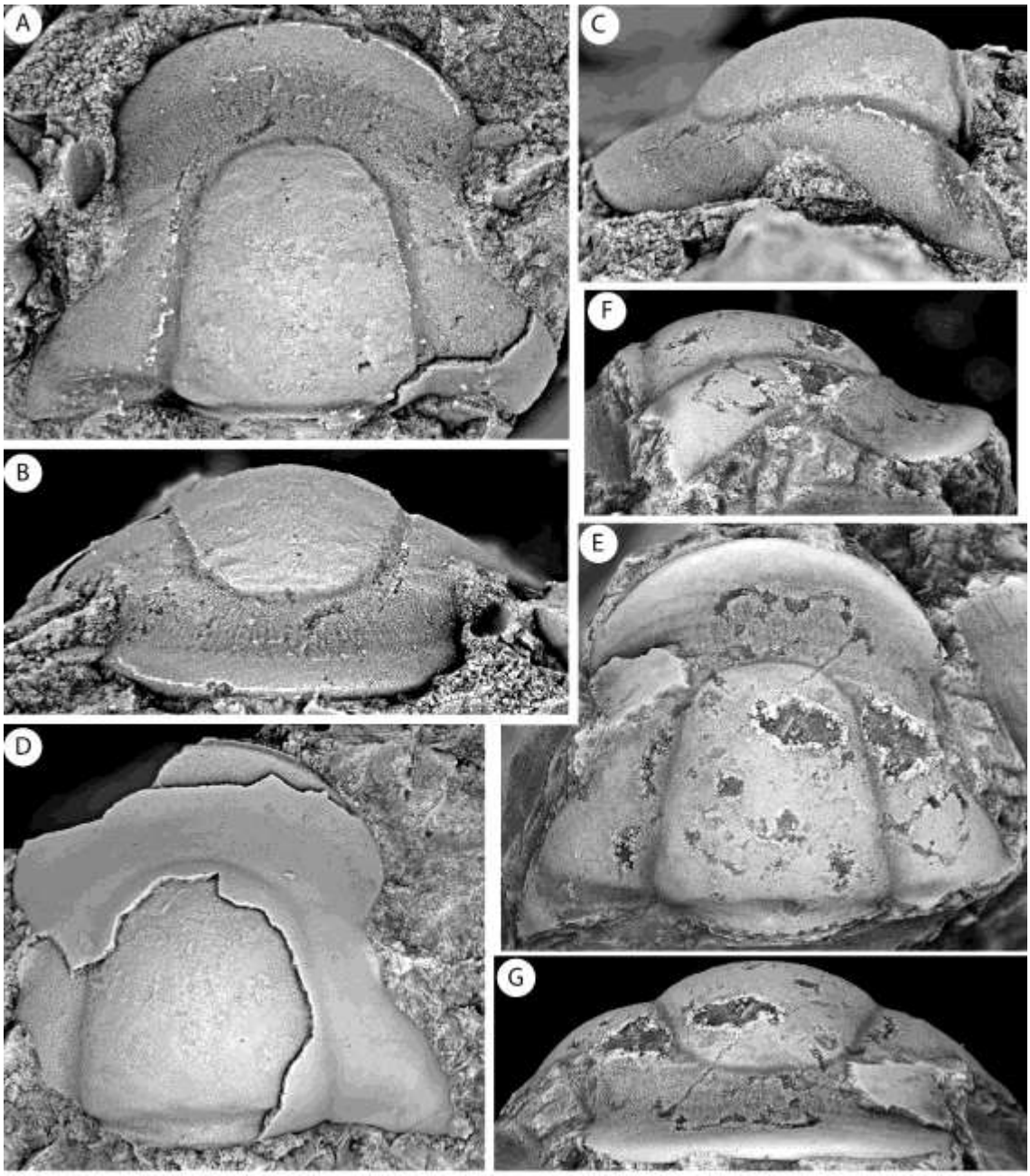
A
C
F
B
E
D
G

Plate 25

Blountia newfoundlandensis n. sp. from the Cow Head Group, Newfoundland, section Cowhead (CH) 48.

A–C, holotype cranidium, dorsal, anterior, lateral views, x13.2.

D–F, cranidium, dorsal, anterior, lateral views, x10.5.

G–I, cranidium, dorsal, lateral, anterior views, x16.7.

J, partially exfoliated cranidium, dorsal view, x9.5.

K, partially exfoliated cranidium, dorsal view, x9.

L, cranidium, dorsal view, x14.2.

M–N, free cheek, dorsal, lateral views, x7.5.

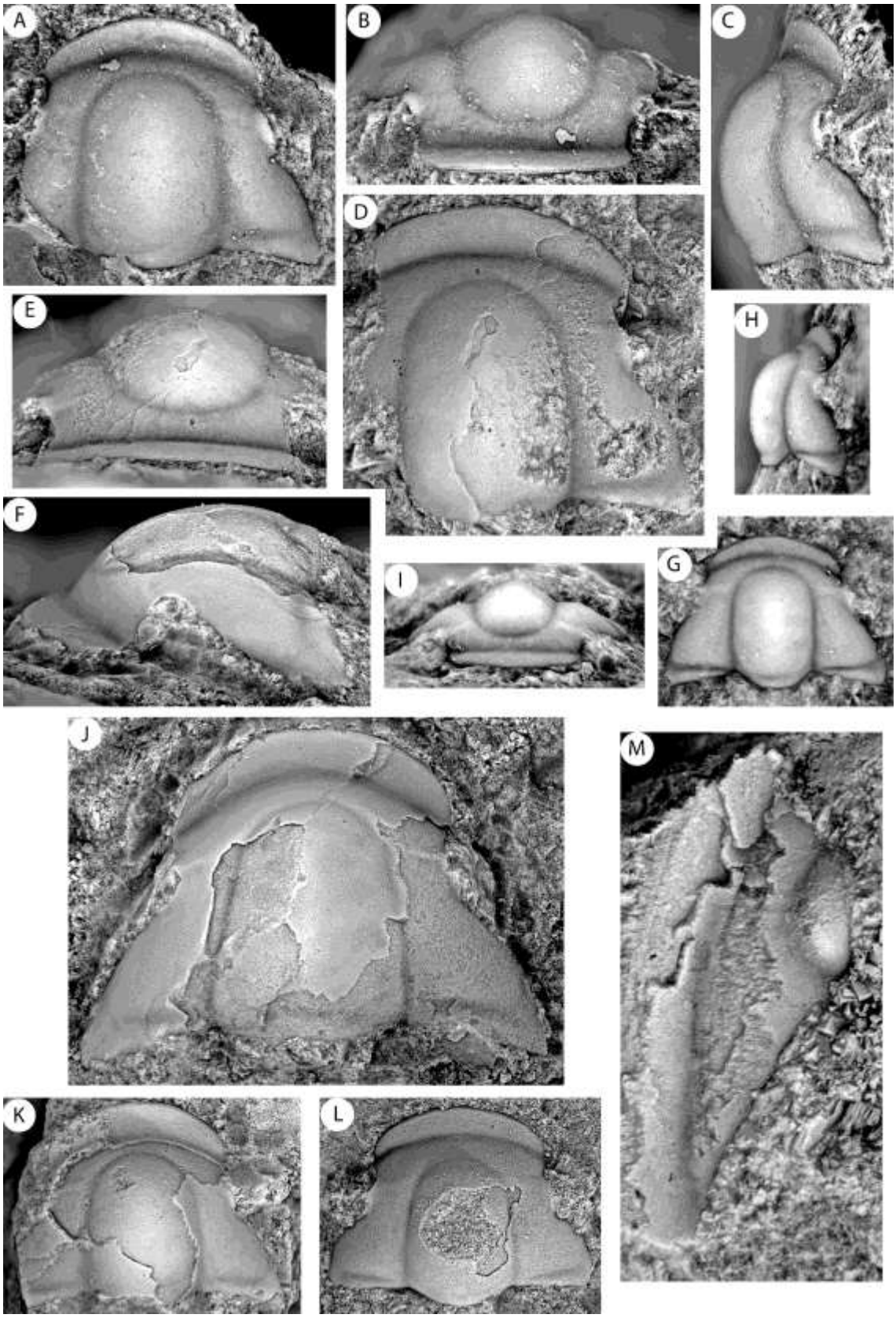
A
B
C
D
E
H
F
I
G
J
M
K
L

Plate 26

Blountia newfoundlandensis n. sp. from the Cow Head Group, Newfoundland section Cowhead (CH) 48.

A–B, partially exfoliated pygidium, dorsal, posterior views, x10.2.

C–E, exfoliated pygidium, dorsal, posterior, lateral views, x8.

F–G, pygidium, dorsal, posterior views, x12.

H–I, pygidium, dorsal, posterior views, x15.

J–L, pygidium, dorsal, lateral, posterior views, x15.

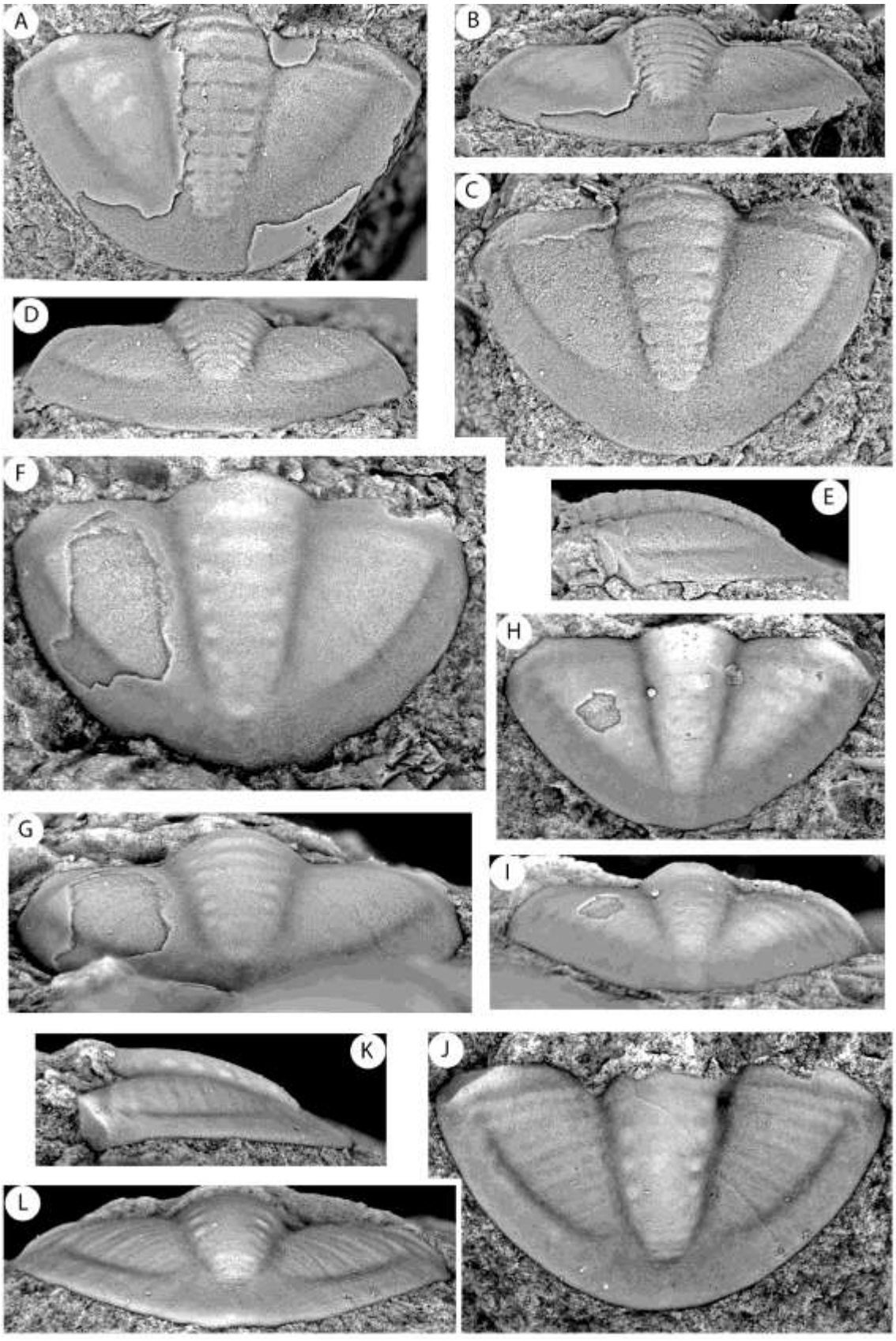
A
B
C
D
F
E
H
G
I
K
J
L

Plate 27

Aphelaspis* cf. *walcotti (Resser, 1938) from the Cap Mountain Limestone, Riley Formation, Texas (MCNe1 7.1).

A–C, partly exfoliated cranidium (OU 238054), dorsal, anterior, lateral views, x7.

D, cranidium (OU 238055), dorsal view, x7.

E–F, cranidium (OU 238056), dorsal, anterior view, x17.6.

G–H, partly exfoliated pygidium (OU 238057), dorsal, posterior view, x8.

I–J, free cheek (OU 238058), dorsal, lateral view, x6.

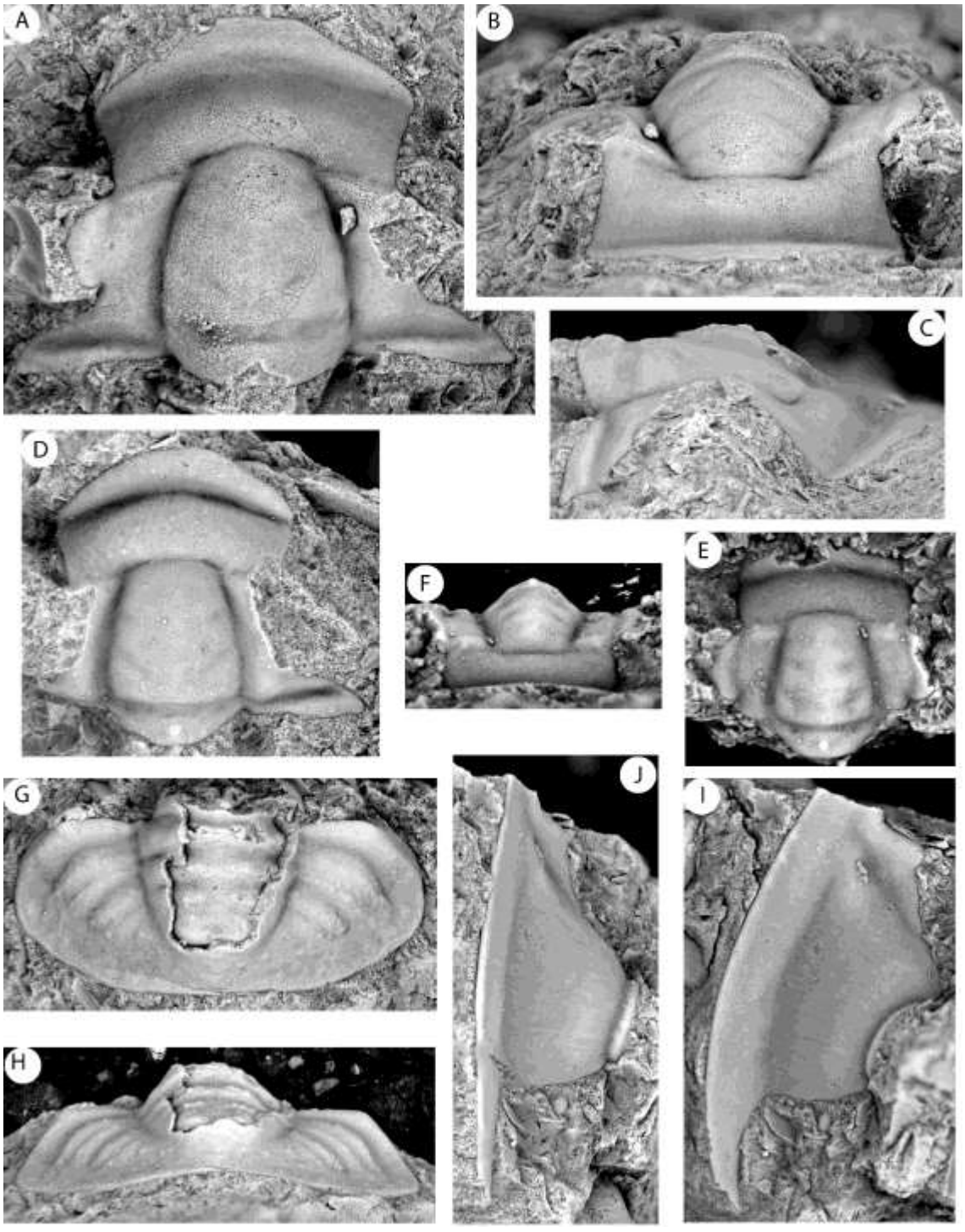
A
B
C
D
E
F
G
H
J
I

Plate 28

Aphelaspis* cf. *walcotti (Resser, 1938) from the Cap Mountain Limestone, Riley Formation, Texas (LB 0.8).

A–B, cranidium (OU 238059), dorsal, anterior view, x9.

C–E, cranidium (OU 238061), dorsal, anterior view, x10.

F, cranidium (OU 238060), dorsal view, x10.

G–H, free cheek (OU 238062), dorsal, lateral view, x9.

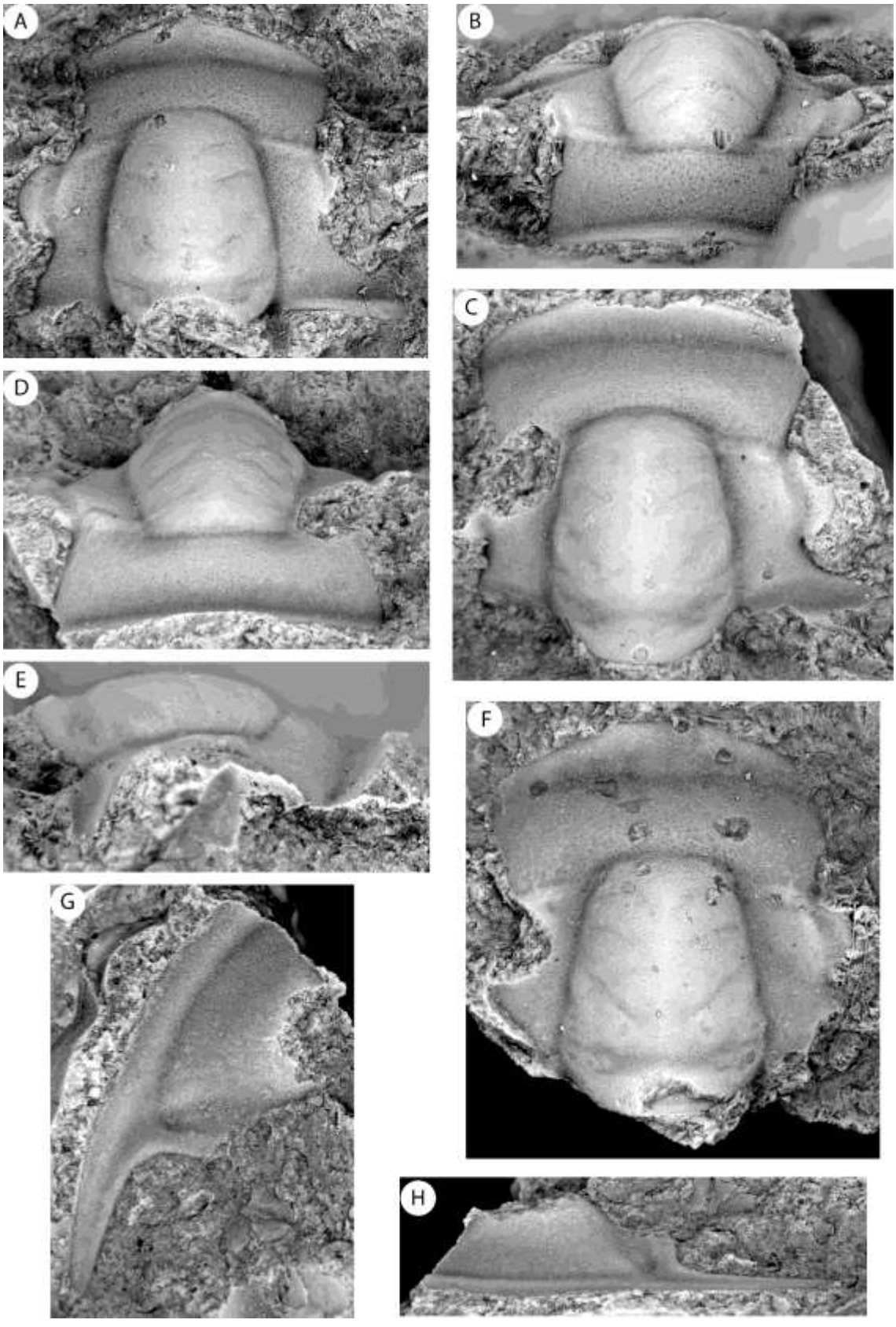
A
B
C
D
E
F
G
H

Plate 29

Aphelaspis constricta Palmer, 1954 from the Cap Mountain Limestone, Riley Formation, Texas (HP 2.5 Pulloff).

A–C, partially exfoliated cranidium (OU 238063), dorsal, anterior, lateral views, x9.3.

D–F, cranidium (OU 238064), dorsal, anterior, lateral views, x11.

G, cranidium (OU 238065), dorsal view, x23.5.

H, cranidium (OU 238065), dorsal view, x14.

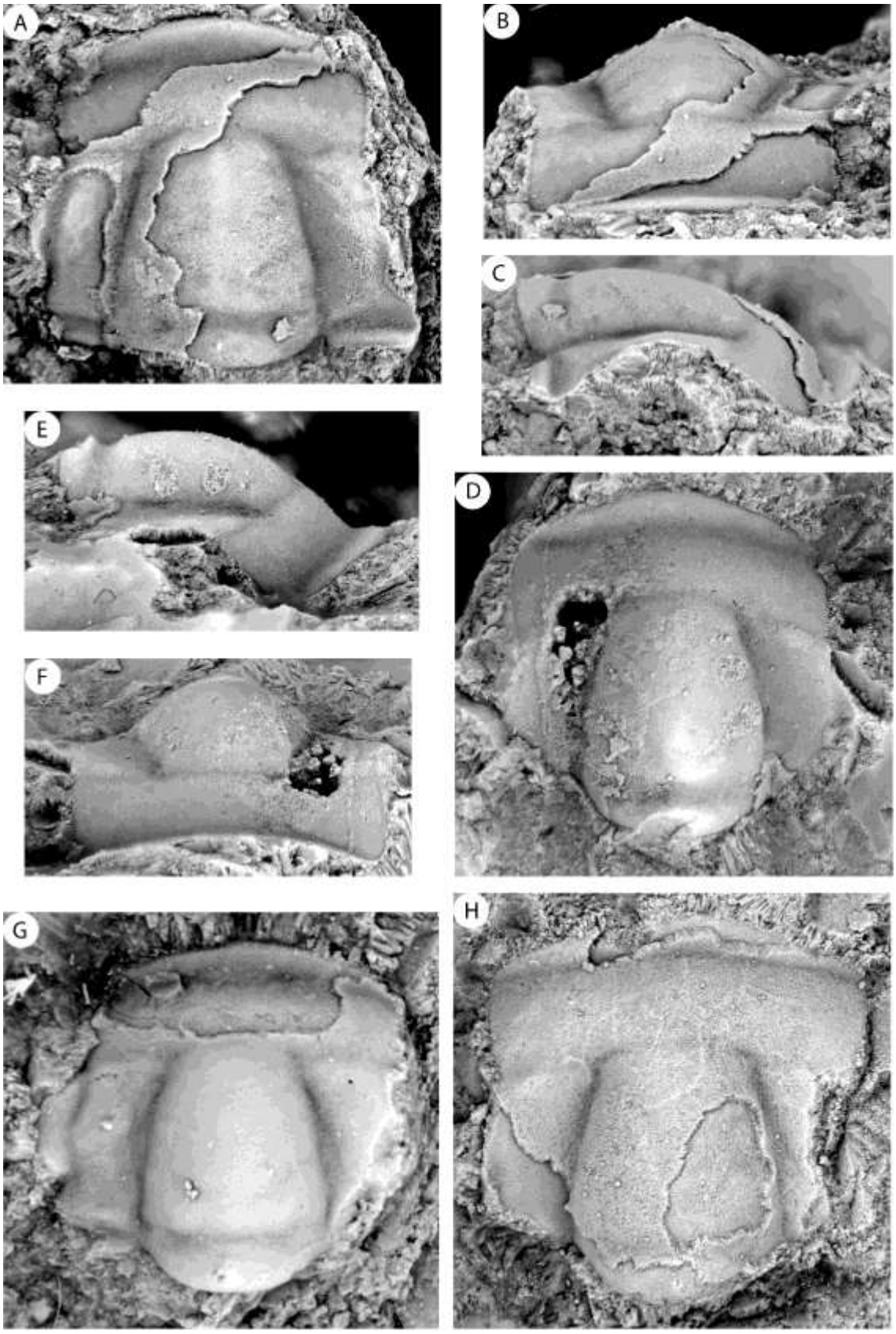
A
B
C
E
D
F
G
H

Plate 30

Aphelaspis constricta Palmer, 1954 from the Cap Mountain Limestone, Riley Formation, Texas (HP 2.5 Pulloff).

A–C, cranidium (OU 238067), dorsal, anterior, lateral views, x17.

D–F, exfoliated cranidium (OU 238068), dorsal, anterior, lateral views, x16.5.

G–H, exfoliated cranidium (OU 238069), dorsal, anterior views, x16.5.

I, cranidium (OU 238070), dorsal view, x18.

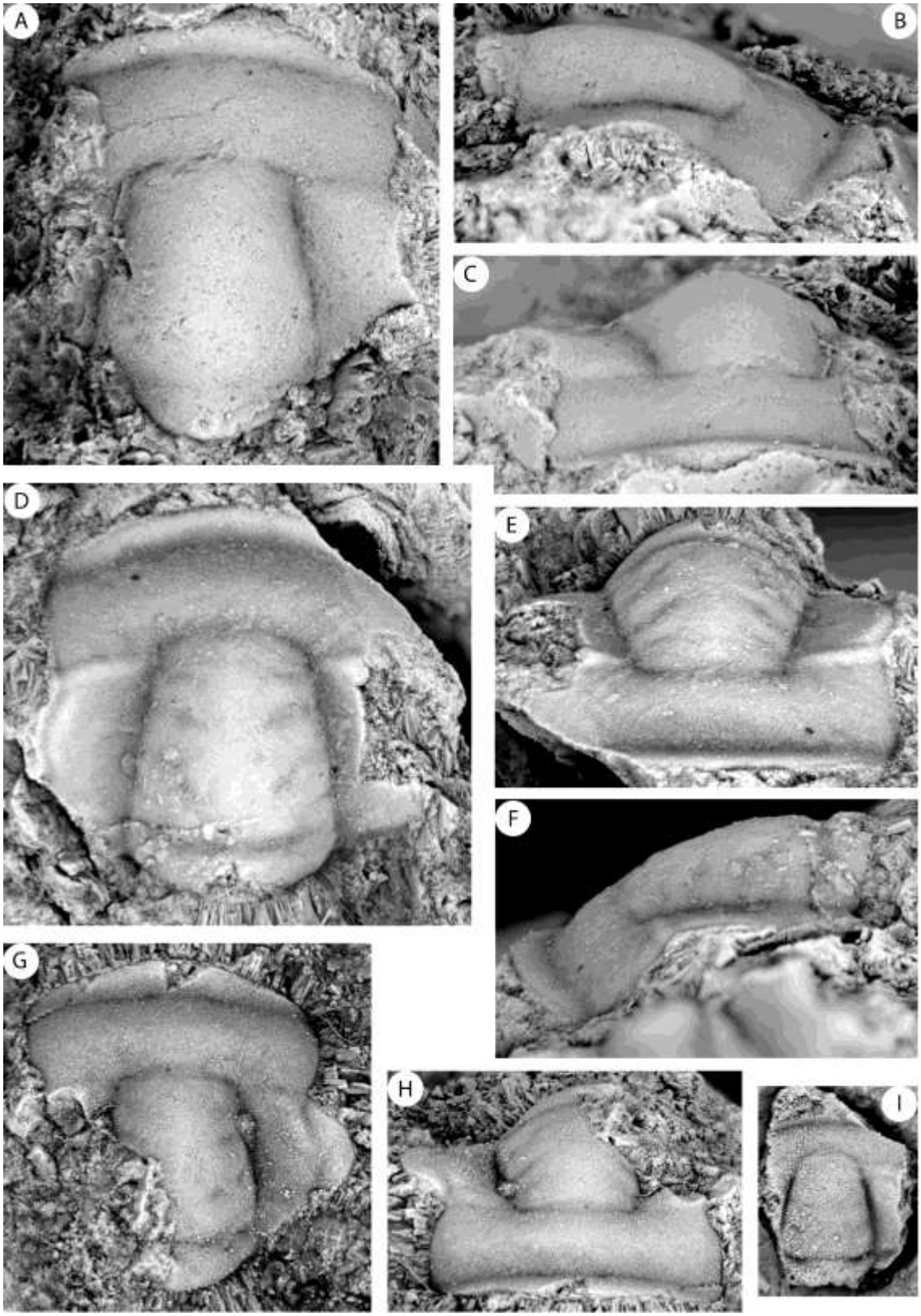
A
B
C
D
E
F
G
H
I

Plate 31

Aphelaspis constricta Palmer, 1954 from the Cap Mountain Limestone, Riley Formation, Texas.

A–B, exfoliated cranidium (OU 238071), dorsal, anterior views, x17.5 (HP 2.5 Pulloff).

C–E, partially exfoliated cranidium (OU 238074), dorsal, anterior, lateral views, x17.5 (HP 2.6 Pulloff).

F–G, cranidium (OU 238072), dorsal, anterior views, x23 (HP 2.5 Pulloff).

H–I, cranidium (OU 238073), dorsal, lateral views, x11 (HP 2.5 Pulloff).

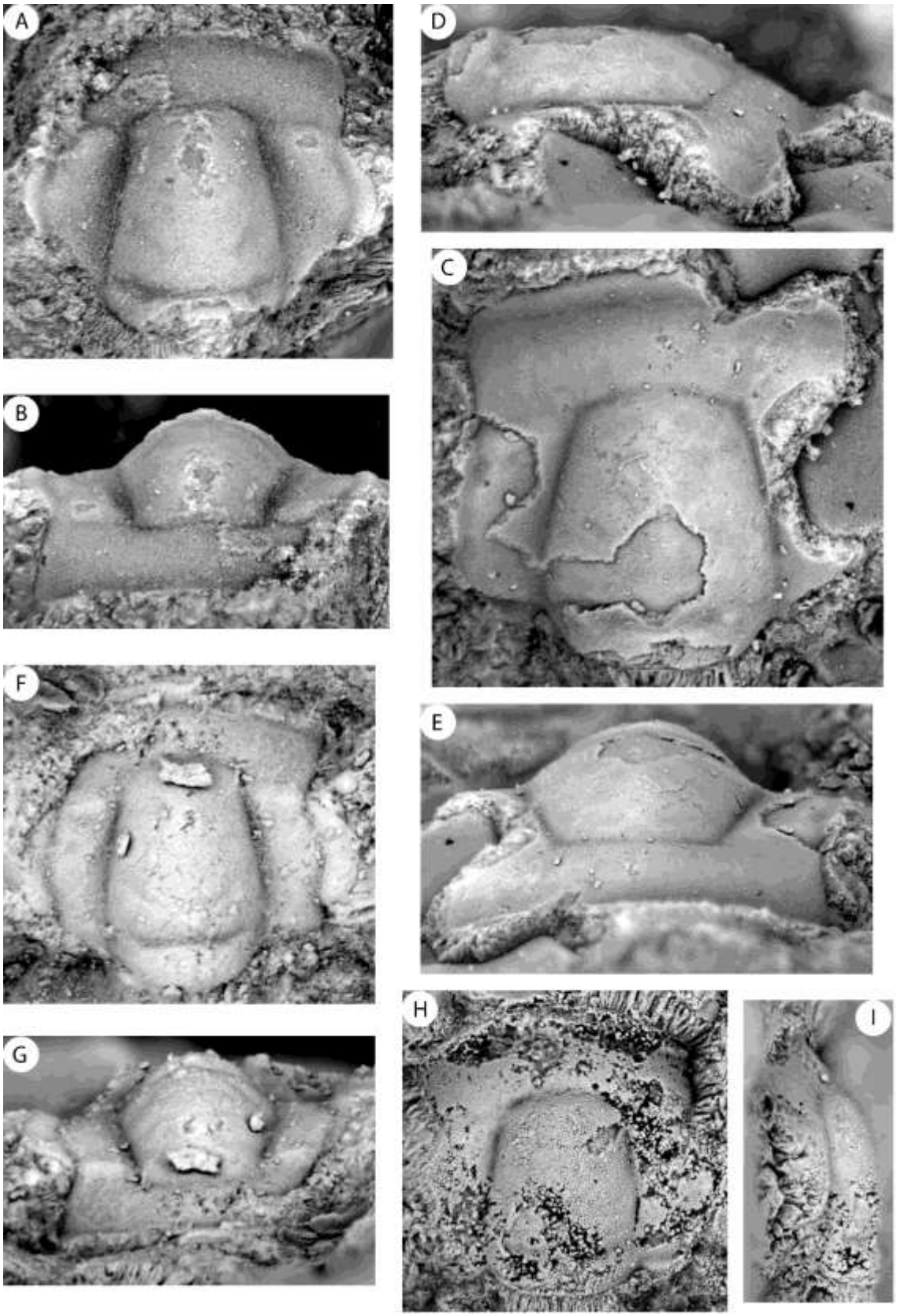
A
D
C
B
F
E
H
I
G

Plate 32

Aphelaspis longifrons Palmer, 1954 from the Cap Mountain Limestone, Riley Formation, Texas (HP 2.5 Pulloff).

A–B, free cheek (OU 238075), dorsal, lateral views, x9.

C–D, cranidium (OU 238076), dorsal, lateral views, x7.

E–F, cranidium (OU 238078), dorsal, anterior views, x5.3.

G, cranidium (OU 238077), dorsal view, x4.

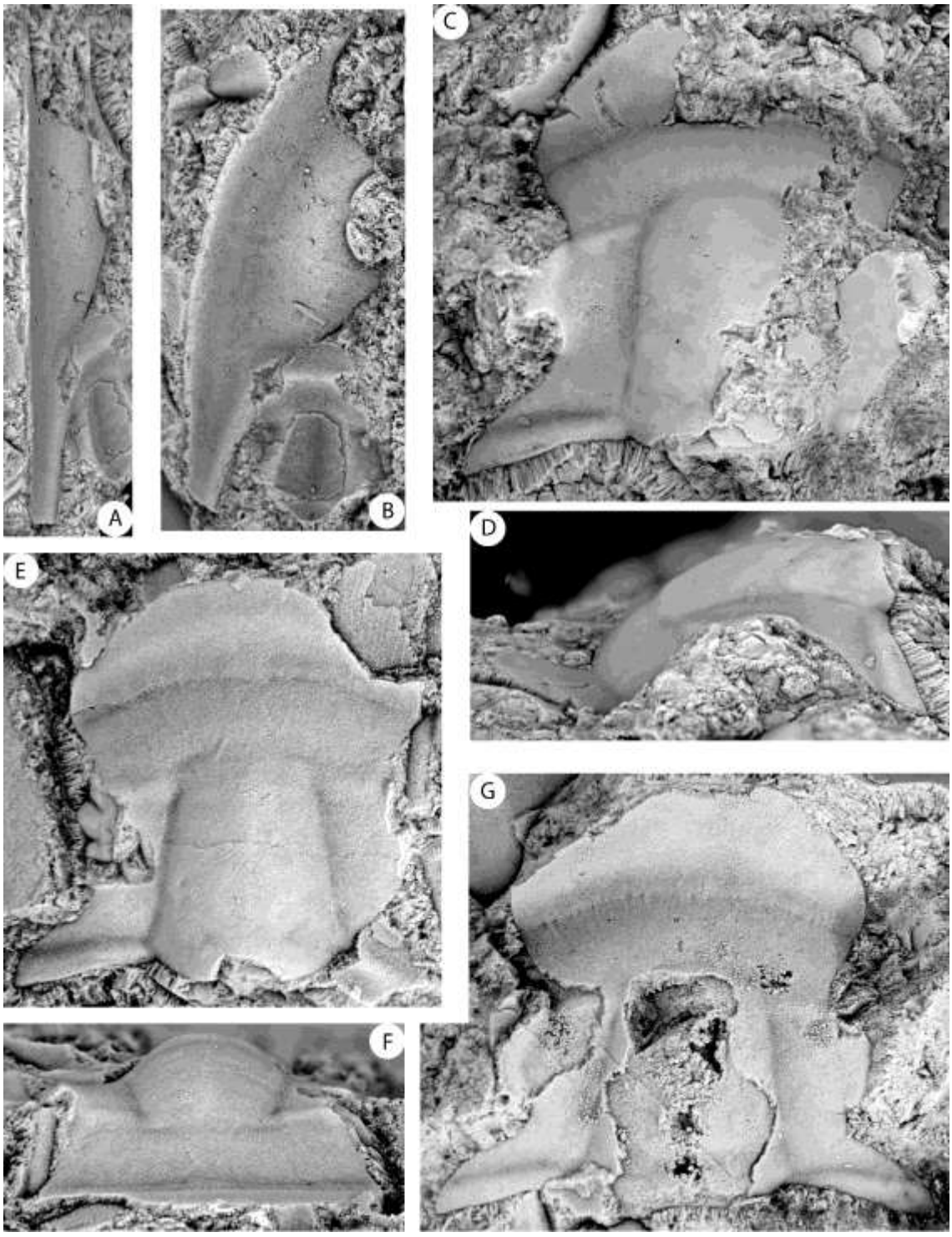
A
B
C
D
E
F
G

Plate 33

Aphelaspis longifrons Palmer, 1954 from the Cap Mountain Limestone, Riley Formation, Texas.

A–C, pygidium (OU 238079), dorsal, ventral, lateral views, x9 (HP 2.5 Pulloff).

D, free cheek (OU 238080), dorsal view, x15 (HP 2.5 Pulloff).

E–F, partially exfoliated pygidium (OU 238083), dorsal, lateral views, x15 (HP 2.6 Pulloff).

G, partially exfoliated pygidium (OU 238081), dorsal view, x15 (HP 2.5 Pulloff).

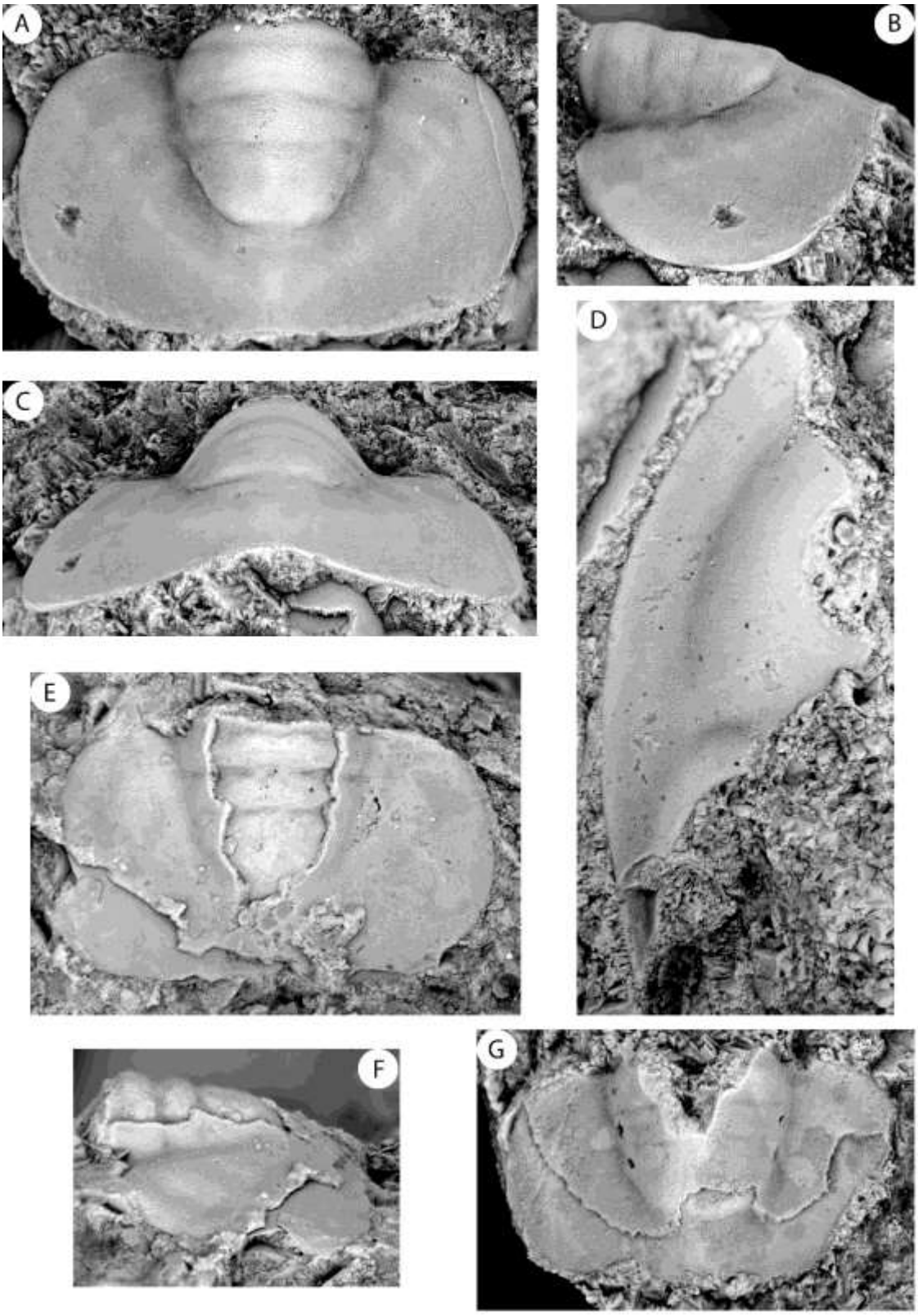
A
B
C
D
E
F
G

Plate 34

Aphelaspis longifrons Palmer, 1954 from the Cap Mountain Limestone, Riley Formation, Texas (HP 2.5 Pulloff).

A–B, partially exfoliated cranidium (OU 238082), dorsal, lateral views, x3.5.

C, partially exfoliated cranidium (OU 238083), dorsal view, x4.5.

D–E, cranidium (OU 238084), dorsal, anterior, lateral view, x6.

G, cranidium (OU 238085), dorsal view, x5.5.

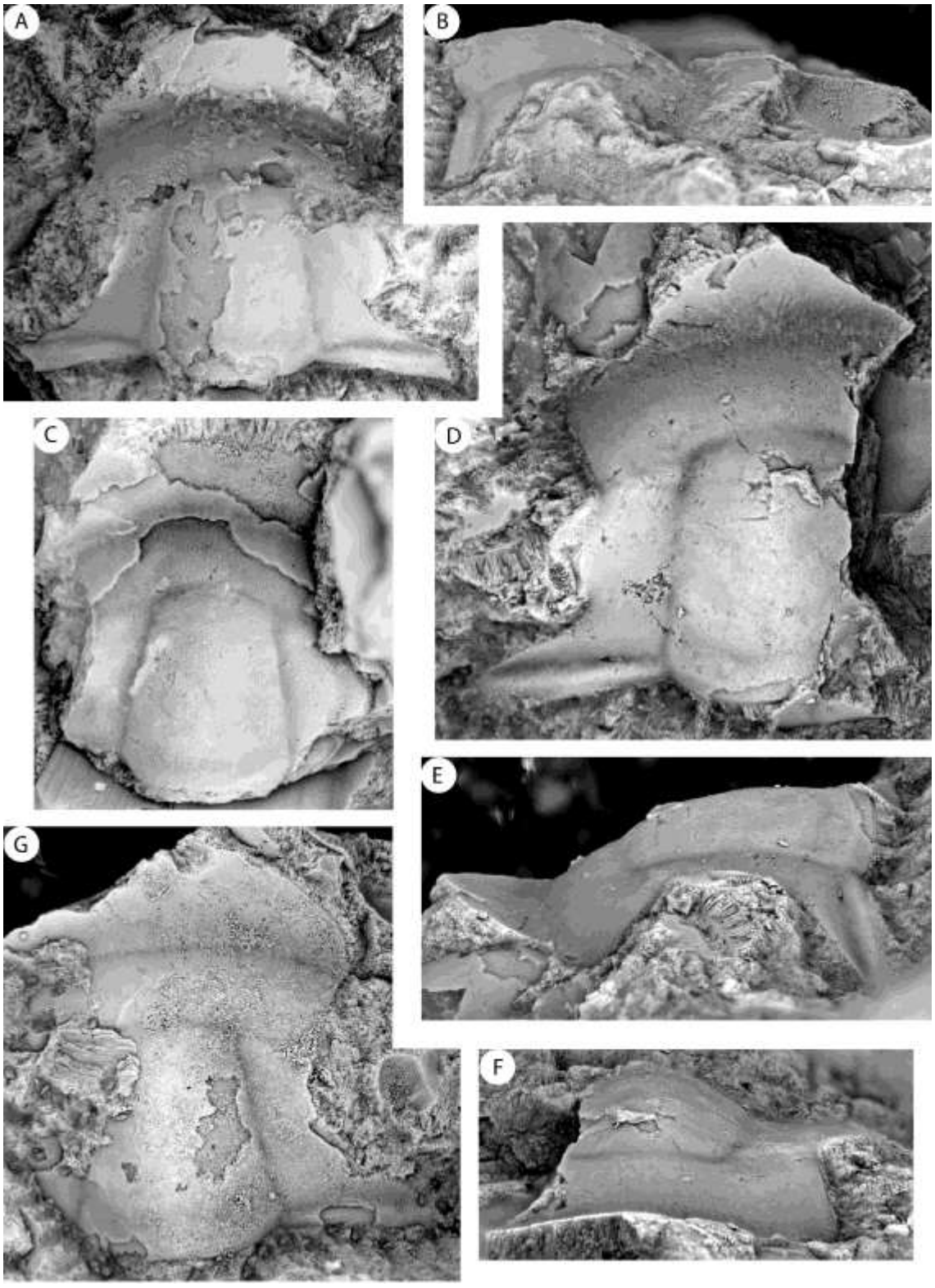
A
B
C
D
E
F
G

Plate 35

Aphelaspis spinosa Palmer, 1954 from the Cap Mountain Limestone, Riley Formation, Texas (MCNe1 5.8–5.9).

A–C, cranidium (OU 238087), dorsal, anterior, lateral views, x9.5.

D–E, partially exfoliated cranidium (OU 238088), dorsal, lateral views, x12.5.

F–H, pygidium (OU 238090), dorsal, posterior, lateral views, x10.5.

I–J, pygidium (OU 238089), dorsal, posterior, lateral views, x16.

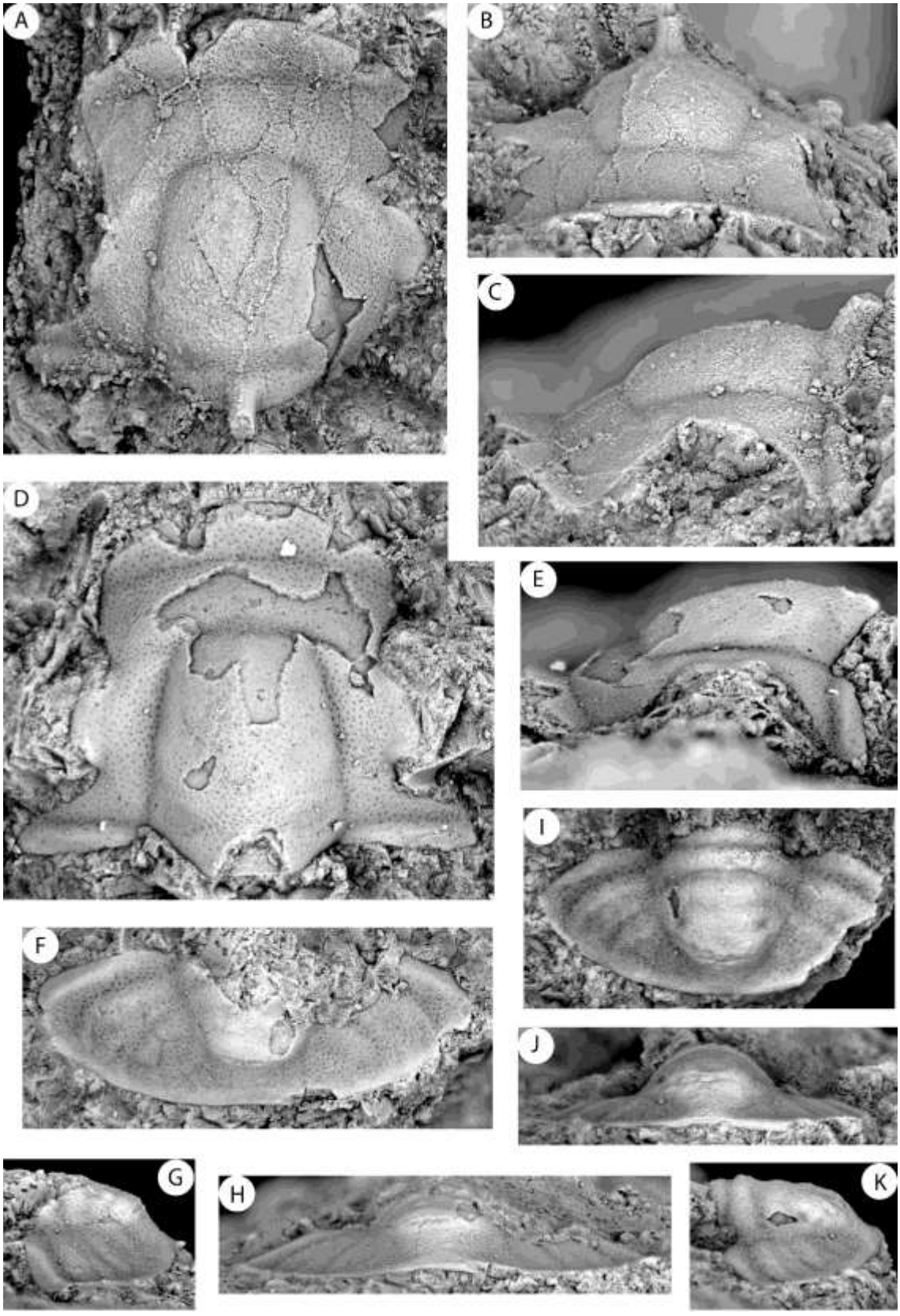
A
B
C
D
E
I
F
J
G
H
K

Plate 36

Aphelaspis spinosa Palmer, 1954 from the Cap Mountain Limestone, Riley Formation, Texas.

A–C, mostly exfoliated cranidium (OU 238091), dorsal, anterior, lateral views, x7 (MCNe1 2.1).

D–F, cranidium (OU 238092), dorsal, anterior, lateral views, x6.5 (LB 0.9–1.0).

G–H, pygidium (OU 238093), dorsal, posterior views, x14 (LB 0.9–1.0).

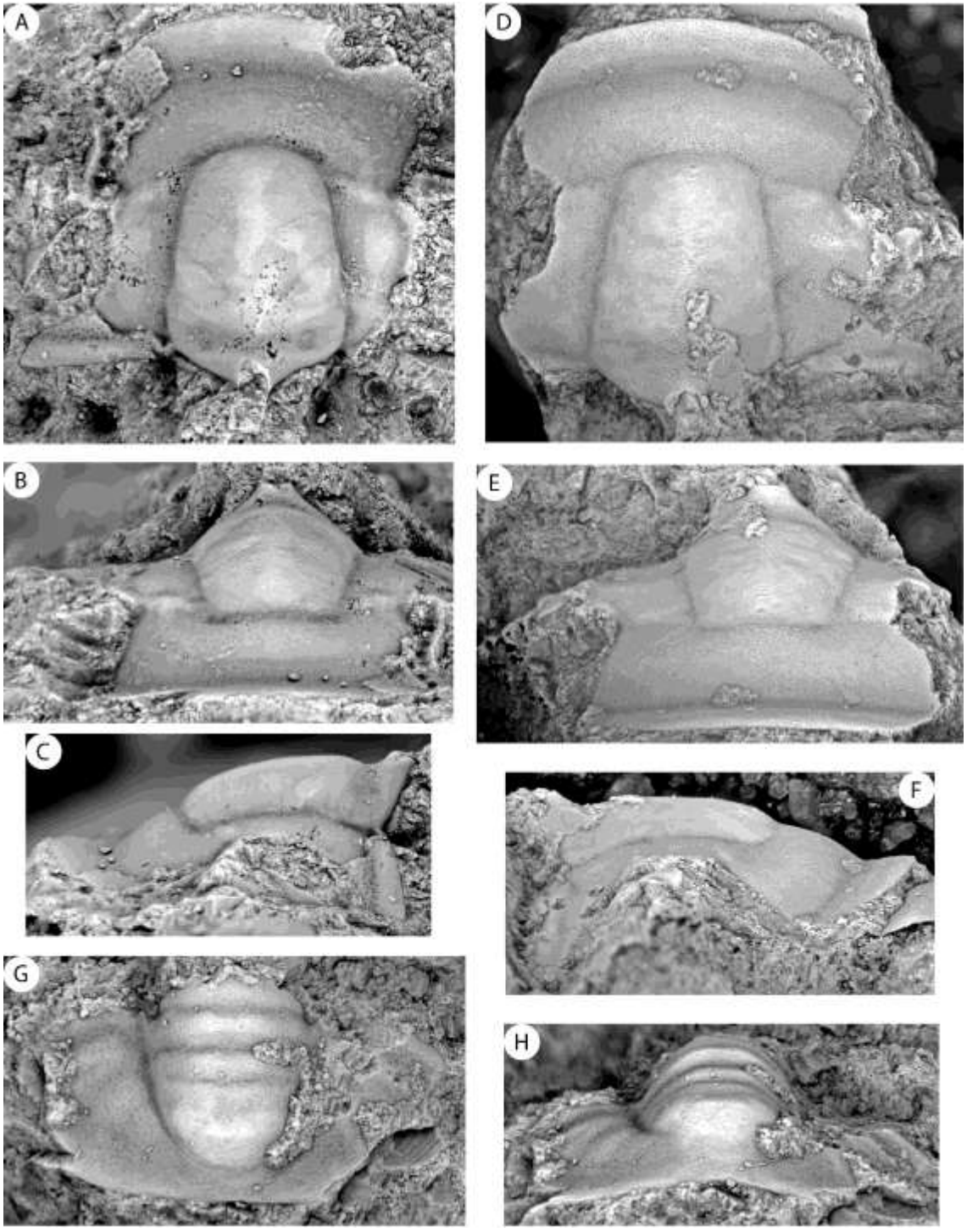
A
D
B
E
C
F
G
H

Plate 37

Aphelaspis spinosa Palmer, 1954 from the Cap Mountain Limestone, Riley Formation, Texas (LB 0.9–1.0).

A–C, cranidium (OU 238094), dorsal, anterior, lateral views, x7.

D–F, pygidium (OU 238096), dorsal, posterior, lateral views, x18.

G, free cheek (OU 238097), dorsal view, x7.6.

H–J, cranidium (OU 238095), dorsal, anterior, lateral views, x18.

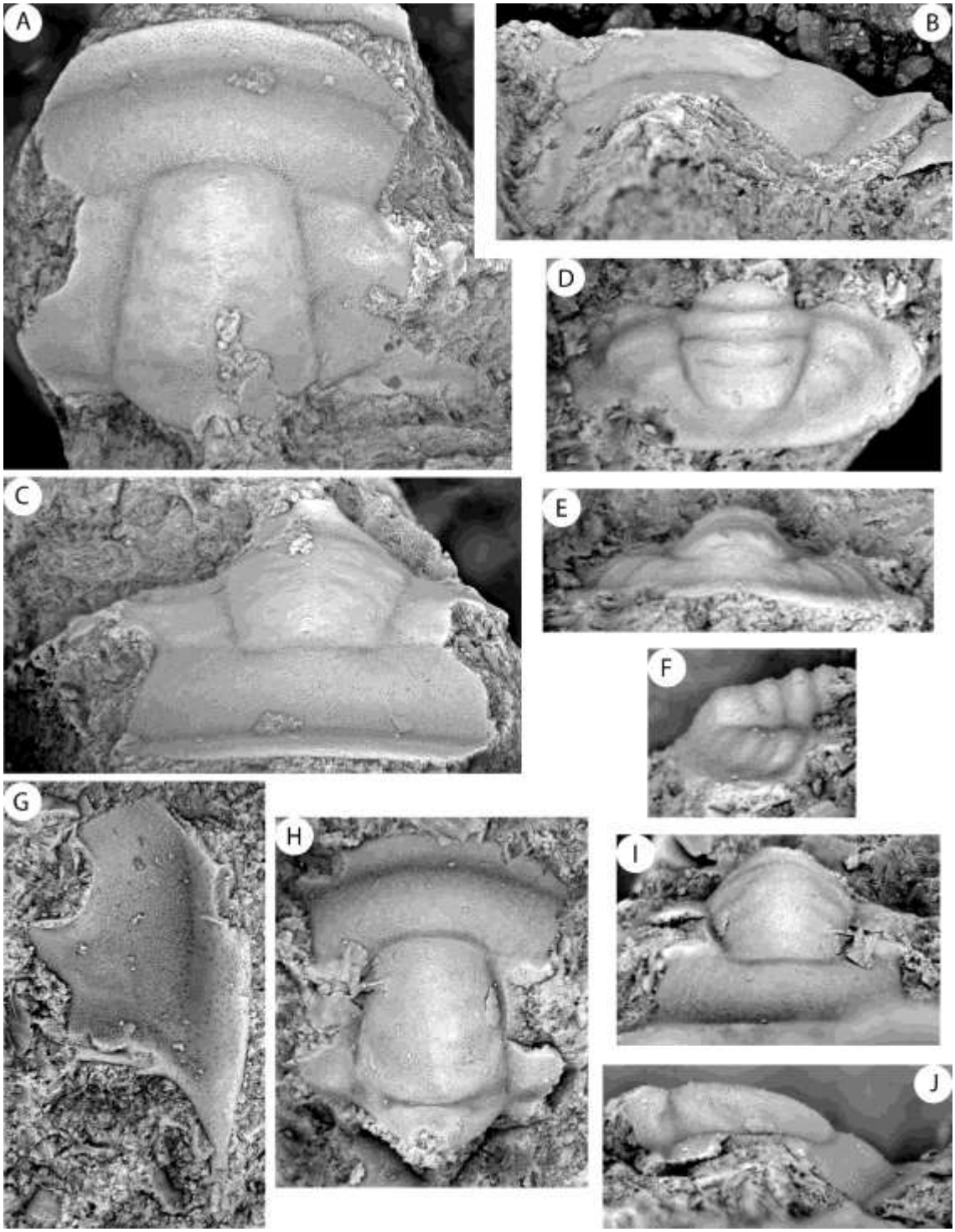
A
B
D
C
E
F
G
H
I
J

Plate 38

Cheilocephalus brevilobus Walcott, 1916 from the Lion Mountain Sandstone, Riley Formation, Texas.

A–C, cranidium (OU 238103), dorsal, anterior, lateral views, x3.5 (HP 3.7).

D–F, exfoliated pygidium (OU 238104), dorsal, posterior, lateral views, x5.3 (MCS 4.5).

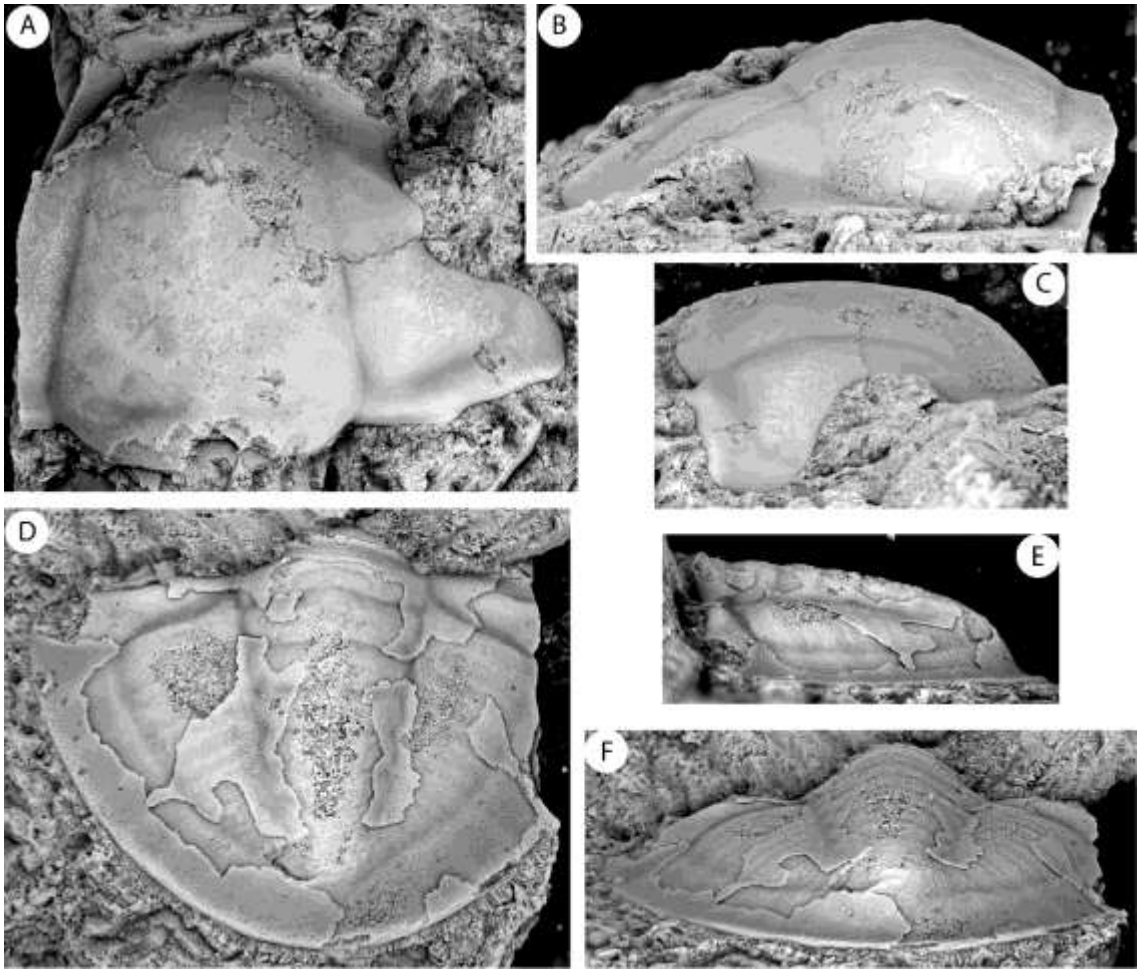
A
B
C
D
E
F

Plate 39

Cheilocephalus* cf. *granulosa (Palmer, 1965) from the Cap Mountain Limestone, Riley Formation, Texas.

A–C, incomplete, partially exfoliated cranidium (OU 238105), dorsal, anterior, lateral views, x3.7 (LB -0.15).

D–E, incomplete, exfoliated cranidium (OU 238106), dorsal, lateral views, x4.6 (MCNe1 2.1).

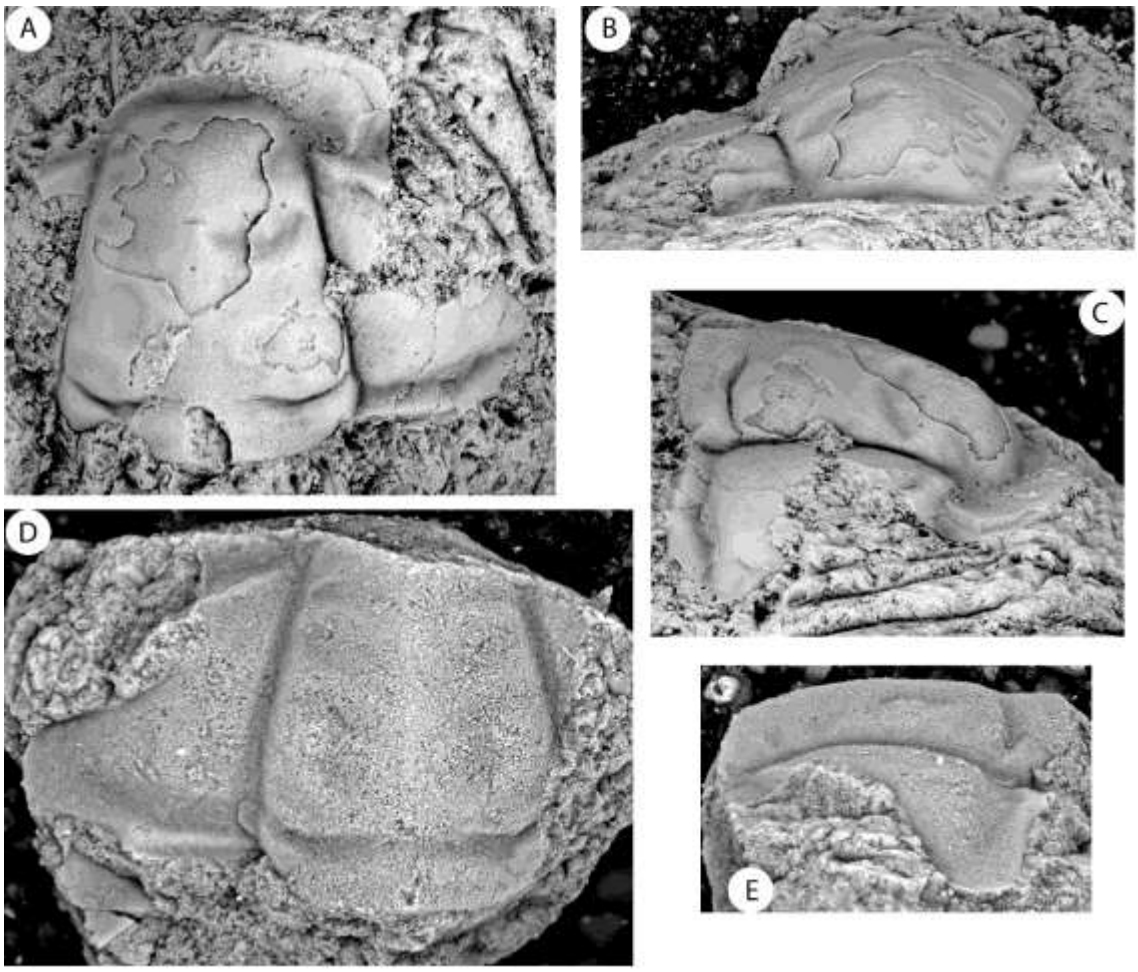
A
B
C
D
E

Plate 40

Dunderbergia* cf. *variagranula (Palmer, 1954) in the Lion Mountain Sandstone, Riley Formation, Texas (HP 3.65).

A–C, partially exfoliated cranidium (OU 238114), dorsal, anterior, lateral views, x6.

D, partially exfoliated cranidium (OU 238115), dorsal view, x3.5.

E–G, exfoliated pygidium (OU 238116), dorsal, anterior, lateral views, x4.5.

H–I, partially exfoliated pygidium (OU 238117), dorsal view, x12.

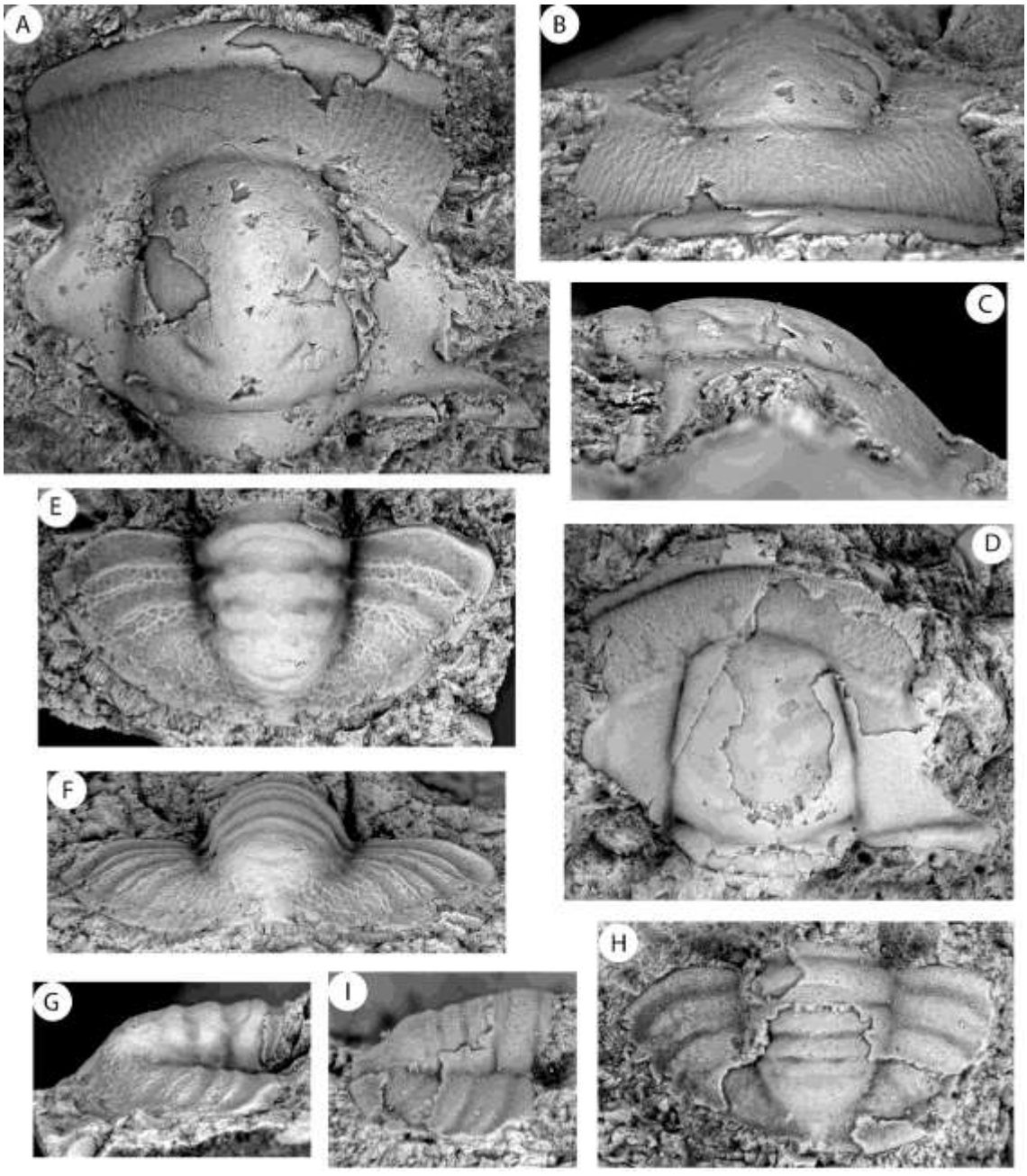
A
B
C
E
D
F
H
G
I

Plate 41

Glaphyraspis parva Walcott, 1899 from the Cap Mountain Limestone, Riley Formation, Texas.

A–C, cranidium (OU 238127), dorsal, anterior, lateral views, x17.5 (MCNe1 2.1).

D–F, cranidium (OU 238128), dorsal, anterior, lateral views, x16.7 (MCNe1 2.1).

G–I, pygidium (OU 238130), dorsal, posterior, lateral views, x17.6 (MCNe1 2.1).

J–K, cranidium (OU 238129), dorsal, lateral views, x16.7 (MCNe1 2.1).

L–N, cranidium (OU 238133), dorsal, anterior, lateral views, x17.5 (MCNe1 5.8–5.9).

O, cranidium (OU 238131), dorsal view, x17.5 (MCNe1 5.8–5.9).

P, cranidium (OU 238132), dorsal view, x17.5 (MCNe1 2.1).

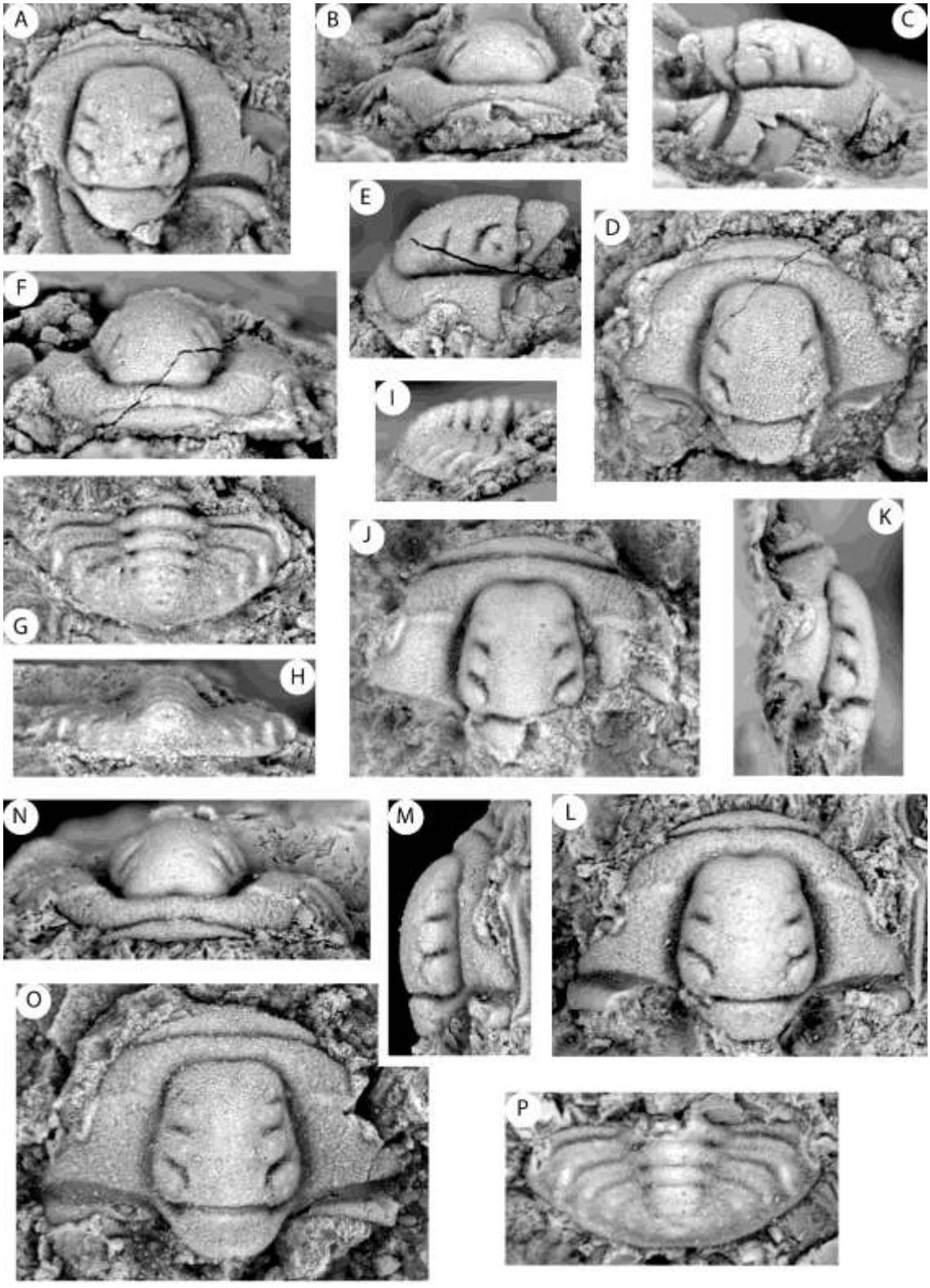
A
B
C
E
D
F
I
G
J
K
H
N
M
L
O
P

Plate 42

Glaphyraspis dianae n. sp. from the Cap Mountain Limestone, Riley Formation, Texas (MCNe1 7.1).

A–C, holotype cranidium (OU 238118), dorsal, anterior, lateral views, x15.8.

D–F, pygidium (OU 238119), dorsal, anterior, lateral, x16.7.

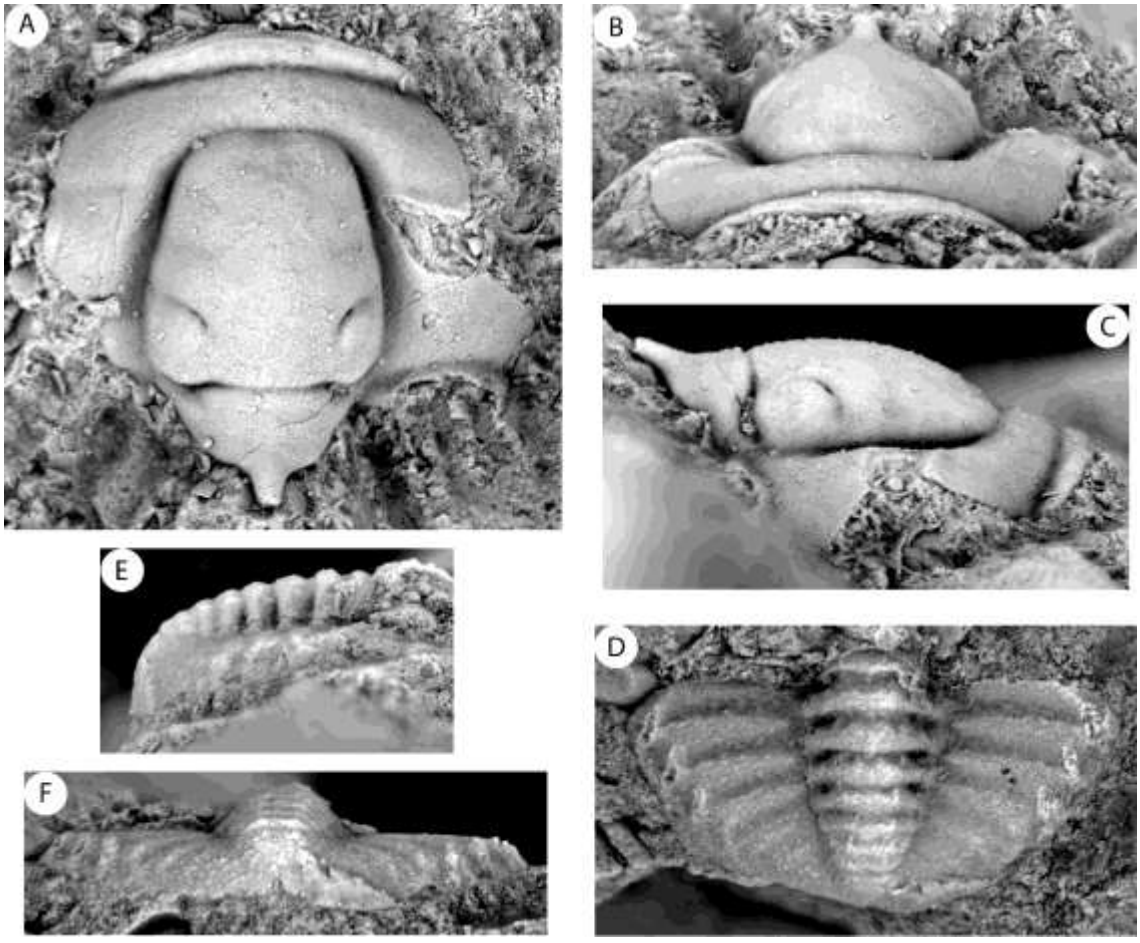
A
B
C
E
D
F

Plate 43

Glaphyraspis dianae n. sp. from the Cap Mountain Limestone, Riley Formation, Texas (LB 0.8).

A–C, cranidium (OU 238120), dorsal, anterior, lateral views, x16.7.

D–F, pygidium (OU 238121), dorsal, anterior, lateral views, x16.7.

G–I, cranidium (OU 238124), dorsal, anterior, lateral views, x10.5.

J–L, free cheek (OU 238125), dorsal, anterior, lateral views, x16.7.

M–N, free cheek (OU 238123), dorsal, lateral views, x16.7.

O–P, pygidium (OU 238122), dorsal, posterior views, x22.

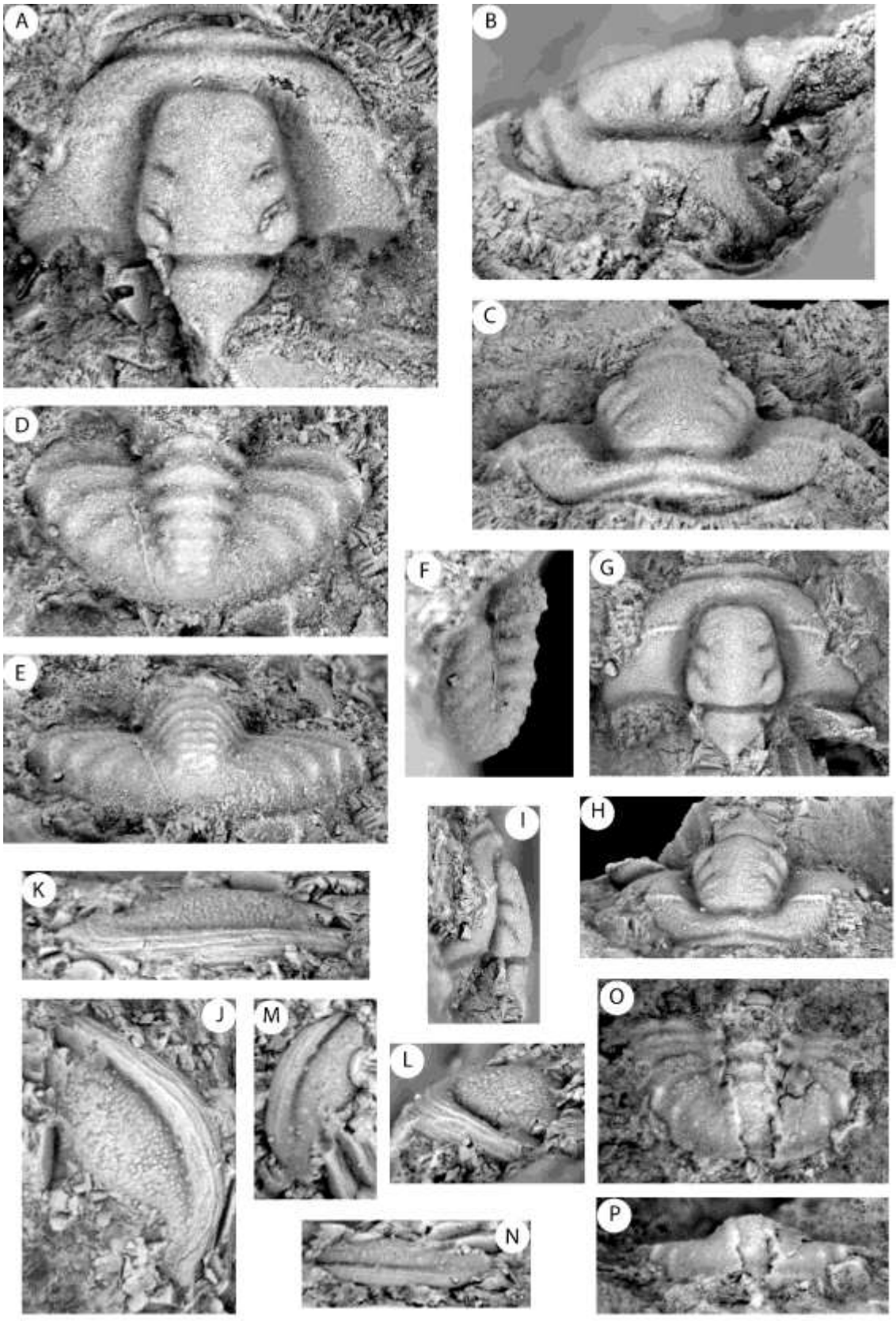
A
B
C
D
E
F
G
H
I
K
J
M
L
O
N
P

Plate 44

Glaphyraspis richardi n. sp. from the Cap Mountain Limestone, Riley Formation, Texas (LB 0.9–1.0).

A–C, holotype cranidium (OU 238134), dorsal, anterior, lateral views, x25.

D–E, pygidium (OU 238136), dorsal, posterior views, x19.

F–G, pygidium (OU 238135), dorsal, lateral views, x25.

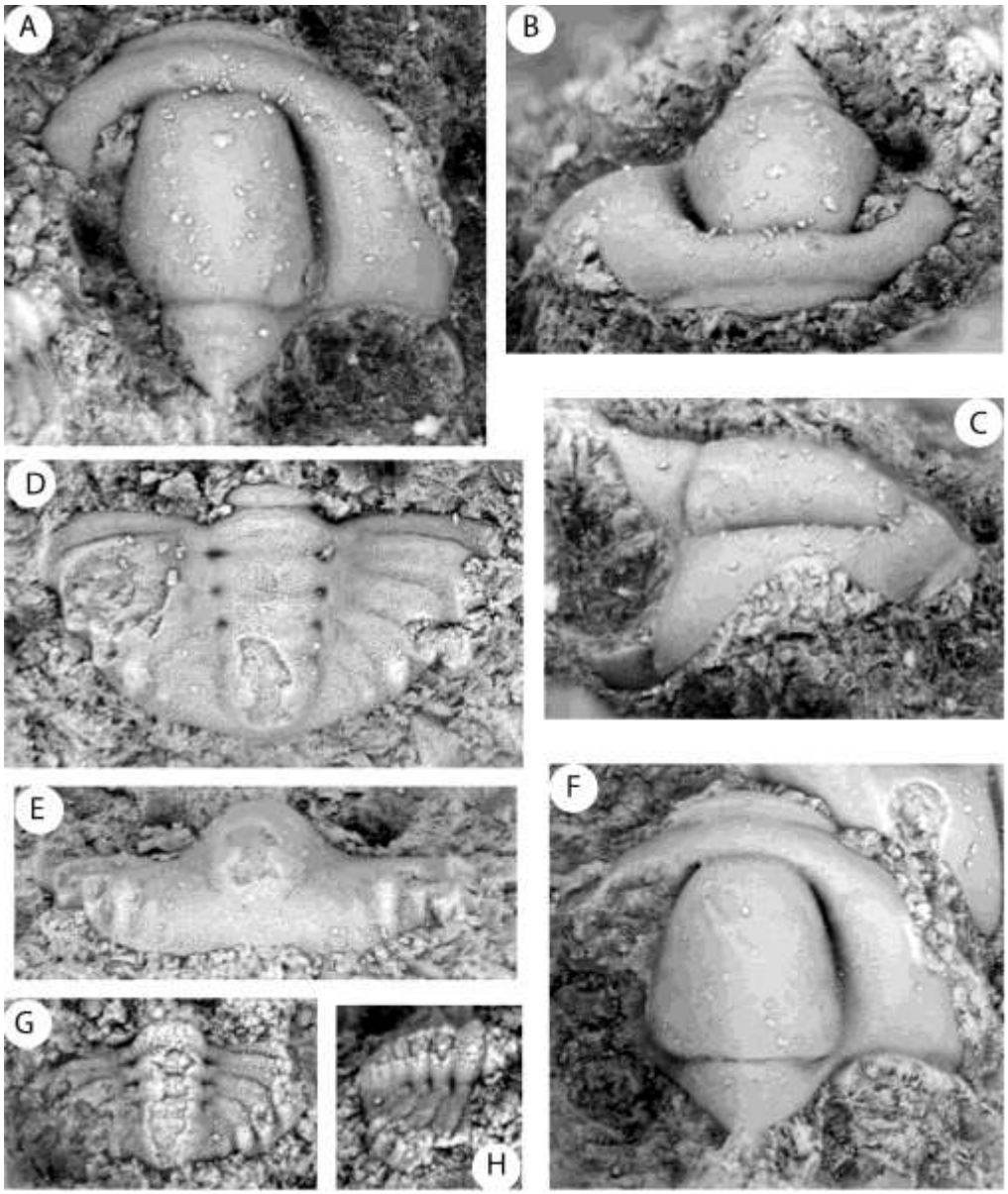
A
B
C
D
E
F
G
H

Plate 45

Coosina* cf. *ariston (Walcott, 1916) from the Cap Mountain Limestone, Riley Formation, Texas (MCNe2 3.9).

A–C, poorly preserved cranidium (OU 238110), dorsal, anterior, lateral views, x7.3.

D–E, exfoliated pygidium (OU 238111), dorsal, posterior view, x9.

Llanoaspis* cf. *peculiaris (Resser, 1938) from the Cap Mountain Limestone, Riley Formation, Texas (MCNe2 3.9).

F–H, cranidium (OU 238112), dorsal, anterior, lateral views, x9.

I. cranidium (OU 238113), dorsal view, x9.

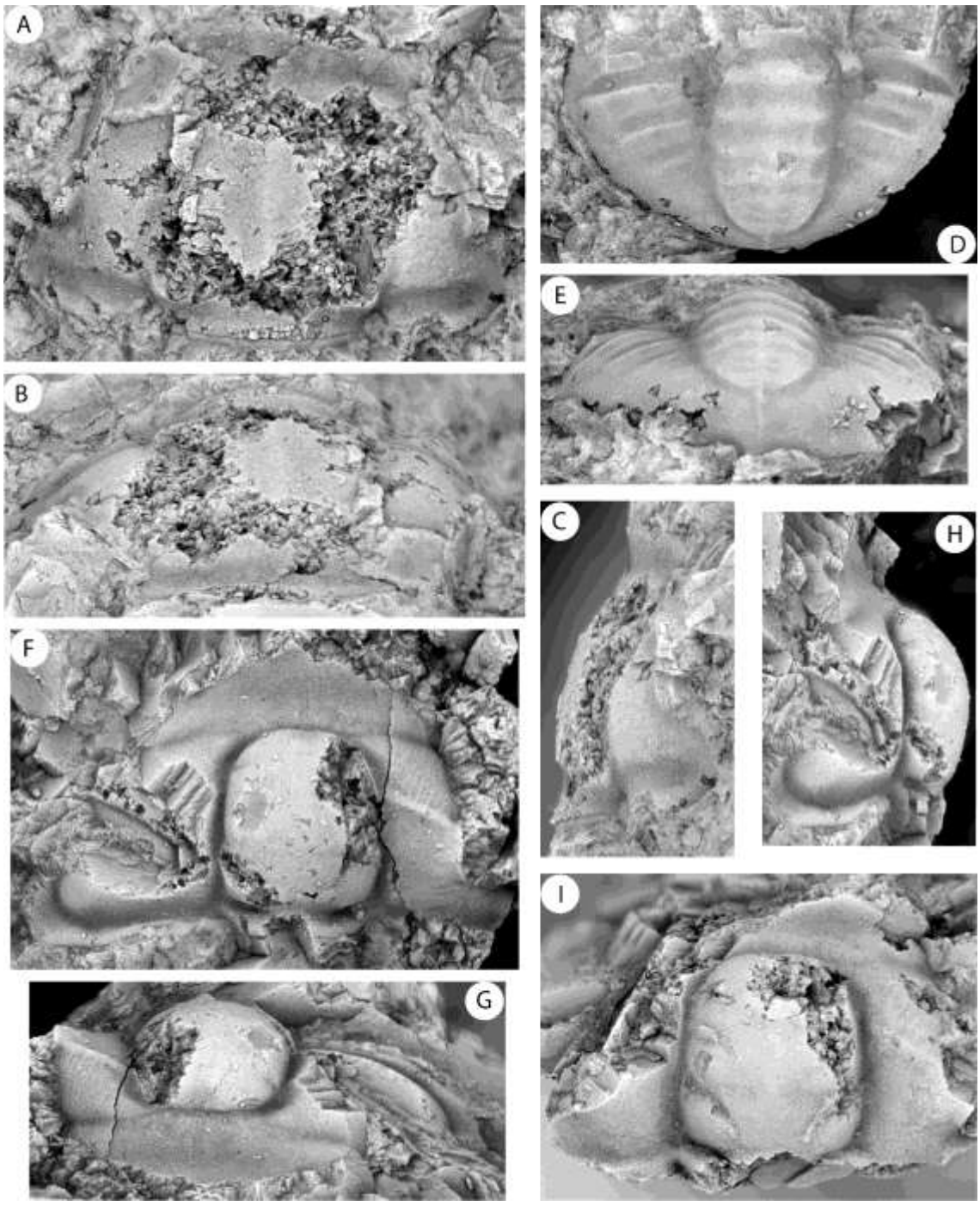
A
B
C
D
E
F
G
H
I

Plate 46

Coosella* cf. *perplexa (Palmer, 1954) from the Cap Mountain Limestone, Riley Formation, Texas (MCNe2 3.9)

A, incomplete cranidium (OU 238107), dorsal view, x8.

B–D, small pygidium (OU 238107), dorsal, posterior, lateral views, x11.7.

E–F, large pygidium (OU 238107), dorsal, posterior views, x2.7.

Coosella perplexa Palmer, 1954 from the Cap Mountain Limestone, Riley Formation, Texas.

G–I, cranidium, dorsal, anterior, lateral views, x5.4 (USNM 185797; figured in Palmer 1954, pl. 77, fig. 2).

J–K, pygidium, dorsal, posterior, lateral views, x6.3 (USNM 185798; figured in Palmer 1954, pl. 77, fig. 4).

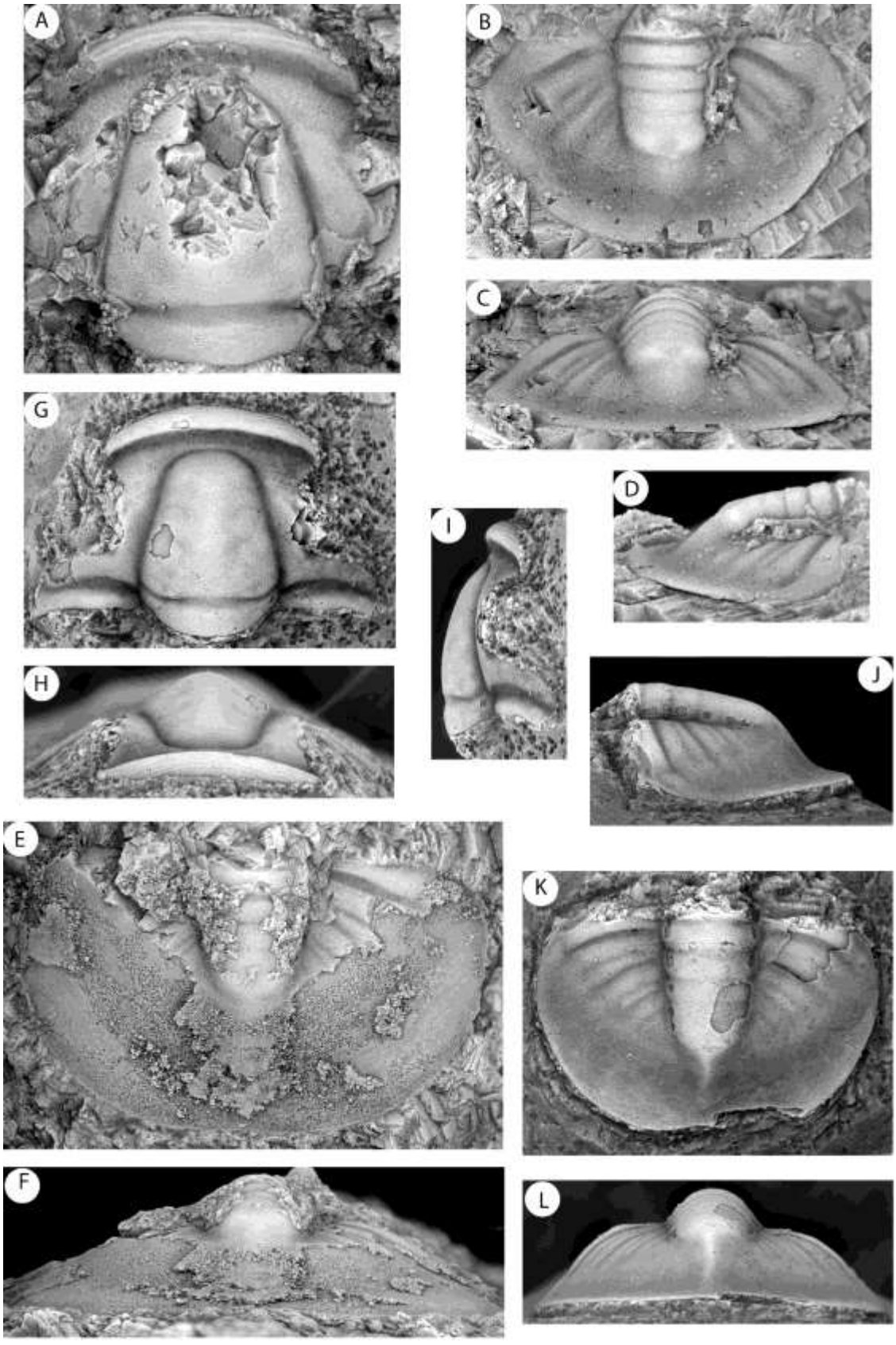
A
B
C
G
D
I
H
J
E
K
F
L

Plate 47

Blandicephalus texanus Palmer, 1954 in the Lion Mountain Sandstone, Riley Formation, Texas.

A, incomplete exfoliated cranidium (OU 238099), dorsal view, x4.5.

B–C, cranidium (OU 238098), dorsal, anterior views, x10.5.

D–E, exfoliated cranidium (OU 238100), dorsal, lateral views, x5.5.

F–H, partially exfoliated pygidium (OU 238102), dorsal, posterior, lateral views, x7.

I–J, free cheek (OU 238101), dorsal view, x4.5.

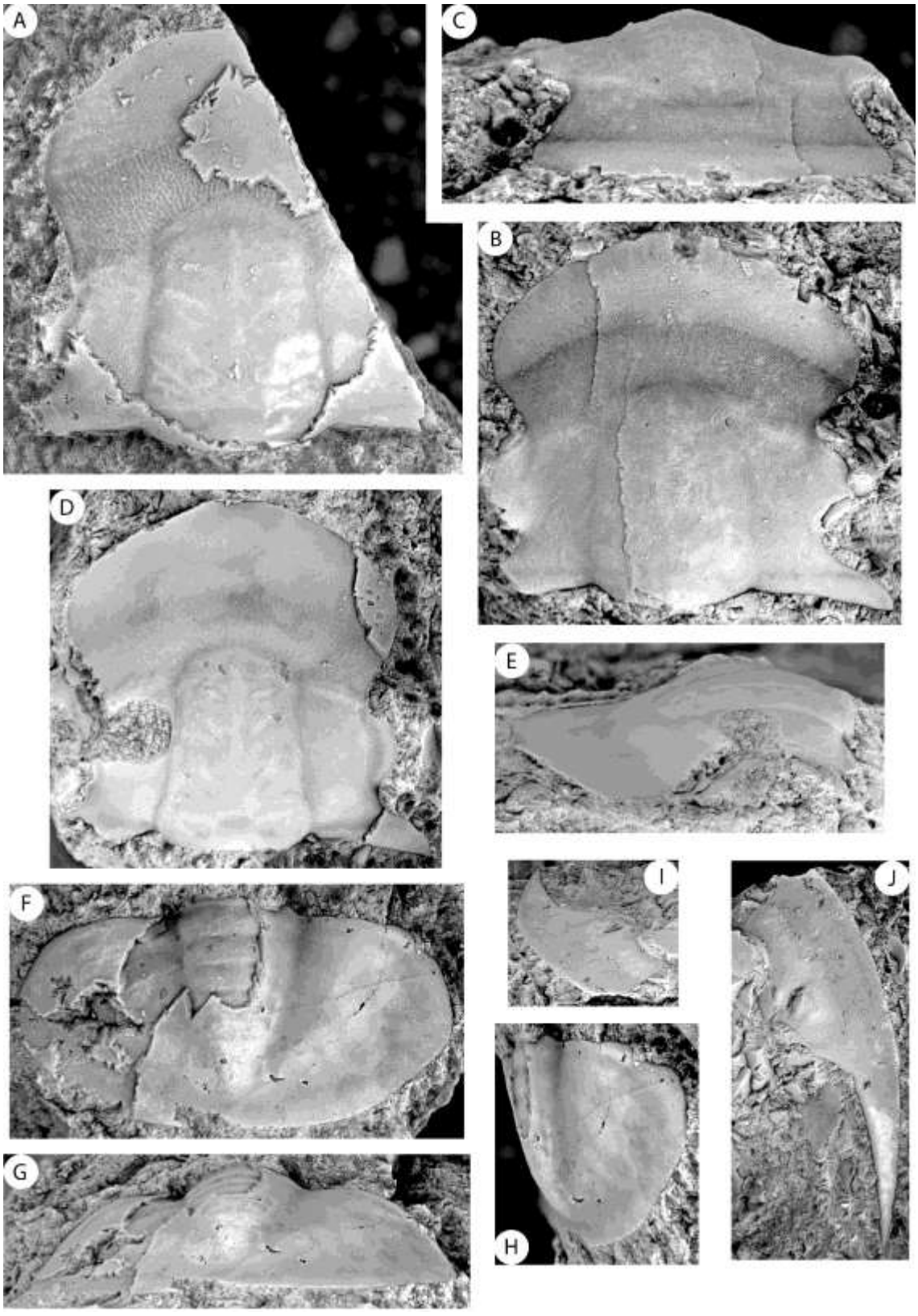
A
C
B
D
E
F
I
J
G
H

Plate 48

Labiostria conveximarginata Palmer, 1954 from the Riley Formation, Texas.

A–**C**, cranidium, dorsal, anterior, lateral views, x5.3 (USNM 185962; figured in Palmer 1954, pl. 86, fig. 4).

Labiostria platifrons Palmer, 1954 from the Riley Formation, Texas.

D–**E**, cranidium, dorsal, anterior, lateral views, x5.8 (USNM 185965; figured in Palmer 1954, pl. 86, fig. 6).

Labiostria sigmoidalis Palmer, 1954 from the Riley Formation, Texas.

G–**I**, cranidium, dorsal, anterior, lateral views, x5.8 (USNM 185968; figured in Palmer 1954, pl. 86, fig. 5).

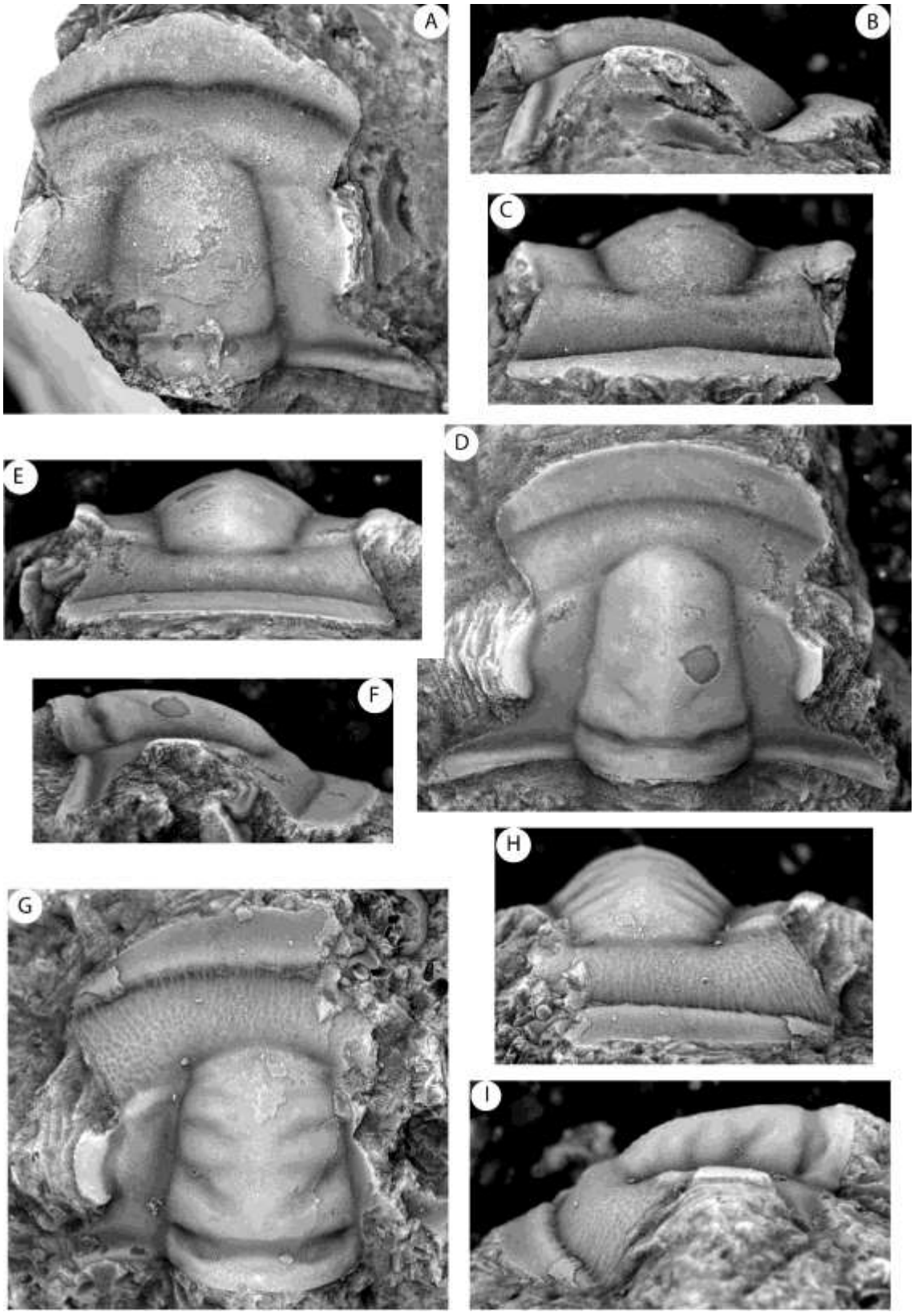
A
B
C
D
E
F
G
H
I

Plate 49

Labiostria conveximarginata Palmer, 1954 from the Riley Formation, Texas.

A–B, cranidium, dorsal, lateral view, x5 (USNM 123322; figured in Palmer 1954, pl. 86, fig. 3).

C, free cheek, dorsal view, x5.3 (USNM 185964; figured in Palmer 1954, pl. 86, fig. 2).

Labiostria platifrons Palmer, 1954 from the Riley Formation, Texas.

D. cranidia, dorsal view, x12 (USNM 185966; figured in Palmer 1954, pl. 86, fig. 8).

E–F, pygidium, dorsal, posterior views, x5 (USNM 185966).

G, free cheek, dorsal view, x5.3 (USNM 185967; figured in Palmer 1954, pl. 86, fig. 7).

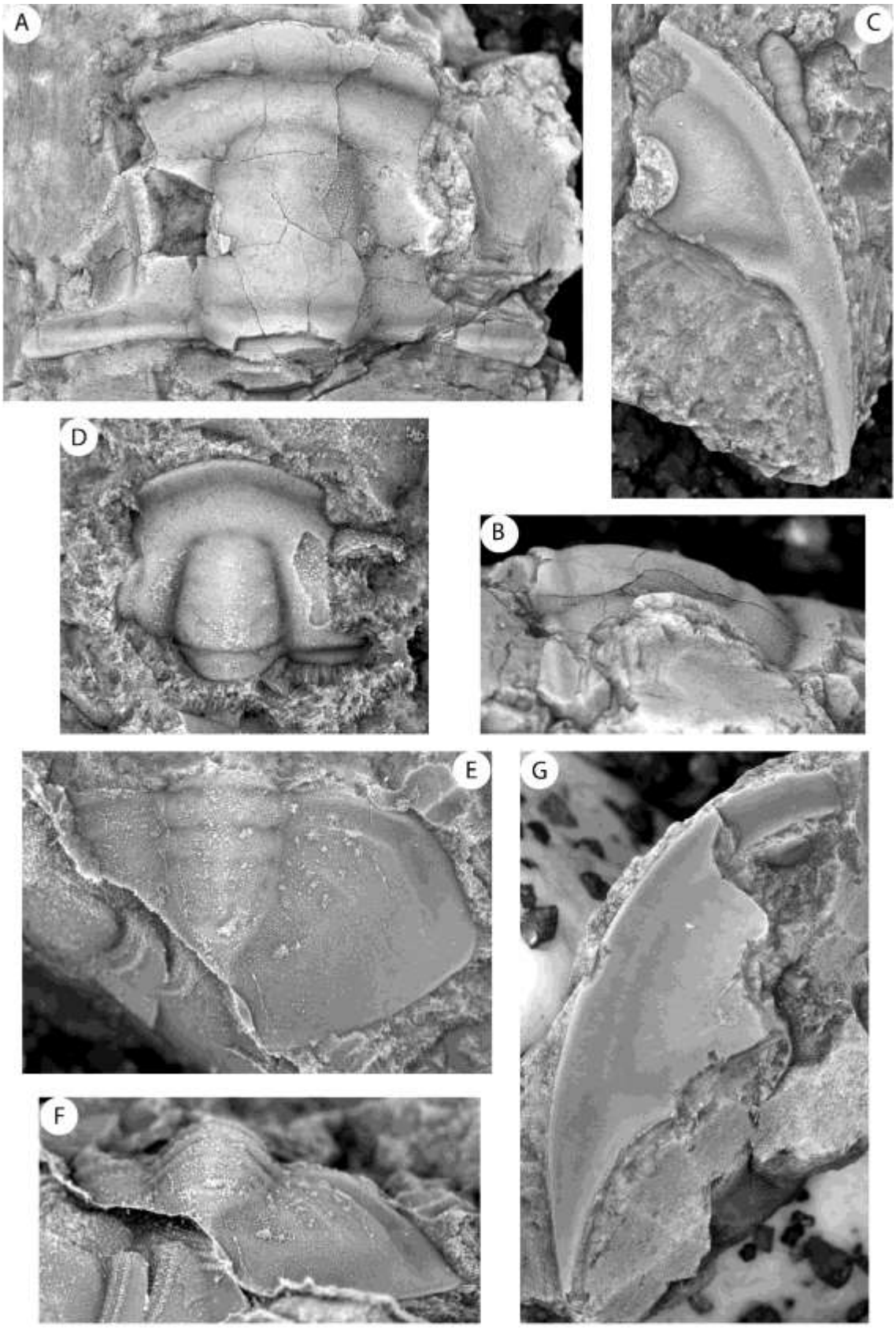
A
C
D
B
E
G
F

Plate 50

Labiostria conveximarginata Palmer 1954 from the Lion Mountain Sandstone, Riley Formation, Texas (MCS 4.5).

A–C, cranidium (OU 238153), dorsal, lateral, and anterior views, x7.5.

D–E, pygidium (OU 238154), dorsal, posterior views, x7.5.

Labiostria sigmoidalis Palmer 1954 from the Lion Mountain Sandstone, Riley Formation, Texas (MCS 4.5).

F–G, exfoliated cranidium (OU 238155), dorsal, anterior views, x8.5.

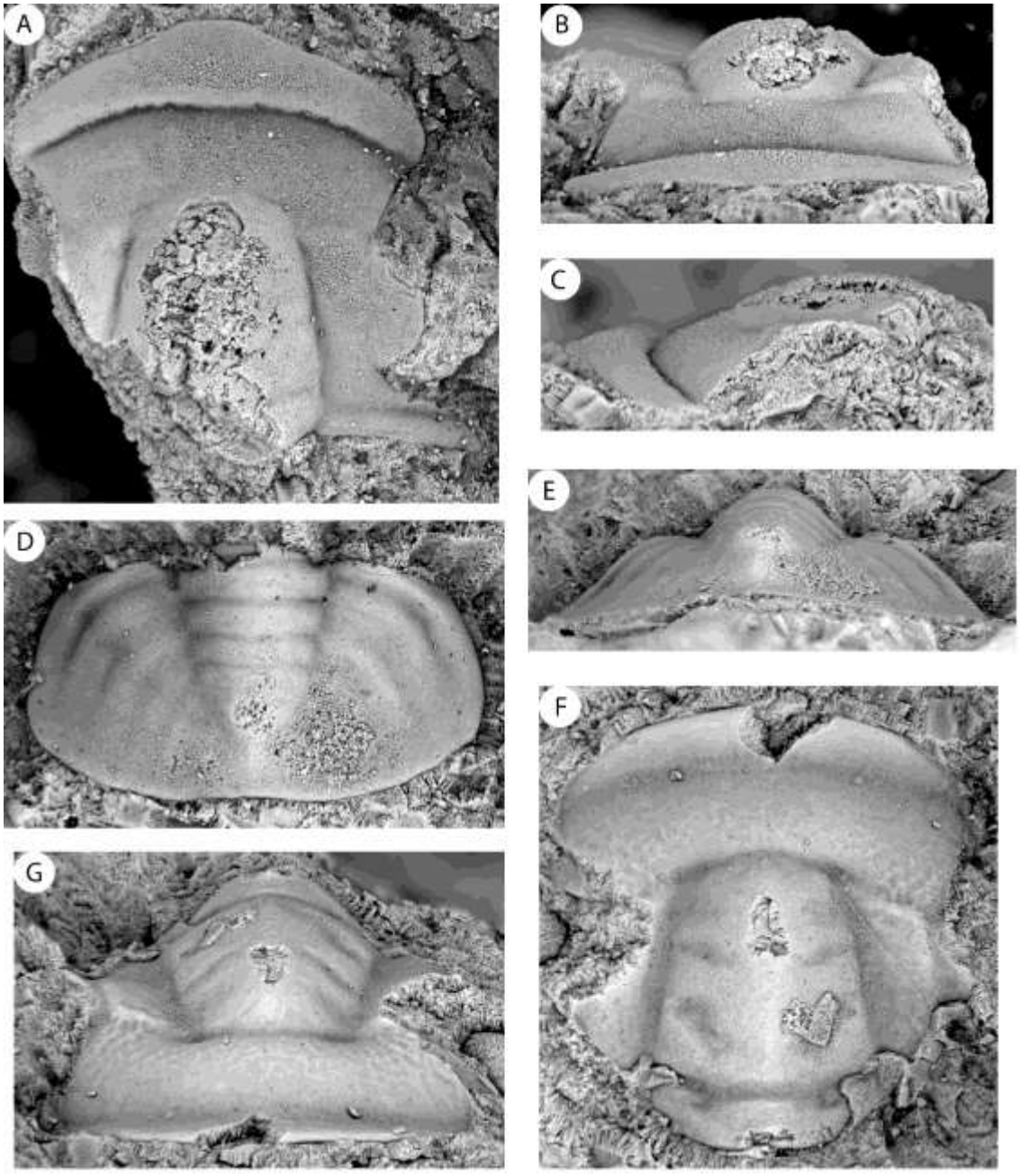
A
B
C
D
E
F
G

Plate 51

Gen. nov. aff. *Dunderbergia* from the Lion Mountain Sandstone, Riley Formation, Texas.

A–C, cranidium (OU 238138), dorsal, anterior, lateral views, x7 (HP 3.1).

D–F, cranidium (OU 238139), dorsal, anterior, lateral views, x9 (HP 3.1).

G–H, free cheek (OU 238141), dorsal, anterior views, x6.5 (HP 3.1).

I, exfoliated cranidium (OU 238140), dorsal view, x8.2 (HP 3.7).

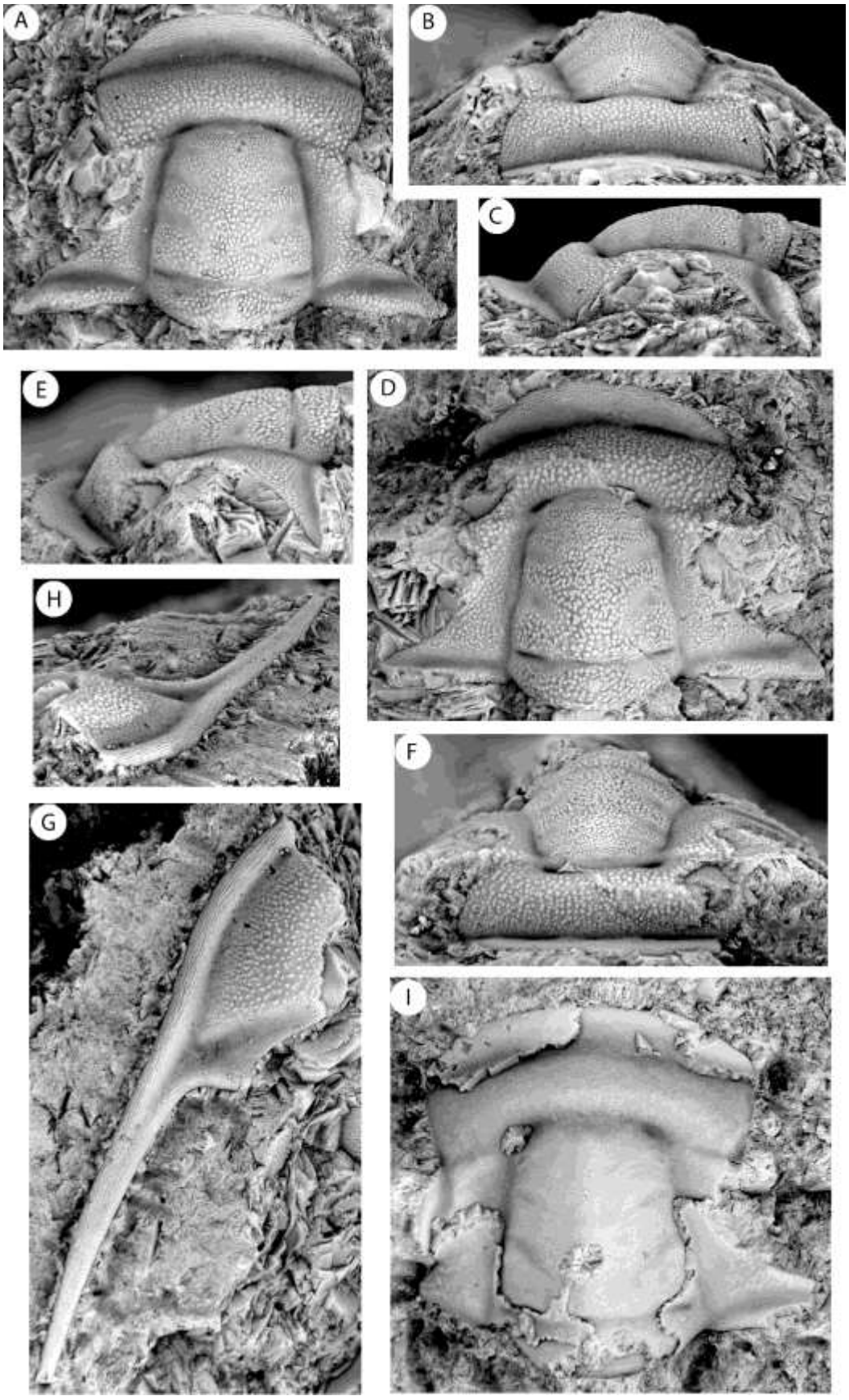
A
B
C
E
D
H
F
G
I